CURIS RESOURCES (ARIZONA) INC.

APPLICATION FOR TEMPORARY INDIVIDUAL AQUIFER PROTECTION PERMIT

ATTACHMENT 14A – HYDROLOGIC STUDY PART A, GROUNDWATER FLOW MODEL (ITEM 25.H)

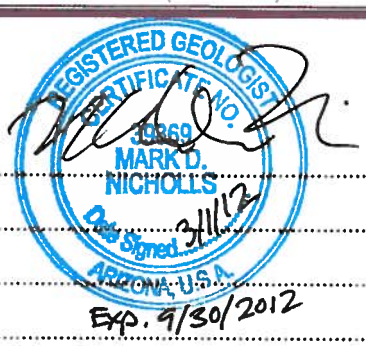

Table of Contents

Table of Contents 1

List of Figures 2

List of Tables 3

List of Exhibits 4

14A.1 Introduction 5
14A.1.1 Background 6

14A.2 Study Area Setting 6
14A.2.1 Physiography 6
14A.2.2 Climate 7
14A.2.3 Surface Water 7
14A.2.4 Land and Water Use 7

14A.3 Hydrogeology and Conceptual Model 8
14A.3.1 Previous Studies 8
14A.3.2 Regional Geology and Hydrostratigraphy 11
14A.3.2.1 Structural Geology 11
14A.3.2.2 Hydrostratigraphy 12
14A.3.2.2.1 Upper Basin Fill Unit (UBFU) 13
14A.3.2.2.2 Middle Fine Grained Unit (MFGU) 13
14A.3.2.2.3 Lower Basin fill Unit (LBFU) 14
14A.3.2.2.4 Oxide Bedrock Zone 14
14A.3.2.2.5 Hydrologic Bedrock 15
14A.3.3 Regional Hydrogeologic System 16
14A.3.3.1 Inflows 16
14A.3.3.1.1 Surface Water Flow and Groundwater Subflow 16
14A.3.3.1.2 Gila River Recharge 16
14A.3.3.1.3 Mountain Front Recharge 17
14A.3.3.1.4 Canal Leakage 17
14A.3.3.1.5 Permitted Recharge Facilities 17
14A.3.3.1.6 Agricultural Returns 17
14A.3.3.2 Outflows 18
14A.3.3.2.1 Groundwater Pumping 18
14A.3.3.2.2 Evapotranspiration 18
14A.3.3.2.3 Underflow 18
14A.3.4 Groundwater Elevations and Gradients 18

14A.4 Production Test Facility Groundwater Model 19
14A.4.1 Production Test Facility Model Development 19
14A.4.2 Computer Code Description 19
14A.4.2.1 Solution Techniques 20
14A.4.2.2 Assumptions 20
14A.4.2.3 Limitations 20
14A.4.3 Model Domain 21
14A.4.3.1 Units and Coordinate System 22
14A.4.3.2 Boundary Conditions 22

14A.4.3.3 Model Grid Discretization and Layering 22
14A.4.4 Stress Periods 23
14A.4.5 Initial Conditions 23
14A.4.6 Hydraulic Parameterization 23
14A.4.7 Sources and Sinks 23

14A.5 Model Results and Calibration 24
14A.5.1 Approach 24
14A.5.2 Qualitative Calibration 25
14A.5.3 Simulated Water Levels and Quantitative Calibration 25
14A.5.3.1 Calibration Statistics and Targets 25
14A.5.3.2 Simulated Water Level Conditions 2010 26
14A.5.3.3 Simulated Water Budget 27

14A.6 Predictive Simulations 27
14A.6.1 Predictive Scenario Development 27
14A.6.2 Discharge Impact Area 28
14A.6.2.1 Transport Simulation Initial Conditions and Parameters 28
14A.6.2.2 DIA Evaluation Criterion 29
14A.6.2.3 Results of DIA Transport Simulation 29
14A.6.3 Particle Tracking 29

14A.7 Water Level Impacts of ISCR 29

14A.8 Impacts from Off-Site Pumping 30

14A.9 References 31

List of Figures

Figure 14A-1 Location Map
Figure 14A-2 Block Diagram Showing Typical ISCR Wells
Figure 14A-3 Mean Monthly Precipitation
Figure 14A-4 Total Annual Precipitation
Figure 14A-5 Monthly Mean Gila River Stage Values – Kelvin, AZ
Figure 14A-6 Land Use and Key Wells
Figure 14A-7 Bedrock Topography
Figure 14A-8 Generalized Regional Geologic Cross Section A-A'
Figure 14A-9 Generalized Regional Geologic Cross Section B-B'
Figure 14A-10 Measured Groundwater Elevations 2008
Figure 14A-11 Hydraulic Conductivity of Basin Fill and Bedrock Units
Figure 14A-12 Well Hydrographs
Figure 14A-13 Model Grid with Boundary Conditions
Figure 14A-14 Refined Model Grid
Figure 14A-15 Water Level Initial Conditions - 1984

List of Figures (continued)

Figure 14A-16 Hydraulic Conductivity Model Layer 1
Figure 14A-17 Hydraulic Conductivity Model Layer 2
Figure 14A-18 Hydraulic Conductivity Model Layer 3
Figure 14A-19 Hydraulic Conductivity Model Layer 4
Figure 14A-20 Hydraulic Conductivity Model Layer 5
Figure 14A-21 Hydraulic Conductivity Model Layer 6
Figure 14A-22 Hydraulic Conductivity Model Layer 7
Figure 14A-23 Hydraulic Conductivity Model Layer 8
Figure 14A-24 Hydraulic Conductivity Model Layer 9
Figure 14A-25 Hydraulic Conductivity Model Layer 10
Figure 14A-26 Regional Water Budget
Figure 14A-27 Calibrated Water Levels and Residuals
Figure 14A-28 Simulated Transient Water Budget
Figure 14A-29 Initial Concentrations, Sulfate Distribution Transport Simulations
Figure 14A-30 Model Layering in the Vicinity of the PTF Well Field
Figure 14A-31 Simulated Sulfate Distribution Model Layer 5 (Lower LBFU), 5 Years after Closure
Figure 14A-32 Simulated Sulfate Distribution Model Layer 6 (Oxide Exclusion Zone), 5 Years after Closure
Figure 14A-33 Simulated Sulfate Distribution Model Layer 7 (Upper Oxide), 5 Years after Closure
Figure 14A-34 Simulated Sulfate Distribution Model Layer 8 (Upper Oxide), 5 Years after Closure
Figure 14A-35 Simulated Sulfate Distribution Model Layer 9 (Upper Oxide), 5 Years after Closure
Figure 14A-36 Simulated Sulfate Distribution Model Layer 10 (Lower Oxide), 5 Years after Closure
Figure 14A-37 Extent of Sulfate Migration within the Oxide (All Layers), 5 Years after Closure
Figure 14A-38 Discharge Impact Area 5 Years after Closure

List of Tables

Table 14A-1 Application Attachments Addressing Hydrologic Study Requirements Defined in A.A.C. R18-9-A202A.8
Table 14A-2 Measured Hydraulic Conductivity Values for MFGU Samples
Table 14A-3 Specifications of the PTF Groundwater Model
Table 14A-4 Aquifer Parameter Value Ranges by Model Layer
Table 14A-5 Transient Model Calibration Statistics
Table 14A-6 Simulated Water Budget Values

List of Exhibits

Exhibit 14A-1	Aquifer Test Data, Volume II, Appendix E, 1996 Florence APP Application (Provided on CD)
Exhibit 14A-2	MFGU Hydraulic Conductivity Testing Laboratory Report (300), 1995; MFGU Hydraulic Conductivity Testing Laboratory Report (283-288), 2011 MFGU Hydraulic Conductivity Testing Laboratory Report (292-297), 2011
Exhibit 14A-3	Site Characterization Report Section 2.3.1, Florence 1996 APP Application

14A.1 Introduction

This attachment has been prepared in response to the information requirements of Item 25.H of the Individual Aquifer Protection Permit (APP) Application Form (Form). Arizona Administrative Code (A.A.C.) R18-9-A202A.8 requires a hydrologic study that defines the Discharge Impact Area (DIA) associated with the permitted activities for the planned life of the proposed Production Test Facility (PTF). Requirements of the hydrologic study are defined in A.A.C. R18-9-A202A.8 as follows:

a. The hydrologic study is required to demonstrate:
   i. That the facility will not cause or contribute to a violation of an Aquifer Water Quality Standard (AWQS) at the applicable point of compliance (POC); or
   ii. If an AWQS for a pollutant is exceeded in an aquifer at the time of permit issuance, and that no additional degradation of the aquifer relative to that pollutant and determined at the applicable POC will occur as a result of the discharge from the proposed facility.

b. Based on the quantity and characteristics of pollutants discharged, methods of disposal, and Site conditions, the Department may require the applicant to provide:
   i. A description of the surface and subsurface geology, including a description of all borings;
   ii. The location of any perennial, intermittent, or ephemeral surface water bodies;
   iii. The characteristics of the aquifer and geologic units with limited permeability, including depth, hydraulic conductivity, and transmissivity;
   iv. The rate, volume, and direction of surface water and groundwater flow, including hydrographs, if available, and equipotential maps;
   v. The precise location or estimate of the location of the 100-year flood plain and an assessment of the 100-year flood surface flow and potential impacts on the facility;
   vi. Documentation of the existing quality of the water in the aquifers underlying the Site, including, where available, the method of analysis, quality assurance (QA), and quality control (QC) procedures associated with the documentation;
   vii. Documentation of the extent and degree of any known soil contamination at the Site;
   viii. An assessment of the potential of the discharge to cause the leaching of pollutants from surface soils or vadose materials;
   ix. For an underground water storage facility, an assessment of the potential of the discharge to cause the leaching of pollutants from surface soils, or vadose materials, or cause the migration of contaminated groundwater. (Not applicable to the PTF).
   x. Any changes in the water quality expected because of the discharge;
   xi. A description of any expected changes in the elevation or flow directions of the groundwater expected to be caused by the facility;
   xii. A map of the facility's DIA; or
   xiii. The criteria and methodologies used to determine the DIA.

Of the hydrologic study requirements outlined above, items A.A.C. R18-9-A202A.8.a.i, 8.b.i-iv, and 8.b.x-xiii are addressed in this Attachment. Item 8.a.ii is described in detail in Attachment 12, *Compliance with Aquifer Water Quality Standards*. Item 8.b.ix is not applicable to the present application, and items 8.b.v-viii are described in Attachment 14B, *Hydrologic Study Part B*. Table 14A-1 includes a directory of the requirements outlined in A.A.C. R18-9-A202.A.8, and where each are addressed in this application.

14A.1.1 Background

Curis Resources (Arizona) Inc. (Curis Arizona) has proposed development of a small, pilot-scale test facility referred to as the PTF located on undeveloped desert land 2.5 miles from the business district of the Town of Florence, Pinal County, Arizona (Figure 14A-1). The proposed PTF will be constructed on State land within an Arizona State Mineral Lease held by Curis Arizona that is fully encompassed by property owned by Curis Arizona. The proposed facility will be constructed on portions of Section 28 of Township 4 South, Range 9 East, of the Gila River Baseline and Meridian.

The proposed PTF consists of a small number of test injection and recovery wells that will be used to dissolve copper bearing minerals within the ore body, and to recover the copper in solution. The injection wells will be used to inject a sulfuric acid-based lixiviant solution that will dissolve copper oxide minerals, liberating the copper into solution. The copper laden solution, referred to as pregnant leach solution (PLS), will be recovered from the formation by a closely-spaced array of recovery wells. The copper will be extracted from the PLS by solvent extraction/electrowinning (SX/EW). A schematic of the PTF well field is shown in Figure 14A-2.

The anticipated injection rate is expected to be approximately 240 gallons per minute (gpm), and the extraction is expected to be approximately 300 gpm. At completion of the PTF injection and recovery process, the ore body will be rinsed with native groundwater until permit closure conditions are met. The PTF and SX/EW plant are described in greater detail in Attachments 2 and 9. Chemistry of the lixiviant and PLS solutions are described in detail in Attachment 10, Characterization of Discharge.

This Attachment documents the development and calibration of, and predictive simulations produced from, a sub-regional scale computer-based groundwater flow model that includes the proposed PTF site and approximately 124 square miles around the proposed PTF.

14A.2 Study Area Setting

14A.2.1 Physiography

The PTF site is located within the Sonoran Desert portion of the Basin and Range Physiographic province, which is characterized by gently sloping alluvial valleys separated by north-northwest trending fault block mountain ranges. The PTF site is located on relatively flat land within an unnamed alluvial basin between the Santan and Tortilla Mountains that straddles the boundary between the Eloy sub-basin of the Upper Gila Watershed (Eloy sub-basin) and the East Salt River Valley (ESRV). The PTF site is located a few miles to the south of this boundary, within the Eloy sub-basin.

The Eloy sub-basin is a hydrographic basin bounded on the east by the Tortilla and Tortolita Mountains, on the south by a topographic divide at the margin of the Aguirre Valley, to the west by a groundwater divide to the west of Casa Grande, and on the north by the Santan Mountains and a topographic divide at the margin of the ESRV. The study area includes an area of approximately 124 square miles located at the northern margin of the Eloy sub-basin. The study area straddles the Eloy-ESRV topographic divide and covers less than 10 percent of the greater Eloy sub-basin.

The PTF site is located on undeveloped desert land approximately 0.6 mile north of the Gila River, which drains the Eloy sub-basin. Ground surface at the PTF site generally slopes southward toward the Gila River and has ground surface elevations ranging between approximately 1,470 and 1,490 feet above mean sea level (amsl).

14A.2.2 Climate

The climate in the vicinity of the proposed PTF site is typical of an arid to semi-arid desert region with low precipitation, low humidity, and high summer temperatures. Temperatures often exceed 100 degrees Fahrenheit (°F) during summer months and seldom fall below freezing during the winter. Precipitation is seasonal and bimodal with winter rainfall resulting from cold fronts originating over the Pacific Ocean occurring from December through March; and summer precipitation resulting from convection of moist air originating over the Gulf of Mexico and Gulf of California occurring from July through September.

Precipitation is generally lower intensity, longer duration in the winter and higher intensity, lower duration in the summer. Mean relative humidity ranges from 19 percent in the winter to 65 percent in the summer (Montgomery and Harshbarger, 1989). Average annual precipitation is 10.3 inches (National Oceanic and Atmospheric Administration [NOAA], 2010). Histograms showing monthly mean precipitation and annual precipitation totals for the period 1931 to 2008 are shown on Figures 14A-3 and 14A-4, respectively.

Evaporation exceeds precipitation in the region, consequently little recharge is received from direct infiltration of precipitation. Estimated potential evaporation is approximately 65 inches (Montgomery and Harshbarger, 1989). The combined effects of evaporation and transpiration (evapotranspiration) are discussed in more detail in Section 14A.3.

14A.2.3 Surface Water

The study area is drained by the Gila River which lies approximately 0.6 mile south of the proposed PTF. The Gila River is a regionally extensive river that originates at headwaters in southwestern New Mexico. The Gila River is the principal surface water feature in the vicinity of the PTF site and traverses the central portion of the 124 square mile study area.

Coolidge Dam is located approximately 55 miles to the east of the PTF site and has regulated Gila River flow in the vicinity of the PTF site since it was completed in 1928. The San Pedro River flows into the Gila River below Coolidge Dam and is the primary source of unregulated flow in the Gila River. Most surface water flowing in the Gila River upstream of the PTF site is diverted into the Florence-Casa Grande Canal at the Ashurst-Hayden Diversion Dam. In the vicinity of the PTF site, the Gila River flows from northeast to southwest and is dry most of the year, except during extended periods of local precipitation and runoff. A hydrograph of historic monthly mean Gila River flows measured at Kelvin, Arizona, located 26 miles east of and hydrographically above the PTF site, is included in Figure 14A-5. The Gila River system and the various irrigation projects that receive water from it are described in greater detail in Brown and Caldwell (1996a).

Besides the Gila River, there are no other significant naturally occurring perennial or ephemeral surface water bodies within the PTF model study area.

14A.2.4 Land and Water Use

The PTF model domain covers an area of approximately 124 square miles or approximately 79,350 acres. Within this area, principal land uses include agricultural, urban, industrial, and undeveloped desert. Approximately 24,500 acres (31 percent of the study area) are currently, or historically have been, under cultivation. Urban areas account for approximately 5,700 acres or slightly more than 7 percent of the PTF model study area. Industrial land uses include primarily aggregate mining operations covering approximately 1,400 acres, less than two percent of the PTF model study area. Undeveloped desert lands account for the majority of the PTF model study area, covering an area of approximately 47,750 acres or 60 percent of the study area. The PTF well field is approximately 4.5 acres in size. Land use within the PTF model study area is shown on Figure 14A-6.

Agricultural land uses account for the largest proportion of developed land use and water use with the PTF model domain. Both surface water and groundwater are used to irrigate fields growing a wide variety of food and fiber crops. Urban water uses within the study area rely solely on groundwater and include residential and public space irrigation, domestic uses, and other incidental uses. Industrial water use within the study area also relies solely on groundwater and consists primarily of material washing at aggregate mines. Anthropogenic water use in the undeveloped desert areas within the PTF model study area is insignificant in magnitude.

Groundwater pumping was not segregated by water use during development of the current PTF groundwater flow model. The groundwater pumping rates used in the model were obtained from the Arizona Department of Water Resources (ADWR), and are described in detail in Section 14A.4.7.

14A.3 Hydrogeology and Conceptual Model

14A.3.1 Previous Studies

Portions of the PTF model study area have been the subject of numerous geologic and hydrologic studies since the 1950s, when the potential for copper oxide mineralization was identified in the vicinity of Poston Butte. Previous studies described herein are limited to relevant hydrologic and groundwater modeling studies covering all or portions of the PTF model study area:

- Brown and Caldwell, 1996a. Magma Florence In-Situ Project Aquifer Protection Permit Application, Volume II of V, Site Characterization Report.
- Brown and Caldwell, 1996b. Magma Florence In-Situ Project Aquifer Protection Permit Application, Volume IV of V, Modeling Report.
- ADWR, 1990. Pinal Active Management Area Regional Groundwater Flow Model.
- ADWR, 1994. Salt River Valley Regional Groundwater Flow Model.

Brown and Caldwell (1996a)

Magma Copper Company (Magma) originally proposed production of cathode copper at the site by using combined in-situ copper recovery (ISCR) and SX/EW in the mid 1990s. Magma retained Brown and Caldwell to perform hydrologic and geochemical studies in support of applications for the required environmental and operational permits from State and Federal agencies. Brown and Caldwell (1996a) summarized geologic and hydrogeologic characteristics of the proposed ISCR site, associated property, and the surrounding vicinity using existing published and unpublished data and data generated during site-specific investigations.

Site-specific investigations performed in support of Brown and Caldwell (1996a) included, but were not limited to:

- Assessment of bedrock properties based on lithologic logs of approximately 700 coreholes drilled into the ore body and the surrounding vicinity.
- Analysis of lithologic and hydrologic data collected from 52 boreholes drilled at the site and surrounding vicinity in 1994 and 1995 to depths ranging from 240 to 1,580 feet.
- Downhole geophysical logging of 16,340 linear feet of boreholes drilled in 1994 and 1995.
- Construction data, water quality data, and water level data available from eighteen monitoring wells constructed in six clusters in and around the ore body.
- Twenty-six aquifer tests conducted at test well and monitoring well clusters at the site and surrounding vicinity.
- Fourteen hydraulic (packer) tests conducted in open boreholes.

The aquifer parameters and hydrostratigraphic unit descriptions developed from data collected in support of Brown and Caldwell (1996a) were used to support the creation of a sub-regional groundwater flow model described in Brown and Caldwell (1996b). These data remain the best available data describing hydrogeologic characteristics at the PTF site and surrounding vicinity. No significant additional hydrogeologic characterization activities have been conducted at the PTF site and surrounding vicinity since the Brown and Caldwell (1996a) study was completed. Data developed in support of Brown and Caldwell (1996a) were used as direct input into the current PTF groundwater flow model described in this report. Hydrostratigraphic unit descriptions presented in Brown and Caldwell (1996a) serve as the conceptual basis for hydrostratigraphic units represented in the PTF groundwater flow model described herein.

Brown and Caldwell (1996b)

Following the hydrogeologic characterization of the PTF site and surrounding vicinity described in Brown and Caldwell (1996a), Brown and Caldwell prepared a sub-regional numerical groundwater flow model for the purpose of simulating the potential effects of ISCR activities on the regional alluvial aquifer. The flow field represented in the 1996 groundwater model was developed using the MODFLOW (McDonald and Harbaugh, 1988) computer code, and particle tracking simulations were performed using PATH 3D (Zheng, 1989).

The 1996 groundwater flow model included a domain that covered approximately 100 square miles, centered roughly on the PTF site and surrounding vicinity. The model grid used a 1,000-foot by 1,000-foot cell size at the periphery of the domain and reduced to a cell size of 50 feet by 50 feet at the center of the domain at the PTF site, and was divided into eight layers corresponding to the various hydrostratigraphic units.

Model inputs included temporal head, recharge, and pumping inputs, and used a one year calibration period. The groundwater flow model drew heavily from the site-specific hydrogeologic data reported in Brown and Caldwell (1996a) and data available from ADWR.

Advances in groundwater modeling software, modeling techniques, and changing groundwater conditions at the PTF site have necessitated the development of the current PTF groundwater model described herein as a replacement for the groundwater model described in Brown and Caldwell (1996b). However, the Brown and Caldwell (1996b) groundwater model provided the basic framework for the current model with minor adjustments to the PTF model domain and a revision of the model layering to reflect the full body of geologic data currently available.

Hydraulic parameters used as inputs to the Brown and Caldwell (1996b) groundwater flow model were developed and reported in the Brown and Caldwell (1996a) Site Characterization Report, which also serves as the primary source for hydrologic properties used in the current groundwater flow model. Other inputs used in the 1996 groundwater model such as General Head Boundaries (GHBs), temporal head distributions, recharge values, and groundwater pumping were not carried forward to the current model because a greater temporal range of detailed data are now available from ADWR.

ADWR, 1990

In 1990, ADWR released a numerical groundwater flow model for the Pinal Active Management Area (AMA) which covers an area of approximately 4,100 square miles located within portions of Pinal, Pima, and Maricopa Counties and includes the PTF site. The Pinal AMA groundwater model was developed using the MODFLOW (McDonald and Harbaugh, 1988) computer code and had a model domain equivalent to the approximate 4,100 square mile AMA area. ADWR developed this model for the purpose of developing a groundwater management tool that would be useful in predicting future groundwater conditions within the AMA. The Brown and Caldwell (1996b) and the current PTF groundwater flow models cover a domain that is less than 2 percent of the 1990 Pinal AMA groundwater flow model.

The original Pinal AMA model used two layers to represent the three hydrogeologic units generally recognized to extend throughout the AMA. The hydrogeologic units are the Upper Alluvial Unit (UAU), the Middle Silt and Clay Unit (MSCU), and the Lower Conglomerate Unit (LCU). The layer thicknesses were defined using more than 2,000 driller's logs; however, the actual thicknesses of the MSCU and LCU are not represented in the model. The 1990 Pinal AMA model grid used a uniform cell size of one square mile roughly oriented to correspond with the Township-Range-Section grid.

The hydrogeologic units used in the 1990 Pinal AMA model and their associated properties roughly correspond to the hydrogeologic units used in the 1996 groundwater model prepared by Brown and Caldwell (1996b). The Brown and Caldwell model used hydrogeologic unit names and descriptions reported in Brown and Caldwell (1996a), namely; the Upper Basin Fill Unit (UBFU), Middle Fine Grained Unit (MFGU), and Lower Basin Fill Unit (LBFU). However, the UBFU corresponds with the UAU, the MFGU corresponds with the MSCU and the LBFU corresponds with the LCU. The hydrogeologic unit names and descriptions used in Brown and Caldwell (1996b) are used in the current PTF groundwater flow model.

Although the 1990 Pinal AMA model grid discretization and layering are too coarse to provide the localized high resolution required for the present modeling effort, the extensive published datasets associated with the model have been a valuable resource in constructing and calibrating the current PTF groundwater flow model.

ADWR is currently in the process of redeveloping and refining the Pinal AMA groundwater flow model to represent expanded pumping and recharge datasets, a refined understanding of the basin and sub-basin morphology, and more refined hydrographic boundaries at the downstream edge of the model. The revised model was planned to be completed in 2010, however it had not yet been made available at the time of this publication. However, ADWR graciously made several of the updated Pinal AMA model input datasets available to Brown and Caldwell on a provisional basis in support of development of the current PTF groundwater flow model. Provisional updated Pinal AMA groundwater model datasets made available by ADWR for use in the current model are described in Section 14A.4.7.

ADWR, 1994

In 1994, ADWR released a computer model that represented the groundwater flow regime of the Salt River Valley (SRV). The SRV is an extensive and complex groundwater basin that includes seven sub-basins and the confluence of four rivers that together drain more than 50 percent of the State. The domain of the 1994 SRV model covers only about 2,500 square miles and does not include the entire SRV, but focuses on the most significant hydrologic features of the valley for the purpose of developing a groundwater management tool. ADWR is currently in the process of updating the SRV model and expanding the model domain, however the results of that effort are not yet available.

Similar to the 1990 Pinal AMA model, the 1994 SRV model used a cell size of one square mile, but differed in that it used three layers to represent the three principal hydrogeologic units within the basin. The layers were designed to discretely represent the three principal hydrogeologic units occurring within the SRV, which units generally correspond to those described in the 1990 Pinal AMA groundwater flow model. The SRV layers include the UAU, Middle Alluvial Unit (MAU), and Lower Alluvial Unit (LAU).

The domain of the 1996 (Brown and Caldwell, 1996b) and the current (2010) PTF sub-regional groundwater flow model lies primarily within the domain of the Pinal AMA groundwater model. However, because the PTF site location is very near the boundary between the Pinal AMA and the Phoenix AMA, a small portion of the PTF model domain lies within the domain of the SRV model. Approximately 20 percent of the PTF model domain lies within the domain of the 1994 SRV model, an area located at the extreme southeast corner of the SRV model domain that represents less than one percent of the entire SRV model domain.

Recognizing that the current PTF groundwater flow model has less than 20 percent of its domain in common with the SRV model, the SRV model construction details such as grid discretization, layering, and boundary conditions were not incorporated in the current modeling effort. However, datasets from the SRV model that were useful in construction and calibration of the current (2010) PTF groundwater model included updated geology and temporal head distributions. Input datasets for the current PTF groundwater model are described in Section 14A.4.

14A.3.2 Regional Geology and Hydrostratigraphy

14A.3.2.1 Structural Geology

The PTF site is located within the Sonoran Desert portion of the Basin and Range Physiographic Province. The Basin and Range Province is defined by the residual effects of extensional forces that stretched the earth's crust throughout western North America, resulting in a series of pull-apart physiographic features that include alternating elongated mountain ranges separated by alluvial basins bounded by normal faults. The basins and ranges are the surface expression of alternating down-thrown blocks of crust (grabens) lying between crustal blocks that remain elevated (horsts) relative to the surrounding terrain.

The Basin and Range Orogeny, an extensional event, was the last major orogenic event to affect the Western United States and occurred from the early Miocene to the Pleistocene (17-5 Ma). Tectonic processes associated with the Basin and Range Orogeny exposed metamorphic core complexes and resulted in igneous activity that included batholith, stock and dike emplacement, and volcanism (Nason and others, 1982).

Basin and Range faulting resulted in partial to complete erosion of older Oligocene to Miocene sediments. Consequently, as much as 4,000 feet of basin-fill has been deposited in the resulting Tertiary alluvial fan and lake bed environments. Figure 14A-7 shows a bedrock surface of the PTF site and limited surrounding vicinity based on well log and corehole data.

Basin and Range faulting and tilting in the vicinity of the PTF resulted in north-northwest trending horst and graben structures bounded by normal faults with large displacements to the west (Nason and others, 1982). The ore body associated with the PTF occurs on a complex horst block which is bounded on the east and west by grabens. The Party Line Fault, a major normal fault on the east side of the ore body, strikes north 35 degrees west and dips 45 to 55 degrees southwest. This fault is reported to have a vertical displacement of over 1,000 feet (Conoco, 1976; Nason and others, 1982). Field studies (Brown and Caldwell, 1996a) have shown that intense fracturing in the vicinity of the fault zone has resulted in elevated hydraulic conductivity parallel to the fault. A series of en-echelon normal faults striking north-south to northwest occur west of the Party Line Fault, which form the transition to the graben structure west of the proposed PTF well field.

The Sidewinder Fault occurs near the west side of the proposed PTF well field and has a displacement of more than 1,200 feet (Conoco, 1976), and represents a continuation of a complex of northwest-southeast trending normal faults east of the PTF site. Field studies (Brown and Caldwell, 1996a) have shown that intense fracturing in the vicinity of the fault zone has resulted in elevated hydraulic conductivity. Additionally, an east-west trending fault system has truncated the south end of the horst, causing bedrock elevations south of the Gila River to drop away by more than 1,500 feet (Conoco, 1976). Additional en-echelon, north to northwest trending normal faults located east of the Sidewinder Fault form the transition to another graben structure east of the PTF site, which strikes north to northwest.

Following the Basin and Range Orogeny, alluvial basin-fill sediments were deposited over the Precambrian bedrock surface in the vicinity of the PTF site. The sediments consist of unconsolidated to moderately well-consolidated interbedded clay, silt, sand, and gravel in variable proportions and thicknesses. Interbedded basalt flows were emplaced during basin fill deposition to the west and northwest of the proposed PTF well field. Total thickness of basin-fill materials in the vicinity of the property ranges from 300 to over 900 feet, and exceeds 2,000 feet at a distance of 1.5 miles southwest of the proposed PTF well field.

14A.3.2.2 Hydrostratigraphy

The saturated geologic formations underlying the PTF site have been divided into three distinct water bearing hydrostratigraphic units referred to as the UBFU, LBFU, and the Bedrock Oxide Unit. Although locally productive, the Bedrock Oxide Unit is considered to be hydrologic bedrock by the ADWR (1989). The UBFU and LBFU are separated by a thin regionally extensive aquitard referred to as the MFGU. Each of these units generally corresponds to regionally extensive hydrostratigraphic units described by ADWR (1989). Generalized cross sections depicting the distribution and thickness of the hydrostratigraphic units are shown on Figures 14A-8 and 14A-9. Recent water levels (2008) within the PTF model domain are shown on Figure 14A-10.

The geologic and hydrologic characteristics of these units have been defined by a series of studies conducted by previous companies associated with the PTF site including Conoco, Magma, and BHP Copper.

Conoco began hydrologic characterization of the ore body in 1971 in order to determine the dewatering requirements for a planned underground mine, and later an open pit mine to be developed at the PTF site. Between 1973 and 1976, Conoco conducted a total of 34 aquifer (pumping) tests that included tests conducted in individual water bearing units and various combinations of the LBFU and Bedrock Oxide Units. No aquifer tests were conducted in the period between 1976 and 1992, when Magma began hydrologic characterization for the purpose of completing a pre-feasibility study.

Magma purchased the PTF site and surrounding vicinity from Conoco in 1992, and initiated an intensive hydrologic characterization program that included a series of 49 pumping tests conducted at 17 locations at the PTF site and surrounding vicinity. The tests, conducted by Brown and Caldwell, included 17 pumping wells and 46 monitoring wells screened within the various water bearing units. Eight wells were completed within the UBFU, 17 within the LBFU, and 38 wells within the Bedrock Oxide Unit including the hanging wall and footwall zones of the major faults. Each of the pumping tests was conducted at pumping rates of at least 0.25 gpm per foot of screen. After completion of the pumping tests, Golder Associates (Golder, 1995) analyzed the pump test data to derive hydrologic parameter values describing each of the water bearing units. The values derived by Golder Associates for each of the water bearing units confirmed, and expanded on, those derived by Conoco. A copy of the 1995 Golder Associates report is submitted as Exhibit 14A-1.

In January 1996, BHP Copper acquired Magma and the PTF site and surrounding vicinity, and continued hydrologic characterization of the associated ore body. BHP Copper did not conduct any additional aquifer tests. However, in order to further characterize hydrologic properties of the ore body, BHP Copper installed a pilot five-spot ISCR well pattern with adjacent, perimeter, and observation wells for the purpose of conducting a commercial-scale pilot test to demonstrate the feasibility of establishing and maintaining hydraulic control. No additional hydrologic characterization activities were completed between the conclusion of the BHP Copper pilot test in 1998 and the purchase of the PTF site and surrounding vicinity by Curis Arizona.

Curis Arizona acquired the PTF site and surrounding vicinity in the first quarter of 2010. The only hydrologic characterization activities conducted by Curis Arizona since their acquisition of the site have been laboratory testing of two samples of MFGU sediments to determine hydraulic conductivity. The results of those tests are described below. The laboratory reports for those analyses are included as Exhibit 14A-2.

The range of hydraulic conductivity values measured for each of the water bearing units are shown on Figure 14A-11. Hydraulic conductivity values plotted on Figure 14A-11 include values derived from tests of individual water bearing units conducted by Conoco and Magma. Hydraulic conductivity values derived from tests that included multiple water bearing units were excluded from Figure 14A-11.

No vadose zone characterization activities have been conducted since 1995 when BHP completed site characterization. Vadose zone characterization activities performed in support of the BHP site characterization are described in Section 2.3.1, Volume II, of that application. A copy of Section 2.3.1, Volume II of the 1996 APP application is included as Exhibit 14A-3.

14A.3.2.2.1 Upper Basin Fill Unit (UBFU)

The UBFU is locally overlain by recent alluvial floodplain sediments emplaced by the Gila River and tributary washes in the vicinity of the PTF site. The recent alluvium is unsaturated, and consists of unconsolidated silt, sand, gravel, and boulders that locally overlie the basin fill deposits of the UBFU. The width of recent alluvium emplacement is approximately one mile on either side of the Gila River. The thickness of the recent alluvium at the PTF site ranges from zero near the bedrock outcrops to approximately 60 feet at the Gila River (Brown and Caldwell, 1996a).

The UBFU consists primarily of unconsolidated to slightly consolidated sands and gravel, with lenses of finer-grained material and ranges in thickness between 50 feet near mountain fronts to approximately 1,200 feet in the basin center. The thickness of the corollary unit within the ESRV Sub-basin is typically between 100 and 200 feet (ADWR, 1993). The UBFU is estimated to range between 200 and 220 feet in thickness within the proposed PTF well field.

The upper portion of the UBFU is not saturated and forms the lower vadose zone, which extends to depths ranging from 100 to 150 feet below ground surface (bgs). The upper portions of the unit are generally fine-grained and calcareous, consisting of a gradational succession of poorly graded, moist silt and sand with minor gravel. The lower portions are generally coarser-grained, with gravel interbeds common at depth. Although more cohesive than the overlying recent alluvium, the UBFU is generally described as unconsolidated (Brown and Caldwell, 1996a).

The UBFU is primarily unconfined with locally confined conditions apparent in portions of the Eloy sub-basin (ADWR, 1989). However, unconfined conditions prevail within the UBFU in the proposed PTF well field. Hydraulic conductivity within the UBFU in the study area ranges from 20 to 130 feet per day and specific yield ranges from approximately 13 to 20 percent (ADWR, 2010).

Based on 2011 groundwater level measurements, the saturated portion of the UBFU within the proposed PTF well field is estimated to be between approximately 275 and 295 feet thick. Depth to groundwater measurements at proposed POC wells completed in the UBFU are provided in Attachment 14B Table 14B-2.

14A.3.2.2.2 Middle Fine Grained Unit (MFGU)

The MFGU underlies the UBFU along a very gently sloping contact that is interpreted to be an unconformity, based on a basin-wide shift in lithofacies. The unit is generally 20 to 30 feet thick at the proposed ISCR site but increases to a maximum thickness of about 55 feet at the southwest corner of the site. The unit is nearly continuous, although it may pinch out or grade to coarser-grained materials in some locations (Brown and Caldwell, 1996a).

Locally, the MFGU ranges from calcareous clay to silty sand, and includes desiccation cracks, reworked broken clay clasts, carbonaceous film, and thin interbeds of fine sand or pebbles up to 1-inch thick. In places, the unit is massive with no detectable internal structure. It is generally calcareous and may be associated with thin zones of caliche. The base of the unit slopes very gently (one to two percent) to the southwest and is generally marked by a change from silty sand to gravel. In light of the numerous faults that are known to affect the bedrock at the in-situ mine site, the relatively flat-lying base of the MFGU is an indication that faulting ceased prior to the deposition of this unit (Brown and Caldwell, 1996a).

The MFGU in the Eloy sub-basin ranges in thickness from less than 50 feet near the sub-basin margins to greater than 6,500 feet in the sub-basin center, and can be locally productive if the well penetrates a sand and gravel lens within the unit; however well productivity in the MFGU is otherwise limited (ADWR, 1989).

No aquifer tests have been conducted within the MFGU. The MFGU is too thin and exhibits a hydraulic conductivity that is too low to support aquifer pumping tests. The thinness of the MFGU also precludes reliable construction of test wells that might be used to perform slug tests. For this reason, Magma Copper

Company, a previous owner of the site and surrounding vicinity elected to collect a sample from bore hole M16-GU for laboratory analysis to determine hydraulic properties of the MFGU. Curis Arizona recently collected two additional MFGU samples from core hole CMP-11-03, which was drilled in August of 2011. The laboratory hydraulic conductivity values determined for these samples are listed in Table 14A-2.

Copies of the original laboratory reports for each of the samples listed in Table 14A-2 are included herewith as Exhibit 14A-2.

The depth, thickness, and extent of the MFGU within the PTF well field, as determined from core hole logs, is shown on detailed cross sections included in Attachment 14C as Figures 14C-48 through 14C-51.

14A.3.2.2.3 Lower Basin fill Unit (LBFU)

The LBFU underlies the MFGU at the proposed PTF site and comprises the lower portion of the sedimentary fill overlying Precambrian bedrock. The MFGU-LBFU contact at the proposed PTF site ranges in depth from 260 to 300 feet bgs. The thickest deposits of LBFU occur west of the proposed PTF well field, along the east flank of a graben structure. The increased thickness is the result of faulting, subsidence, and lithostatic loading of the basin. The thinnest deposits overlie a 400- to 500-foot wide bedrock ridge west of the proposed PTF well field. Beneath the eastern portion of the PTF site, the thickness of the LBFU generally ranges from about 30 to 80 feet.

The LBFU consists of coarse gravel, fanglomerate, conglomerate, and breccia, and is distinguished by a greater degree of consolidation than is exhibited by the UBFU. Lithologically, clasts appear similar to the overlying UBFU, with the exception of the occurrence of bedrock derived gravel conglomerate, immediately above the bedrock contact that is locally well-lithified. The conglomerate portion of the LBFU may correlate with the Gila and Whitetail Conglomerates described in the region (Conoco, 1976).

Where overlain by the MFGU, the LBFU typically exhibits confined or semi-confined characteristics (ADWR, 1989). Hydraulic conductivity within the LBFU ranges from 5 to 25 feet per day and specific storage is approximately 1e-5 ft-1 (ADWR, 2010). Hydraulic conductivity for the LBFU calculated by Montgomery (1994) was approximately 93.0 ft/day. Aquifer parameters reported for the Gila Conglomerate include transmissivities reported by Halpenny (1976) that range from 113,000 to 233,000 gallons per day per foot (gpd/ft). Studies performed by Halpenny and Green (1972) suggest that a transmissivity value of 125,000 gpd/ft is a reasonable mean value.

Beneath the proposed PTF well field, the LBFU is fully saturated and exhibits confined to semi-confined characteristics. As noted on the cross sections submitted in Attachment 14C (Figures 14C-48 through 14C-51), the water levels in the LBFU are measured at points well above the top of that unit. Aquifer tests conducted at the PTF site, and measured groundwater elevations, have demonstrated that the LBFU and Bedrock Oxide Unit are in hydrologic communication with one another. Depth to groundwater measurements for proposed POC wells completed in the LBFU are included in Attachment 14B, Table 14B-2.

14A.3.2.2.4 Oxide Bedrock Zone

Bedrock underlying the LBFU in the proposed PTF well field consists primarily of Precambrian quartz monzonite and Tertiary granodiorite porphyry. Based on the copper mineral assemblage, the bedrock is divided into an upper oxide zone and lower sulfide zone. The oxide bedrock zone is estimated to range in thickness from approximately 200 feet to over 1,500 feet (Brown and Caldwell, 1996a). The depth and extent of the Oxide Bedrock Zone beneath the PTF well field is shown on the generalized geologic cross sections in Figures 14A-8 and 14A-9.

The top of the oxide bedrock zone consists of a weathered rubbly mixture of fracture filling and angular bedrock fragments, and is expected to be a zone of enhanced hydraulic conductivity. On available well logs, this zone is included with the LBFU in some locations as it is difficult to distinguish in-place weathering products from overlying colluvial materials. Below this weathered zone, the oxide consists of extensively fractured quartz monzonite, granodiorite, and associated dikes. Movement of groundwater through the oxide bedrock zone is expected to be largely controlled by secondary permeability resulting from faults, fractures, and associated brecciation.

Fracture intensity is greatest near the Party Line and Sidewinder faults, and decreases further away from these features. The Party Line fault post-dates mineralization and partially bounds mineralization in the eastern portion of the ore body. A vertical displacement of approximately 1,000 feet has been estimated on the Party Line fault. The Sidewinder fault occurs in the western portion of the in-situ mine site and exhibits an estimated 1,200 feet of vertical displacement. Rubblization and subsequent erosion associated with the Sidewinder fault has resulted in a bedrock trough that underlies the western portion of the PTF site.

Hydraulic conductivity within the oxide bedrock zone ranges from 0.1 to 2.51 ft/day and specific storage ranges from 5e-6 to 1e-5 ft-1 (Brown and Caldwell, 1996a). Transmissivity within the oxide bedrock zone in the vicinity of the PTF site has been estimated to range from 10,000 to 12,000 gpd/ft (Halpenny and Green, 1972).

Beneath the proposed PTF well field, the Bedrock Oxide Unit is fully saturated and exhibits confined to semi-confined characteristics. As noted on the cross sections submitted in Attachment 14C (Figures 14C-48 through 14C-51), the water levels measured in wells completed in the Bedrock Oxide Unit are observed at points well above the top of that unit. Due to the low hydraulic conductivity of the Sulfide Unit, there is no demonstrable hydraulic connection between it and the Bedrock Oxide Unit.

14A.3.2.2.5 Hydrologic Bedrock

The oxide bedrock zone is underlain locally by a zone of sulfide mineralization that occurs in the same quartz monzonite and granodiorite rocks that compose the oxide zone, and is of unknown lateral and vertical extent. The fracture frequency and resulting permeability of the fracture network within the sulfide zone is significantly less than that observed in the overlying oxide zone.

The Sulfide Unit is a bedrock unit that underlies the Bedrock Oxide Unit, and is distinguished from that unit by differences in mineralogical composition. In addition to having a different mineralogical composition than the Bedrock Oxide Unit, the Sulfide Unit is substantially less fractured, and consequently has a much lower hydraulic conductivity. Pumping and injection tests conducted in 1995 included tests conducted in wells constructed in the Sulfide Unit. During these tests, it was observed that the Sulfide Unit wells dewatered quickly and did not recover within a timeframe that allowed meaningful analysis of test data. For this reason, slug tests were conducted in the Sulfide Unit wells which produced hydraulic conductivity values between one and three orders of magnitude lower than those measured in the Bedrock Oxide Unit. Sulfide bedrock hydraulic conductivity values, developed by Brown and Caldwell (1996a), ranged from 0.0055 to 0.05 ft/day.

Within the broader study area, hydrologic bedrock consists primarily of Precambrian granite, gneiss, and schist with Mesozoic granite and related crystalline intrusive rocks, volcanic flows, sedimentary and metamorphic rocks and is assumed to be impermeable (ADWR, 1989). In the context of defining regional groundwater resources, the sulfide bedrock zone does not yield appreciable quantities of water (ADWR, 1989). Local areas of intense fracturing may yield groundwater from the bedrock complex; however; previous ADWR groundwater models (ADWR, 1990 and 1994) have assumed all bedrock (including the oxide bedrock zone) within the study area is impermeable. No flow bedrock areas are shown on Figure 14A-10.

14A.3.3 Regional Hydrogeologic System

The Eloy sub-basin is a structurally controlled hydrographic basin in the middle reach of the upper Gila River watershed that is bounded by topographic divides on the north, east, and south and by a groundwater divide on the west. The Eloy sub-basin represents a series of graben structures that have been overlain with basin fill sediments shed from the surrounding mountains. The basin fill sediments extend in depth to more than 4,000 feet at the center of the sub-basin and are generally water bearing in the uppermost 1,800 feet of thickness, with the exception of a series of fine grained deposits that extend nearly basin wide. The ephemeral Gila River is a losing stream within the Eloy sub-basin and also drains the sub-basin.

In the eastern portion of the Eloy sub-basin, and the eastern portion of the PTF model domain, groundwater flow generally follows the course of the Gila River but turns north-northwest in the vicinity of the Town of Florence and the PTF site.

The PTF model study area lies principally within the Eloy sub-basin. Groundwater inflows and outflows of the Eloy sub-basin that pertain to the domain of the PTF groundwater model are described below.

14A.3.3.1 Inflows

14A.3.3.1.1 Surface Water Flow and Groundwater Subflow

The Gila River is an ephemeral losing stream within the PTF model domain and is the principal source of groundwater recharge in the region. The flow control and diversion structures located on the Gila River are described in Brown and Caldwell (1996a). Within the study area, there are no other significant ephemeral or perennial surface water bodies that contribute to groundwater recharge. All other drainages within the PTF model domain consist of dry ephemeral washes that are tributaries to the Gila River and only flow during infrequent heavy precipitation events. Surface water infiltration estimates used in the model were compiled by ADWR for the ongoing update of the Pinal AMA groundwater flow model and were provided by ADWR on provisional basis for use in the current PTF groundwater flow model. Estimated surface water infiltration values are discussed in Section 14A.4.7

There is no documented sub-flow associated with the Gila River entering the Eloy sub-basin at the eastern margin of the basin, and no other potential sources of sub-flow exist within the Eloy sub-basin.

14A.3.3.1.2 Gila River Recharge

The Gila River is the primary source of recharge to the alluvial aquifers in the vicinity of the PTF site. Both historical and recent water level records demonstrate that there is a close relationship between the magnitude of flows in the Gila River and local groundwater elevations. This relationship is illustrated by the hydrographs plotted on Figure 14A-12. Figure 14A-12 is a map with hydrographs for Groundwater Site Inventory (GWSI) wells and PTF and surrounding vicinity wells plotted relative to a discharge hydrograph of the Gila River. The hydrographs plotted on Figure 14A-12 clearly show that as Gila River flow increases, groundwater elevations also increase shortly thereafter. As Gila River flows decrease, groundwater pumping causes groundwater elevations to decline. Hydrographs plotted on Figure 14A-12 show that recharge derived from Gila River flows affects groundwater elevations as far as approximately 3.5 miles from the Gila River.

No direct measurements of groundwater recharge derived from Gila River flows are available. The best available quantification of recharge derived from Gila River flow was developed by ADWR in conjunction with the groundwater model the Department developed to simulate groundwater conditions in the Pinal AMA (ADWR, 1990). The recharge array used in this model was directly imported from provisional data files prepared for the update of the Pinal AMA groundwater flow model (ADWR, 1990). These data were made available to Curis Arizona by ADWR on a provisional basis.

14A.3.3.1.3 Mountain Front Recharge

Analyses performed by ADWR (1989) demonstrated that mountain front recharge is negligible within the domain of the Pinal AMA groundwater flow model. Based on provisional data provided by ADWR, the revision of the Pinal AMA groundwater flow model that is currently in progress will validate the earlier ADWR conclusion that there is no significant mountain front recharge within the domain of the Pinal AMA groundwater flow model. Accordingly, the current PTF groundwater flow model does not include mountain front recharge.

14A.3.3.1.4 Canal Leakage

Three irrigation districts serve water to farms within the PTF model study area through a network of unlined canals: New Magma Irrigation and Drainage District, Maricopa Stanfield Irrigation and Drainage District, and the San Carlos Irrigation and Drainage District. Seasonally, canal water is obtained from surface water diversions on the Gila River and from the Central Arizona Project (CAP). When insufficient surface water supplies are available to meet irrigation demand, the irrigation districts pump groundwater into the canal network to meet the demand. The location of these canals within the model domain is shown on Figure 14A-6. Leakage from the unlined canals is a significant source of recharge water within the Eloy sub-basin and the PTF model domain. Canal leakage data used in this model were compiled by ADWR for the ongoing update of the Pinal AMA groundwater flow model and were provided by ADWR on a provisional basis for use in the current PTF groundwater flow model. Canal leakage model input values are discussed in Section 14A.4.7.

14A.3.3.1.5 Permitted Recharge Facilities

There is one permitted Underground Storage Facility (USF) no. 70-431125 within the PTF model study area. The USF is permitted to recharge 135 acre-feet per year (AFY) of reclaimed wastewater generated at the North Florence Wastewater Treatment Plant operated by the Town of Florence. The location of the North Florence recharge facility is shown on Figure 14A-1. Permitted USFs seldom operate at the maximum permitted volume on a continuous basis, and typically are permitted for excess capacity to allow for facility expansion. Based on ADWR records, the Town of Florence groundwater Long-Term Storage Account increased by a total of 73 acre-feet between 2007 and 2010 due to recharge from this facility.

The amount of recharge contributed by the North Florence USF is relatively insignificant compared to the recharge received from the nearby Gila River, which can fluctuate by as much as 10,000 to 100,000 AFY. Consequently recharge from the North Florence USF was not included in the current PTF groundwater flow model.

14A.3.3.1.6 Agricultural Returns

Because much of the agricultural land within the PTF model domain is irrigated by flood (furrow) methods, typical irrigation efficiency is assumed by ADWR to be in the range of 65 to 70 percent, which means that 30 to 35 percent of all water applied to the surface infiltrated beyond the root zone and is recharged to groundwater. Because there is a relatively large volume of irrigation water used within the study area, agricultural returns are a significant source of recharge used in the model. Irrigation return data used in the model were compiled by ADWR for the ongoing update of the Pinal AMA groundwater flow model and were provided by ADWR on a provisional basis for use in the current PTF groundwater flow model. Agricultural return model input values are discussed in Section 14A.4.7.

14A.3.3.2 Outflows

14A.3.3.2.1 Groundwater Pumping

Groundwater pumping is the principal outflow of groundwater within the study area. Pumping for irrigation generally makes up more than half of the groundwater extracted from the aquifer on an annual basis. Groundwater pumping data used in the model were compiled by ADWR for the ongoing update of the Pinal AMA groundwater flow model and were provided by ADWR on a provisional basis for use in the current PTF groundwater flow model. Pumping data from 1984 to 2006 was compiled by ADWR from San Carlos Irrigation Project (SCIP) reports and from the Registry of Groundwater Rights (RoGR) database. Pumping data after 2006 was compiled by Brown and Caldwell from the ADWR wells 55 database, specifically the pump-year data within that database. Annual groundwater extraction within the study area ranges from 21,100 to 73,100 AFY.

14A.3.3.2.2 Evapotranspiration

Evapotranspiration is associated with vegetation along the Gila River. Due to the depth of the water table, evapotranspiration from the aquifer is minimal. Significant evapotranspiration only occurs during flood years when water levels in, and adjacent to, the Gila River channel are higher than the evapotranspiration extinction depth. Evapotranspiration data used in the PTF groundwater flow model were compiled by ADWR for the ongoing update of the Pinal AMA groundwater flow model and were provided by ADWR on a provisional basis for use in the current PTF groundwater flow model. The evapotranspiration rate used by ADWR (1990) is discussed in Section 14A.4.7.

14A.3.3.2.3 Underflow

The PTF model domain does not encompass the entire Eloy sub-basin; consequently, underflow identified by ADWR (2010) does not represent underflow simulated at the perimeter of the PTF study area. Underflow out of the 124 square mile study area is comprised of underflow from the study area toward the south and west into the broader Eloy sub-basin, and underflow northward into the SRV. Estimates of underflow were calculated by examining measured groundwater gradients over time.

14A.3.4 Groundwater Elevations and Gradients

Hammett (1992) reported that prior to about 1900, the groundwater system in the PTF study area was in dynamic equilibrium, with the amount of water entering the groundwater system approximately equal to that extracted, with no appreciable change in storage. During the pre-development period (circa 1900), the general direction of groundwater flow through the PTF study area was from the east-southeast to the west-northwest, with a gradient of 8 or 9 feet per mile (Hammett, 1992).

By the 1980s, the groundwater flow direction and gradient had changed from that observed in the pre-development period (circa 1900) to a more pronounced southeast to northwest pattern, toward areas of greatest groundwater pumping. By the 1980s flows in the Gila River had also been eliminated in all but the wettest years, limiting infiltration of river water into the basin-fill sediments to periods of flooding.

In 1995, Brown and Caldwell (1996a) observed that groundwater flow was generally to the northwest at an approximate gradient of 33 feet per mile in alluvial units in the northern portion of the PTF study area. Montgomery (1994) reported the hydraulic gradient across the proposed PTF well field to range from approximately 25 to 65 feet per mile in the UBFU and LBFU.

Beginning in the fall of 1995, Brown and Caldwell has conducted quarterly water level monitoring at the proposed PTF well field in conjunction with a quarterly groundwater quality monitoring program. Observations resulting from the water level monitoring program are described below.

Seasonal changes in groundwater elevations and flow direction were observed in each of the water producing zones beneath the PTF site. Seasonal fluctuations in groundwater elevations in the LBFU and Oxide Zone have been as great as 20 feet, but typically range between 10 and 15 feet in magnitude. Seasonal fluctuations in groundwater elevations in the UBFU are less pronounced, ranging between 5 and 8 feet.

Hydrographs depicting seasonal groundwater elevation changes at the PTF site during the years 1996 through 2011 are included in Attachment 14C Figures 14C-1 through 14C-31.

Potentiometric surface maps depicting groundwater elevations and flow directions at the PTF site during the years 1996 through 2011 in each of the three water bearing units beneath the PTF site are included in Attachment 14C Figures 14C-32 through 14C-46.

Recent hydrographs depicting groundwater elevations in four key wells located at and near Curis Arizona property are shown on Figure 14A-12. These wells were selected as key wells based on the relatively extensive length of the monitoring record, and the distribution within the active portion of the model domain. The water level data plotted in Figure 14A-12 was obtained from the ADWR GWSI database.

Regional potentiometric maps depicting groundwater elevations and flow directions in the vicinity of the PTF site are included in Attachment 14C Figures 14C-1 through 14C-31. Current (December 2010) groundwater gradients within the PTF study area range between approximately 12 feet per mile in the eastern and southern portions of the study area, to approximately 22 feet per mile in the northern portion of the PTF study area. Groundwater gradients at the site of the proposed PTF well field range between approximately 11 feet per mile in the UBFU and approximately 22 feet per mile in the Bedrock Oxide Unit, with a northwest groundwater flow direction in the UBFU, LBFU, and Oxide Zone.

14A.4 Production Test Facility Groundwater Model

14A.4.1 Production Test Facility Model Development

The conceptual model described above was used as the basis to develop a numerical, three-dimensional (3-D) groundwater flow model that is representative of groundwater flow conditions within the PTF study area. The model development process consisted of the generation of both regional and local scale 3-D geologic models, which were then imported into the groundwater modeling software along with estimates of aquifer hydraulic properties and components of the hydrologic water budget. Once the model was refined and calibrated, it was used to simulate pre-development (or steady state), historic, present day, and predicted future groundwater conditions under a variety of operating and closure scenarios.

This section summarizes model specifications, model development, and the methods and assumptions used for estimating initial numerical model inputs. An overview of the numerical model specifications are presented in Table 14A-3.

14A.4.2 Computer Code Description

The computer code used to simulate both groundwater flow and solute transport was MODFLOW-SURFACT™ (Version 3.0), a modular, finite-difference, 3-D groundwater modeling program based on the U.S. Geological Survey (USGS) code MODFLOW (HydroGeoLogic, Inc., 1996; Harbaugh et al., 2000). MODFLOW-SURFACT™ adds additional features to the MODFLOW code in order to better simulate desaturation/resaturation of aquifers as well as unsaturated flow conditions. MODPATH (Pollock, 1994) was used in conjunction with the results from the groundwater flow model to perform particle tracking simulations, which estimate the travel distances of the recharged water. Groundwater Vistas™ Version 5.48 (Environmental Simulations, Inc. [ESI], 2008) was used as the pre- and post-processor and was coupled with ArcGIS™ (ESRI, 2006) to facilitate the development of input files and analyses of model output. The generation of 2-D gridded and contour data by geostatistical interpolation techniques (i.e., kriging) was performed using the Surfer® software package (Golden Software, Inc., 2008), which produces output that can be imported into the numerical model or geographic information system (GIS).

The transport and migration of sulfate was modeled using the Analysis of Contaminant Transport (ACT) modules, which are fully integrated and consistent with MODFLOW SURFACT™ (HydroGeoLogic, Inc., 1996). These modules are fully integrated with the MODFLOW-SURFACT code and greatly expand the capabilities of traditional MODFLOW-compatible solute transport modules by running simultaneously with the MODFLOW-SURFACT flow solution and allowing for advanced solute fate and transport mechanisms to be considered explicitly within the fully integrated MODFLOW flow solution.

14A.4.2.1 Solution Techniques

MODFLOW-SURFACT™ supports two solution packages: the Preconditioned Conjugate Gradient Version 4 (PCG4); and Version 5 (PCG5). All model simulations presented in this report were generated using the PCG5 package.

14A.4.2.2 Assumptions

MODFLOW uses a finite-difference numerical method for solving a form of the 3-D groundwater flow equation. This technique essentially solves for hydraulic head by discretizing the flow domain into a computational grid composed of orthogonal blocks, with a node located at the center of each block. In general, the finite-difference approximation assumes that all hydraulic parameters, stresses, and inputs are constant over the area of a single cell and over the time elapsed during a stress period. Likewise, calculated hydraulic head and groundwater fluxes are also averaged over the areal extent of a single cell. Using the model for a specific application requires the definition of boundary and initial conditions, estimates of key hydraulic parameters, and groundwater inflows and outflows as a function of time.

14A.4.2.3 Limitations

Numerical solutions using MODFLOW-SURFACT™ are dependent upon the scale of the model grid, the time frame of interest, and the behavior of the various model inputs and boundary conditions. For large-scale applications such as the PTF Model, results may have limited usefulness in investigating groundwater issues with: 1) spatial scales smaller than a single cell or small grouping of cells; and 2) substantially varying groundwater stresses or inputs at a time scale less than a single stress period.

Model cells are sized at 500 feet by 500 feet at the model periphery and telescope down to 12.5 feet by 12.5 feet in size at the model center. At 4.5 acres, the PTF well field represents roughly 1,254 model cells in size. Consequently, the model grid discretization is fine enough to appropriately simulate groundwater conditions at the PTF well field scale and the domain is sufficiently large to ensure that regional and sub-regional factors are considered in those simulations.

Model stress periods vary in length. Input datasets available from ADWR and other sources are typically compiled at annual intervals rather than monthly, weekly, or smaller time increments. Input datasets were kept at one year intervals, and stress periods of various shorter lengths were used to simulate the 23-month active pumping period and portions of the five year post pumping closure period. The model stress periods of one year are sufficient to simulate the impacts of PTF activities five years after closure.

Large water level changes that are basin-wide, or intersect model boundary conditions, have the potential to introduce some error into the model results along basin boundaries due to large numbers of dry cells and losses of groundwater stresses, such as pumping or recharge. However, such large water level changes within the Eloy sub-basin are more likely to occur during predictive scenario time periods based on committed demands and other administrative conditions rather than during the historical, transient time period to which the model was calibrated. No large water level declines and associated loss of stresses were observed in the predictive model runs.

The finite-difference solution technique also assumes that the majority of groundwater flow occurs orthogonal to the cell faces, and error can be introduced into the simulation if significant vertical or oblique-angle flow components are evident within a single layer at a local scale. Extrapolation or interpolation of the model results over large time frames are subject to uncertainties inherent in long-term, transient, predictive model stresses. Such uncertainties arise from differences in population growth and climatic conditions relative to predicted values for related groundwater pumping or recharge parameters.

The use of a finite-difference modeling scheme applies stresses and inputs to the model evenly across a model cell. Likewise, hydraulic parameters are uniform within a model cell, limiting the resolution of the model to the size of the grid. The grid cell spacing for the PTF Model has a minimum 12.5 feet by 12.5 feet, equal to 178,421 cells per square mile. Model results, such as groundwater elevations or drawdown are also averaged across each model cell and may not be appropriate for assessing conditions at a small scale adjacent to major pumping stresses.

14A.4.3 Model Domain

The areal extent of the active PTF groundwater model domain is shown on Figure 14A-10. The domain includes the PTF site and an area that extends at least five miles from the Site in all directions. This domain was chosen because it includes a sufficient portion of the Eloy sub-basin to include key hydrographic features and boundaries affecting the PTF site and the immediate vicinity. The PTF model domain extends from the Santan Mountains on the west, to the Tortilla Mountains on the east, and straddles the boundary between the Eloy sub-basin and the ESRV. The PTF model domain is 10.4 miles across from north to south, and approximately 12 miles across from east to west, covering a total area of approximately 124 square miles. The northernmost portion of the PTF model domain extends approximately three miles into the ESRV, with the southern seven miles extending into the Eloy sub-basin.

Within this domain, mountains and mountain front regions are considered to be "no-flow" areas and are represented numerically as inactive cells. Areal extent of the entire active PTF model domain is approximately 97 square miles.

No continuity issues related to joining the boundaries of the ADWR Pinal and Phoenix AMA groundwater models were encountered. No such issues were encountered because no effort was made to join and run the Pinal and Phoenix AMA models together to create the PTF groundwater model. The 125 square mile PTF model domain only covers a very small fraction of the larger Pinal and Phoenix AMA groundwater model domains, which cover a combined area of approximately 6,600 square miles. The effort required to join and run the Pinal and Phoenix AMA models was not warranted to simulate groundwater conditions at, or in the vicinity of the PTF site.

Approximately 20 percent of the PTF model domain lies within the domain of the 1994 Phoenix AMA model; the remaining 80 percent of the model domain lies within the Pinal AMA groundwater model domain. Grid discretization, layering, and boundary conditions from the Phoenix AMA model were not incorporated into the PTF Model, but were analyzed to develop an understanding of ADWR interpretations of geologic and hydrologic properties. Layering and boundary conditions from the Pinal AMA groundwater model were incorporated at the periphery of the model domain. Updated geology and temporal head distributions recently developed by ADWR for the Phoenix and Pinal AMA groundwater model were used for construction and calibration of the PTF Model.

During calibration of the PTF Model, both model heads and fluxes across the northern boundary were reviewed against the Phoenix and Pinal AMA model heads and fluxes for the same time period. This comparison was one of many such comparisons performed during calibration of the PTF Model and showed that heads and fluxes predicted by the PTF Model and the Phoenix AMA model were consistent.

14A.4.3.1 Units and Coordinate System

The PTF Model uses linear units of feet, temporal units of days, and all model features georeferenced within the State Plane NAD27 Central Arizona projection.

14A.4.3.2 Boundary Conditions

As stated previously, ADWR is in the process of updating the Pinal AMA groundwater flow model and has made selected data supporting that update available for use on a provisional basis for the PTF groundwater model. ADWR no-flow boundaries were generally maintained along the front of the Santan and Tortilla Mountains, and a dewatered area of approximately five square miles in the southeastern portion of the domain. No-flow boundaries to the northwest and northeast were refined from the ADWR data during the model layering process. Areas within the interior of the PTF model domain that were too thin for saturation were converted to no-flow.

GHBs were placed to represent the underflow from the Pinal AMA to the Salt River AMA to the north, and flow to the broader Eloy sub-basin in the southwest. Reference heads for the GHBs were set to approximate groundwater elevations two miles away from the PTF model domain. GHB cell widths, lengths, and thicknesses correspond exactly to individual grid cell dimensions. Hydraulic conductivity for all GHBs was set to the hydraulic conductivity values for each model layer. During model calibration, GHB reference heads were adjusted to produce a groundwater flow regime representative of regional water level elevations and gradients over time.

14A.4.3.3 Model Grid Discretization and Layering

The PTF Model grid consists of 298 rows and 305 columns covering an area of approximately 124 square miles. Grid cell spacing has a minimum discretization of 12.5 feet by 12.5 feet in the area of the PTF site and telescopes out to 500 feet by 500 feet at the edges of the PTF model domain. The model grid for the entire study area is shown on Figure 14A-13, and the grid in the vicinity of the proposed PTF well field is shown on Figure 14A-14. The model is georeferenced in the coordinate system as noted in Section 14A.4.3.1.

The hydrostratigraphy of the PTF Model is divided into 10 layers. The top of the highest active layer at any location within the model represents ground surface. Elevations were interpolated from a 30-meter Digital Elevation Model (DEM).

Layers 1 and 2 represent the UBFU, layer 3 represents the MFGU, and, layers 4 and 5 represent the LBFU. Layers 6 through 10 represent the Bedrock Oxide Unit, with layer 6 representing the uppermost 40 feet of that unit, which is excluded from injection.

Data used to determine layer contact elevations and extent was obtained from historic on-site corehole data (SRK, 2010), on-site well lithologic logs (Brown and Caldwell, 1996a), and geologic layering of the Pinal AMA model (ADWR, 1990). The historic site corehole database includes Rock Quality Descriptions (RQD) data generated by previous owners of the Site of the past 40 years, and includes data from approximately 700 on-site or near-site coreholes. On-site well lithologic logs were developed in 1994 and 1995 when Brown and Caldwell (1996a) drilled and installed 52 exploratory wells and observation wells at the PTF site.

In the vicinity of the PTF site, the corehole database was used to define the extent and thickness of the UBFU, MFGU, LBFU, and Bedrock Oxide Unit. Throughout the remainder of the PTF model domain, the extent and thickness of the UBFU, MFGU, and LBFU were derived from the Pinal AMA (ADWR, 1990) and SRV (ADWR, 1993) groundwater flow models.

The Bedrock Oxide Unit is not identified within the Pinal AMA model (ADWR, 1990) as a water bearing unit. The extent and water bearing characteristics of the Bedrock Oxide Unit are defined entirely by data collected on site and near site during mineral exploration and ore body characterization activities. The extent

and depth of the Bedrock Oxide Unit was interpolated from RQD data included in the historic corehole database, and was truncated or pinched out at appropriate structural features near the edges of the available corehole data coverage. Bedrock beneath the Bedrock Oxide Unit and beyond the extent of the corehole data coverage is considered to be impermeable.

14A.4.4 Stress Periods

The calibrated model consists of 28 annual (365.25 days) stress periods from 1984 to 2010. Stress period 1 is a steady state stress period that precedes the transient portion of the model representing conditions in 1900. Stress periods 2 through 28 represent the 1984 to 2010 time period. The Adaptive Time-Stepping and Output Control (ATO4) package was utilized allowing for automatic time step generation. Time steps were allowed to fall to a minimum of 0.1 days and grow to a maximum of 200 days using a 1.2 multiplier.

The predictive model simulates the time period from 2012 through 2014, and consists of seven stress periods of various lengths. The first two stress periods include 14 months of PTF operational pumping, and 9 months of PTF well field rinsing. The last five stress periods a one year in length and represent the 5-year closure period. The ATO4 package was utilized to optimize time step sizes and improve model performance.

14A.4.5 Initial Conditions

The steady state stress period 1 uses the drain down method to solve for a steady state head array. Since this array represents conditions from 1900, these heads are not allowed to carry over as starting heads for the transient portion of the model. Instead water levels for the year 1984 were obtained from the GWSI database. These data were then spatially interpolated, contoured, and attached to model grid nodes to serve as initial heads for the beginning of the transient portion of the model simulation. Water table elevations were used for starting heads in every model layer. Initial water level elevations are shown on Figure 14A-15.

14A.4.6 Hydraulic Parameterization

Horizontal hydraulic conductivity, vertical hydraulic conductivity, specific storage, specific yield, and porosity were used by ADWR in the Pinal AMA model (ADWR, 1990) for layers 1 through 5. In layer 3 where the MFGU pinches out to the east, the model was assigned values associated with the UBFU rather than those of the MFGU because as bedrock elevations rise, the LBFU thins in this area. Bedrock Oxide Unit and fault hydraulic conductivity and porosity values were derived from aquifer tests conducted in 1994 and 1995 (Brown and Caldwell, 1996a). Figures 14A-16 through 14A-25 show the hydraulic conductivity distribution for each model layer.

14A.4.7 Sources and Sinks

The PTF Model contains groundwater sources of recharge and underflow. Groundwater outflow is represented in evapotranspiration (ET), wells, and underflow. Recharge was directly imported from the ADWR Pinal AMA model. The ADWR recharge array represents recharge from the Gila River, agriculture, canals, Gila River Indian Community, and Picacho effluent.

To estimate recharge derived from Gila River flows, ADWR calculated the difference between flow at the Ashurst-Hayden Spilled and Sluiced gage and the Laveen or Maricopa gage (Maricopa was used post-1995), and distributed it in a non-linear fashion across each reach of the river based on reach specific parameters. This method assigns a fixed percentage of Gila River recharge to each model cell based on the length of river segments assigned to each model cell, relative to the total length of the river within the model domain. The ADWR methodology results in larger volumes of Gila River derived recharge to the regional aquifer system in the upper reaches of the river, which is consistent with physical observations of conditions in the groundwater basin.

Recharge values included in the ADWR recharge array for the year 1993 are provided as example estimates of groundwater recharge derived from Gila River flow during that year. Gila River flow in 1993 was more than six times greater than the long-term annual average flow, and was greater than any recorded annual flow before or since. For the year 1993, the ADWR recharge calculation method yields a recharge range of approximately 447 to 17,363 acre feet per model cell for the uppermost 25 miles of the Gila River, and 74 to 9,986 acre feet per model cell for the lower 25-mile portion of the Gila River.

In the vicinity of the PTF site, groundwater recharge derived from Gila River flow during 1993 ranged from 6,930 to 12,221 acre feet per model cell. In the ADWR groundwater model, four model cells measuring 0.5 miles square are located adjacent to the south side of the PTF site. This recharge represents a small fraction of the total recharge of approximately 364,400 acre feet received from the Gila River within the 125 square-mile domain of the Curis Arizona groundwater model for the year 1993.

The Gila River induced recharge calculated by ADWR was reduced by half for input into the Curis Arizona groundwater model based on the assumption that Gila River flood flows during that year reached a limiting condition with respect to the amount of recharge that was able to infiltrate to the regional aquifer system. This adjustment was made to the ADWR recharge value for 1993 because direct application of the ADWR recharge for that year caused groundwater elevations to rise significantly higher than observed levels. The ADWR recharge values were not adjusted for any other year of the 28-year simulation period.

In 2010, total recharge within the model domain was 35,405 acre feet. The total recharge for 1993 within the model domain was 184,254 acre feet after adjustment.

Evapotranspiration was also imported directly from the ADWR Pinal AMA model. Evapotranspiration was applied in the western portion of the model along the Gila River with a rate of 0.015 feet per day, with a 30-foot extinction depth. However, this extinction depth results in little evapotranspiration in the model.

GHBs represent underflow into the SRV to the north and underflow to and from the remainder of the Eloy sub-basin in the southwest.

Provisional data provided by ADWR (2010) included pumping values derived from SCIP reports for the period of 1984 to 2006. These data were then extended to 2010 by assuming 2006 pumping values for 2007 through 2010. ADWR (2010) also used pumping data from the RoGR database for 1984 through 2006. These pumping values were not extended into 2010; instead pumping data for 2007 and 2008 were obtained from the pump-year dataset within ADWR's wells 55 database. The 2008 pumping values obtained from the pump-year dataset were then extended for 2009 and 2010. Model water budget elements within the study area are shown on Figure 14A-26.

14A.5 Model Results and Calibration

14A.5.1 Approach

Calibration is the process of adjusting model parameters to achieve a good match between the simulated and observed hydraulic heads or other relevant hydrologic data such as water budget components. These observed data are called calibration "targets". Initial estimates for hydrogeologic parameters are varied within an observed or estimated range of values to improve the model's ability to simulate these targets.

The calibration exercise is completed prior to performing predictive simulations to provide confidence that the model is capable of simulating the historical and observed groundwater conditions. The range of plausible estimates for hydrogeologic parameters provides constraints on the calibration exercise to ensure that inputs remain defensible, and to limit the non-unique nature of the model results to a set of realistic input conditions. The adjustable model variables include hydrogeologic parameters such as hydraulic conductivity, specific storage, and specific yield.

The model was calibrated from 1984 through 2010. Additionally a qualitative steady state calibration was performed for conditions in 1900. Water level elevations from the GWSI database and PTF site water level monitoring data were used as calibration targets.

14A.5.2 Qualitative Calibration

Prior to the calculation of calibrations statistics, a qualitative review of the model-calculated flow regime was performed to assess the general groundwater flow system and to provide a subjective indication of the agreement between model-calculated groundwater elevations and flow gradients relative to observed conditions. This qualitative review was performed for the steady state simulation as well as the initial set of transient calibration simulations.

Initially, a steady state calibration was used to match regional groundwater levels across the PTF model domain by adjusting the GHB conditions. Steady state water levels for the year 1900 provided by ADWR were used as the qualitative calibration target. Steady state water levels range from a high of approximately 1,500 feet amsl where the Gila River enters the PTF model domain, to a low of approximately 1,380 feet amsl where the Gila River exits the model. Model simulated water levels generally had good agreement between regional groundwater elevations and flow directions. Groundwater flow proceeds from the east and southeast edges of the PTF model domain towards the west and northwest. This flow regime is consistent with the conceptual model, which assumes that the bulk of model inflows are from Gila River flows and incidental recharge from irrigated lands within the PTF model domain. The dominant outflow components are groundwater underflow along the north and west model boundaries, where the model domain adjoins to the regional aquifer systems for the SRV and central Pinal AMA groundwater basins, respectively.

14A.5.3 Simulated Water Levels and Quantitative Calibration

The quantitative analysis of the model calibration utilized both statistical measures of model residuals and direct comparisons of simulated and observed water levels to assess the accuracy and precision of the PTF modeling tool. Variations between the simulated and observed water levels were analyzed as functions of space and time.

14A.5.3.1 Calibration Statistics and Targets

Groundwater elevations and depths to water recorded for monitoring well locations within the model domain were compiled in a GIS-compatible database (geodatabase). The integration of the water levels with GIS coverages of well locations allows for the interpretation of water level trends both spatially and temporally during the model development and calibration process. Two sources of observed water levels were combined into the PTF Model water level geodatabase: 1) ADWR's GWSI database; and 2) the water level database for the PTF site that has been maintained by Brown and Caldwell since 1995. The compiled water levels were used to develop interpolated water level distributions at various times and serve as target values for the quantitative model calibration. The recorded water levels from ADWR's GWSI database were primarily used during the calibration of the regional groundwater flow regime; whereas, the more localized and higher resolution distribution of water levels and monitoring wells from the PTF database were used in refinement of the localized calibration for the refined portion of the model grid surrounding the PTF well field.

Although water levels from wells located outside of the PTF model domain were used to conceptualize regional flow conditions and identify temporal water level trends along model boundaries, these data were removed from the final target data set. Likewise, water level data from wells located within model no flow areas were also removed, as no simulated water levels were produced for these areas. Target wells were assigned to specific model layers based upon their total depths and assumed or known screened intervals to improve the vertical resolution and accuracy of the final model calibration.

Following calibration of the model to industry accepted standards (Anderson and Woessner, 1992), water levels from wells located within cells that had "dried out" by the end of the simulation were also removed from the target data set. These wells were all located in regions of the model where saturated aquifer units thin to the point where they should no longer be considered to be significant component of the regional aquifer system.

Generally, American Society of Testing Materials (ASTM) standards were followed whenever possible during the quantitative calibration of the model (ASTM, 2008). During calibration, residuals are calculated to assess the "fit" of the model-calculated (or simulated) heads to those actually observed. A residual is defined as the observed (or field-measured) water level minus the simulated water level at the same location. Positive residuals represent a model-calculated head value that is lower than the observed head value, and negative residuals represent a model-calculated head value that is higher than the observed value. A residual value of 0 represents a perfect fit between the model-calculated and observed values. During calibration, the goal is to minimize the residual statistics while remaining within the acceptable range for water budget components, hydraulic parameters, and flow regime requirements.

Plotting the residuals on a map with simulated water level contours provides an indication of the spatial distribution of model error and helps guide the calibration process. Trends in the distribution of error, such as clusters of values that are all too high or too low, indicate spatial bias. The spatial distribution of PTF model residual values for 2008-2010 is shown on Figure 14A-27 along with simulated water levels. From review of the residual distribution for this time frame as well as all simulated model time frames, no substantial spatial bias was observed that would significantly affect the results of predictive simulations.

Calibration statistics based on the residual values are used as a quantitative measure of the overall ability of the model to match calibration targets. Calibration statistics that were calculated to quantify the average error included:

- Absolute Residual Mean (ARM), the arithmetic average of the absolute value of the residuals;
- Residual Mean (RM), the arithmetic average of the residuals; and
- Residual Standard Deviation (RSD), the standard deviation of the residuals.

When the ratio of the ARM to the range of observed head values in the system is small, discrepancies between simulated and observed values comprise only a small part of the overall model response (Anderson and Woessner, 1992). One of the goals of the quantitative calibration process was for the ratio of the ARM to the range in observed heads to be less than five percent for any given calibration period. Total interpreted head change across the PTF model domain is approximately 400 feet based on the range of observed heads over the full 28-year model simulation time period; therefore, the ARM should be less than 20 feet to meet this goal. A listing of the key calibration metrics for the PTF Model is presented in Table 14A-5. All calibration statistics and metrics are reflective of the water level target values for the entire simulation time period of 1984 through the end of 2010. The ARM is approximately 12 feet, producing a ratio of ARM to observed head range of three percent, well below the predefined calibration goal. The principle industry standards for model calibration are an ARM/Head Range of less than 5 percent and a RSD/Head Range of less than 10 percent. Model calibration metrics are well within industry standard guidelines for successful model calibration.

14A.5.3.2 Simulated Water Level Conditions 2010

Simulated water levels at the end of the calibrated model simulation time frame (end of 2010) are shown on Figure 14A-27. The model reproduces the general flow gradients and absolute water level elevations throughout the PTF model domain. Simulated flow gradients are generally directed along the course of the Gila River and flow exits the PTF model domain along the northern and western GHBs. By the end of the simulation time period, groundwater underflow into the PTF Model is observed along the southern model

boundary. Localized pumping and Gila River recharge produces a saddle-shaped water table feature in the central portion of the PTF model domain, causing diverging flow gradients to the north towards the PTF site and towards the south and the central portion of the Pinal AMA regional aquifer system. Overall, the simulated groundwater conditions match the conceptual understanding of the water levels and flow within the Eloy sub-basin, as well as matching observed water level measurements.

14A.5.3.3 Simulated Water Budget

The simulated water budget for the PTF study area for 1984, 2003, and at the end of the calibrated time period in 2010 is presented in Table 14A-6 and for the entire simulation time frame in Figure 14A-28. Water budget components that exhibit the largest changes from 1984 to 2010 include storage, fluxes from general head cells, and recharge. Recharge in 1984 represents a "wetter" year and therefore storage outflows represent addition of water to aquifer reserves.

Inflows from storage in 1984 were very low or negligible because that year followed a high precipitation year during which the Gila River experienced extremely high flood flows. These flows and high precipitation caused a large amount of groundwater recharge along the course of the river and also caused a reduction in the amount of agricultural pumping. The net effect was that groundwater levels rose throughout the model area, hence the large amount of storage outflows (refilling of the regional aquifer) and no storage inflows (no net aquifer depletion). The recharge and pumping reduction was so pronounced for this year that there was no simulated groundwater depletion at the spatial scale of the model cells. Higher fluxes in the general head cells in 1984 corroborate with higher water levels and increased flows out of the study area.

In the lowest recharge year of the simulation time frame (2003), storage inflows represent depletion of the aquifer, pumping increases, and there is a drastic reduction in general head flux out of the study area compared to 1984. Although 2003 was a dry year, the relatively higher GHB flux out of the study area represents continued drain down of recharge received in earlier years. The year 2010 has recharge value typical of an average year and fluxes adjust accordingly compared to 1984 and 2003.

14A.6 Predictive Simulations

The calibrated PTF Model was adjusted to simulate and predict future conditions at and in the vicinity of the PTF well field. This was accomplished by keeping all model groundwater fluxes at 2010 magnitudes and distributions and shifting the time frame to cover a specified future period of time. Two predictive scenarios were developed to assess 1) the migration potential of groundwater away from the PTF well field using a full fate and transport model and advective particle tracking, and 2) the impact of groundwater containment pumping over the estimated, cumulative 23-month timeframe of PTF activities and rinsing periods.

14A.6.1 Predictive Scenario Development

Two predictive scenarios were developed that differ primarily by the presence or absence of containment pumping at the PTF well field over a 23-month timeframe. These two scenarios and associated simulations are identified as "pumping" and "no pumping", respectively. For the pumping predictive simulation, an additional 5 years (2014 through 2019) was included after the initial 23 months to facilitate the simulation of potential post-closure sulfate transport.

Simulation of the future DIA was performed using modeled groundwater conditions that prevailed following cessation of PTF pumping. For the advective particle tracking analysis, the 3-D groundwater flow field at the end of the calibrated model (end of 2010) was used to simulate flowpaths after pumping had stopped. A comparison of the results of the PTF pumping and agricultural-only pumping predictive scenarios over the 23-month PTF well field life allowed the estimation of the impact of PTF pumping on future water levels by comparing simulated water levels both with and PTF operations at the end of the 23-month period.

14A.6.2 Discharge Impact Area

The DIA is defined in Arizona Revised Statutes (A.R.S.) § 49-201 as the "potential areal extent of pollutant migration, as projected on the land surface, as the result of discharge from a facility." The simulated DIA is based on the potential areal extent of sulfate migration from the proposed PTF facility following completion of copper recovery and restoration activities. The DIA was defined using sulfate because the proposed lixiviant is a sulfuric acid based solution, and over the life of the proposed PTF project, a substantial quantity of the lixiviant will be circulated through the associated ore body. By mass, sulfate comprises the greatest quantity of material to be removed during restoration activities.

Site restoration activities consist primarily of post-production rinsing of the ore body using native groundwater to remove residual lixiviant and residual constituents dissolved by the lixiviant. During restoration, rinsing the pH of the residual fluids will rise to the point that it is near background levels. As the pH rises, constituents of interest such as metals will complex out of solution or otherwise precipitate in insoluble forms. There is expected to be sufficient gypsum precipitated in the ore body during PTF operations to ensure that sulfate will exist in residual formation water in substantial quantities as the other constituents are immobilized by the elevated pH. Geochemical modeling presented in Attachment 10 has demonstrated that no constituent other than sulfate will migrate to the POC after cessation of PTF operations.

Simulation of the future migration of sulfate and delineation of the DIA was performed using the MODFLOW SURFACT™ ACT module, described in Section 14A.4.2, fully coupled with the transient groundwater flow simulated for the pumping predictive scenario. Post-closure sulfate mass was allowed to migrate through and away from the PTF well field via advection, dispersion, and diffusion for 5 years, commencing immediately after the cessation of containment pumping. The horizontal distribution of initial sulfate concentrations is shown on Figure 14A-29. The discretization of model layers relative to the hydrostratigraphic units described above is shown on Figure 14A-30. Figures 14A-31 through 14A-36 show the maximum extent of sulfate migration at the DIA concentration criterion of two milligrams per liter (mg/L) above background in each model layer with sulfate concentrations above that level.

Sulfate transport simulations did not result in any sulfate migration into model layers 1 through 4 (Figure 14A-30), which represent the upper portion of the LBFU or the UBFU. Transport simulations indicate that following restoration, sulfate generally remains confined to the Bedrock Oxide Unit, with limited migration into the LBFU over time. The maximum extent of sulfate migration in the Bedrock Oxide Unit is shown on Figure 14A-37, and for the LBFU on Figure 14A-31

The DIA is the vertical projection of the maximum aerial extent of sulfate migration from the PTF well field at 5 years after closure in all model layers combined. Combination of the sulfate migration extent in each model layer results in a composite image of the maximum horizontal extent of sulfate migration 5 years after PTF well field closure. As described above, beside sulfate, no other residual water quality constituents are transported beyond the PTF well field boundary once restoration has been completed. The DIA as defined by sulfate migration 5 years after PTF well field closure is shown on Figure 14A-38.

14A.6.2.1 Transport Simulation Initial Conditions and Parameters

Geochemical modeling originally performed by Brown and Caldwell (1996b), and subsequently updated as presented in Attachment 10 to this application, has demonstrated that the process of post-production rinsing of the ore body to a target sulfate concentration of 750 mg/L, will remove other constituents of interest from the ore body to near background concentrations, or below AWQS levels. For this reason, proposed restoration activities include rinsing of the ore body until sulfate concentrations reach a level of 750 mg/L, at which point restoration will be complete. Therefore, for the purposes of the transport simulation, this sulfate concentration was used as an initial condition and was emplaced in model layers 7 though 10 within the

boundaries of the PTF well field (Figure 14A-27). This distribution of initial sulfate concentrations represents the volume of Bedrock Oxide Unit targeted for injection and recovery and excludes the uppermost 40 feet of the Bedrock Oxide Unit.

A uniform dispersivity value of 10 feet was used for all model cells, and a uniform diffusion coefficient of 1 x 10-3 ft^2/day was also applied. The transport of sulfate was assumed to be fully conservative; therefore, no solute degradation was considered in the simulation and all model cells were assigned a sulfate distribution coefficient of zero. Porosity of the basin fill porous media, as well as the oxide and fault zones, are presented in Table 14A-4 and range from 0.05 for the lower oxide to 0.20 for the LBFU.

14A.6.2.2 DIA Evaluation Criterion

The DIA described herein is defined by the Practical Quantitation Limit (PQL), for sulfate concentration as determined by USEPA Test Method 300. The current PQL for sulfate analyses performed by the laboratory used for site water quality analyses (Test America, Phoenix) is 2.0 mg/L. Consequently, the laboratory cannot certify sulfate analytical results below this concentration, and cannot reliably reproduce analytical results with a precision of less than 2.0 mg/L using USEPA Test Method 300. Therefore, the greatest areal extent of sulfate migration as a result of operation of discharging facilities proposed under this APP application was defined at a sulfate concentration of 2 mg/L above background conditions.

14A.6.2.3 Results of DIA Transport Simulation

For model layers 1 through 4 (representing the UBFU, MFGU, and upper LBFU) (Figure 14A-28) there were no sulfate concentrations simulated to be greater than 2 mg/L above background conditions 5 years after closure. The maximum extent of simulated sulfate concentrations greater than or equal to 2 mg/L above background for layers 5 through 10 are shown on Figures 14A-31 through 14A-36. The simulated maximum distance of down-gradient migration of sulfate, approximately 150 feet beyond the edge of the PTF well field in the lower bedrock oxide unit (Layer 10).

Although sulfate appears to migrate from the Bedrock Oxide Unit into the LBFU, sulfate concentrations in the LBFU were simulated to be substantially lower than those within the Oxide Bedrock Unit, reaching a maximum of less than 10 mg/L above background in a relatively small area (Figure 14A-31). Sulfate concentrations in the Bedrock Oxide Unit 5 years after closure were simulated to be approximately 500 mg/L above background concentrations near the center of the PTF well field in model layers 7 through 10. The transport distances and areal distribution of sulfate within the Bedrock Oxide Unit layers are relatively limited, migrating only approximately 150 feet down-gradient along the trend of the more permeable Sidewinder fault zone.

14A.6.3 Particle Tracking

14A.7 Water Level Impacts of ISCR

Localized water level impact was defined as the change in simulated water levels at seven days after the end of PTF operations as a result of pumping within the PTF well field. Water level impacts were calculated by subtracting the simulated water levels of the PTF Pump Scenario from the simulated water levels of the No PTF Pump Scenario (agricultural pumping only) after 23 months of future PTF pumping. Water levels were allowed to recover for seven days following the 23 month pumping period. This analysis of impact reflects the relative water level change due to pumping at the PTF well field without bias from regional hydrologic declines or increases.

Pumping at the PTF well field was assumed to be a total of 60 gpm for a period of 14 months, and 260 gpm for a period of 9 months, distributed evenly the PTF well field. This pumping represents the planned over pumping necessary to maintain hydraulic control during PTF operations. To distribute the pumping evenly

across the site, four extraction points were used that are not intended to represent production phases or operational conditions. The 43 extraction points represent an evenly spaced array that is used to distribute pumping evenly across the Site for the period of PTF operations. Simulated water levels after 23 months of pumping reflect residual water level impact that is less than 1 foot and less than the ability of the model to quantify, given that regional water levels fluctuate between 1 and 4 feet in response to recharge form the Gila River and agricultural groundwater pumping. Similar to the residual water level impacts simulated in the LBFU, water levels in the Bedrock Oxide Unit after 23 months of pumping are less than regional water level fluctuations induced by recharge irrigation pumping stresses, and are therefore indiscernible from background fluctuations.

14A.8 Impacts from Off-Site Pumping

This groundwater model was developed using site-specific and published regional geologic and hydrologic data. The groundwater model included the most up to date groundwater pumping data available from ADWR at the time of model development. ADWR is the official repository of groundwater data generated and reported throughout the State of Arizona. No other entity, public or private, maintains as thorough or current hydrologic datasets, including groundwater pumping datasets, for the State of Arizona.

As described above, groundwater pumping data used in the PTF Model were compiled by ADWR for the ongoing update of the Pinal AMA groundwater flow model and were provided by ADWR on a provisional basis for use in the PTF groundwater flow model. Pumping data from 1984 to 2006 were compiled by ADWR from SCIP reports and from the RoGR database. Pumping data after 2006 were compiled by Brown and Caldwell from the ADWR wells 55 database, specifically the pump-year dataset within that database. Future groundwater pumping conditions were simulated based on these historical records, and were projected into the future using annual stress periods.

Given that the most current groundwater pumping data available were used to develop the PTF groundwater flow model, the groundwater elevation impacts on the proposed PTF facility resulting from off-site pumping are already represented in the PTF groundwater model. Groundwater pumping represented in the PTF groundwater model was distributed at the locations identified by ADWR throughout the PTF model domain. ADWR assigned groundwater pumping to individual model cells where reporting wells were located. The finite-difference approximation assumes that all hydraulic parameters, stresses, and inputs are constant over the area of a single cell and over the time elapsed during a stress period. Likewise, calculated hydraulic head and groundwater fluxes, such as pumping, are also averaged over the areal extent of a single cell. Within the PTF groundwater model, cells sizes range from 500 feet by 500 feet at the model periphery to 12.5 feet by 12.5 feet in size at the PTF well field, in center of the model.

Pumping trends, both on and off site were projected for a period of 23 months, using stress periods of various lengths. Based on this simulation, off site pumping does not materially affect groundwater flow direction or gradients at the proposed PTF well field relative to current groundwater conditions, and will not materially affect PTF operations.

14A.9 References

American Society for Testing and Materials (ASTM), 2008. *Standard Guide for Calibrating a Ground-Water Flow Model Application.* ASTM D5981-96(2008).

Anderson, M.P. and Woessner, W. W., 1992. *Applied Groundwater Modeling: Simulation of Flow and Advective Transport.* Academic Press Inc., San Diego, California, 381 p.

Arizona Department of Water Resources (ADWR), 1989. *Pinal Active Management Area Regional Groundwater Flow Model, Phase One: Hydrogeologic Framework, Water Budget and Phase One Recommendations, Model Report 1.*

ADWR., 1990. *Pinal Active Management Area Regional Groundwater Flow Model, Modeling Report No. 2.*

ADWR., 1993. *A Regional Groundwater Flow Model of the Salt River Valley - Phase I, Phoenix Active Management Area Hydrogeologic Framework and Basic Data Report.*

ADWR, 1994. *A Regional Groundwater Flow Model of the Salt River Valley - Phase II. Numerical Model, Calibration, and Recommendations*. Corell and Corkhill . Modeling Report No. 8

ADWR, 2010. *Regional Groundwater Model of the Pinal Active Management Area; Provisional Data.*

Brown and Caldwell, 1996a. *Magma Florence In-Situ Project Aquifer Protection Permit Application, Volume IV of V, Modeling Report.* January 1996.

Brown and Caldwell, 1996b. *Focused Facilities Investigation October 1995, Magma Florence In-Situ Project.*

Conoco, 1976. *Conoco Copper Project, Florence, Arizona, Phase III Feasibility Study, Volume III, Hydrology, Geology, and Ore Reserves*: Conoco Minerals Department.

Environmental Simulations, Inc. (ESI), 2008. *Groundwater Vistas*, Advanced Model Design and Analysis, version 5.25.

ESRI, 2006. Arc GIS™ software, version 9.2.

Golden Software, Inc., 2008. *Surfer*, Surfer Mapping System, version 8.

Halpenny, L.C., 1976. *Evaluation of Northward Groundwater Movement Near Conoco Proposed Mine, Florence, Arizona*: Water Development Corporation, Tucson, Arizona.

Halpenny, L.C., and Green, D.K., 1972. *Preliminary Report on Hydrogeology of Poston Butte Area, Arizona, and Relationship to Proposed In-Situ Leaching.* Water Development Corporation, Tucson, Arizona.

Hammett, B.A., 1992. Maps Showing Groundwater Conditions in the Eloy and Maricopa/Stanfield Sub-basins of the Pinal Active Management Area, Pinal, Pima, and Maricopa Counties; Department of Water Resources Hydrologic Map Series Report No. 23.

Harbaugh, A.W., Banta, E.R., Hill, M.C., and McDonald, M.G., 2000. *MODFLOW-2000, The U.S. Geological Survey Modular Ground-water Model – User Guide to Modularization Concepts and the Ground-water Flow Process.* U.S. Geological Survey Open-File Report 00-92.

HydroGeoLogic, Inc., 1996. *MODHMS Software, (Version 2.0) Documentation*, 426p, Herndon,VA (1996)

McDonald, M.G., and Harbaugh, A.W., 1988. *A Modular Three Dimensional Finite-Difference Groundwater Flow Model.* U.S. Geological Survey Techniques of Water Resource Investigations Book6, ChapterA1.

Montgomery, E.L, and Harshbarger, J.W., 1989. *Arizona Hydrogeology and Water Supply*, in Jenny, J.P. and Reynolds, S.J., Geologic Evolution of Arizona; Arizona Geological Society Digest 17, pp. 827-840.

Montgomery, 1994. *Hydrogeologic Investigation for Prefeasibility Studies for Florence Project, Magma Copper Company, Pinal County, Arizona.* Tucson, Arizona.

Nason, P.W., Shaw, A.V., and Aveson, K.D., 1982. *Geology of the Poston Butte Porphyry Copper Deposit: Advances in Geology of the Porphyry Copper Deposits, Southwestern North America*, Ed. Spencer R. Titley, University of Arizona Press, pp. 375-385.

NOAA, 2010. US Monthly Surface Data, Cooperative Station ID 0.23027.

Pollock, D.W., 1994. *User's Guide for MODPATH/MODPATH-PLOT, Version 3: A Particle Tracking Post-Processing Package for MODFLOW*, the U.S. Geological Survey Finite-Difference Ground-Water Flow Model: U.S. Geological Survey Open-File Report 94-464.

SRK, 2010. Legacy Florence Corehole Database, Provisional Data

Zheng, C. 1989. Applied PATH3D, A Groundwater Path and Travel Time Simulator, Version 3.0

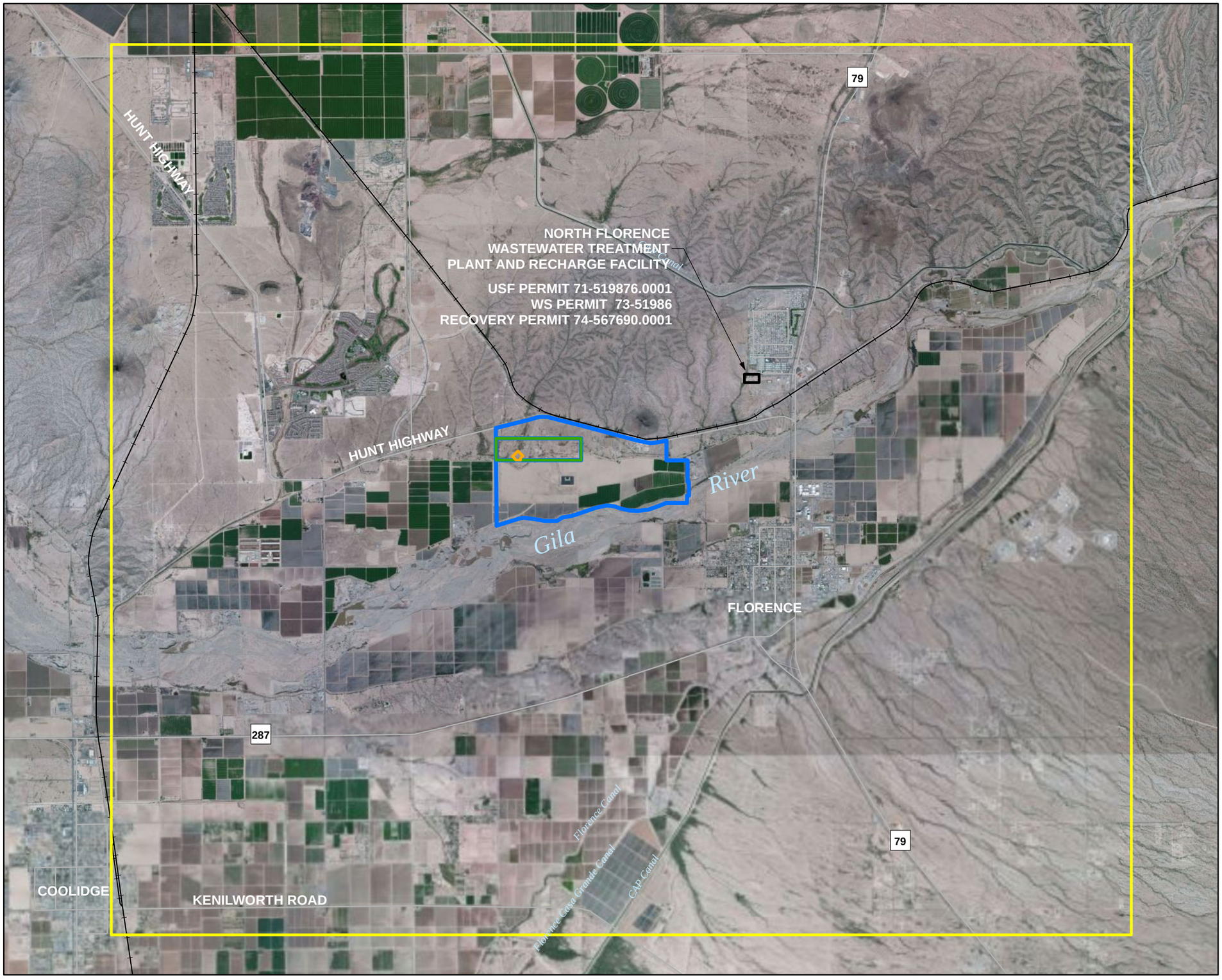

0 3,000 6,000

SCALE IN FEET

EXPLANATION

- MODEL EXTENT
- PTF WELL FIELD
- STATE MINERAL LEASE BOUNDARY
- CURIS PROPERTY BOUNDARY

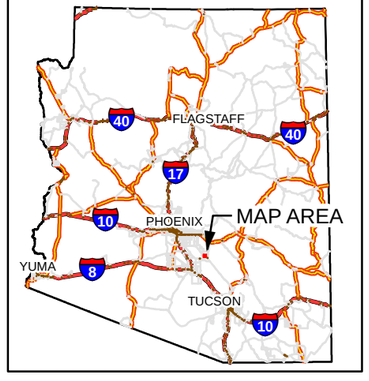

Figure 14A-1
LOCATION MAP

CURIS RESOURCES (ARIZONA) INC.
FLORENCE, ARIZONA

Brown AND Caldwell

HDI CURIS

\\BCPHX03\projects\Hunter Dickinson\Curis GIS\MXDs\Temp Permit2012\G14075334014A1.mxd Updated: 1/25/2012

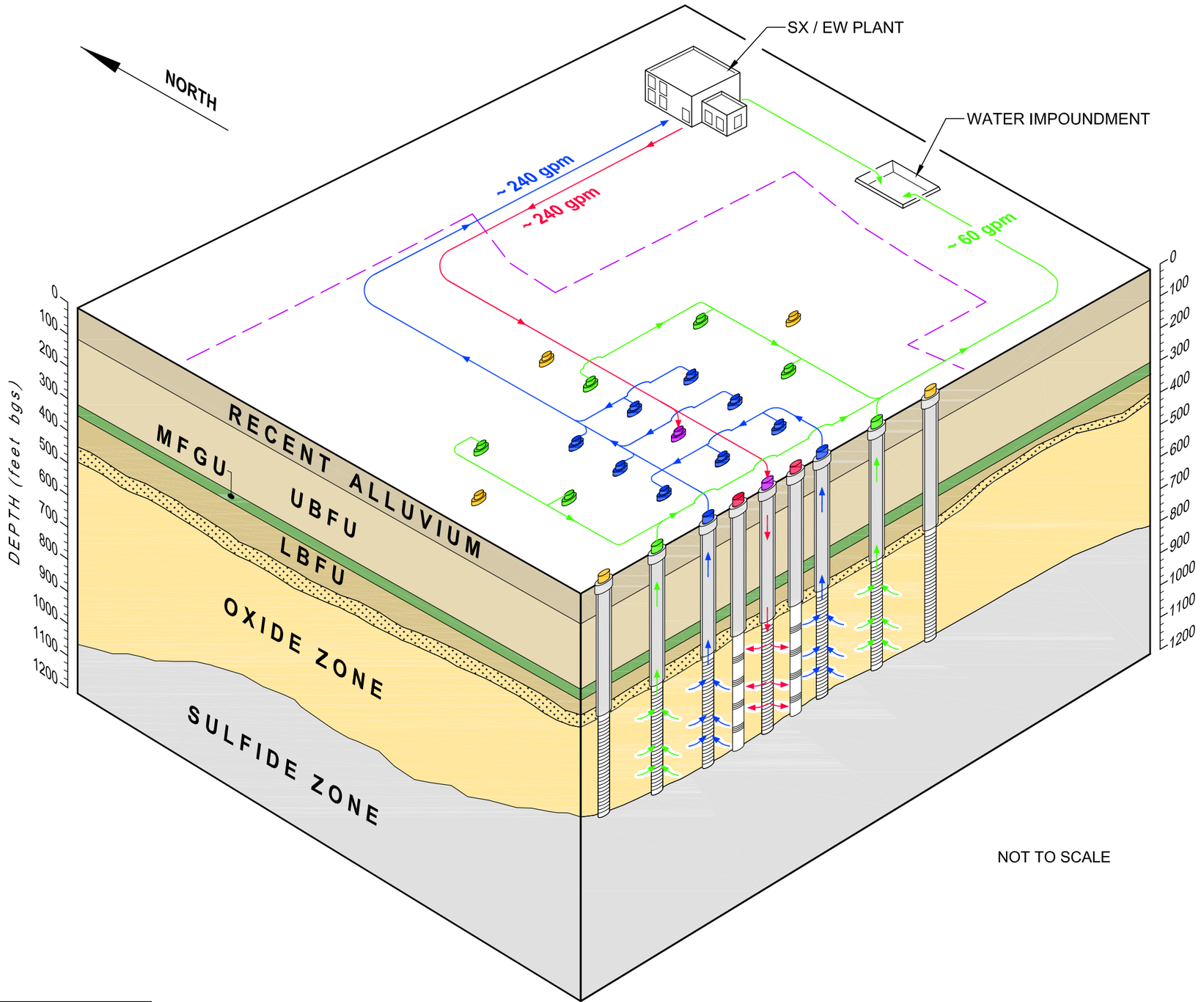

EXPLANATION

- RECOVERY WELL
- INJECTION WELL
- PERIMETER WELL
- OBSERVATION WELL
- WESTBAY WELL
- CEMENT SEAL
- 40-FOOT OXIDE EXCLUSION ZONE
- ISCR BOUNDARY

NOTE: A TOTAL OF FOUR WESTBAY WELLS ARE TO BE USED DURING PTF ISCR ACTIVITIES TO STUDY FORMATION CHEMISTRY. NO WESTBAY WELLS ARE PLANNED FOR USE DURING LATER PHASES OF ISCR ACTIVITIES.

NOT TO SCALE

Brown AND Caldwell

HDI CURIS

Figure 14A-2

BLOCK DIAGRAM SHOWING TYPICAL PTF WELLS

CURIS RESOURCES (ARIZONA) INC.
FLORENCE, ARIZONA

P:\Hunter Dickinson\140913 - Curis - 2011 Mine Plan and GServ\Drawings\ES\140913016.dwg Mar 01, 2012 - 12:32pm jcollier

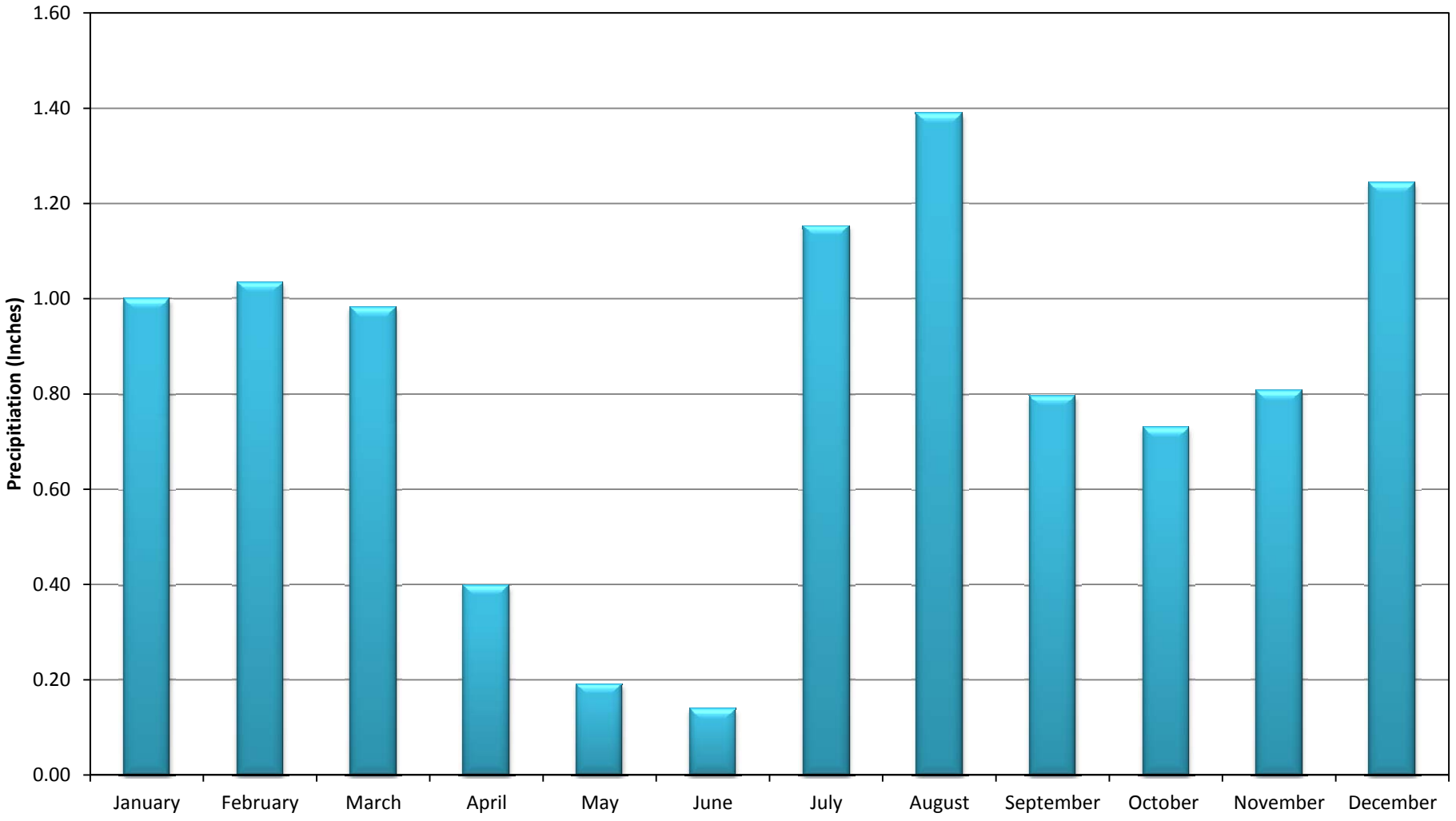

Average Precipitation Values based on 30 year record 1978-2008
NOAA, 2010

Figure 14A-3
Mean Monthly Precipitation
Florence, Arizona

Curis Resources (Arizona) Inc.
Florence, Arizona

Brown AND Caldwell

J:\Hunter Dickinson\138799 - Curis Florence Copper Permitting\Working\Significant Amendment\Figures\Modeling Report\Precipitation Histograms.xlsx 1/17/2012

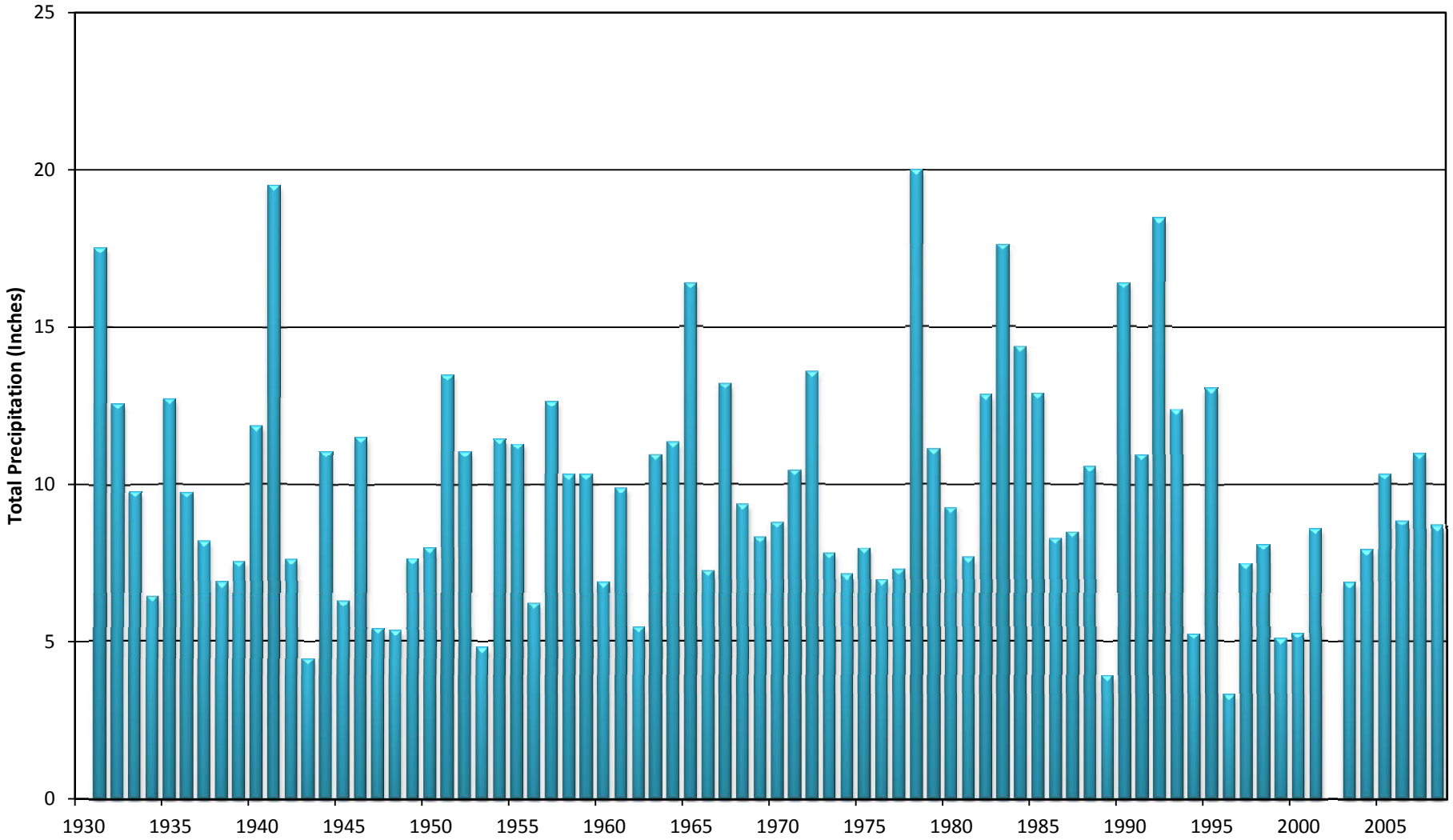

Brown AND Caldwell

NOAA, 2010
Cooperative Station ID 023027
For the year 2002, the record is missing nine months of data

Figure 14A-4
Total Annual Precipitation
Florence, Arizona

Curis Resources (Arizona) Inc.
Florence, Arizona

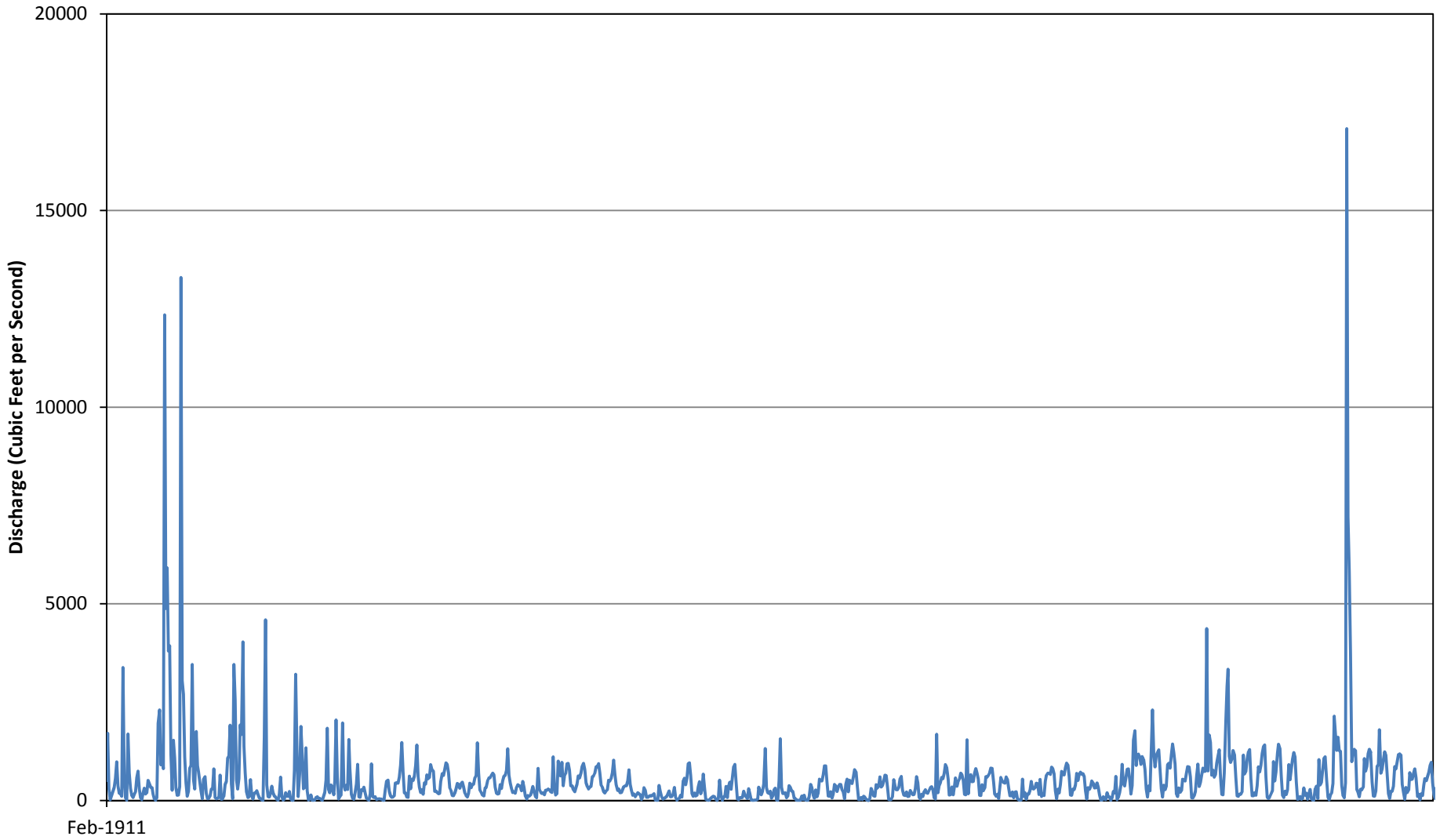

Figure 14A-5
Monthly Mean Gila River Stage Values
Kelvin, Az
Curis Resources (Arizona) Inc.
Florence, Arizona

Brown AND Caldwell

J:\Hunter Dickinson\138799 - Curis Florence Copper Permitting\Working\Significant Amendment\Figures\Modeling Report\Gila River USGS_Monthly_Hydrographs.xlsx 1/17/2012

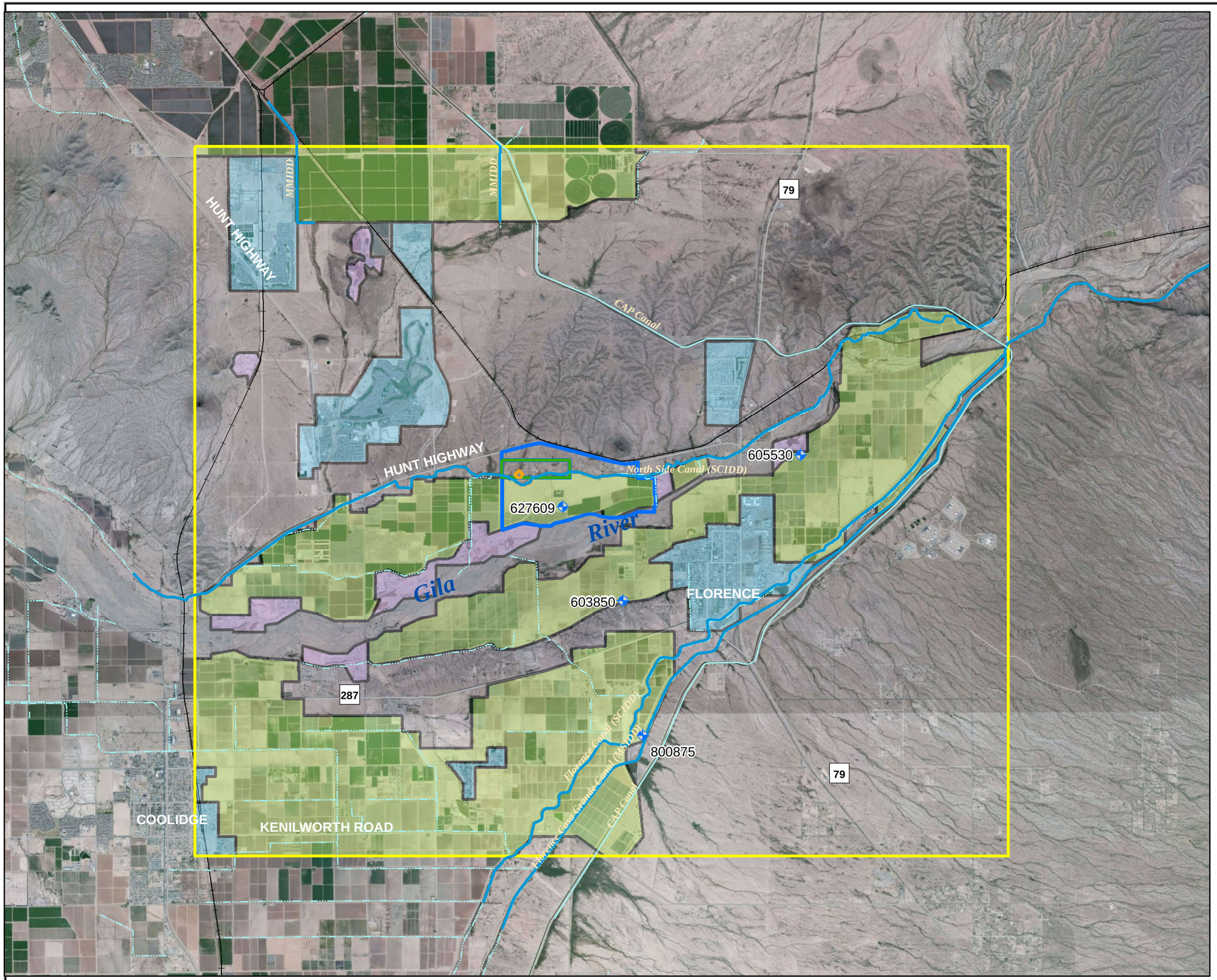

0 3,000 6,000

SCALE IN FEET

EXPLANATION

- KEY WELLS
- CANAL
- MODEL EXTENT
- PTF WELL FIELD
- STATE MINERAL LEASE BOUNDARY
- CURIS PROPERTY BOUNDARY

LAND USE

- Agriculture
- Industrial
- Urban

Figure 14A-6
LAND USE AND
KEY WELLS

CURIS RESOURCES (ARIZONA) INC.
FLORENCE, ARIZONA

Brown AND Caldwell

HDI CURIS

\\BCPHX03\projects\Hunter Dickinson\Curis GIS\MXDs\Temp Permit2012\G14075334014A6.mxd Updated: 1/27/2012

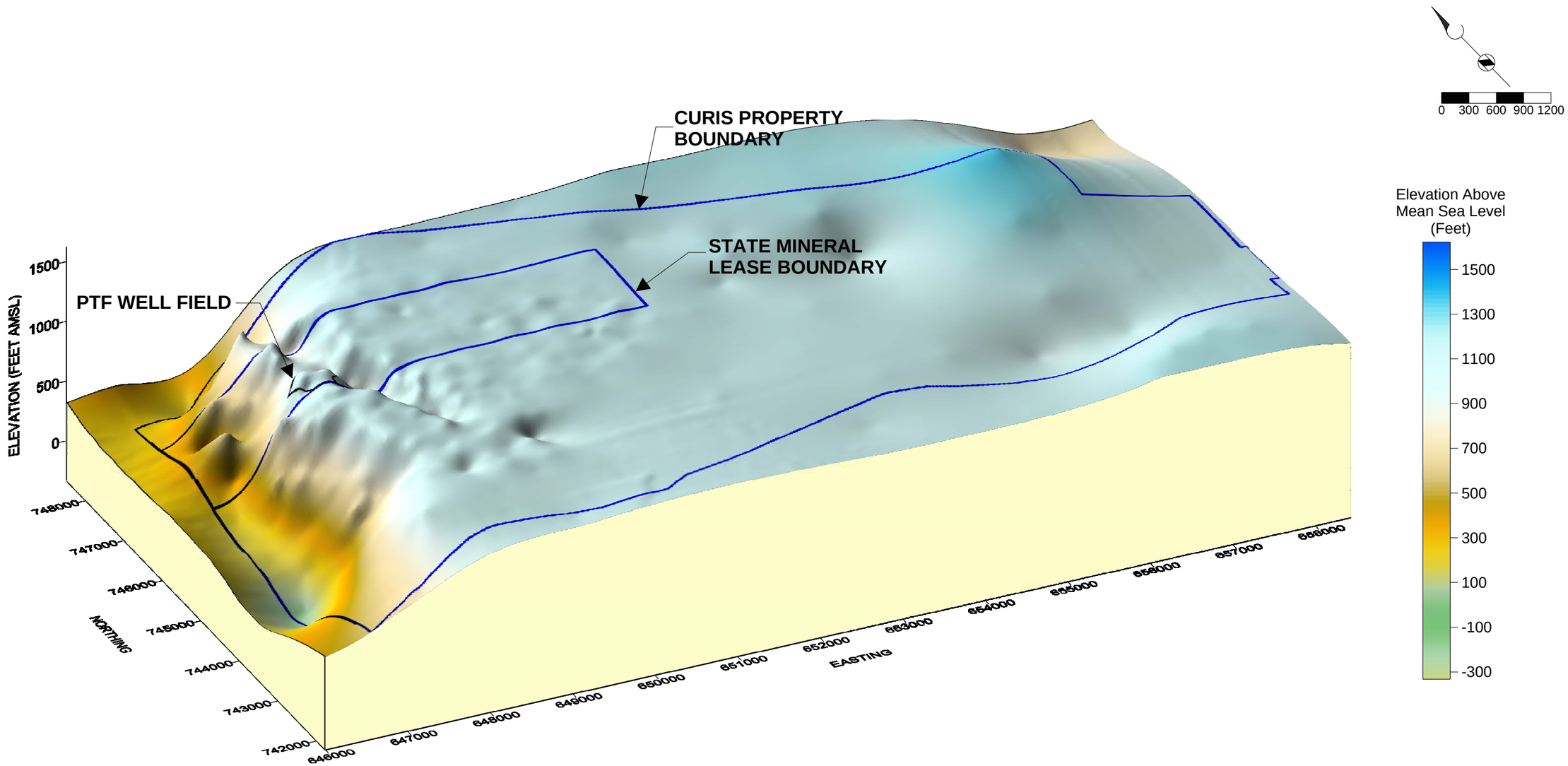

HDI CURIS

Brown AND Caldwell

Figure 14A-7
BEDROCK TOPOGRAPHY

CURIS RESOURCES (ARIZONA) INC.
FLORENCE, ARIZONA

P:\Hunter Dickinson\140753 – Curis – 2011 Environmental Support\GIS\Surfer\S140753001.srf 02/10/12

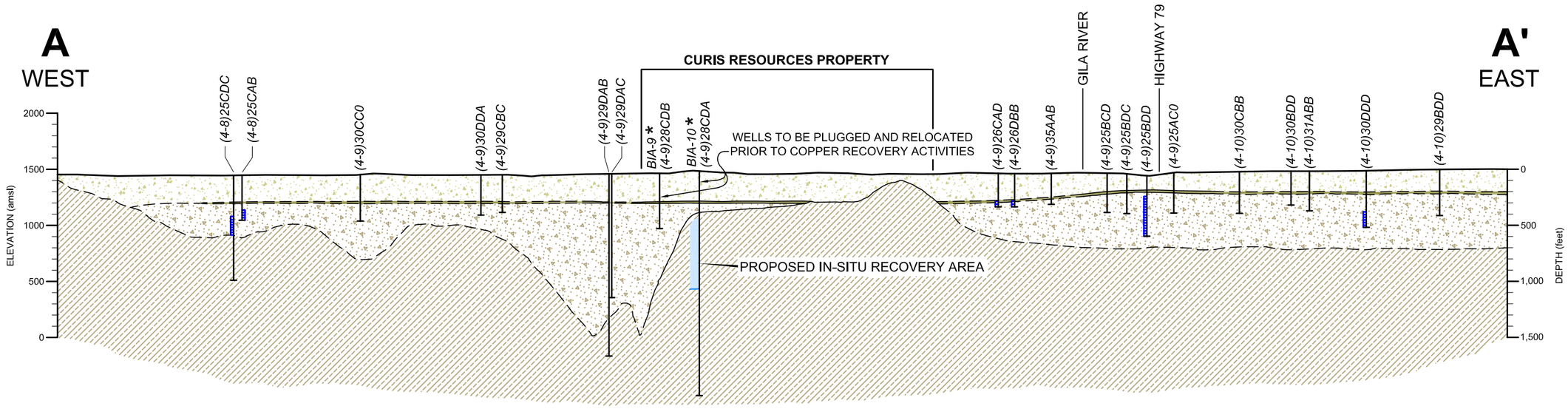

KEYMAP

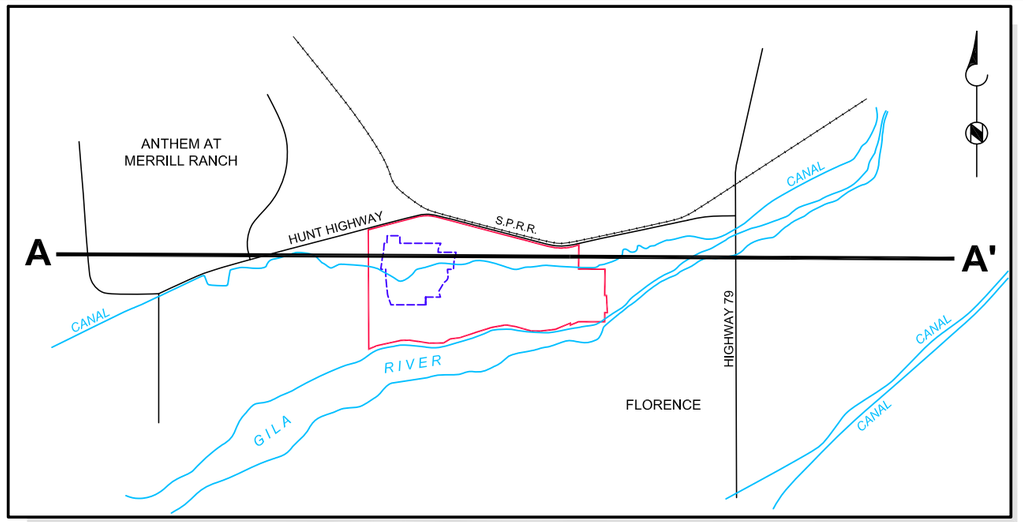

EXPLANATION

- UPPER BASIN FILL ALLUVIAL UNIT
- MIDDLE FINE-GRAINED UNIT
- LOWER BASIN FILL ALLUVIAL UNIT
- BEDROCK

APPROXIMATE WELL LOCATION
(GENERALLY PROJECTED ONTO CROSS-SECTION)

- SCREENED INTERVAL (WHERE DATA IS AVAILABLE)
- TOTAL DEPTH OF BOREHOLE

NOTES: BEDROCK SURFACE CONTOURS COMPILED BY BROWN AND CALDWELL FROM EXISTING WATER WELL LOGS, EXPLORATORY CORE LOGS AND REGIONAL GRAVITY SURVEYS (MAGMA COPPER COMPANY APP APPLICATION, VOLUME II FIGURES 3.4-2 (II) AND 3.4-3 (II), 1996).

* WELLS BIA-9 AND BIA-10 (LOCATED IN THE PROPOSED IN-SITU RECOVERY AREA) WILL BE PLUGGED AND RELOCATED PRIOR TO INITIATING COPPER RECOVERY ACTIVITIES.

UNIT CONTACTS DASHED WHERE INFERRED

HORIZONTAL SCALE: 1" = 4,000'
VERTICAL SCALE: 1" = 1,000'

4X VERTICAL EXAGGERATION

Brown AND Caldwell

HDI CURIS

Figure 14A-8

GENERALIZED REGIONAL GEOLOGIC CROSS-SECTION A-A'

CURIS RESOURCES (ARIZONA) INC.
FLORENCE, ARIZONA

P:\Hunter Dickinson\140913 - Curis - 2011 Mine Plan and GServ\Drawings\ES\140913018.dwg Jan 19, 2012 - 10:06am jcollier

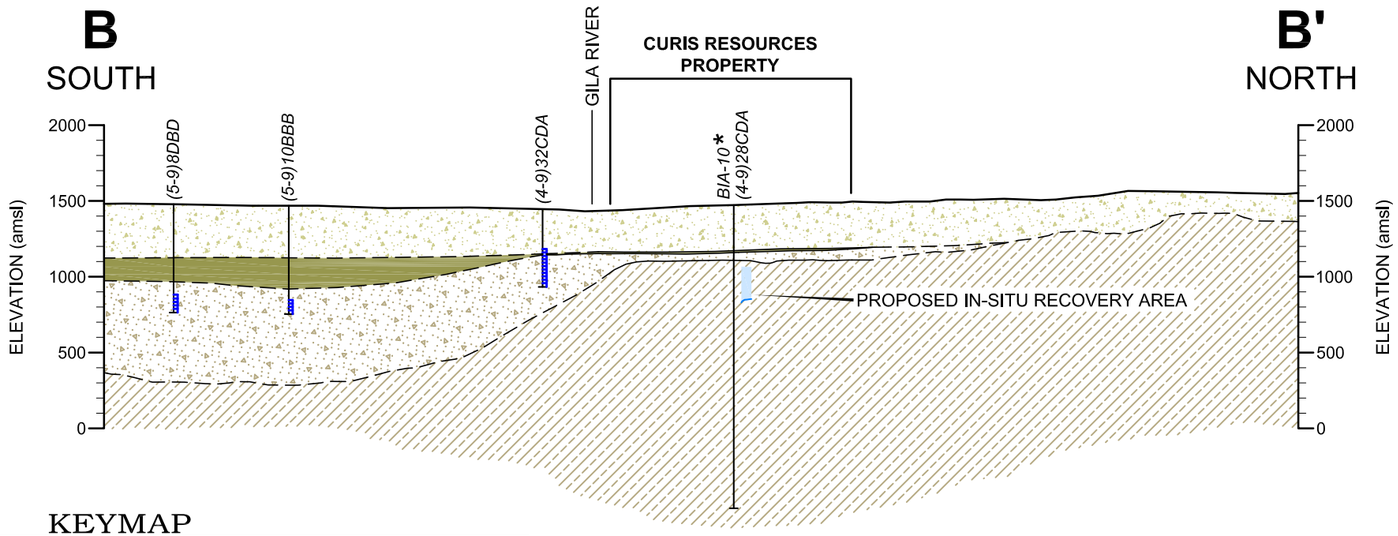

KEYMAP

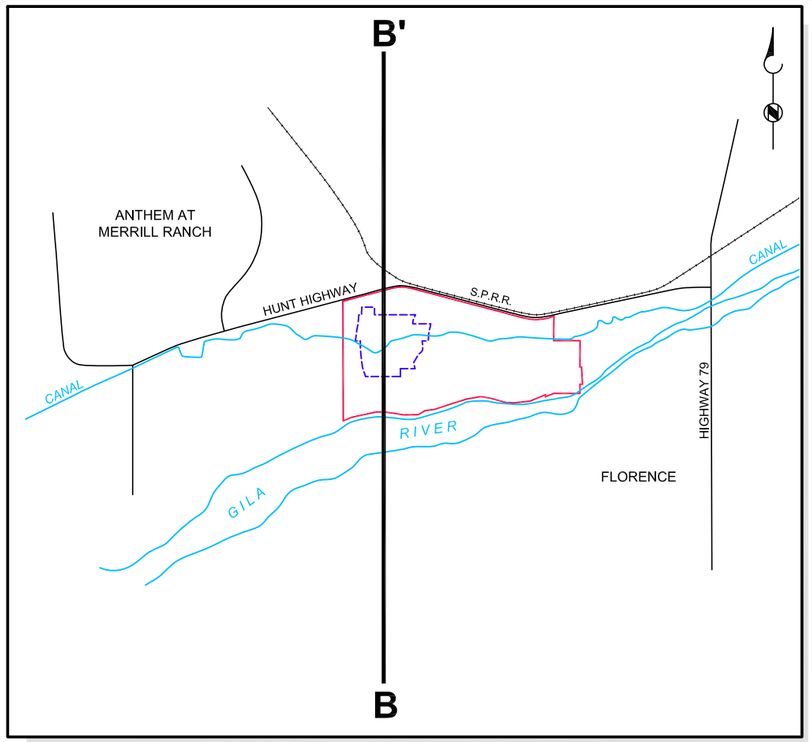

EXPLANATION

- UPPER BASIN FILL ALLUVIAL UNITS
- MIDDLE FINE-GRAINED UNIT
- LOWER BASIN FILL ALLUVIAL UNIT
- BEDROCK

APPROXIMATE WELL LOCATION
(GENERALLY PROJECTED ONTO CROSS-SECTION)

- SCREENED INTERVAL (WHERE DATA IS AVAILABLE)
- TOTAL DEPTH OF BOREHOLE

HORIZONTAL SCALE: 1" = 4,000'
VERTICAL SCALE: 1" = 1,000'

4X VERTICAL EXAGGERATION

NOTES:
1. BEDROCK SURFACE CONTOURS COMPILED BY BROWN AND CALDWELL FROM EXISTING WATER WELL LOGS, EXPLORATORY CORE LOGS AND REGIONAL GRAVITY SURVEYS (MAGMA COPPER COMPANY APP APPLICATION, VOLUME II FIGURES 3.4-2 (II) AND 3.4-3 (II), 1996).
2. * WELL BIA-10 (LOCATED IN THE PROPOSED IN-SITU RECOVERY AREA) WILL BE PLUGGED AND RELOCATED PRIOR TO INITIATING COPPER RECOVERY ACTIVITIES.
3. MIDDLE FINE-GRAINED UNIT SHOWN AT WELLS (5-9)8DBD, (5-9)10BBB AND (4-9)32CDA ESTIMATED FROM ADWR WELL REPORTS.
4. UNIT CONTACTS DASHED WHERE INFERRED.

Brown AND Caldwell

HDI CURIS

Figure 14A-9

GENERALIZED REGIONAL GEOLOGIC CROSS-SECTION B-B'

CURIS RESOURCES (ARIZONA) INC.
FLORENCE, ARIZONA

P:\Hunter Dickinson\140913 - Curis - 2011 Mine Plan and GServ\Drawings\ES\140913017.dwg Jan 19, 2012 - 10:07am jcollier

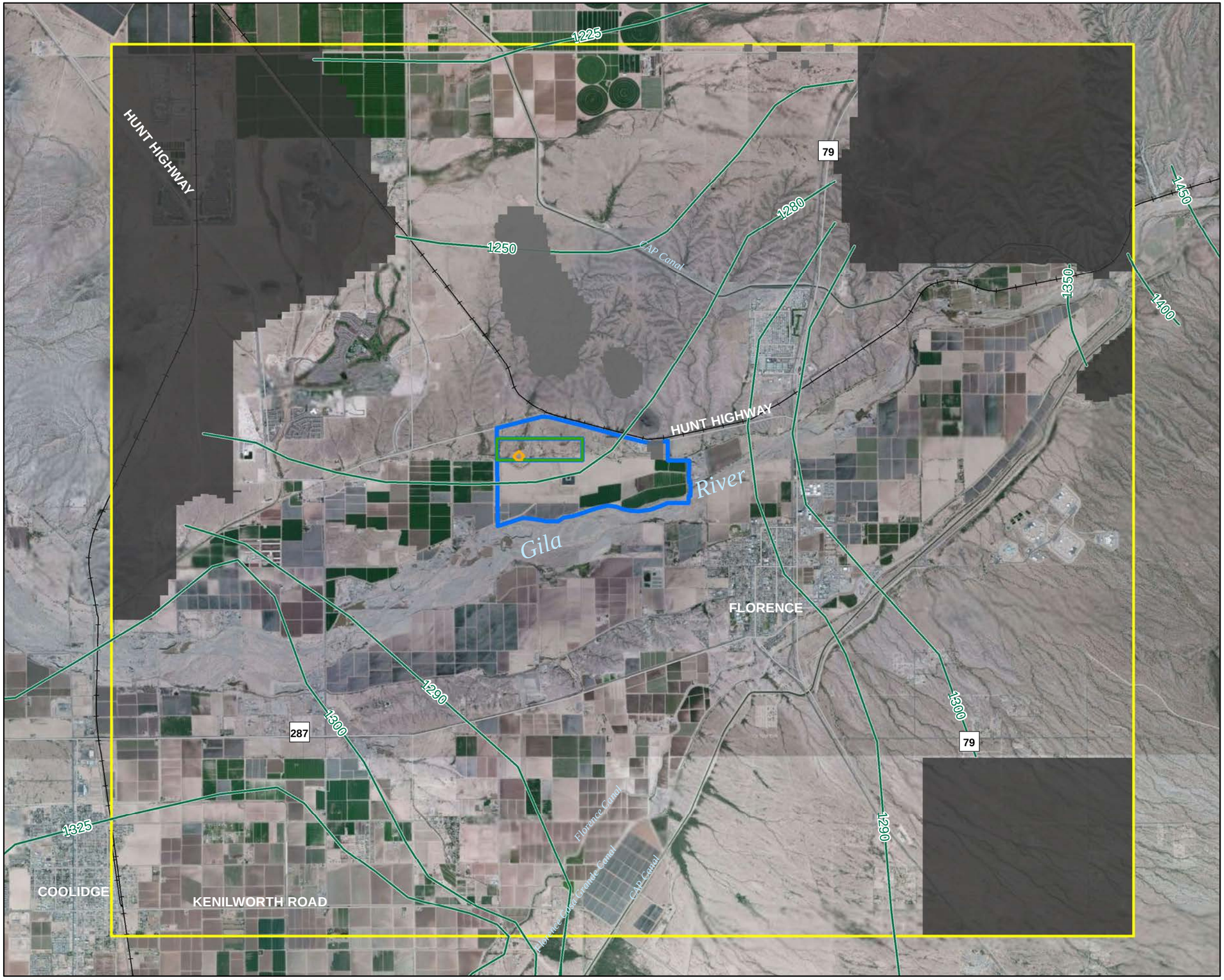

0 3,000 6,000

SCALE IN FEET

EXPLANATION

- DRY CELLS
- GROUNDWATER ELEVATION CONTOUR
- MODEL EXTENT
- PTF WELL FIELD
- NO FLOW CELLS
- STATE MINERAL LEASE BOUNDARY
- CURIS PROPERTY BOUNDARY

Figure 14A-10
MEASURED GROUNDWATER ELEVATIONS
2008

CURIS RESOURCES (ARIZONA) INC.
FLORENCE, ARIZONA

Brown AND Caldwell

HDI CURIS

Path:(BCPhx03) \\BCPHX03\projects\Hunter Dickinson\Curis GIS\MXDs\Temp Permit2012\G140753401A11.mxd Date: 12/4/2012

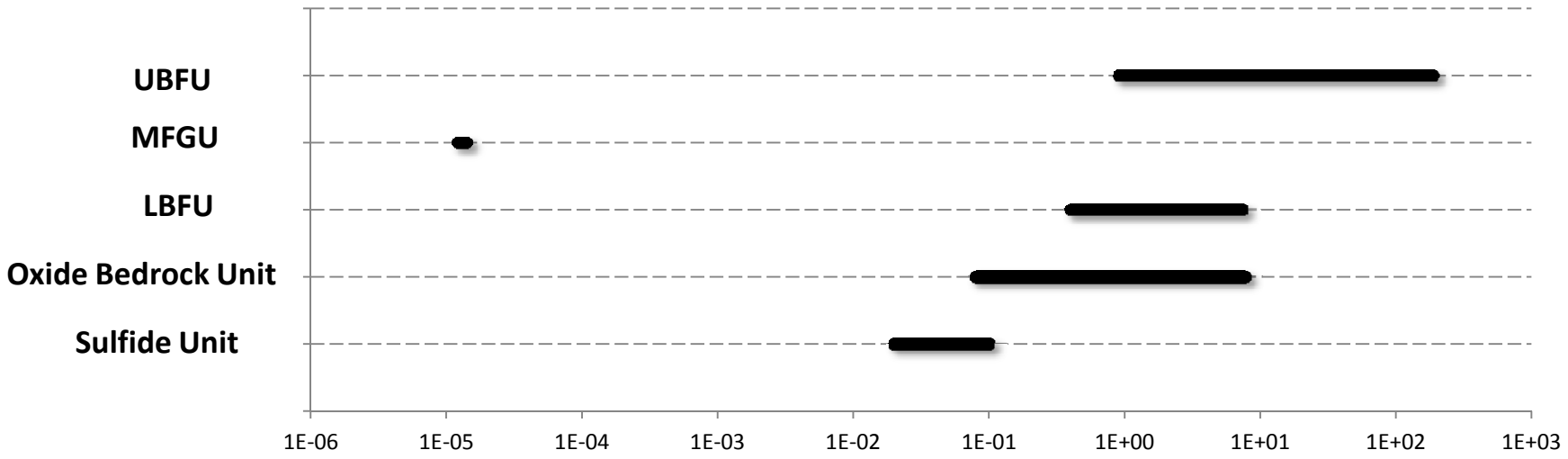

FIGURE 14A-11
HYDRAULIC CONDUCTIVITY
OF BASIN FILL AND BEDROCK UNITS

CURIS RESOURCES (ARIZONA) INC.
FLORENCE, ARIZONA

Brown AND Caldwell

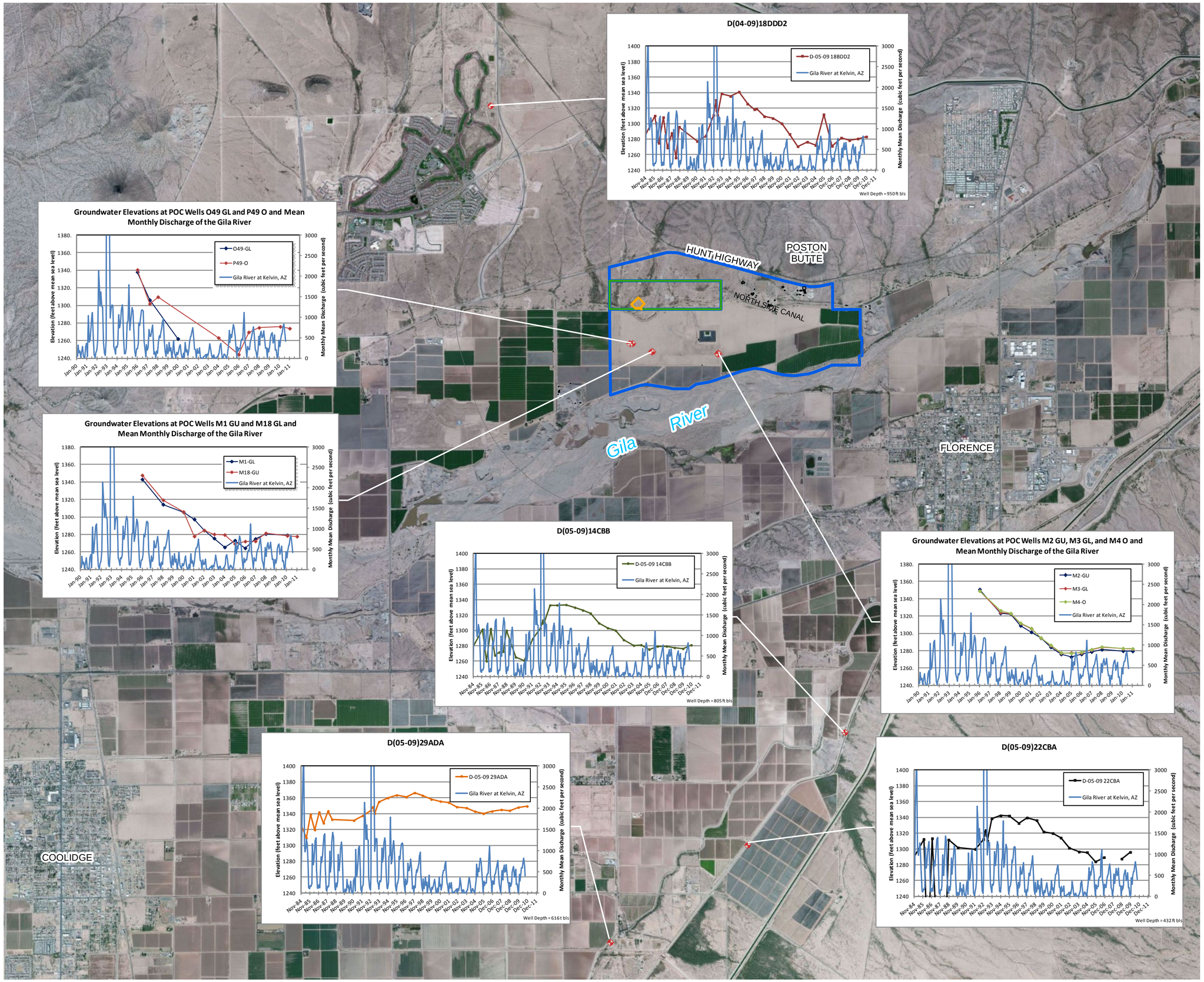

0 1,500 3,000

SCALE IN FEET

EXPLANATION

- HYDROGRAPH WELL
- PTF WELL FIELD
- STATE MINERAL LEASE BOUNDARY
- CURIS PROPERTY BOUNDARY

Groundwater elevation data for wells D(04-09)18DDD2, D(04-09)14CBB, and D(05-09)22CBA obtained from ADWR GWSI database, October 2011.

Groundwater elevation data for wells M1-GL, M18-GU, M2-GU, M3-GL, M4-O, O49-GL AND P49-GL were obtained from Curis Arizona project files.

Gila River discharge data obtained from the USGS October 2011.

HDI CURIS

Brown AND Caldwell

Figure 14A-12
WELL HYDROGRAPHS
CURIS RESOURCES (ARIZONA) INC.
FLORENCE, ARIZONA

J:\Hunter Dickinson\Curis GIS\MXDs\Temp Permit2012\G14075334014A12_Hydrographs.mxd Updated: 2/27/2012

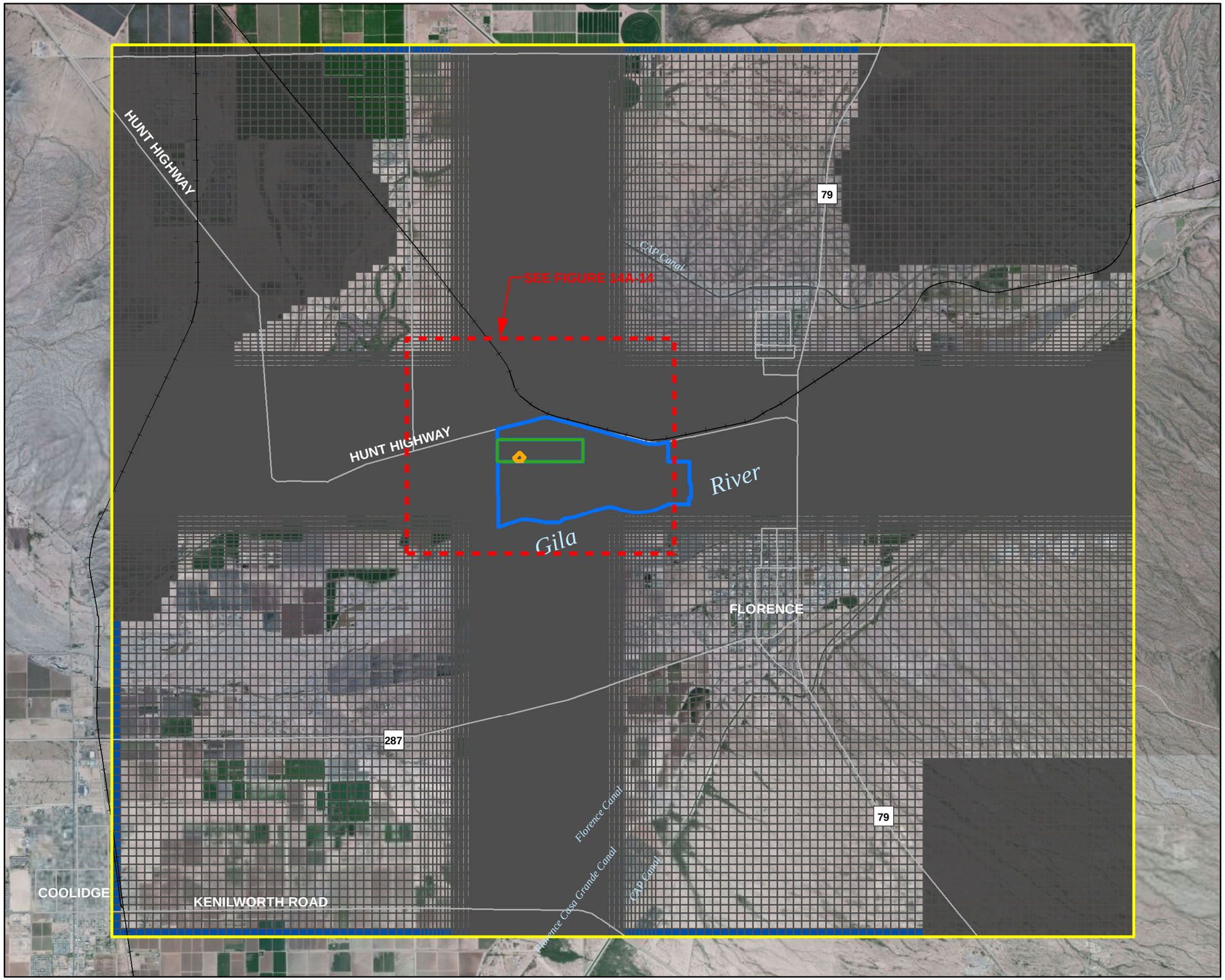

0 3,000 6,000

SCALE IN FEET

EXPLANATION

- MODEL EXTENT
- PTF WELL FIELD
- STATE MINERAL LEASE BOUNDARY
- CURIS PROPERTY BOUNDARY
- MODEL CELL GRID
- GENERAL HEAD BOUNDARY
- NO FLOW CELLS

Figure 14A-13
MODEL GRID WITH
BOUNDARY CONDITIONS

CURIS RESOURCES (ARIZONA) INC.
FLORENCE, ARIZONA

Brown AND Caldwell

HDI CURIS

Path(BCPhx01): P:\Hunter Dickinson\Curis GIS\MXDs\Temp Permit2012\G14075334014A13.mxd Updated: 1/24/2012

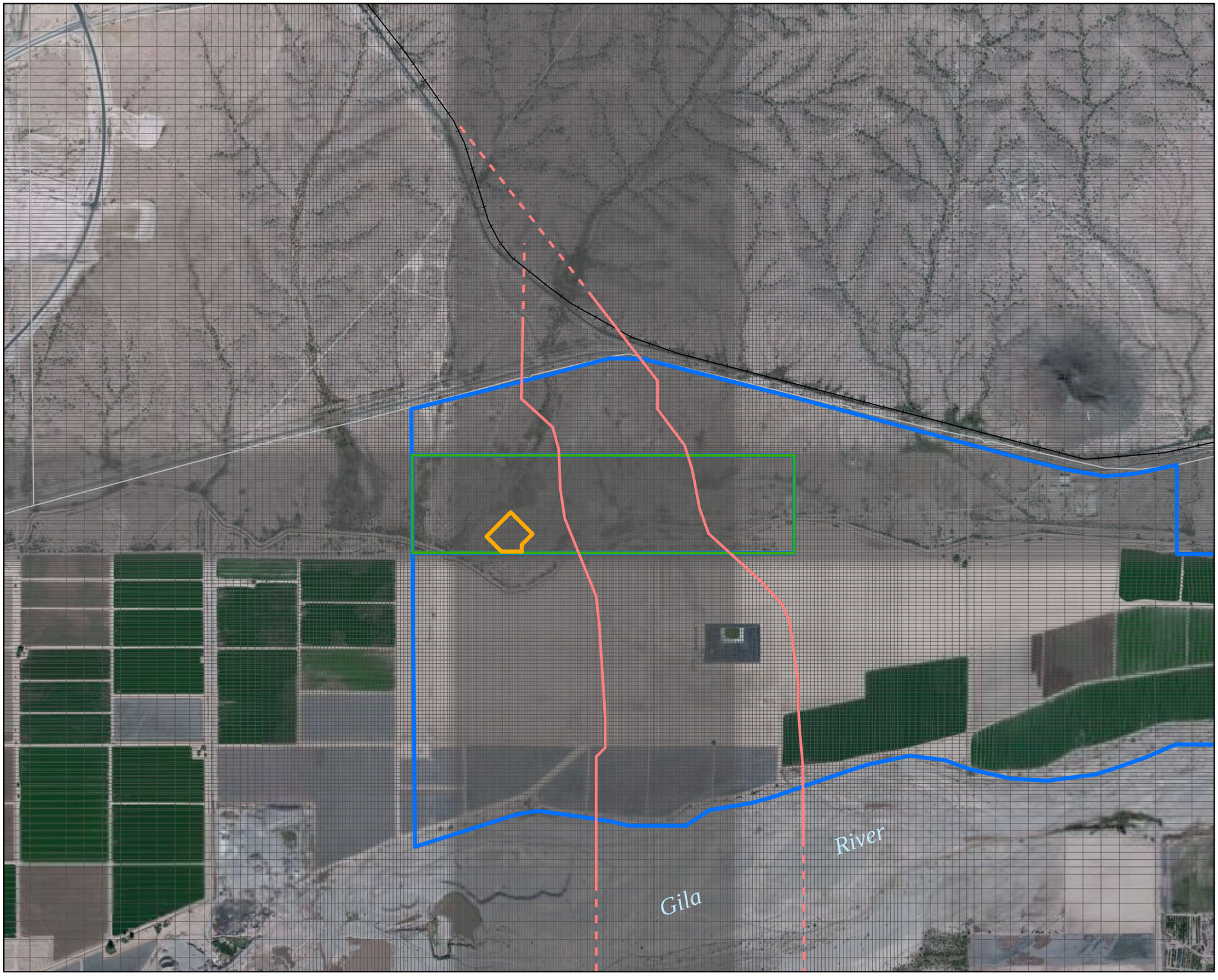

0 750 1,500

SCALE IN FEET

EXPLANATION

- FAULT TRACE
- INFERRED FAULT TRACE
- PTF WELL FIELD
- STATE MINERAL LEASE BOUNDARY
- CURIS PROPERTY BOUNDARY

Figure 14A-14
REFINED MODEL GRID

CURIS RESOURCES (ARIZONA) INC.
FLORENCE, ARIZONA

Brown AND Caldwell

HDI CURIS

Path(BCPhx03): P:\Hunter Dickinson\Curis GIS\MXDs\Temp Permit2012\G14075334014A14.mxd Updated: 1/24/2012

0 3,000 6,000

SCALE IN FEET

EXPLANATION

- MODEL EXTENT
- PTF WELL FIELD
- NO FLOW CELLS
- CURIS PROPERTY BOUNDARY
- STATE MINERAL LEASE BOUNDARY
- GROUNDWATER ELEVATION CONTOUR

Figure 14A-15
WATER LEVEL
INITIAL CONDITIONS - 1984
CURIS RESOURCES (ARIZONA) INC.
FLORENCE, ARIZONA

Brown AND Caldwell

HDI CURIS

\\BCPHX03\projects\Hunter Dickinson\Curis GIS\MXDs\Temp Permit2012\G14075334014A15.mxd Updated: 1/27/2012

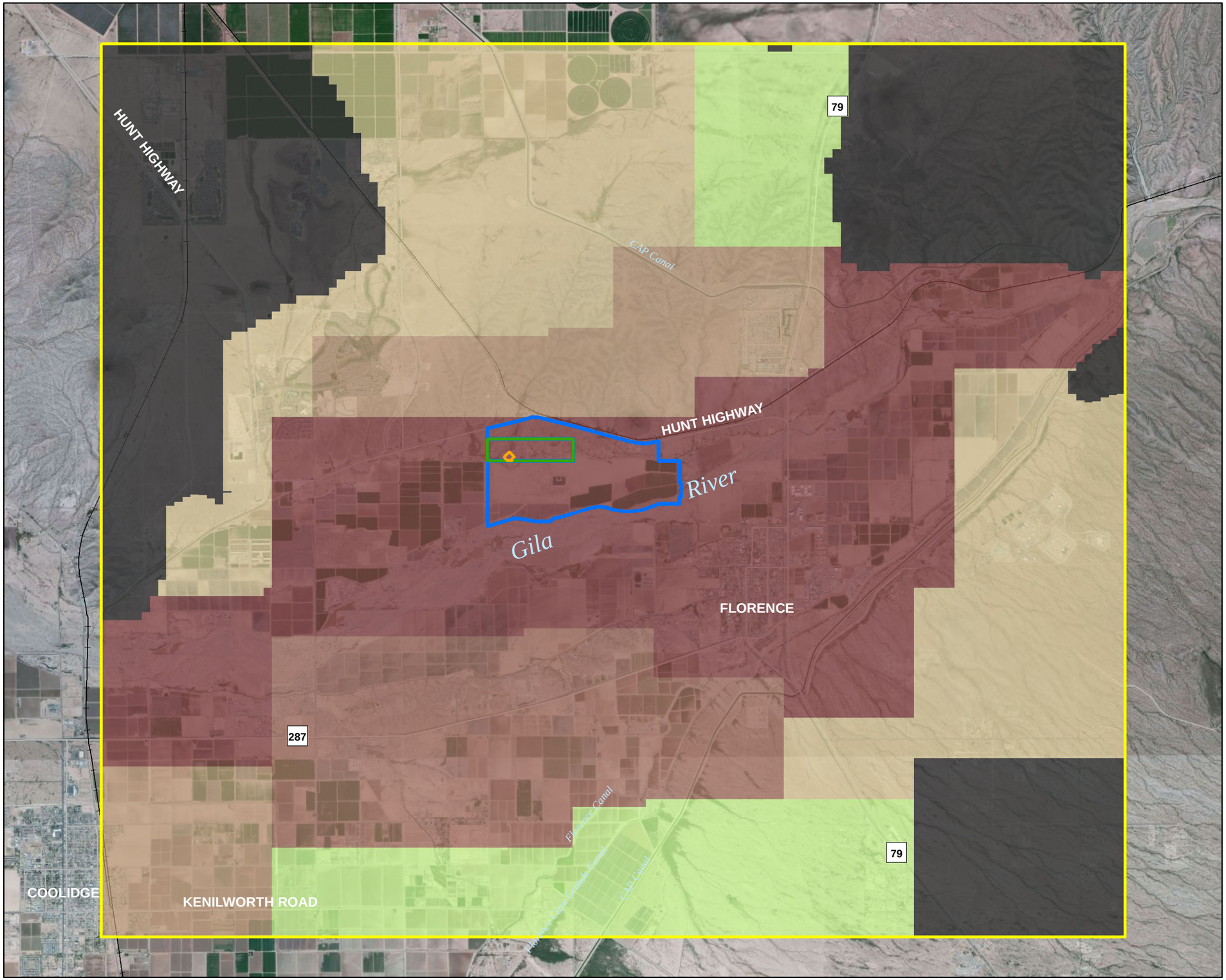

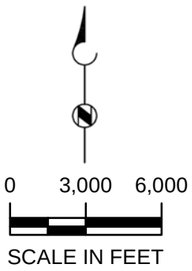

EXPLANATION

- MODEL EXTENT
- PTF WELL FIELD
- NO FLOW CELLS
- STATE MINERAL LEASE BOUNDARY
- CURIS PROPERTY BOUNDARY

HYDRAULIC CONDUCTIVITY (ft/day)

- 0.1
- 0.57
- 1
- 2.51
- 5
- 10
- 15
- 20
- 25
- 30
- 80
- 100
- 130

Figure 14A-16
HYDRAULIC CONDUCTIVITY
MODEL LAYER 1

CURIS RESOURCES (ARIZONA) INC.
FLORENCE, ARIZONA

Brown AND Caldwell

HDI CURIS

\\BCPHX03\projects\Hunter Dickinson\Curis GIS\MXDs\Temp Permit2012\G14075334014A16.mxd Updated: 1/27/2012

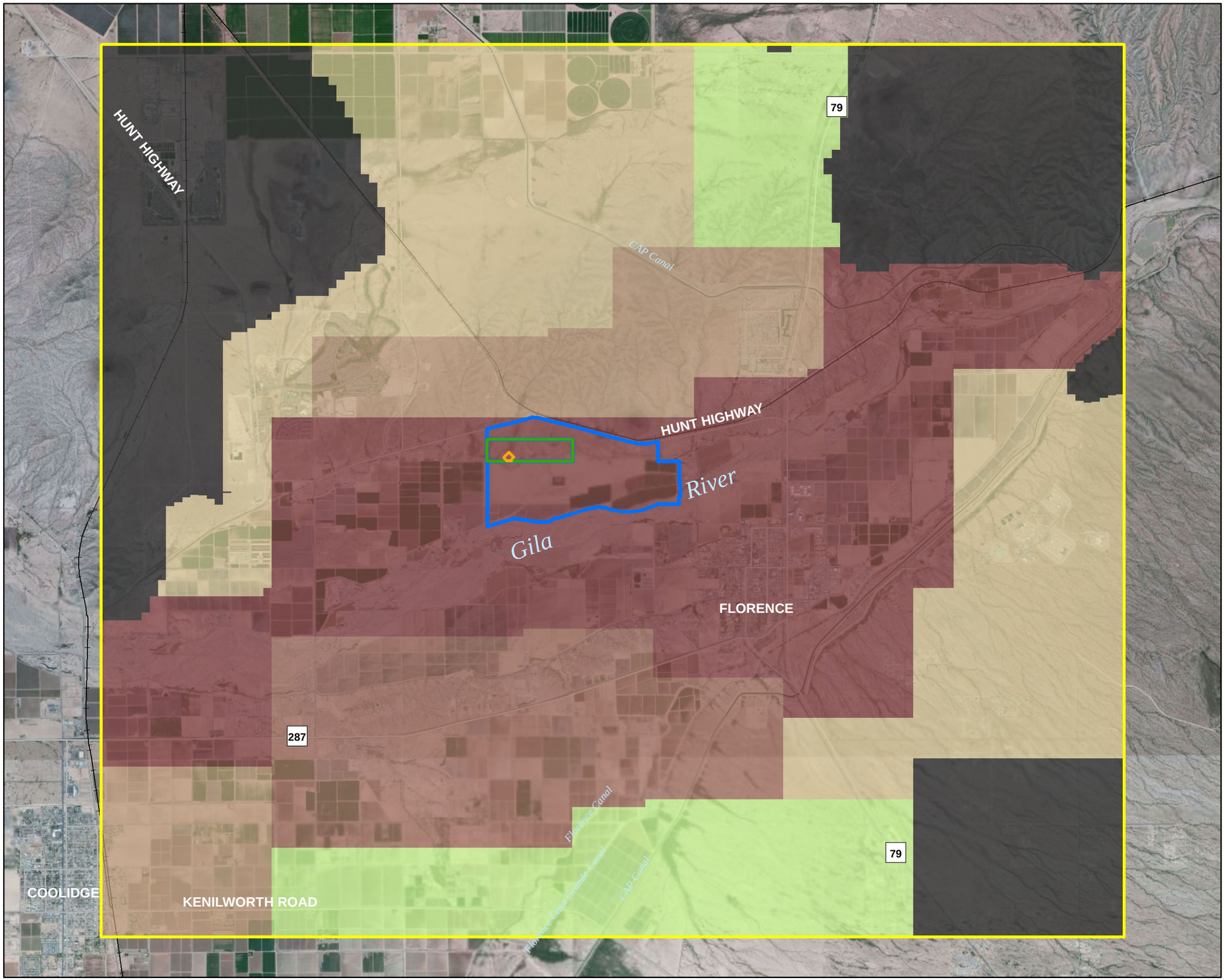

0 3,000 6,000

SCALE IN FEET

EXPLANATION

- MODEL EXTENT
- PTF WELL FIELD
- NO FLOW CELLS
- STATE MINERAL LEASE BOUNDARY
- CURIS PROPERTY BOUNDARY

HYDRAULIC CONDUCTIVITY (ft/day)

- 0.1
- 0.57
- 1
- 2.51
- 5
- 10
- 15
- 20
- 25
- 30
- 80
- 100
- 130

Figure 14A-17
HYDRAULIC CONDUCTIVITY
MODEL LAYER 2

CURIS RESOURCES (ARIZONA) INC.
FLORENCE, ARIZONA

Brown AND Caldwell

HDI CURIS

\\BCPHX03\projects\Hunter Dickinson\Curis GIS\MXDs\Temp Permit2012\G14075334014A16.mxd Updated: 1/27/2012

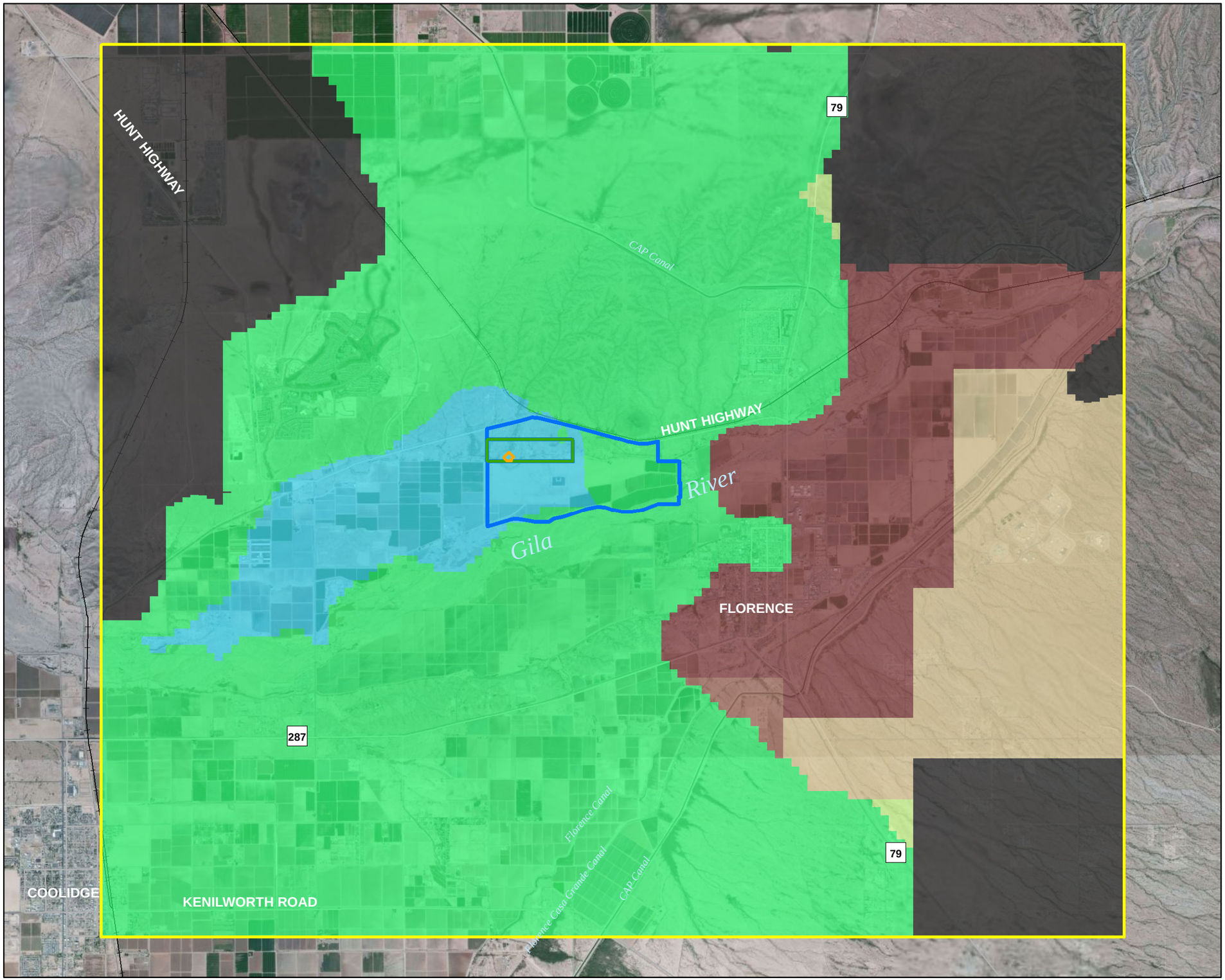

0 3,000 6,000

SCALE IN FEET

EXPLANATION

- MODEL EXTENT
- PTF WELL FIELD
- NO FLOW CELLS
- STATE MINERAL LEASE BOUNDARY
- CURIS PROPERTY BOUNDARY

HYDRAULIC CONDUCTIVITY (ft/day)

- 0.1
- 0.57
- 1
- 2.51
- 5
- 10
- 15
- 20
- 25
- 30
- 80
- 100
- 130

Figure 14A-18
HYDRAULIC CONDUCTIVITY
MODEL LAYER 3

CURIS RESOURCES (ARIZONA) INC.
FLORENCE, ARIZONA

Brown AND Caldwell

HDI CURIS

\\BCPHX03\projects\Hunter Dickinson\Curis GIS\MXDs\Temp Permit2012\G14075334014A16.mxd Updated: 1/27/2012

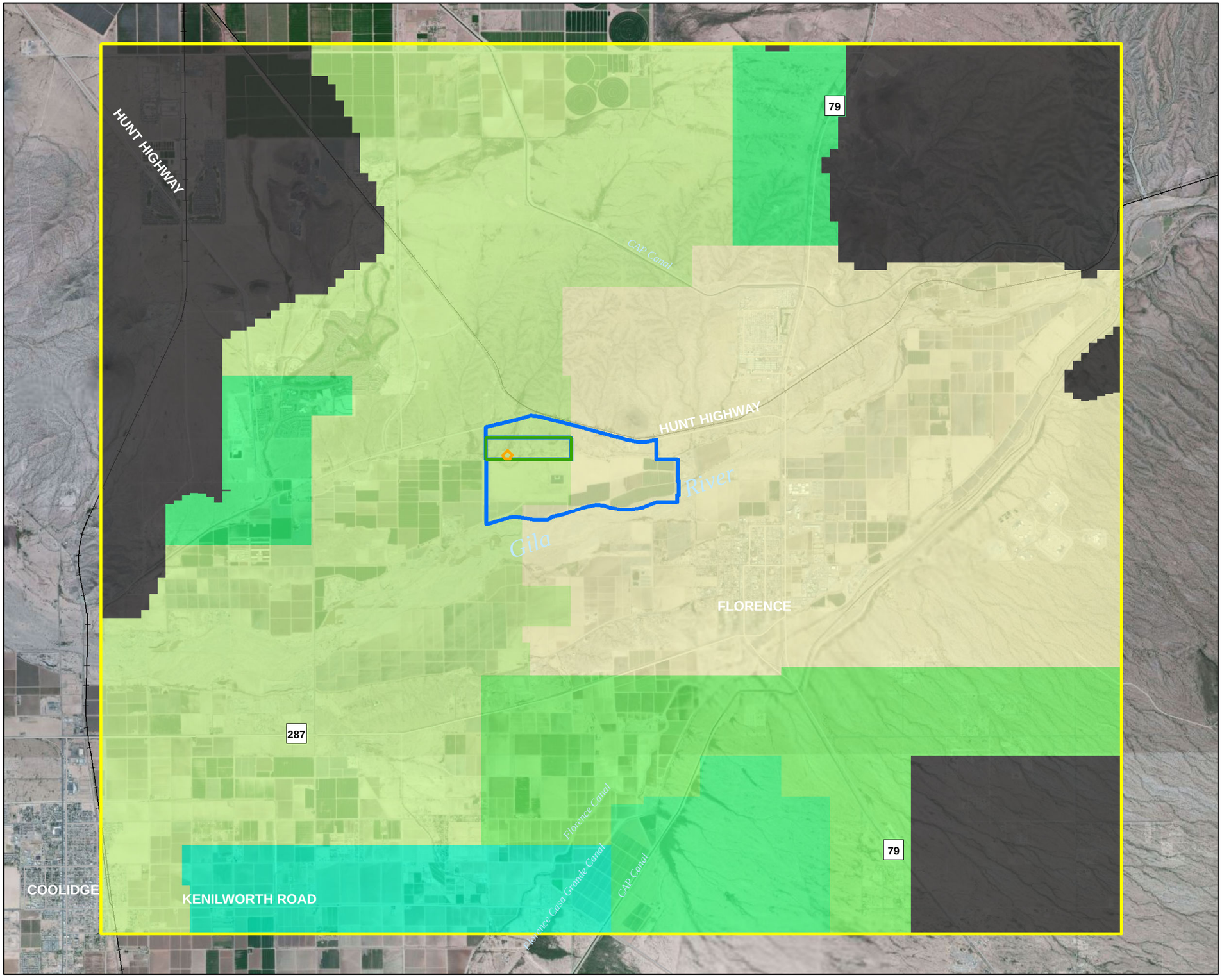

0 3,000 6,000

SCALE IN FEET

EXPLANATION

- MODEL EXTENT
- PTF WELL FIELD
- NO FLOW CELLS
- STATE MINERAL LEASE BOUNDARY
- CURIS PROPERTY BOUNDARY

HYDRAULIC CONDUCTIVITY (ft/day)

- 0.1
- 0.57
- 1
- 2.51
- 5
- 10
- 15
- 20
- 25
- 30
- 80
- 100
- 130

Figure 14A-19
HYDRAULIC CONDUCTIVITY
MODEL LAYER 4

CURIS RESOURCES (ARIZONA) INC.
FLORENCE, ARIZONA

Brown AND Caldwell

HDI CURIS

\\BCPHX03\projects\Hunter Dickinson\Curis GIS\MXDs\Temp Permit2012\G14075334014A16.mxd Updated: 1/27/2012

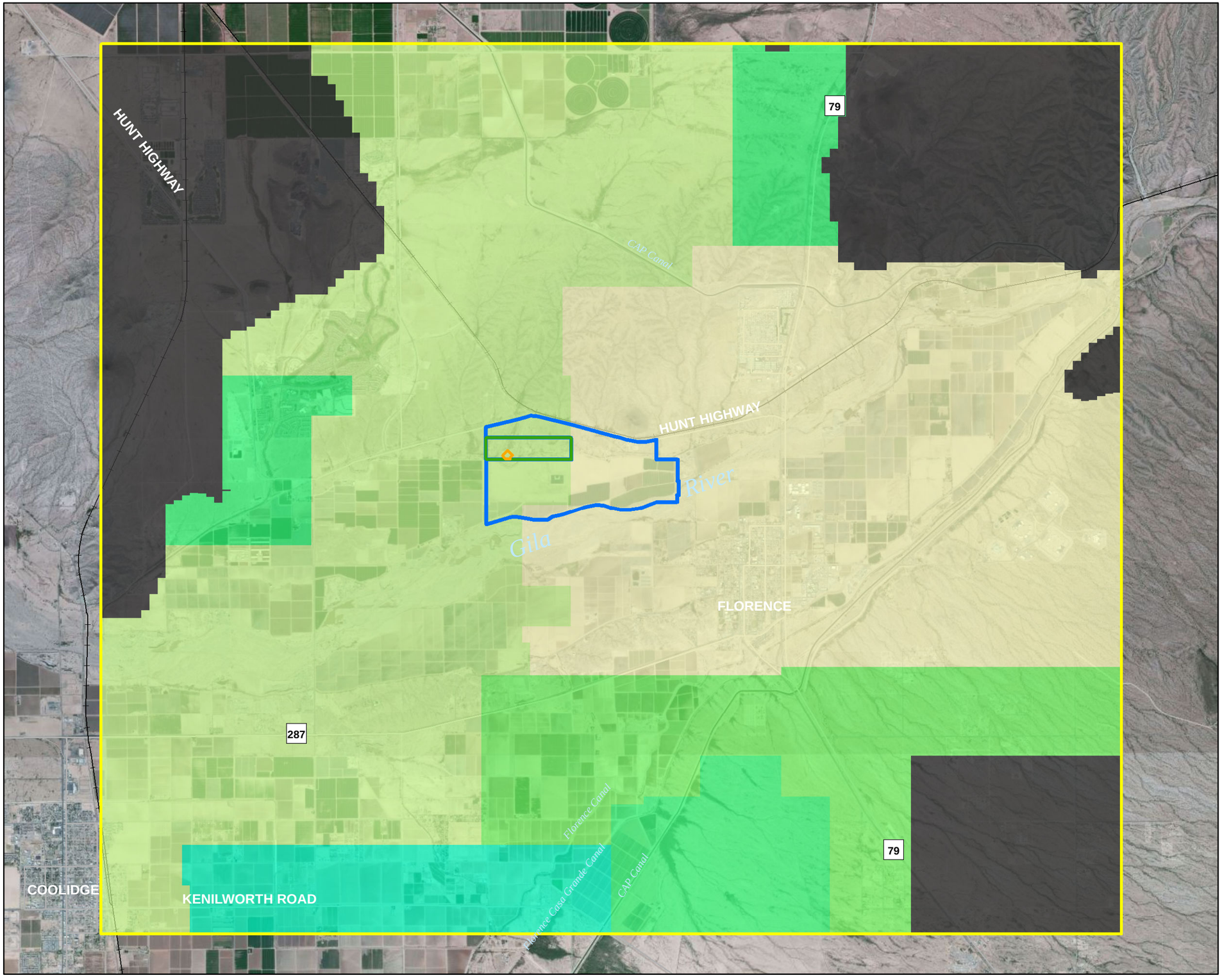

0 3,000 6,000

SCALE IN FEET

EXPLANATION

- MODEL EXTENT
- PTF WELL FIELD
- NO FLOW CELLS
- STATE MINERAL LEASE BOUNDARY
- CURIS PROPERTY BOUNDARY

HYDRAULIC CONDUCTIVITY (ft/day)

- 0.1
- 0.57
- 1
- 2.51
- 5
- 10
- 15
- 20
- 25
- 30
- 80
- 100
- 130

Figure 14A-20
HYDRAULIC CONDUCTIVITY
MODEL LAYER 5

CURIS RESOURCES (ARIZONA) INC.
FLORENCE, ARIZONA

Brown AND Caldwell

HDI CURIS

\\BCPHX03\projects\Hunter Dickinson\Curis GIS\MXDs\Temp Permit2012\G14075334014A16.mxd Updated: 1/27/2012

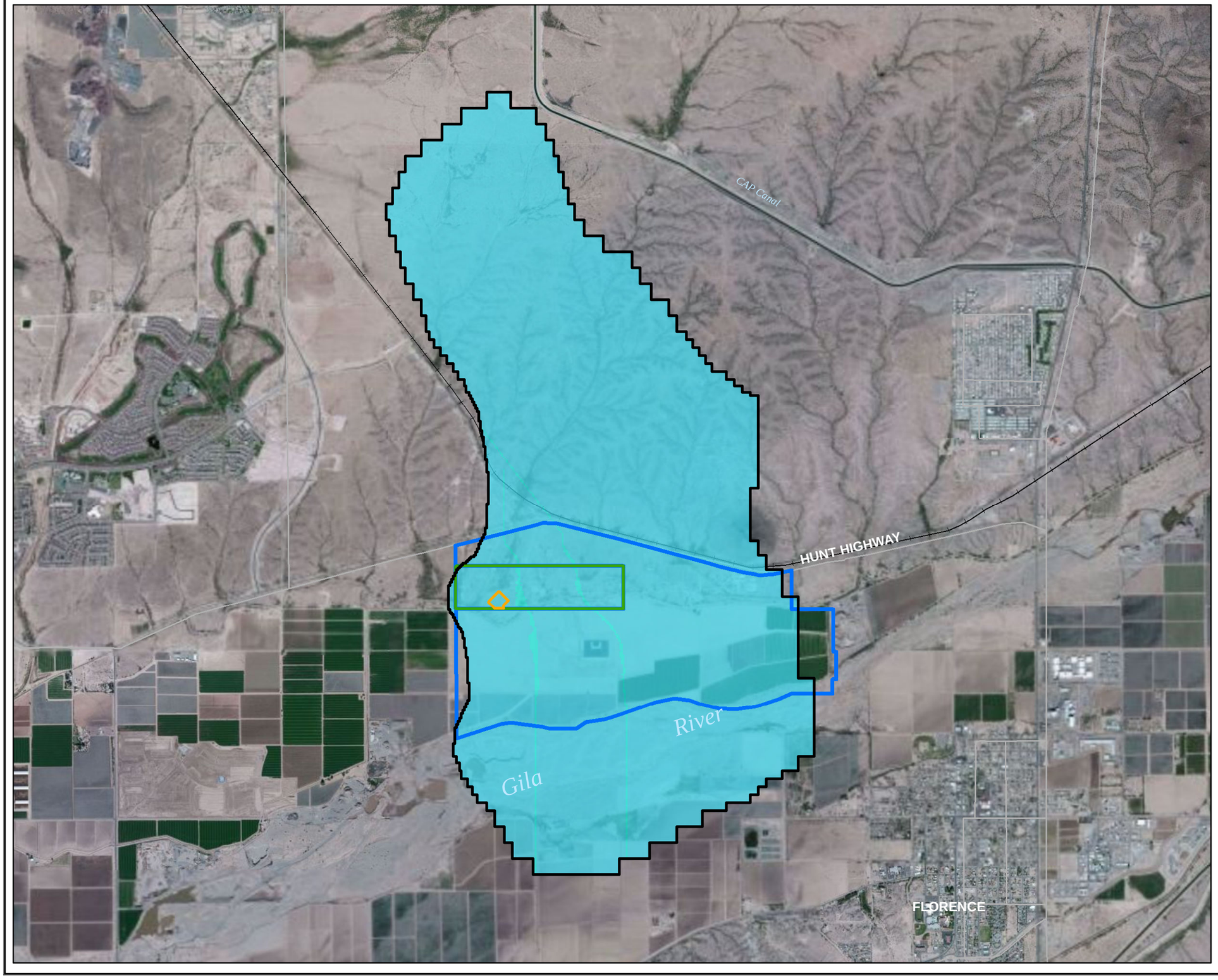

0 1,500 3,000

SCALE IN FEET

EXPLANATION

- ACTIVE AREA
- MODEL EXTENT
- PTF WELL FIELD
- STATE MINERAL LEASE BOUNDARY
- CURIS PROPERTY BOUNDARY

HYDRAULIC CONDUCTIVITY (ft/day)

- 0.1
- 0.57
- 1
- 2.51
- 5
- 10
- 15
- 20
- 25
- 30
- 80
- 100
- 130

Figure 14A-21
HYDRAULIC CONDUCTIVITY
MODEL LAYER 6

CURIS RESOURCES (ARIZONA) INC.
FLORENCE, ARIZONA

Brown AND Caldwell

HDI CURIS

Path(BCPhx03): \\BCPHX03\projects\Hunter Dickinson\Curis GIS\MXDs\Temp Permit2012\G14075334014A21.mxd Date: 1/24/2012

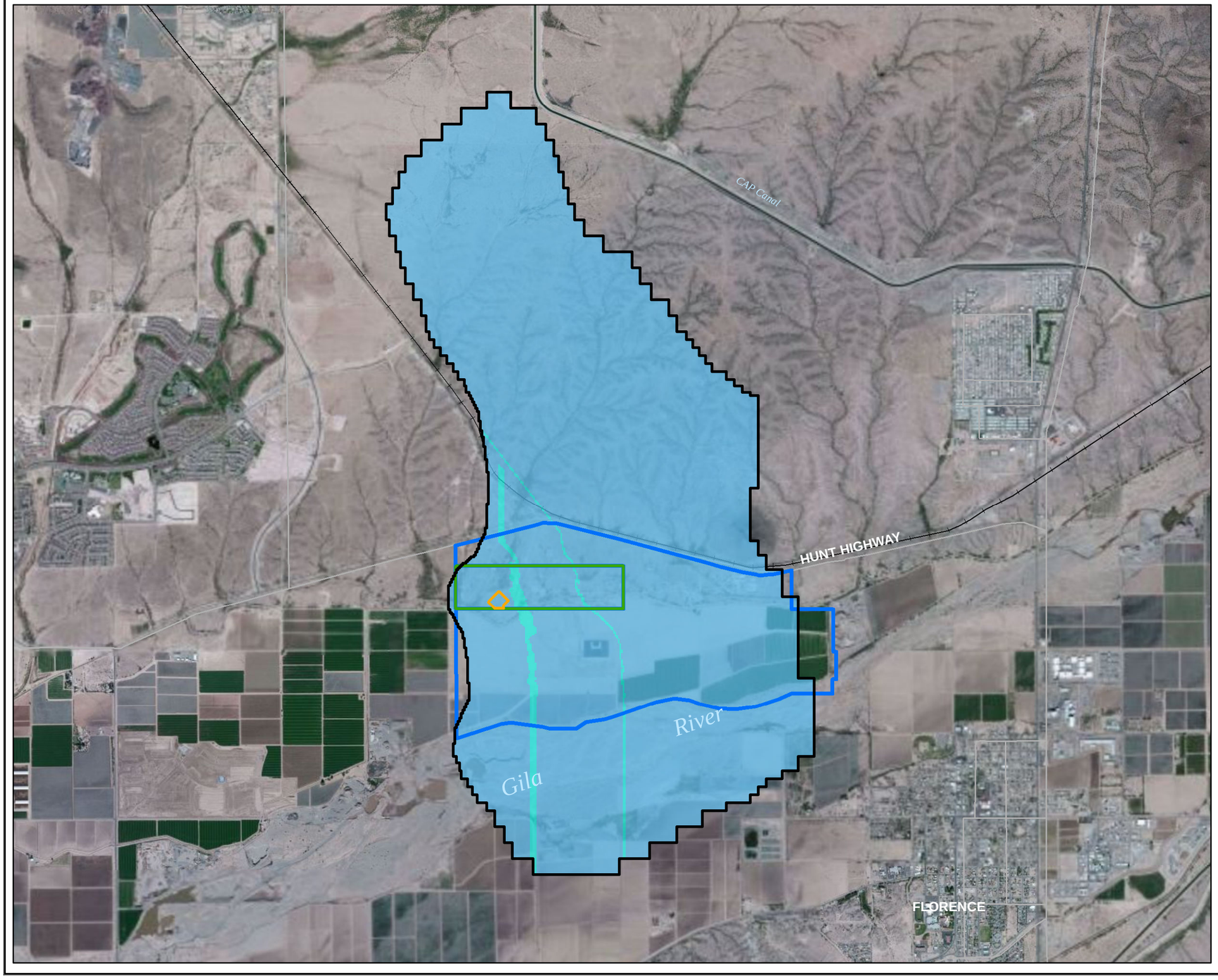

0 1,500 3,000

SCALE IN FEET

EXPLANATION

- ACTIVE AREA
- MODEL EXTENT
- PTF WELL FIELD
- STATE MINERAL LEASE BOUNDARY
- CURIS PROPERTY BOUNDARY

HYDRAULIC CONDUCTIVITY (ft/day)

- 0.1
- 0.57
- 1
- 2.51
- 5
- 10
- 15
- 20
- 25
- 30
- 80
- 100
- 130

Figure 14A-22
HYDRAULIC CONDUCTIVITY
MODEL LAYER 7

CURIS RESOURCES (ARIZONA) INC.
FLORENCE, ARIZONA

Brown AND Caldwell

HDI CURIS

Path(BCPhx03): \\BCPHX03\projects\Hunter Dickinson\Curis GIS\MXDs\Temp Permit2012\G14075334014A21.mxd Date: 1/24/2012

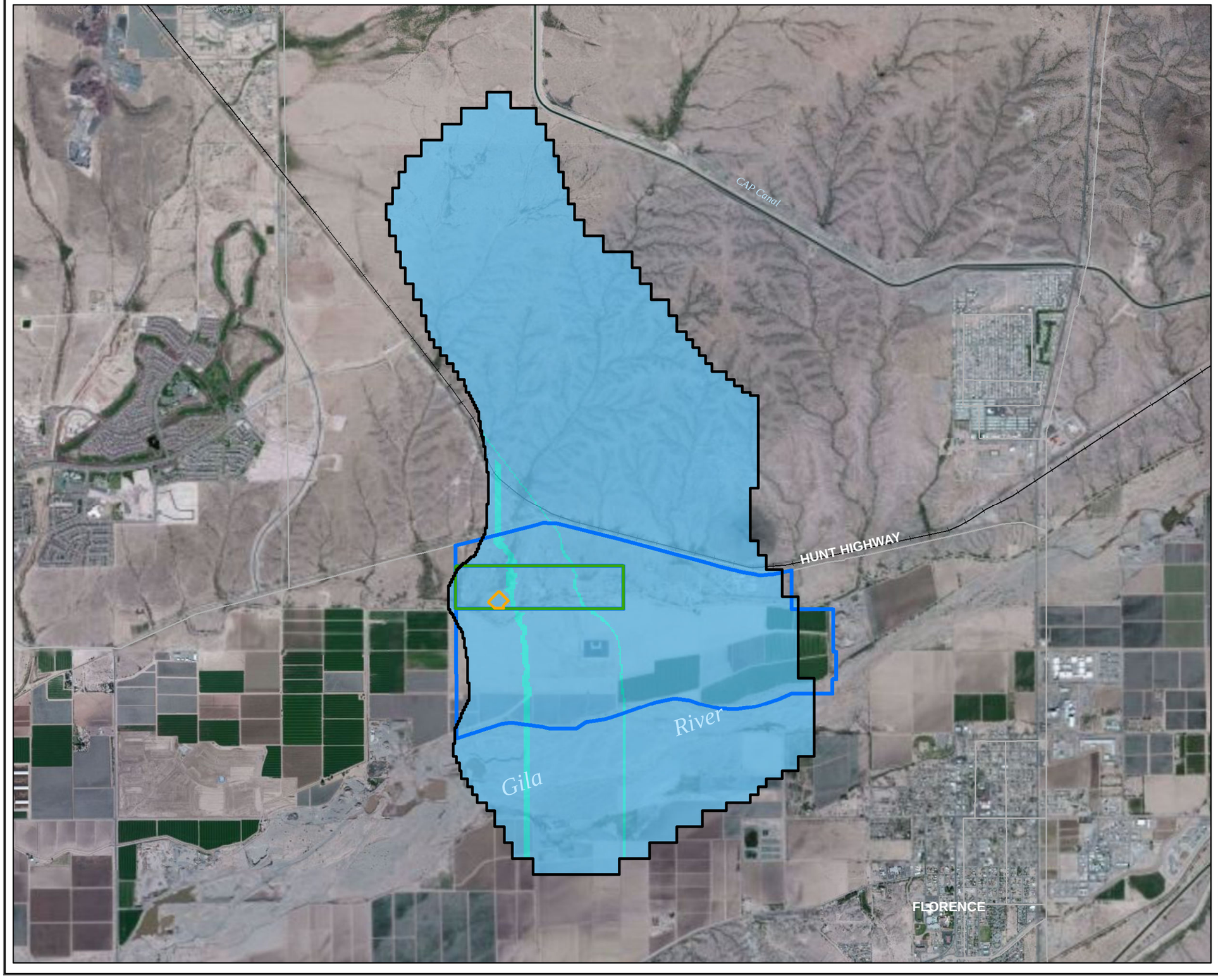

0 1,500 3,000

SCALE IN FEET

EXPLANATION

- ACTIVE AREA
- MODEL EXTENT
- PTF WELL FIELD
- STATE MINERAL LEASE BOUNDARY
- CURIS PROPERTY BOUNDARY

HYDRAULIC CONDUCTIVITY (ft/day)

- 0.1
- 0.57
- 1
- 2.51
- 5
- 10
- 15
- 20
- 25
- 30
- 80
- 100
- 130

Figure 14A-23
HYDRAULIC CONDUCTIVITY
MODEL LAYER 8

CURIS RESOURCES (ARIZONA) INC.
FLORENCE, ARIZONA

Brown AND Caldwell

HDI CURIS

Path(BCPhx03): \\BCPHX03\projects\Hunter Dickinson\Curis GIS\MXDs\Temp Permit2012\G14075334014A21.mxd Date: 1/24/2012

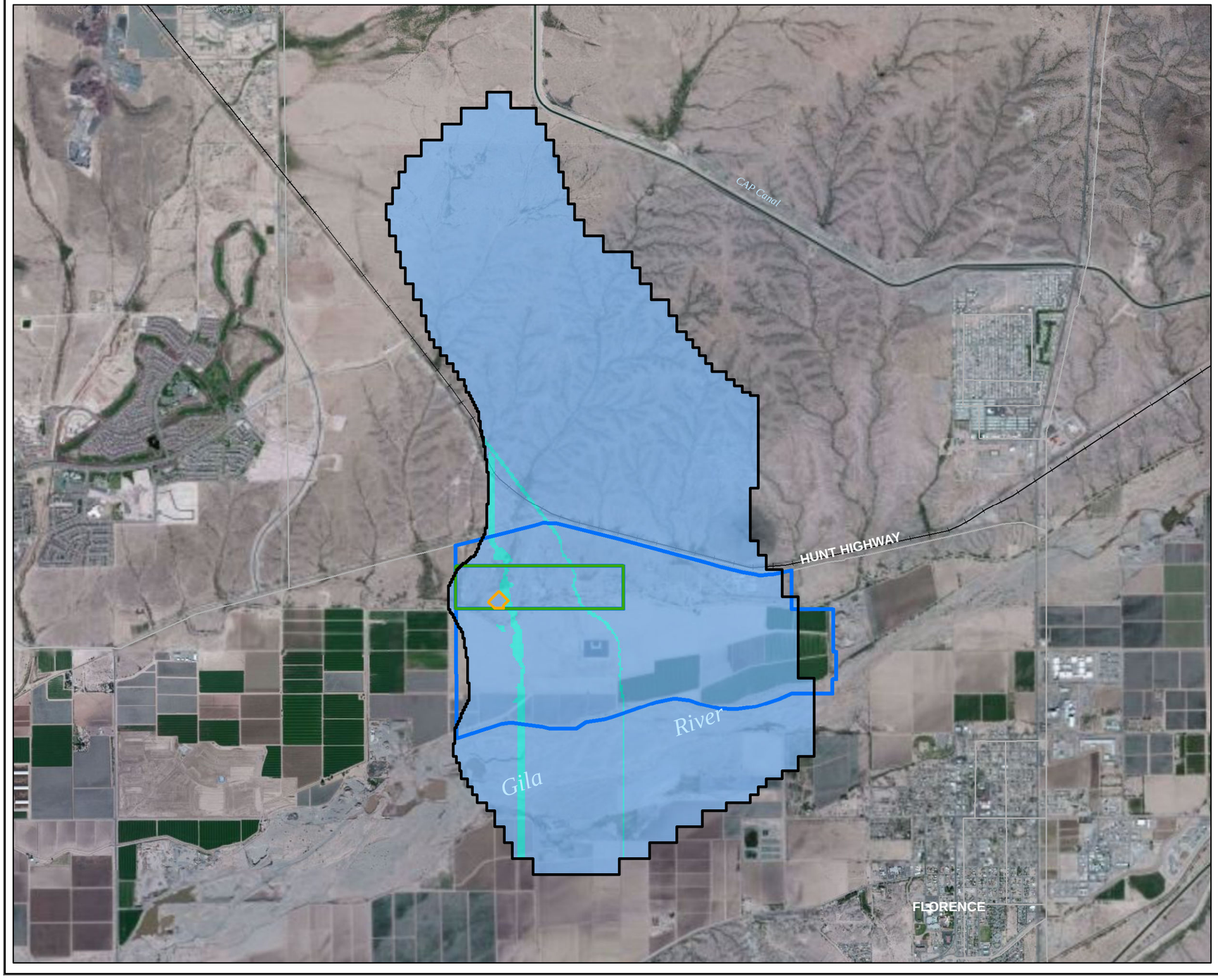

0 1,500 3,000

SCALE IN FEET

EXPLANATION

- ACTIVE AREA
- MODEL EXTENT
- PTF WELL FIELD
- STATE MINERAL LEASE BOUNDARY
- CURIS PROPERTY BOUNDARY

HYDRAULIC CONDUCTIVITY (ft/day)

- 0.1
- 0.57
- 1
- 2.51
- 5
- 10
- 15
- 20
- 25
- 30
- 80
- 100
- 130

Figure 14A-24
HYDRAULIC CONDUCTIVITY
MODEL LAYER 9

CURIS RESOURCES (ARIZONA) INC.
FLORENCE, ARIZONA

Brown AND Caldwell

HDI CURIS

Path(BCPhx03): \\BCPHX03\projects\Hunter Dickinson\Curis GIS\MXDs\Temp Permit2012\G14075334014A21.mxd Date: 1/24/2012

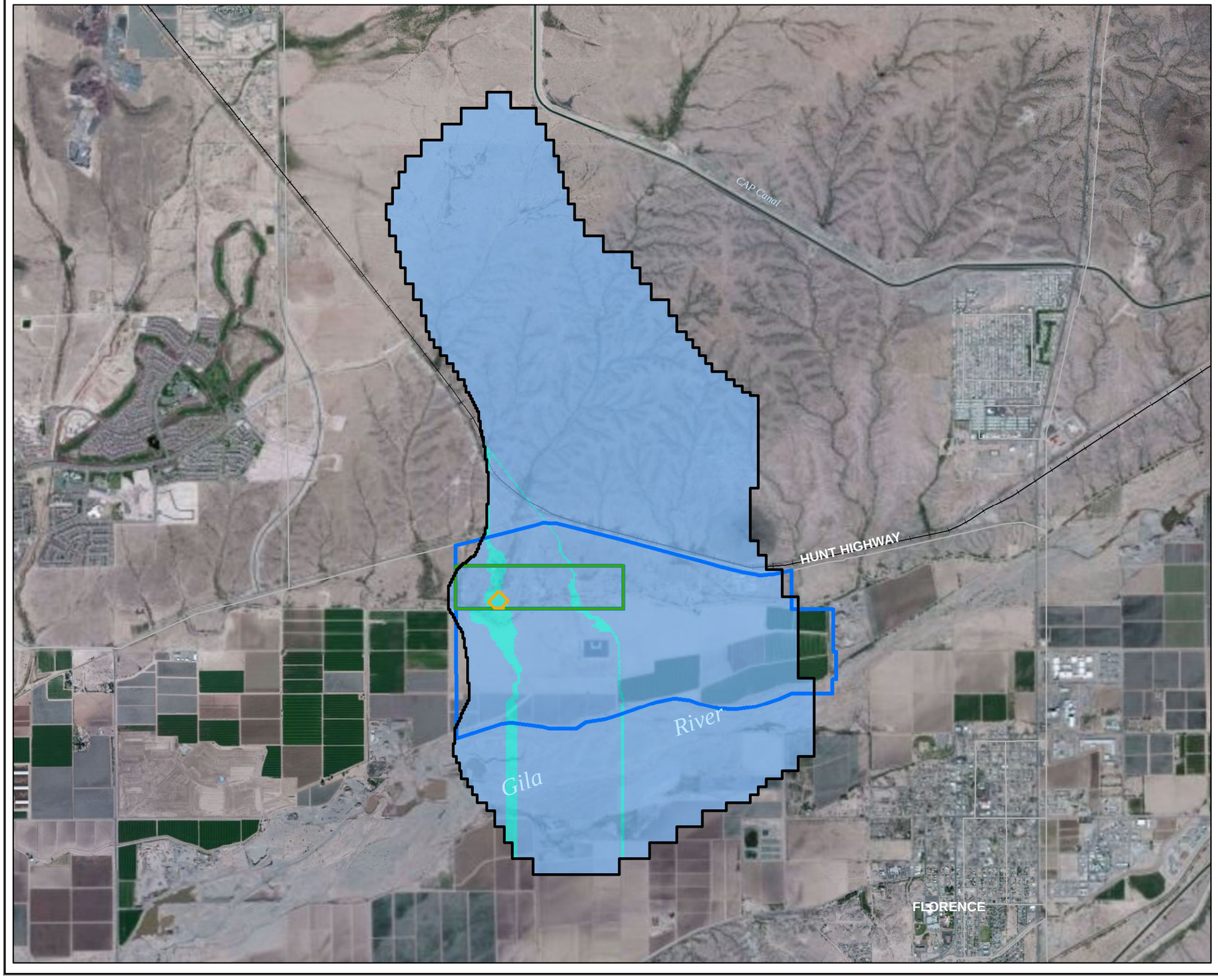

0 1,500 3,000

SCALE IN FEET

EXPLANATION

- ACTIVE AREA
- MODEL EXTENT
- PTF WELL FIELD
- STATE MINERAL LEASE BOUNDARY
- CURIS PROPERTY BOUNDARY

HYDRAULIC CONDUCTIVITY (ft/day)

- 0.1
- 0.57
- 1
- 2.51
- 5
- 10
- 15
- 20
- 25
- 30
- 80
- 100
- 130

Figure 14A-25
HYDRAULIC CONDUCTIVITY
MODEL LAYER 10

CURIS RESOURCES (ARIZONA) INC.
FLORENCE, ARIZONA

Brown AND Caldwell

HDI CURIS

Path(BCPhx03): \\BCPHX03\projects\Hunter Dickinson\Curis GIS\MXDs\Temp Permit2012\G14075334014A21.mxd Date: 1/24/2012

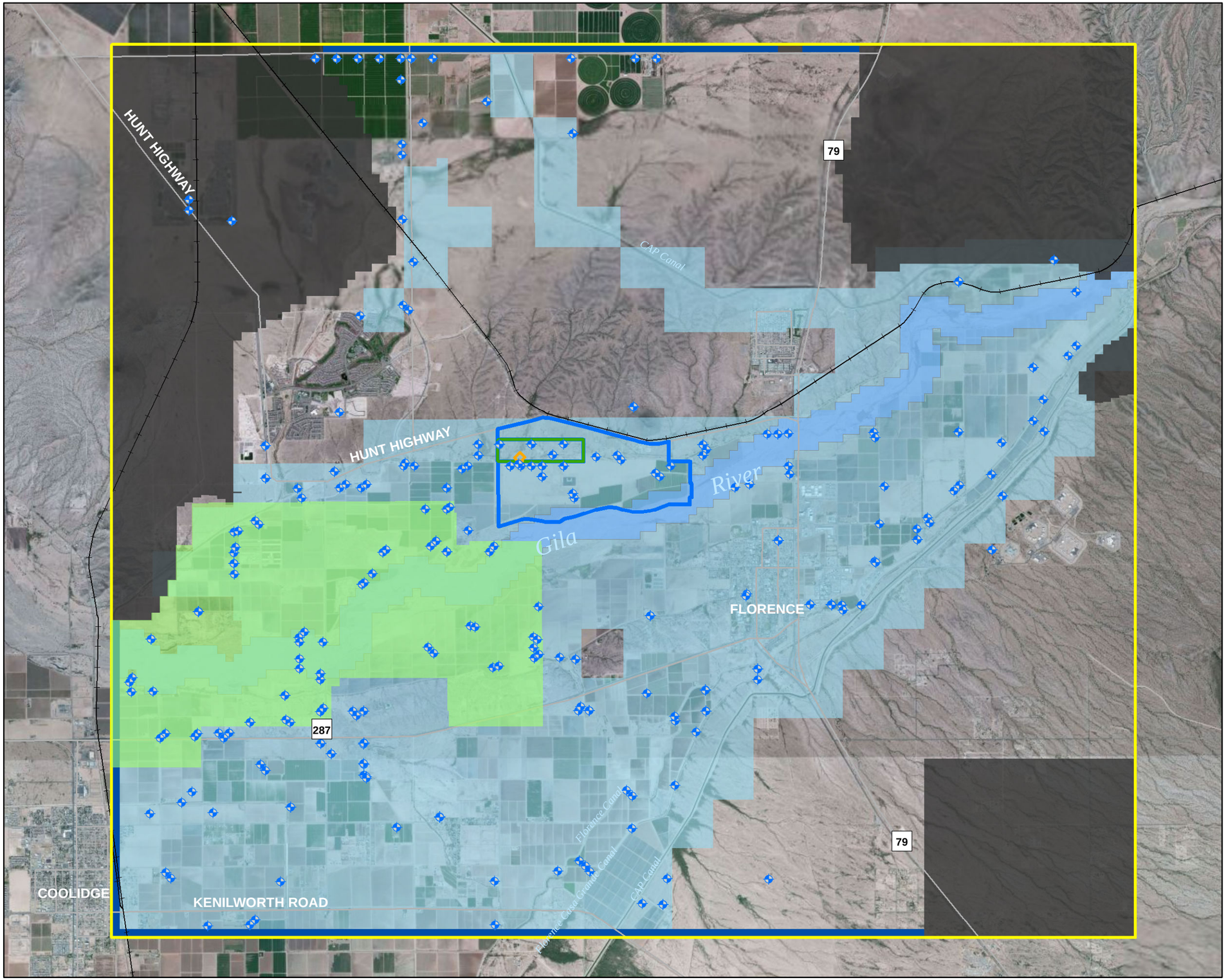

0 3,000 6,000

SCALE IN FEET

EXPLANATION

- WELL
- EVAPOTRANSPIRATION
- MODEL EXTENT
- PTF WELL FIELD
- STATE MINERAL LEASE BOUNDARY
- CURIS PROPERTY BOUNDARY
- NO FLOW CELLS
- RIVER RECHARGE
- RECHARGE

Figure 14A-26
REGIONAL WATER BUDGET
CURIS RESOURCES (ARIZONA) INC.
FLORENCE, ARIZONA

Brown AND Caldwell

HDI CURIS

\\BCPHX03\projects\Hunter Dickinson\Curis GIS\MXDs\Temp Permit2012\G140753340l4A26_RegionalWBudget.mxd Updated: 1/27/2012

0 3,000 6,000

SCALE IN FEET

EXPLANATION

RESIDUALS (YEARS 2000-2010)

Residual

- 75 - -60
- -59 - -40
- -39 - -20
- -19 - 0
- 1 - 20
- 21 - 40
- 41 - 60
- 61 - 75
- MODEL EXTENT
- PTF WELL FIELD
- STATE MINERAL LEASE BOUNDARY
- CURIS PROPERTY BOUNDARY
- NO FLOW CELLS
- CALIBRATED WATER LEVEL

Figure 14A-27

CALIBRATED WATER LEVELS AND RESIDUALS

CURIS RESOURCES (ARIZONA) INC.
FLORENCE, ARIZONA

Brown AND Caldwell

HDI CURIS

\\BCPHX03\projects\Hunter Dickinson\Curis GIS\MXDs\Temp Permit2012\G140753340CalibratedWLResiduals.mxd Updated: 1/27/2012

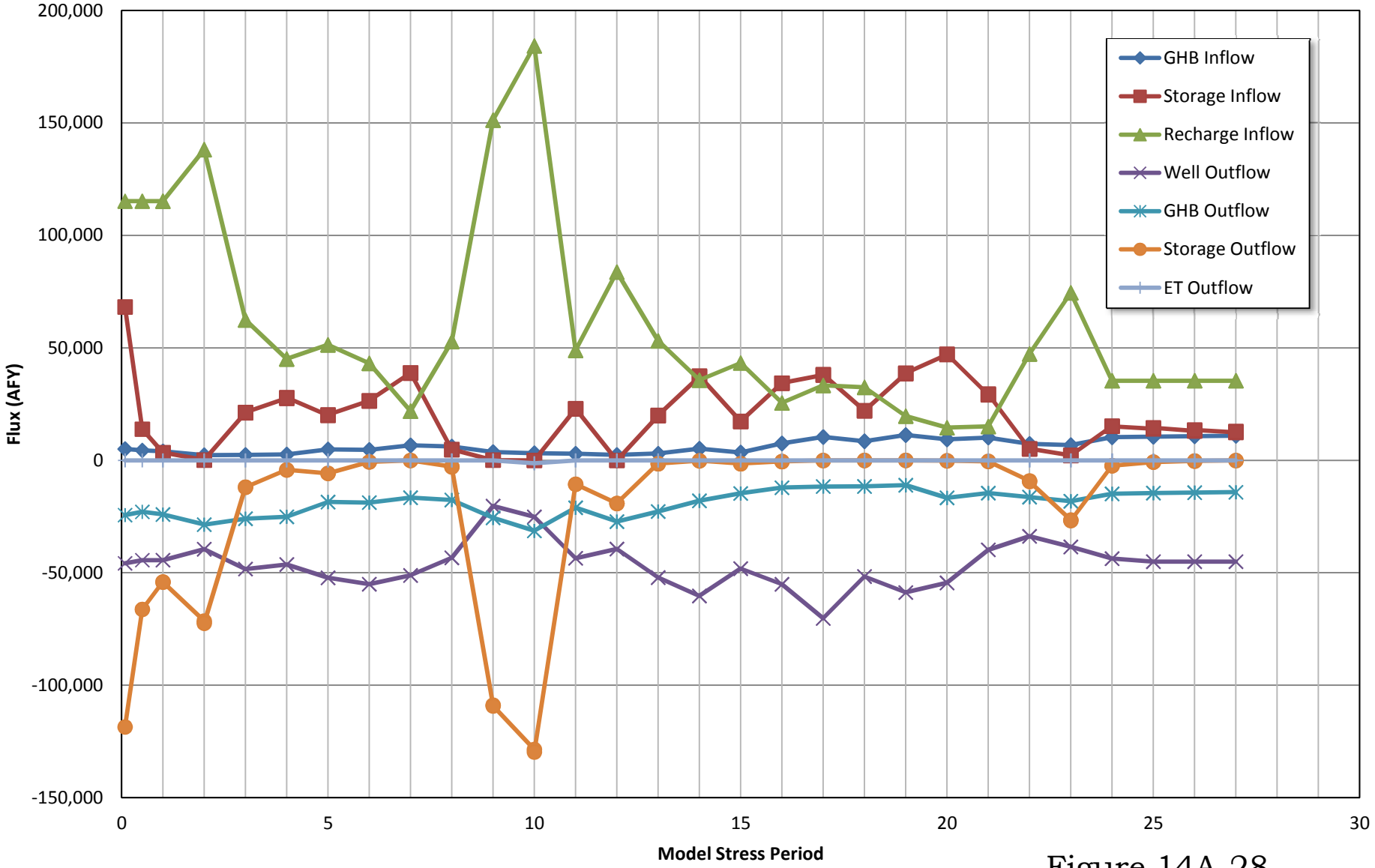

Figure 14A-28
Simulated Transient
Water Budget
Curis Resources (Arizona) Inc.
Florence, Arizona

Brown AND Caldwell

J:\Hunter Dickinson\138799 - Curis Florence Copper Permitting\Working\Significant Amendment\Figures\Modeling Report\Water Budget_Figure.xlsx 1/24/2012

0 250 500

SCALE IN FEET

EXPLANATION

- INITIAL SULFATE CONCENTRATION DISTRIBUTION 750 mg/L
- PTF WELL FIELD
- STATE MINERAL LEASE BOUNDARY
- CURIS PROPERTY BOUNDARY

Figure 14A-29
INITIAL CONCENTRATIONS
SULFATE DISTRIBUTION
TRANSPORT SIMULATIONS
CURIS RESOURCES (ARIZONA) INC.
FLORENCE, ARIZONA

Brown AND Caldwell

HDI CURIS

\\BCPHX03\projects\Hunter Dickinson\Curis GIS\MXDs\Temp Permit2012\G14075334027.mxd Updated: 1/27/2012

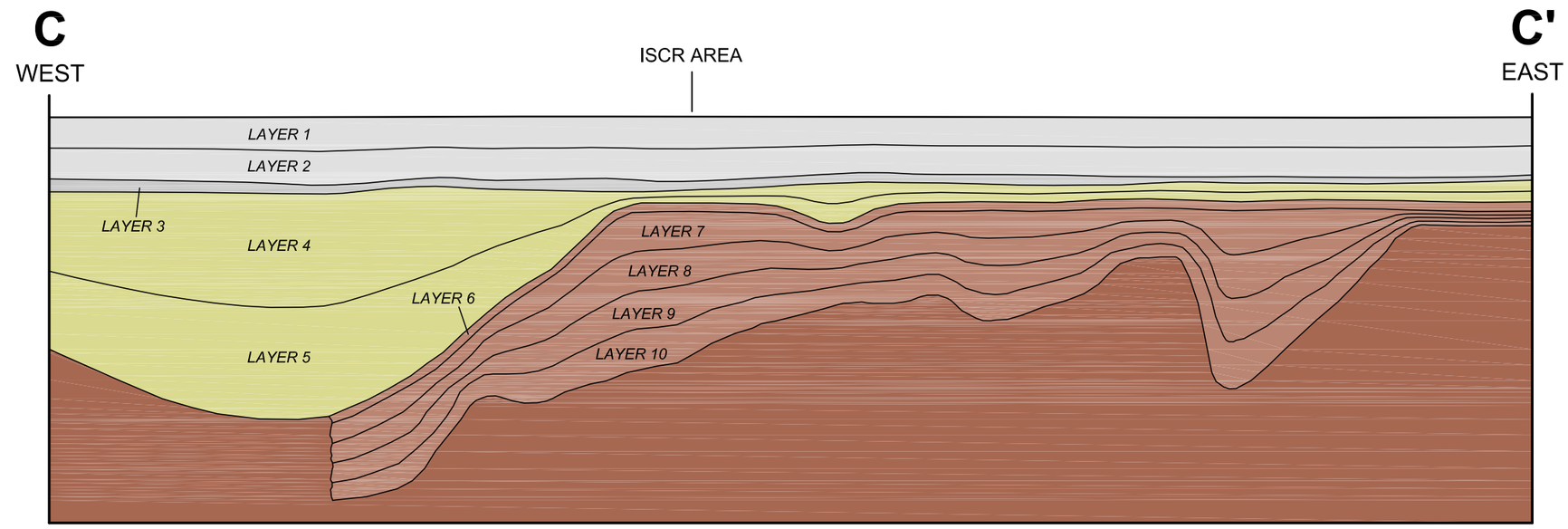

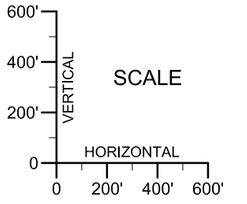

NO VERTICAL EXAGGERATION

KEYMAP

NOT TO SCALE

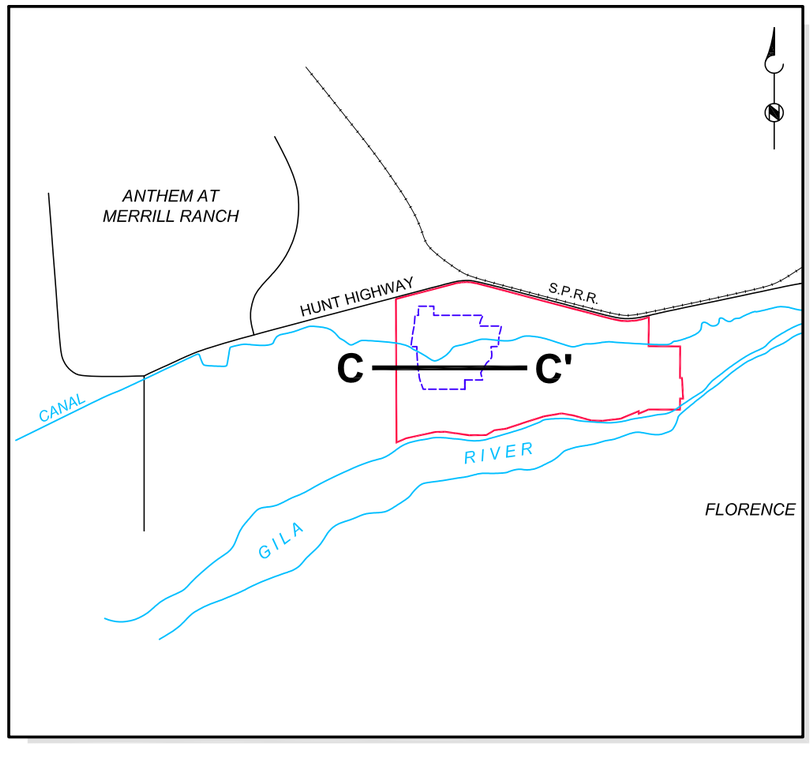

EXPLANATION

- UPPER BASIN FILL UNIT (UBFU)
- MIDDLE FINE GRAINED UNIT (MFGU)
- LOWER BASIN FILL UNIT (LBFU)
- OXIDE BEDROCK ZONE
- SULFIDE BEDROCK ZONE

Brown AND Caldwell

HDI CURIS

Figure 14A-30

MODEL LAYERING IN THE VICINITY OF THE ISCR AREA

CURIS RESOURCES (ARIZONA) INC.
FLORENCE, ARIZONA

P:\Hunter Dickinson\140913 - Curis - 2011 Mine Plan and GServ\Drawings\ES\140913026.dwg Feb 07, 2012 - 11:08am jcollier

0 200 400

SCALE IN FEET

EXPLANATION

- SIMULATED SULFATE DISTRIBUTION AND CONCENTRATION ABOVE BACKGROUND (mg/L)
- PTF WELL FIELD
- CURIS PROPERTY BOUNDARY
- STATE MINERAL LEASE BOUNDARY

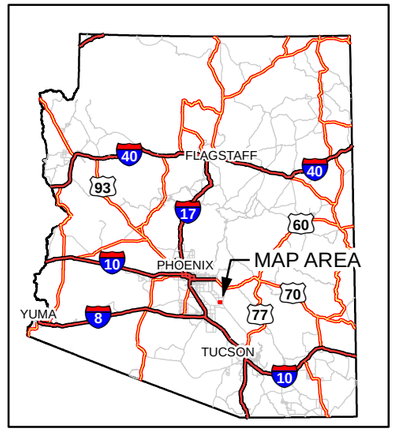

Figure 14A-31
SIMULATED SULFATE DISTRIBUTION
MODEL LAYER 5 (LOWER LBFU)
5 YEARS AFTER CLOSURE
CURIS RESOURCES (ARIZONA) INC.
FLORENCE, ARIZONA

Brown AND Caldwell

HDI CURIS

\\BCPHX03\projects\Hunter Dickinson\Curis GIS\MXDs\Temp Permit2012\G140753340_Sulfate L5_ Lower LBFU updated.mxd Updated: 1/26/2012

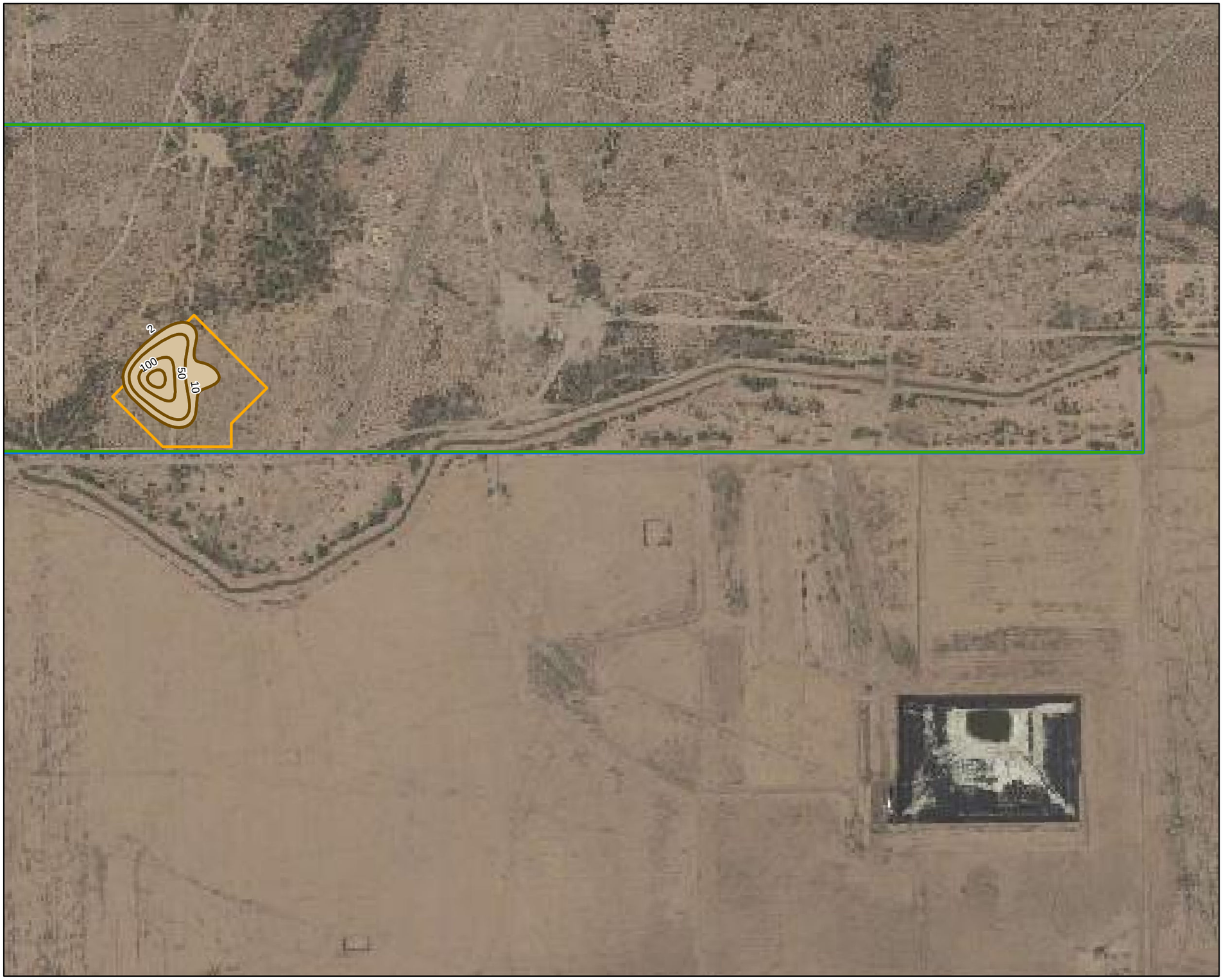

0 200 400

SCALE IN FEET

EXPLANATION

- SIMULATED SULFATE DISTRIBUTION AND CONCENTRATION ABOVE BACKGROUND (mg/L)
- PTF WELL FIELD
- STATE MINERALS LEASE BOUNDARY
- CURIS PROPERTY BOUNDARY

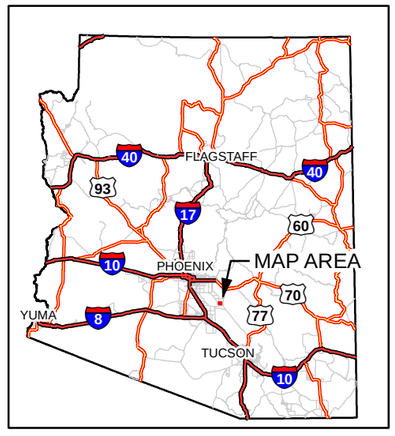

Figure 14A-32
SIMULATED SULFATE DISTRIBUTION
MODEL LAYER 6 (OXIDE EXCLUSION ZONE)
5 YEARS AFTER CLOSURE
CURIS RESOURCES (ARIZONA) INC.
FLORENCE, ARIZONA

Brown AND Caldwell

HDI CURIS

\\BCPHX03\projects\Hunter Dickinson\Curis GIS\MXDs\Temp Permit2012\14075334031_L6 Discharge Impact Oxide Excl.mxd Updated: 1/26/2012

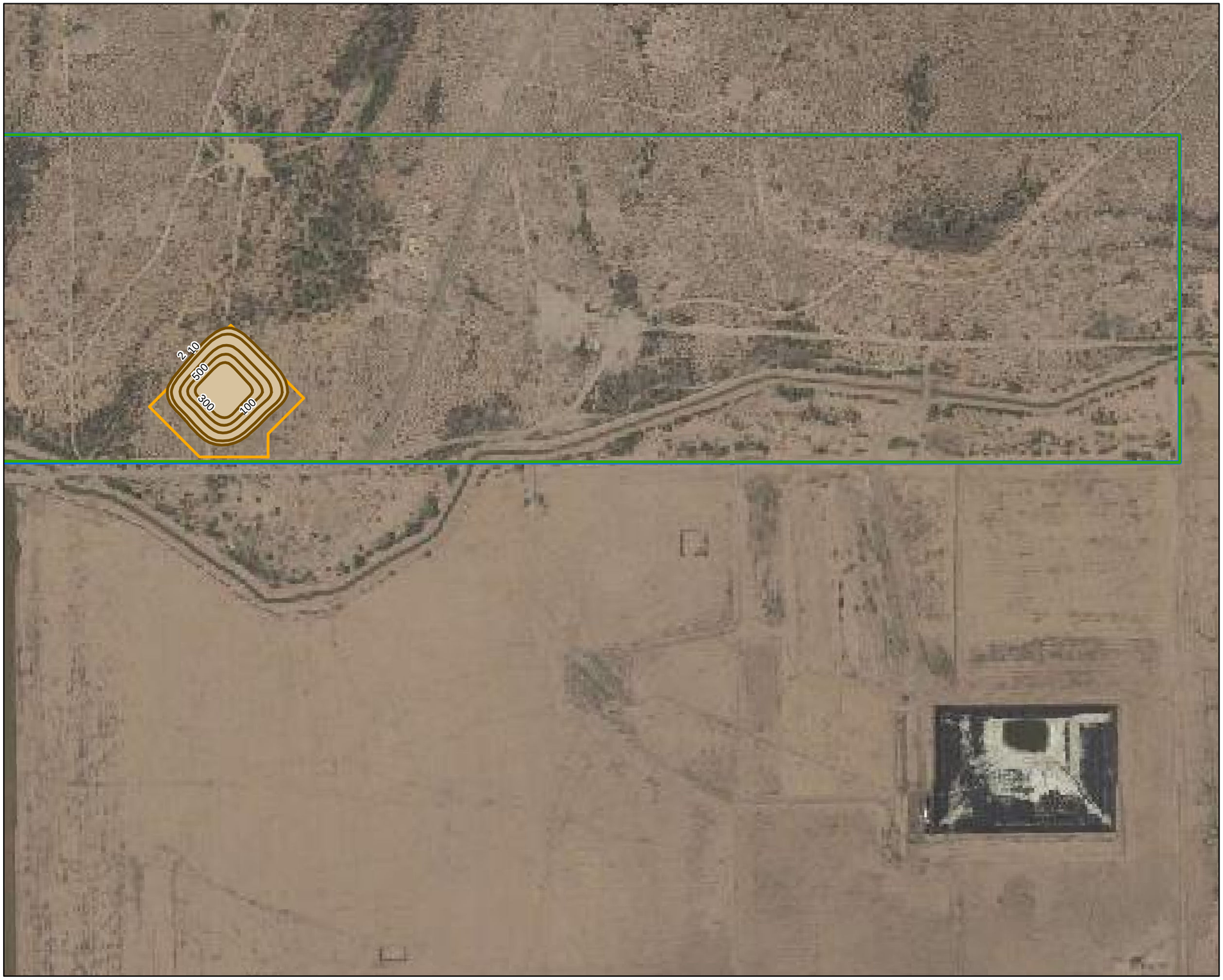

0 200 400

SCALE IN FEET

EXPLANATION

- SIMULATED SULFATE DISTRIBUTION AND CONCENTRATION ABOVE BACKGROUND (mg/L)
- PTF WELL FIELD
- CURIS PROPERTY BOUNDARY
- STATE MINERALS LEASE BOUNDARY

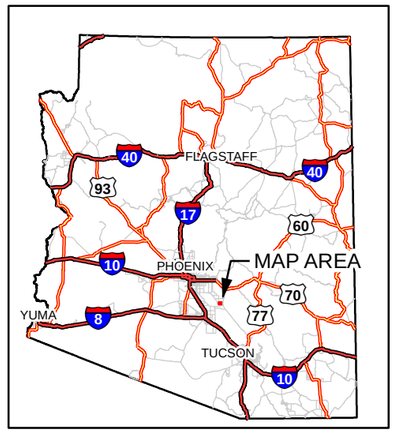

Figure 14A-33
SIMULATED SULFATE DISTRIBUTION
MODEL LAYER 7 (UPPER OXIDE)
5 YEARS AFTER CLOSURE
CURIS RESOURCES (ARIZONA) INC.
FLORENCE, ARIZONA

Brown AND Caldwell

HDI CURIS

\\BCPHX03\projects\Hunter Dickinson\Curis GIS\MXDs\Temp Permit2012\14075334032_L7Discharge Impact Upper Oxide updated.mxd Updated: 1/26/2012

0 200 400

SCALE IN FEET

EXPLANATION

- SIMULATED SULFATE DISTRIBUTION AND CONCENTRATION ABOVE BACKGROUND (mg/L)
- PTF WELL FIELD
- CURIS PROPERTY BOUNDARY
- STATE MINERALS LEASE BOUNDARY

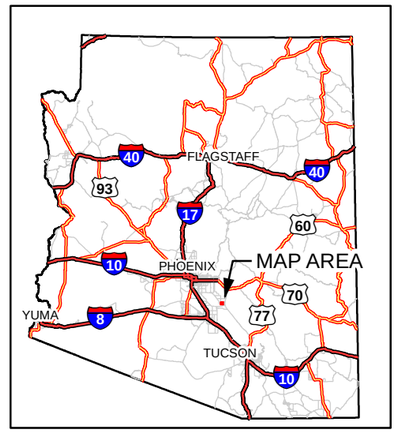

Figure 14A-34
SIMULATED SULFATE DISTRIBUTION
MODEL LAYER 8 (UPPER OXIDE)
5 YEARS AFTER CLOSURE
CURIS RESOURCES (ARIZONA) INC.
FLORENCE, ARIZONA

Brown AND Caldwell

HDI CURIS

\\BCPHX03\projects\Hunter Dickinson\Curis GIS\MXDs\Temp Permit2012\140753340_ Discharge Impact Upper Oxide L8 updated.mxd Updated: 1/26/2012

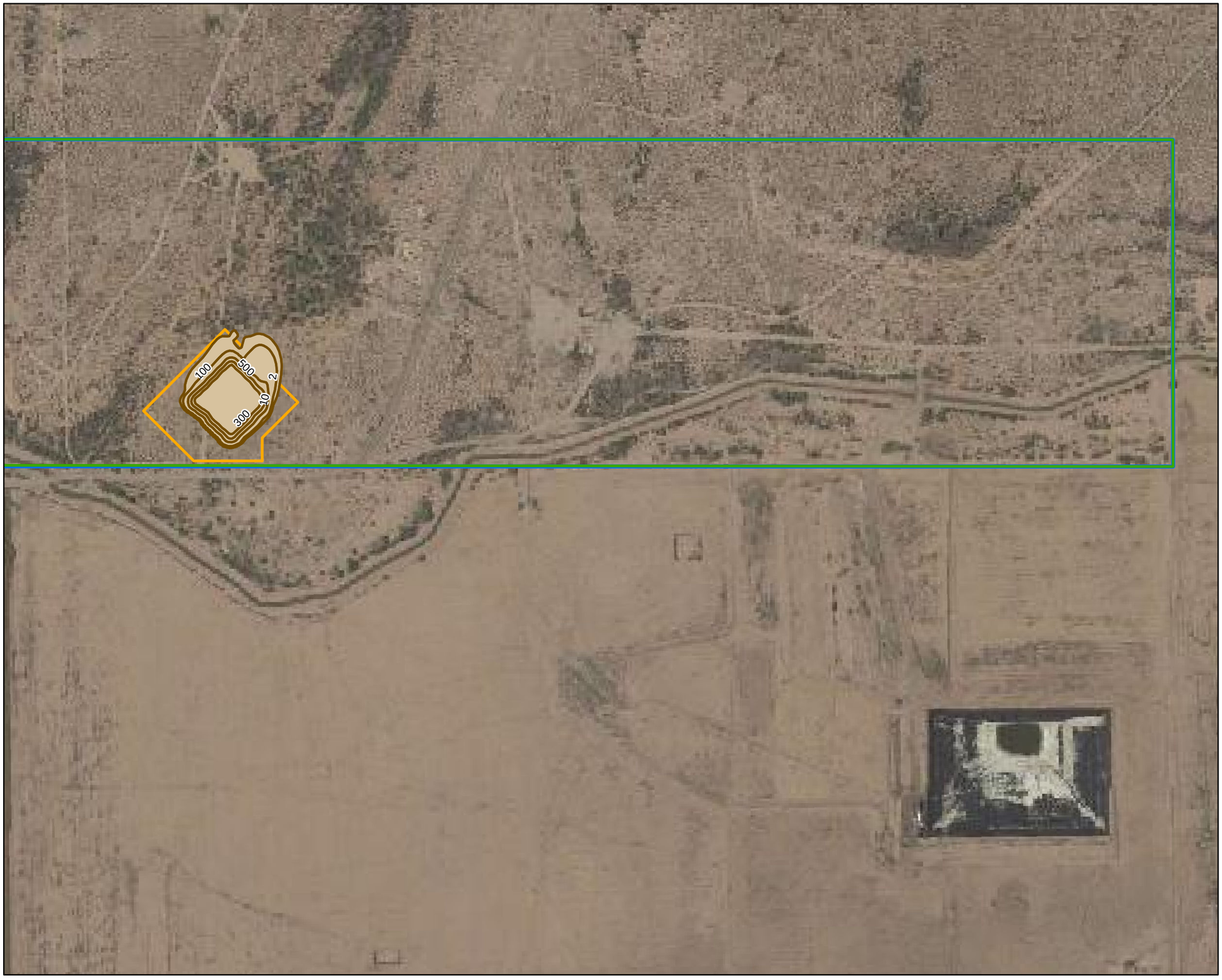

0 200 400

SCALE IN FEET

EXPLANATION

- SIMULATED SULFATE DISTRIBUTION AND CONCENTRATION ABOVE BACKGROUND (mg/L)
- PTF WELL FIELD
- STATE MINERALS LEASE BOUNDARY
- CURIS PROPERTY BOUNDARY

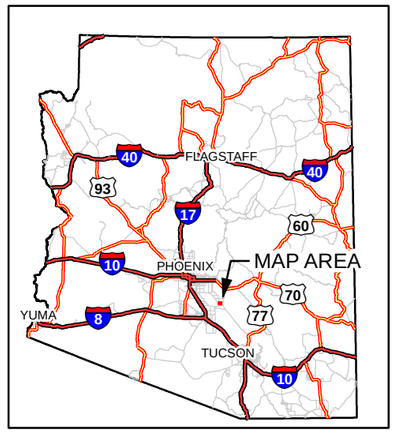

Figure 14A-35
SIMULATED SULFATE DISTRIBUTION
MODEL LAYER 9 (LOWER OXIDE)
5 YEARS AFTER CLOSURE
CURIS RESOURCES (ARIZONA) INC.
FLORENCE, ARIZONA

Brown AND Caldwell

HDI CURIS

\\BCPHX03\projects\Hunter Dickinson\Curis GIS\MXDs\Temp Permit2012\140753340_ L9_Discharge Impact Lower Oxide.mxd Updated: 1/26/2012

0 200 400

SCALE IN FEET

EXPLANATION

- SIMULATED SULFATE DISTRIBUTION AND CONCENTRATION ABOVE BACKGROUND (mg/L)
- PTF WELL FIELD
- STATE MINERALS LEASE BOUNDARY
- CURIS PROPERTY BOUNDARY

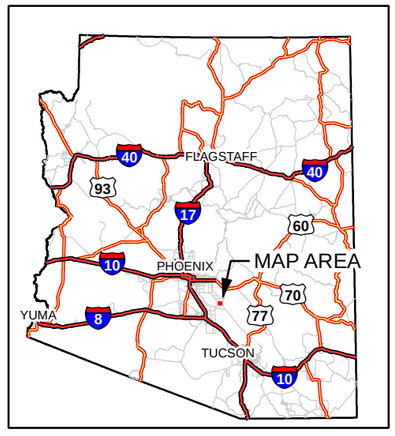

Figure 14A-36
SIMULATED SULFATE DISTRIBUTION
MODEL LAYER 10 (LOWER OXIDE)
5 YEARS AFTER CLOSURE
CURIS RESOURCES (ARIZONA) INC.
FLORENCE, ARIZONA

Brown AND Caldwell

HDI CURIS

\\BCPHX03\projects\Hunter Dickinson\Curis GIS\MXDs\Temp Permit2012\140753340_Discharge Impact Lower Oxide L10 updated.mxd Updated: 1/26/2012

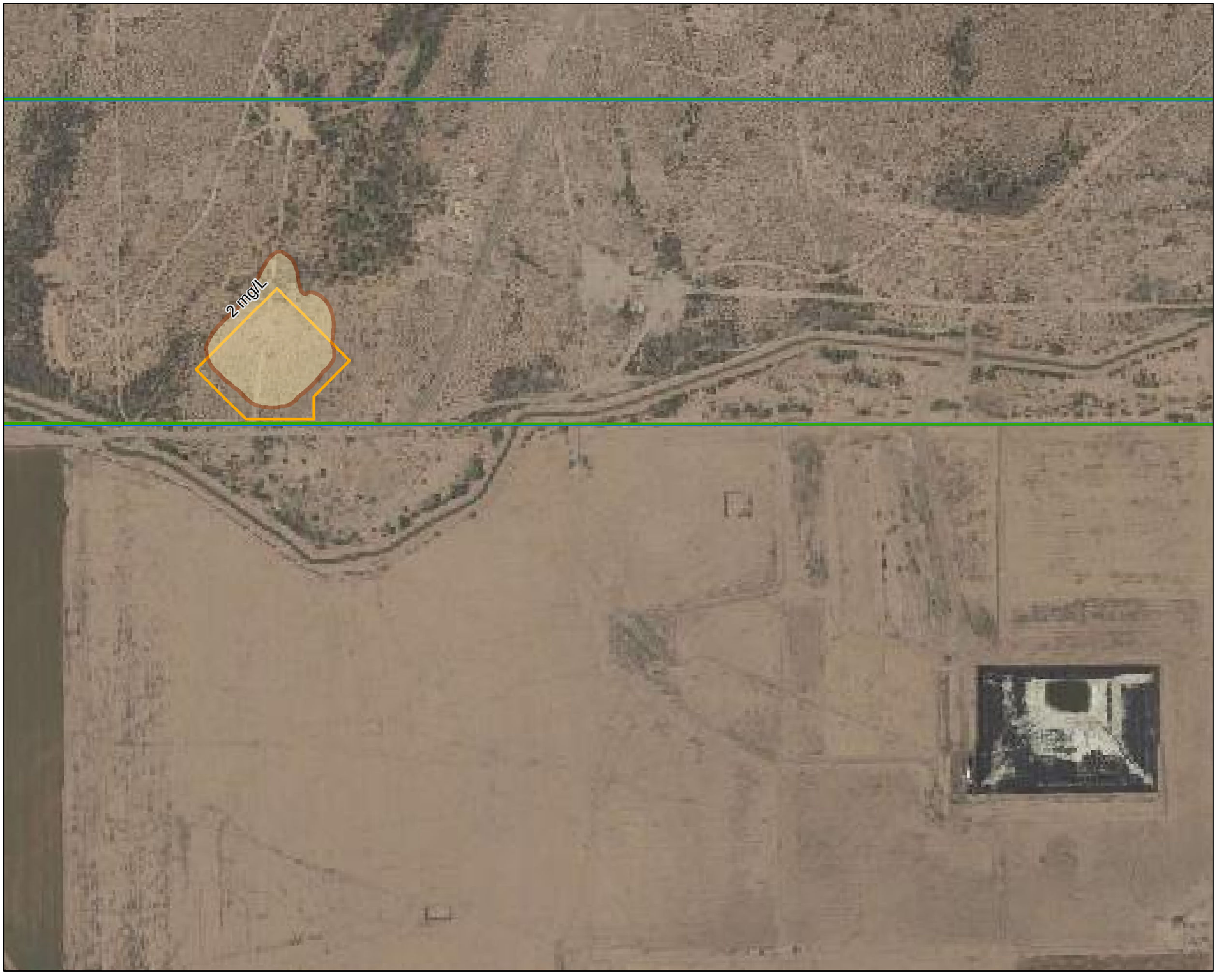

0 200 400

SCALE IN FEET

EXPLANATION

- PTF WELL FIELD
- CURIS PROPERTY BOUNDARY
- STATE MINERAL LEASE BOUNDARY
- MAXIMUM EXTENT OF SULFATE MIGRATION IN THE OXIDE

Figure 14A-37
EXTENT OF SULFATE MIGRATION WITHIN THE OXIDE (ALL LAYERS)
5 YEARS AFTER CLOSURE

CURIS RESOURCES (ARIZONA) INC.
FLORENCE, ARIZONA

Brown AND Caldwell

HDI CURIS

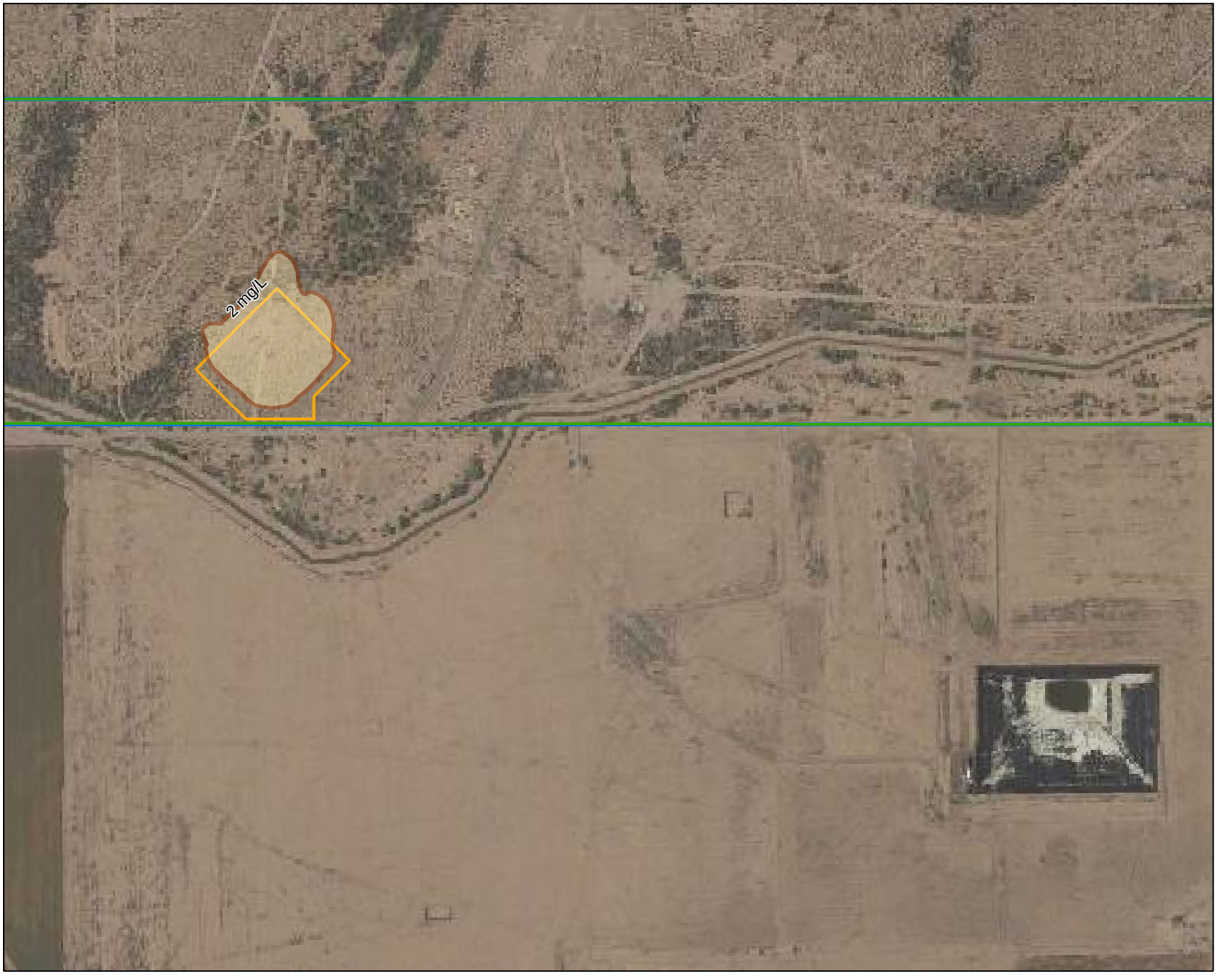

0 200 400

SCALE IN FEET

EXPLANATION

- PTF WELL FIELD
- CURIS PROPERTY BOUNDARY
- STATE MINERAL LEASE BOUNDARY
- MAXIMUM EXTENT OF SULFATE MIGRATION (ALL MODEL LAYERS)

Figure 14A-38
DISCHARGE IMPACT AREA
5 YEARS AFTER CLOSURE

CURIS RESOURCES (ARIZONA) INC.
FLORENCE, ARIZONA

Brown AND Caldwell

HDI CURIS

\\BCPHX03\projects\Hunter Dickinson\Curis GIS\MXDs\Temp Permit2012\G140753340_Composite_5Years.mxd Updated: 1/27/2012

Table 14A-1. Application Attachments Addressing Hydrologic Study Requirements Defined in A.A.C. R18-9-A202A.8

Requirement	Addressed in Attachment
8.a.i	Attachment 14A (This Attachment)
8.a.ii	Attachment 12
8.b.i	Attachment 14A (This Attachment)
8.b.ii	Attachment 14A (This Attachment)
8.b.iii	Attachment 14A(This Attachment)
8.b.iv	Attachment 14A (This Attachment)
8.b.v	Attachment 14B
8.b.vi	Attachment 14B
8.b.vii	Attachment 14B
8.b.viii	Attachment 14B
8.b.ix	Does not pertain to the present application
8.b.x	Attachment 14A (This Attachment)
8.b.xi	Attachment 14A (This Attachment)
8.b.xii	Attachment 14A (This Attachment)
8.b.xiii	Attachment 14A (This Attachment)

Table 14A-2. Measured Hydraulic Conductivity Values for MFGU Samples

Sample Name	Date of Analysis	Hydraulic Conductivity (cm/sec)	Hydraulic Conductivity (ft/day)
M16-60-300	October 11, 1995	5.0×10^{-9}	1.41×10^{-5}
CMP-11-03, 283-288 ft	August 11, 2011	4.4×10^{-9}	1.25×10^{-5}
CMP-11-03, 292.5-297.5 ft	August 11, 2011	4.3×10^{-9}	1.22×10^{-5}

cm/sec = centimeters per second
ft/day = feet per day

Table 14A-3. Specifications of the PTF Groundwater Model	
Model Characteristics	Specifications
Active Model Domain	~ 97 Square Miles
Units	Time: Days Length: Feet (lateral and vertical)
Coordinate System	State Plane NAD27 Arizona Central
Model Grid	392 rows by 540 columns, 2,116,800 total cells, 1,646,985,860 active cells Origin X: 622750 Y: 716500 (No rotation)
Cell Size	12.5 x 12.5 feet up to 500 by 500 feet
Layering –10 Layers	Layer 1 and 2: UBFU Layer 3: MFGU Layer 4 and 5: LBFU Layer 6: Oxide Exclusion Zone Layer 7 through 10: Oxide
Groundwater Flow Model Packages	MODFLOW SURFACT (ver. 3), BCF4, ATO, BAS, GHB, PG5, RCH, WEL
Solute Transport Packages	Solution Fate and Transport: MODFLOW SURFACT - ACT Modules
Simulation Time	Steady State: ~1900 Transient: 1984 to 2010 Predictive: 6 Years and 1 month (14 months with hydraulic control pumping at the ISCR, 9 months formation rinsing pumping, and 5 years with no hydraulic control pumping during closure)
Stress Periods (SP's)	Calibrated Model: 1 Steady State SP; 27 annual transient SPs Predictive Models: 7 SPs of varying lengths
Recharge	Variable, ranging from ~14,500 to ~188,200 AFY
Wells	General Head Boundaries along the central portion of the northern boundary, southern portion of the western boundary, and western portion of the southern boundary. "No flow" conditions along remainder of model boundaries.
Boundary Conditions	Interpolated water levels from observed 1984 groundwater conditions
Initial Conditions	Contoured and kriged water levels from 1984
Solution Method	Preconditioned-Conjugate Gradient 5 (PCG5)

Table 14A-4. Aquifer Parameter Value Ranges by Model Layer

	Horizontal Hydraulic Conductivity Kx (feet/day)	Vertical Hydraulic Conductivity Kz (feet/day)	Specific Storage Ss (feet-1)	Specific Yield Sy (Unitless)	Porosity n (Unitless)
Layers 1 and 2 (UBFU)	20 to 130	2 to 13	1e-5	0.13 to 0.2	0.13 to 0.2
Layer 3 (MFGU/UBFU)	1 to 130	0.01 to 13	5e-6 to 1 e-5	0.08 to 0.2	0.15 to 0.2
Layers 4 and 5 (LBFU)	5 to 25	0.5 to 2.5	1e-5	0.08 to 0.1	0.2
Layer 6	1	1	1e-5	0.08	0.08
Layer 7	0.57	0.57	5e-6	0.08	0.08
Layer 8	0.57	0.57	5e-6	0.08	0.08
Layer 9	0.1	0.1	5e-6	0.05	0.05
Layer 10	0.1	0.1	5e-6	0.05	0.05
Faults	2.51	2.51	5e-6	0.1	0.1

Table 14A-5. Transient Model Calibration Statistics

	Residual Mean (RM) (ft)	Absolute Residual Mean (ARM) (ft)	Residual Standard Deviation (RSD) (ft)	Simulated Range of Heads Values (Range) (ft)	RM/Range (%)	ARM/Range (%)	RSD/Range (%)
1984 to 2010	-2.80	12.10	15.61	398	0.71	3.0	3.9

Table 14A-6. Simulated Water Budget Values			
Inflow Source	1984 Simulated Water Budget (AFY)	2003 Simulated Water Budget (AFY)	2010 Simulated Water Budget (AFY)
Recharge	116,776	14,538	35,541
Storage	-	47,831	12,749
TOTAL INFLOWS	116,776	62,369	48,290

Outflow Source	1984 Simulated Water Budget (AFY)	2003 Simulated Water Budget (AFY)	2010 Simulated Water Budget (AFY)
Evapotranspiration	0	0	0
Pumping Wells	44,352	54,453	45,010
General Head Boundary	20,819	8,180	3,900
Storage	55,183	-	-
TOTAL OUTFLOWS	120,354	62,633	48,910

Exhibit 14A-1

Aquifer Test Data, Volume II, Appendix E
1996 Florence APP Application

APPENDIX E

CURRENT INVESTIGATION AQUIFER TEST ANALYSIS INFORMATION

Table E-1 Summary of Aquifer Test Field Program

Pumping Well	Observation Wells	Screened Interval (ft bgs)	Pump Rate (gpm)	Maximum Drawdown (ft)	Hydraulic Conductivity (ft/day)	Date Test Performed	Comments
PW7-1		540 - 880	38	109.0	0.2	6/16/95 to 6/22/95	Irrigation wells BIA-10B & WW-3 pumped during test.
	OB7-1	540 - 880		67.9	0.1		
	O3-GL	325 - 365		8.7	N/A		
	Corehole OB-1	Not Screened		6.3[3]	N/A		
P5-O		414 - 770	66	51.8	N/A	10/18/95 to 10/24/95	Irrigation wells BIA-10B & BIA-9 pumped during test.
	O5.1-O	674 - 832		29.5	N/A		
	O5.2-O	712 - 771		31.7	N/A		
P8.1-O		400 - 580	12	212.7	N/A	9/7/95 to 9/13/95	Irrigation well BIA-9 is pumped during test.
	P8.2-O	396 - 576		4.5	N/A		
	P8-GU	128 - 248		0.49	N/A		
	08-O	401 - 579		72.6	N/A		
	08-GU	133 - 251		0	N/A		
P8-GU		128 - 248	85	6.9	61.3	9/18/95 to 9/22/95	Irrigation wells BIA-10B & BIA-9 pumped during test.
	P8.1-O	400 - 580		9.2	N/A		
	P8.2-O	396 - 576		9.5	N/A		
	O8-O	401 - 579		8.9	N/A		
	O8-GU	133 - 251		6.9	N/A		
P12-O		440 - 940	64	35.5	0.4	6/1/95 to 6/8/95	Irrigation well WW-3 is pumped during test.
	O12-O	434 - 939		42.8	0.6		
	O12-GL	125 - 165		N/A[4]	N/A		
P13.1-O		772 - 1,449	46	93.1	N/A	10/9/95 to 10/16/95	No irrigation wells pumped during test.
	P13.2-O	781 - 1,379		19.2	N/A		
	P13-GL	690 - 760		0	N/A		
	O13-O	770 - 1,393		4.4	N/A		
P15-O		580 - 1,300	59	40.9	N/A	9/29/95 to 10/5/95	Irrigation wells BIA-10B & BIA-9 pumped during test.
	O15-O	632 - 1,296		22.4	N/A		
	O15-GL	421 - 481		1.3	N/A		

Table E-1 Summary of Aquifer Test Field Program

Pumping Well	Observation Wells	Screened Interval (ft bgs)	Pump Rate (gpm)	Maximum Drawdown (ft)	Hydraulic Conductivity (ft/day)	Date Test Performed	Comments
P19.1-O		402 - 600	24	155.2	0.3	7/3/95 to	Irrigation wells BIA-10B & WW-3 pumped
	P19.2-O	404 - 602		25.7	0.2	7/6/95	during test.
	019-O	410 - 608		16.9	0.2		
	019-GL	375 - 435		2.4	N/A		
	Corehole 138	Not Screened		0	N/A		
P28.1-O		395 - 495	30	7.9	7.7	8/15/95 to	Low pump rate test. No irrigation wells pumped
	P28.2-O	398 - 497		5.4	N/A	8/21/95	during test.
	P28-GL	279 - 309		1.03	N/A		
	028.1-O	394 - 494		4.7	N/A		
	028.2-S	454 - 494		3.2	N/A		
	028-GL	277 - 307		1.7	N/A		
P28.1-O		395 - 495	85	50.4	3.6	9/7/95 to	High pump rate test conducted. Irrigation well
	P28.2-O	398 - 497		28.3	2.7	9/13/95	BIA-9 pumped during test.
	P28-GL	279 - 309		7.1	N/A		
	028.1-O	394 - 494		22.8	N/A		
	028.2-S	454 - 494		14.2	N/A		
	028-GL	277 - 307		10.1	N/A		
P28-GL		279 - 309	75	115.2	8.3	9/18/95 to	Irrigation wells BIA-10B & BIA-9 pumped
	P28.1-O	395 - 495		11.7	N/A	9/28/95	during test.
	P28.2-O	398 - 497		11.6	N/A		
	O28.1-O	394 - 494		11.9	N/A		
	O28.2-S	454 - 494		12.2	N/A		
	O28-GL	277 - 307		18.8	25.5		
P28.2-O		398 - 497	80	33.8	3.1	10/2/95 to	Irrigation wells BIA-10B & BIA-9 pumped until
	P28.1-O	395 - 495		2.3	N/A	10/5/95	10/5/95.
	P28-GL	279 - 309		8.7	N/A		
	O28.1-O	394 - 494		18.5	3.0		
	O28.2-S	454 - 494		15.4	N/A		
	O28-GL	277 - 307		11.9	N/A		

Table E-1 Summary of Aquifer Test Field Program

Pumping Well	Observation Wells	Screened Interval (ft bgs)	Pump Rate (gpm)	Maximum Drawdown (ft)	Hydraulic Conductivity (ft/day)	Date Test Performed	Comments
P39-O		471 - 826	55	108	0.3	5/19/95 to	No irrigation wells pumped during test.
	O39-O	474 - 890		23	0.3	5/21/95	
P49-O		808 - 1,222	40	298	N/A	10/11/95 to	No irrigation wells pumped during test.
	O49-O	812 - 1,227		091	N/A	10/16/95	
	O49-GL	661 - 721		0.47	N/A		
M2-GU		198 - 237	10	0.38	N/A	7/25/95 to	Short duration test(1). Irrigation wells BIA-10B & England No. 3 pumped during test.
	M3-GL	298 - 338		0	N/A	7/26/95	
	M4-O	405 - 465		0	N/A		
	M5-S	516 - 576		0	N/A		
M3-GL		298 - 338	10	5.6	15.9	7/26/95 to	Short duration test(1). Irrigation well England No. 3 pumped during test.
	M2-GU	198 - 237		0	N/A	7/27/95	
	M4-O	405 - 465		0.58	N/A		
	M5-S	516 - 576		0	N/A		
M4-O		405 - 465	15	190.4	0.6	7/28/95 to	Short duration test(1). Irrigation well England No. 3 pumped during test.
	M2-GU	198 - 237		0.445	N/A	7/30/95	
	M3-GL	298 - 338		1.09	14.8		
	M5-S	516 - 576		0	N/A		
M10-GU		218 - 258	15	0.508	N/A	7/25/95 to	Short duration test(1). Irrigation wells BIA-10B & England No.3 pumped during test.
	M11-GL	290 - 330		0.222	N/A	7/29/95	
	M12-O	420 - 480		0.318	N/A		
	M13-S	851 - 911		0	N/A		
M11-GL		290 - 330	15	16.7	N/A	7/29/95 to	Short duration test(1). Irrigation well England No. 3 pumped during test.
	M10-GU	218 - 258		4.5	N/A	7/31/95	
	M12-O	420 - 480		4.6	N/A		
	M13-S	851 - 911		0	N/A		

Table E-1 Summary of Aquifer Test Field Program							
Pumping Well	**Observation Wells**	**Screened Interval (ft bgs)**	**Pump Rate (gpm)**	**Maximum Drawdown (ft)**	**Hydraulic Conductivity (ft/day)**	**Date Test Performed**	**Comments**
M12-O		420 - 480	14	19.5	N/A	7/31/95 to 8/2/95	Short duration test[1]. Irrigation wells BIA-10B & England No. 3 pumped during test.
	M10-GU	218 - 258		1.36	N/A		
	M11-GL	290 - 330		3.08	N/A		
	M13-S	851 - 911		0	N/A		
M18-GU		178 - 218	10	7.7	19.6	8/8/95 to 8/9/95	Short duration test[1].
	M1-GL	315 - 355		0	N/A		
M1-GL		315 - 355	10	5.4	17.3	8/11/95 to 8/12/95	Short duration test[1].
	M18-GU	178 - 218		0.157	N/A		
M15-GU		554 - 594	10	47.5	2.6	8/8/95 to 8/9/95	Short duration test[1].
	M14-GL	778 - 838		0	N/A		
M14-GL		778 - 838	10	30.1	1.7	8/11/95 to 8/12/95	Short duration test[1].
	M15-GU	554 - 594		1.56	N/A		
WW-3[2]		240 - 930	2000	N/A	N/A	8/23/95 to 8/29/95	Large scale aquifer test. No other irrigation well pumped during test.
	OB7-1	540 - 880		13.3	N/A		
	O3-GL	325 - 365		12.5	N/A		
	O12-O	434 - 939		23.2	N/A		
	O12-GL	125 - 165		29.9	N/A		
	P15-O	580 - 1,300		32.7	N/A		
	O15-O	632 - 1,296		26.7	N/A		
	O15-GL	421 - 481		7.4	N/A		
	O19-O	410 - 608		5.19	N/A		
	O19-GL	375 - 435		5.3	N/A		
	P28.1-O	395 - 495		2.1	N/A		
	P28.2-O	398 - 497		2.05	N/A		
	O28.1-O	394 - 494		2.06	N/A		
	028-GL	277 - 307		1.9	N/A		
	M14-GL	778 - 838		10.7	N/A		
	M15-GL	554 - 594		9.9	N/A		
	AIRSHAFT	Not Screened		5.0	N/A		

Table E-1 Summary of Aquifer Test Field Program

Pumping Well	Observation Wells	Screened Interval (ft bgs)	Pump Rate (gpm)	Maximum Drawdown (ft)	Hydraulic Conductivity (ft/day)	Date Test Performed	Comments
BIA-9[2]		80 - 494	2350	N/A	N/A	8/29/95 to 9/6/95	Large scale aquifer test. BIA-10B pumped during test.
	OB7-1	540 - 880		21.5	N/A		
	O3-GL	325 - 365		26.2	N/A		
	O12-O	434 - 939		10.3	N/A		
	O12-GL	125 - 165		10.2	N/A		
	P15-O	580 - 1,300		10.3	N/A		
	O15-O	632 - 1,296		5.3	N/A		
	O15-GL	421 - 481		4.7	N/A		
	O19-O	410 - 608		4.3	N/A		
	O19-GL	375 - 435		3.9	N/A		
	P28.1-O	395 - 495		4.1	N/A		
	P28.2-O	398 - 497		4.1	N/A		
	O28.1-O	394 - 494		4.3	N/A		
	028-GL	277 - 307		4.4	N/A		
	M14-GL	778 - 838		6.3	N/A		
	M15-GL	554 - 594		3.9	N/A		
	AIRSHAFT	Not Screened		11.6	N/A		

[1] Short duration tests performed at the monitoring well clusters. Each test was performed by pumping each well in the cluster for approximately 24 hours (Except sulfide wells).
[2] Regional tests performed using existing high discharge irrigation wells.
[3] Drawdown due to irrigation well not test pumping well.
[4] No information available, transducer malfunctioned.
ft bgs - feet below ground surface
ft/day - feet per day
gpm - gallons per minute
See section 2.3.5 (II) for discussion of aquifer tests.
Additional Aquifer test data is presented in Appendix E (II).

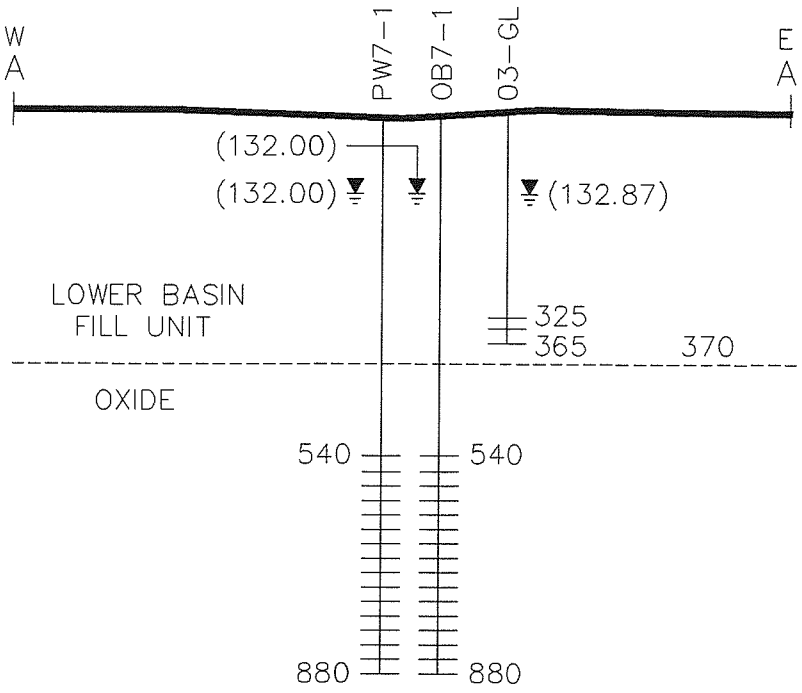

EXPLANATION

POTENTIOMETRIC SURFACE (151.00)

(SHOWN IN FEET BELOW GROUND SURFACE)

WELL PREFIXES

PUMPED WELL	P
MONITOR WELL	M
OBSERVATION WELL	O

WELL SUFFIXES (AQUIFER COMPONENT SCREEN)

BASIN FILL	GU
BASIN FILL	GL
OXIDE BEDROCK	O
SULFIDE BEDROCK	S

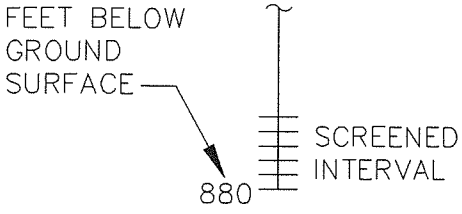

SIMPLIFIED EAST-WEST CROSS SECTION

Approximate Scale: Vertical : 1"= 300'
Horizontal: 1"= 150'

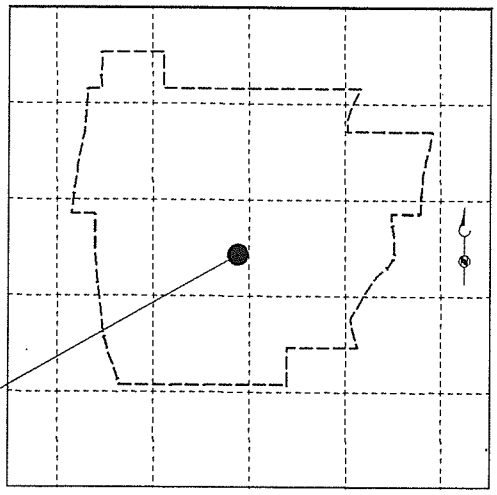

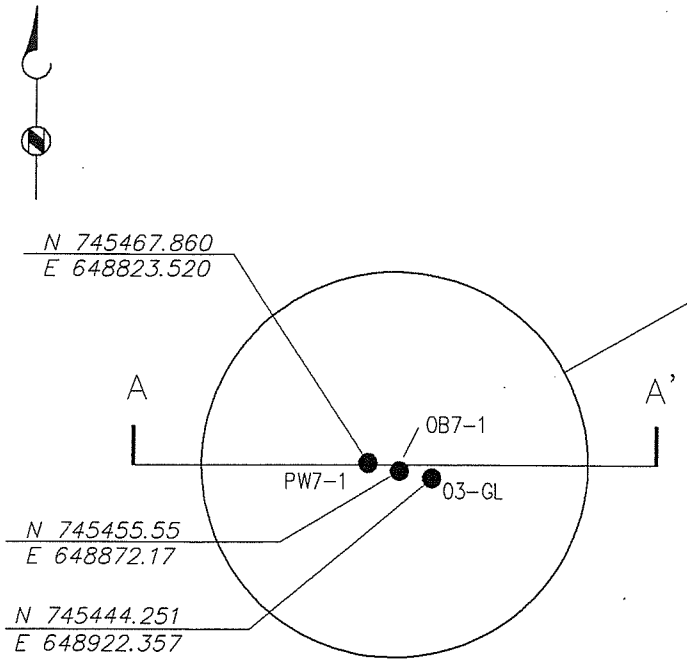

WELL PLAN VIEW

Approximate Scale: 1"= 300'

WELL LOCATION MAP

Approximate Scale: 1"= 2000'

BROWN AND CALDWELL

Figure E-1 (II)
LOCATION SUMMARY
AQUIFER TEST
CLUSTER NO. 3

MAGMA COPPER COMPANY
Florence, Arizona

E-1_2 12-01-95 DanH

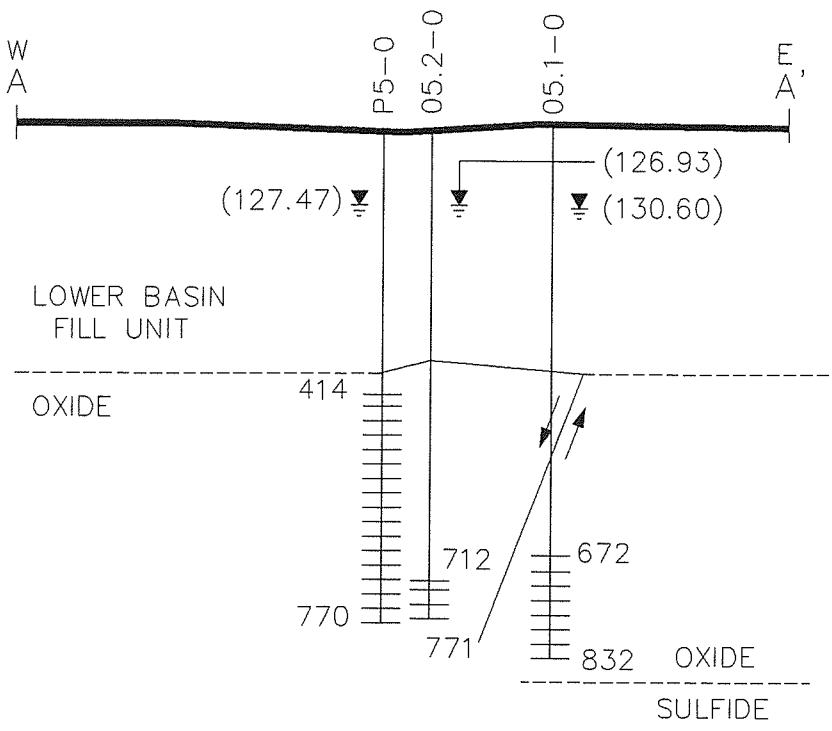

SIMPLIFIED EAST-WEST CROSS SECTION

Approximate Scale: Vertical : 1"= 300'
Horizontal: 1"= 150'

EXPLANATION

POTENTIOMETRIC SURFACE (151.00)

(SHOWN IN FEET BELOW GROUND SURFACE)

WELL PREFIXES

PUMPED WELL	P
MONITOR WELL	M
OBSERVATION WELL	O

WELL SUFFIXES (AQUIFER COMPONENT SCREEN)

BASIN FILL	GU
BASIN FILL	GL
OXIDE BEDROCK	O
SULFIDE BEDROCK	S

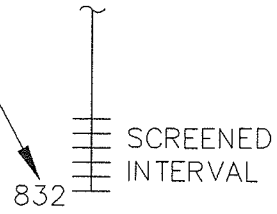

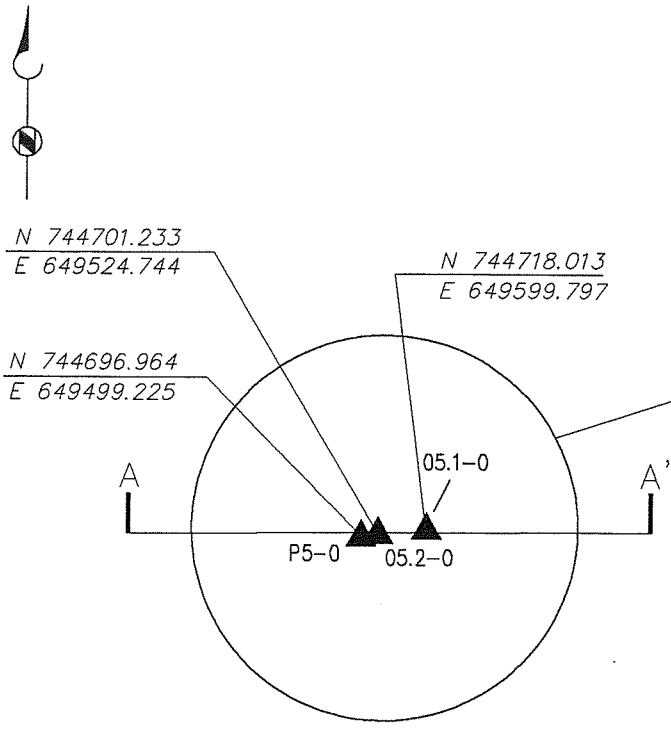

WELL PLAN VIEW

Approximate Scale: 1"= 300'

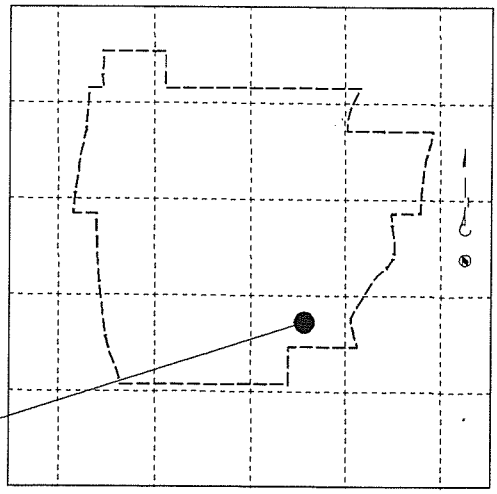

WELL LOCATION MAP

Approximate Scale: 1"= 2000'

Figure E-2 (II)
LOCATION SUMMARY
AQUIFER TEST
CLUSTER 5

BROWN AND CALDWELL

MAGMA COPPER COMPANY
Florence, Arizona

E-2_2 12-01-95 DanH

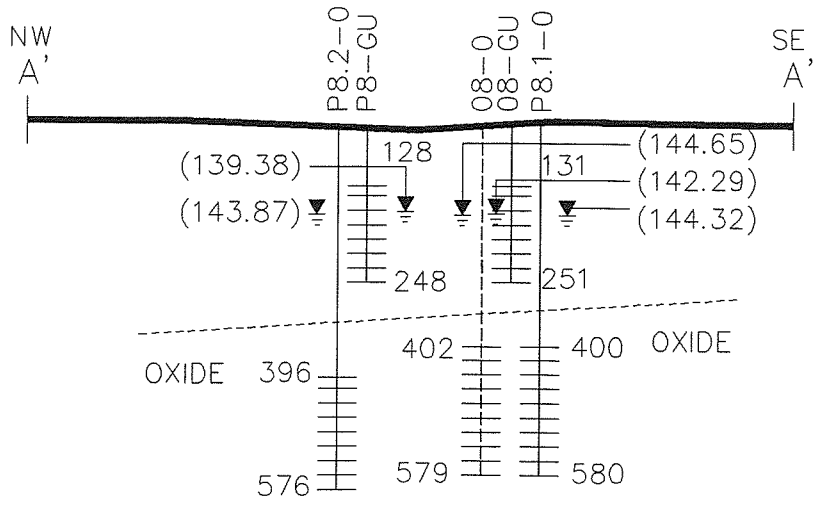

SIMPLIFIED EAST-WEST CROSS SECTION

Approximate Scale: Vertical : 1"= 300'
Horizontal: 1"= 150'

EXPLANATION

POTENTIOMETRIC SURFACE (151.00)▼

(SHOWN IN FEET BELOW GROUND SURFACE)

WELL PREFIXES

PUMPED WELL	P
MONITOR WELL	M
OBSERVATION WELL	O

WELL SUFFIXES (AQUIFER COMPONENT SCREEN)

BASIN FILL	GU
BASIN FILL	GL
OXIDE BEDROCK	O
SULFIDE BEDROCK	S

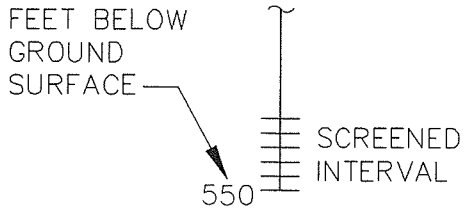

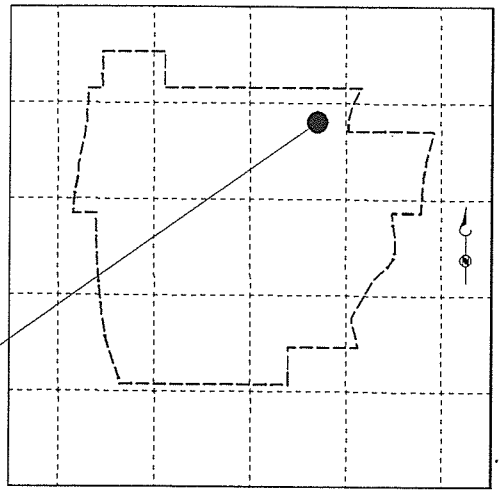

WELL LOCATION MAP

Approximate Scale: 1"= 2000'

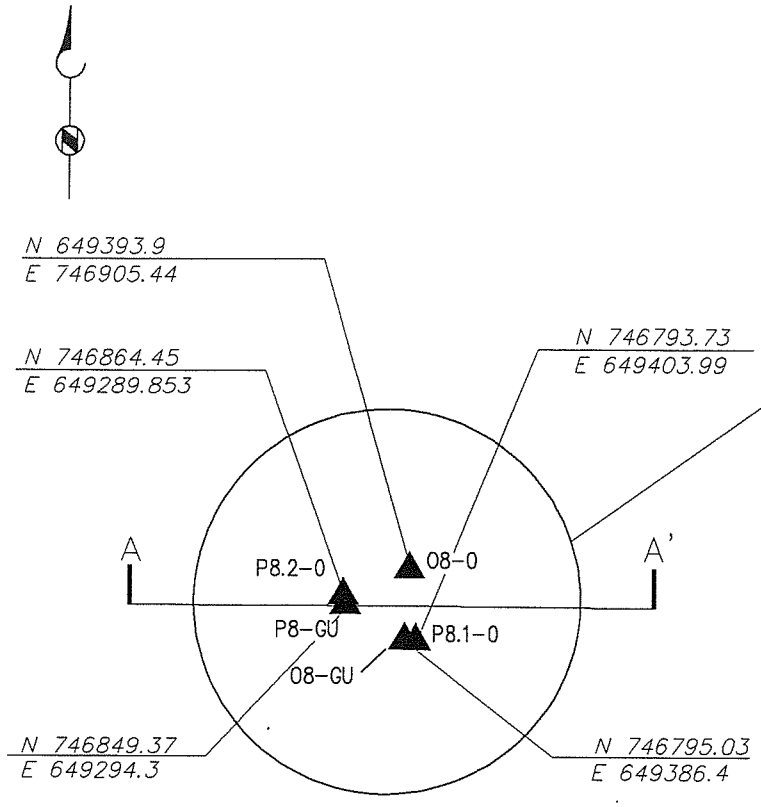

WELL PLAN VIEW

Approximate Scale: 1"= 300'

Figure E-3 (II)
LOCATION SUMMARY
AQUIFER TEST
CLUSTER 8

BROWN AND CALDWELL

MAGMA COPPER COMPANY
Florence, Arizona

E-3_2 12-01-95 DanH

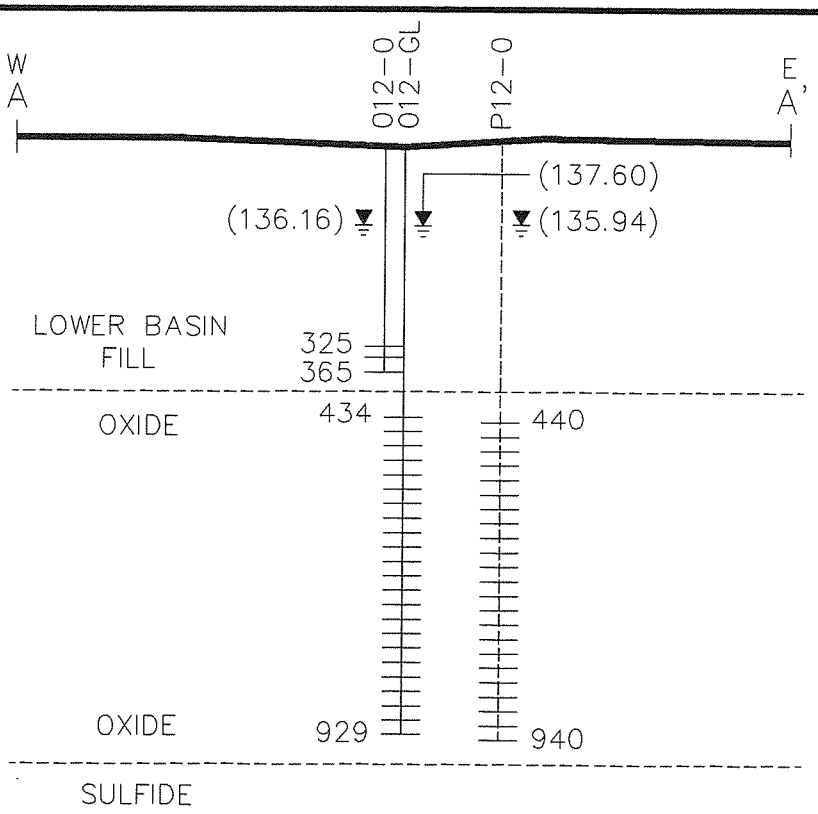

SIMPLIFIED EAST-WEST CROSS SECTION

Approximate Scale: Vertical : 1"= 300'
Horizontal: 1"= 150'

EXPLANATION

POTENTIOMETRIC SURFACE (151.00)

(SHOWN IN FEET BELOW GROUND SURFACE)

WELL PREFIXES

PUMPED WELL	P
MONITOR WELL	M
OBSERVATION WELL	O

WELL SUFFIXES (AQUIFER COMPONENT SCREEN)

BASIN FILL	GU
BASIN FILL	GL
OXIDE BEDROCK	O
SULFIDE BEDROCK	S

FEET BELOW GROUND SURFACE — 940 — SCREENED INTERVAL

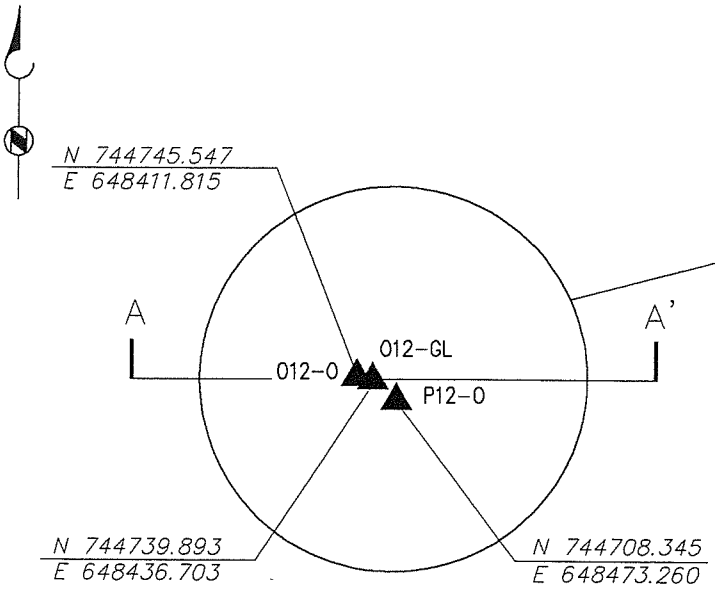

WELL PLAN VIEW

Approximate Scale: 1"= 300'

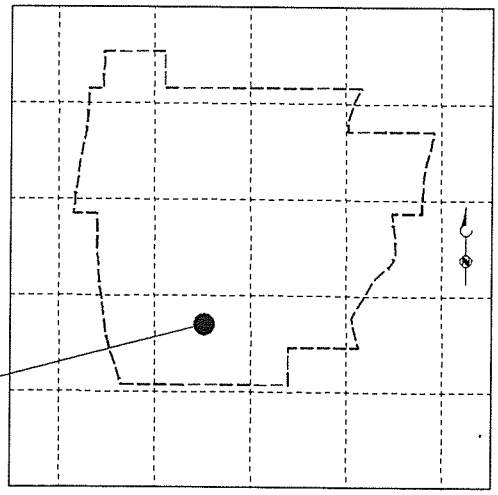

WELL LOCATION MAP

Approximate Scale: 1"= 2000'

Figure E-4 (II)

LOCATION SUMMARY AQUIFER TEST CLUSTER 12

BROWN AND CALDWELL

MAGMA COPPER COMPANY
Florence, Arizona

E-4_2 12-01-95 DanH

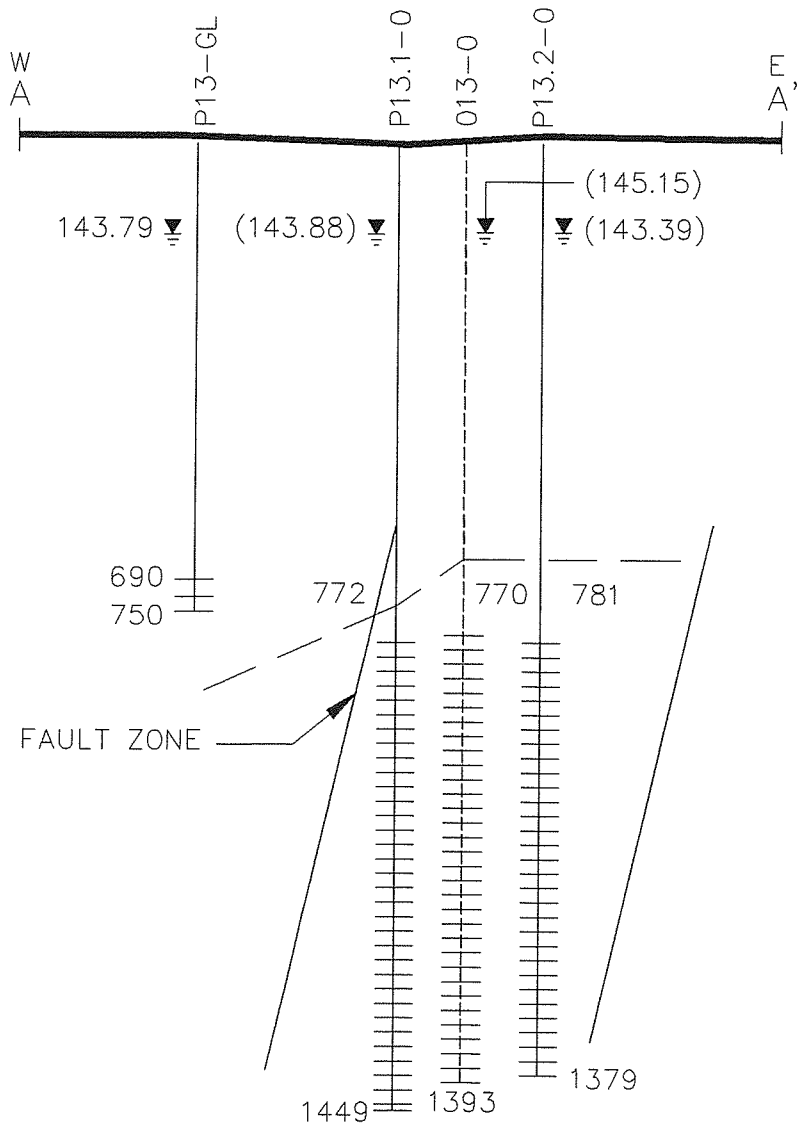

SIMPLIFIED EAST-WEST CROSS SECTION

Approximate Scale: Vertical : 1"= 300'
Horizontal: 1"= 600'

EXPLANATION

POTENTIOMETRIC SURFACE (151.00)

(SHOWN IN FEET BELOW GROUND SURFACE)

WELL PREFIXES

PUMPED WELL	P
MONITOR WELL	M
OBSERVATION WELL	O

WELL SUFFIXES (AQUIFER COMPONENT SCREEN)

BASIN FILL	GU
BASIN FILL	GL
OXIDE BEDROCK	O
SULFIDE BEDROCK	S

FEET BELOW GROUND SURFACE — 1450 — SCREENED INTERVAL

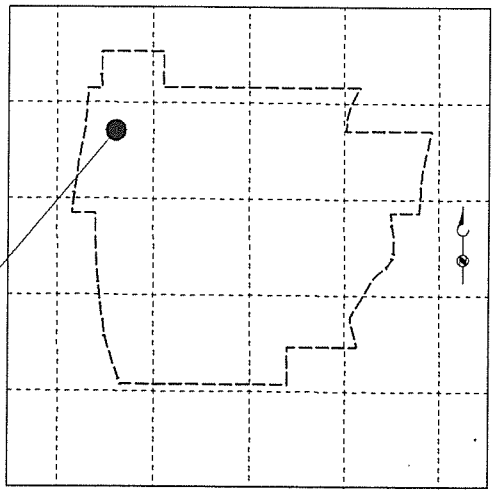

WELL LOCATION MAP

Approximate Scale: 1"= 2000'

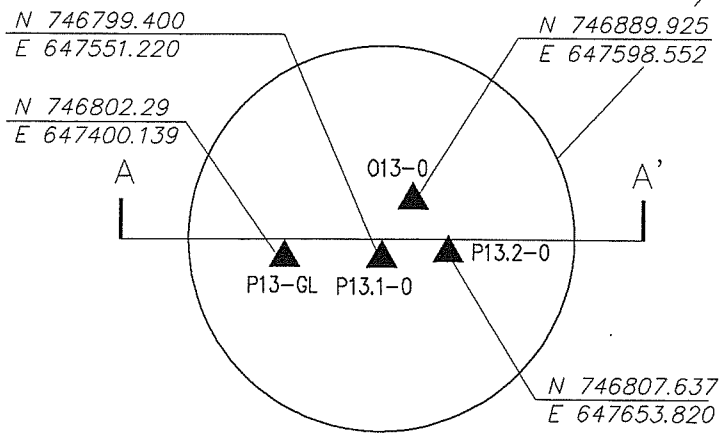

WELL PLAN VIEW

Approximate Scale: 1"= 300'

Figure E-5 (II)
LOCATION SUMMARY
AQUIFER TEST
CLUSTER 13

BROWN AND CALDWELL

MAGMA COPPER COMPANY
Florence, Arizona

E-5_2 12-01-95 DanH

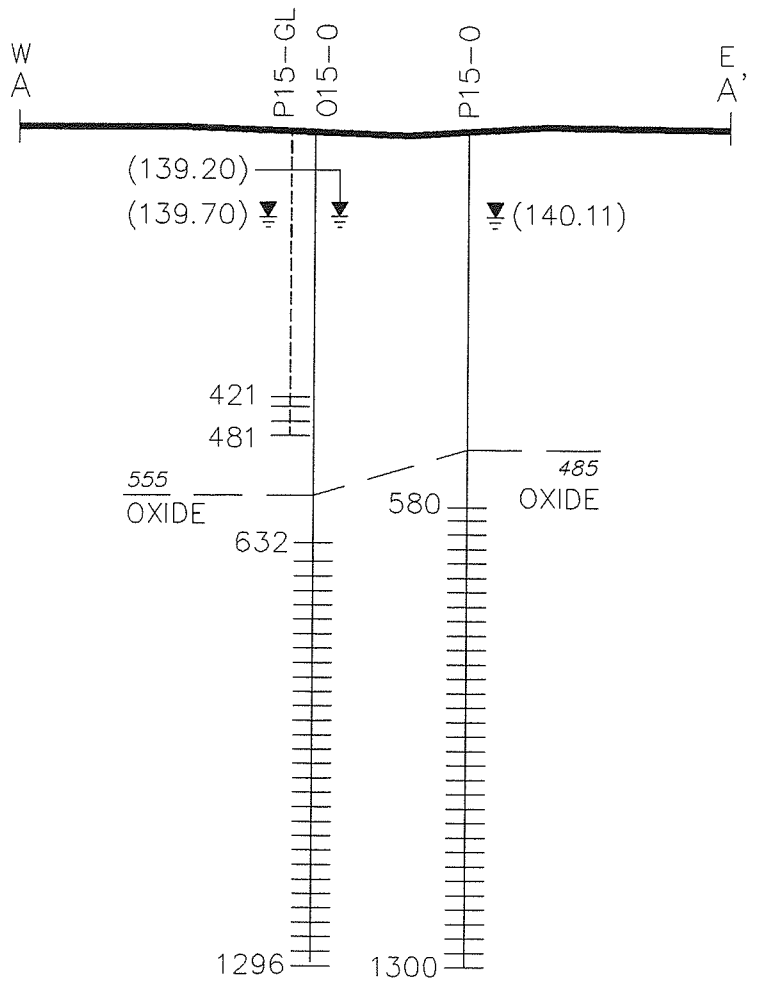

SIMPLIFIED EAST-WEST CROSS SECTION

Approximate Scale: Vertical : 1"= 300'
Horizontal: 1"= 150'

EXPLANATION

POTENTIOMETRIC SURFACE (151.00)

(SHOWN IN FEET BELOW GROUND SURFACE)

WELL PREFIXES

PUMPED WELL	P
MONITOR WELL	M
OBSERVATION WELL	O

WELL SUFFIXES (AQUIFER COMPONENT SCREEN)

BASIN FILL	GU
BASIN FILL	GL
OXIDE BEDROCK	O
SULFIDE BEDROCK	S

FEET BELOW GROUND SURFACE

610

SCREENED INTERVAL

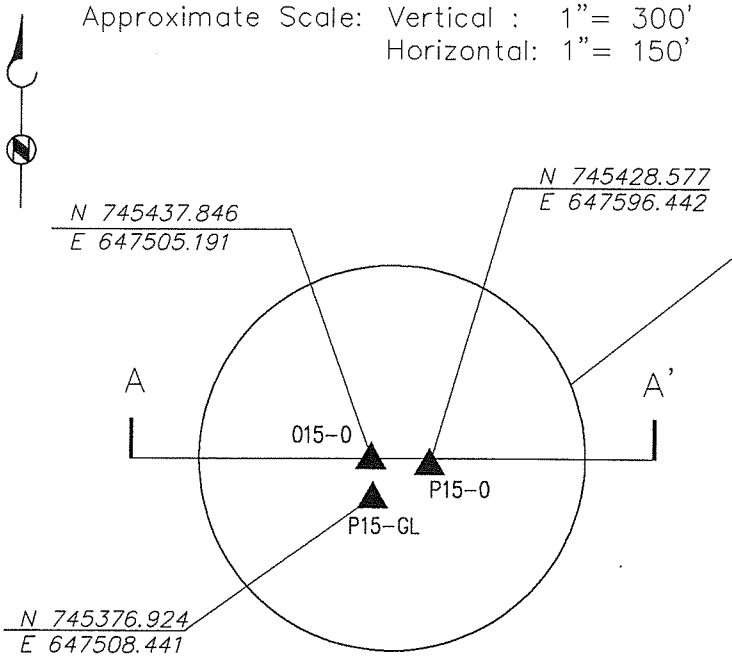

WELL PLAN VIEW

Approximate Scale: 1"= 300'

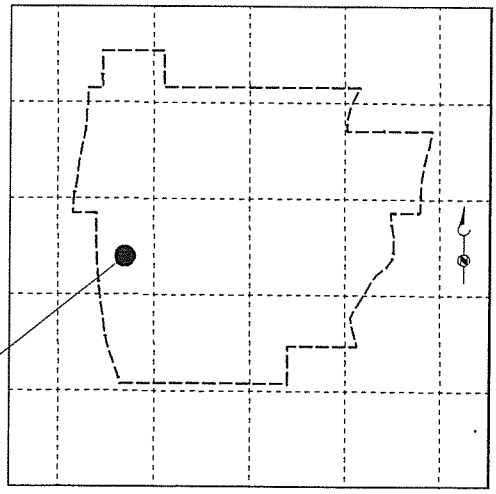

WELL LOCATION MAP

Approximate Scale: 1"= 2000'

Figure E-6 (II)
LOCATION SUMMARY
AQUIFER TEST
CLUSTER 15

BROWN AND CALDWELL

MAGMA COPPER COMPANY
Florence, Arizona

E-6_2 12-01-95 DanH

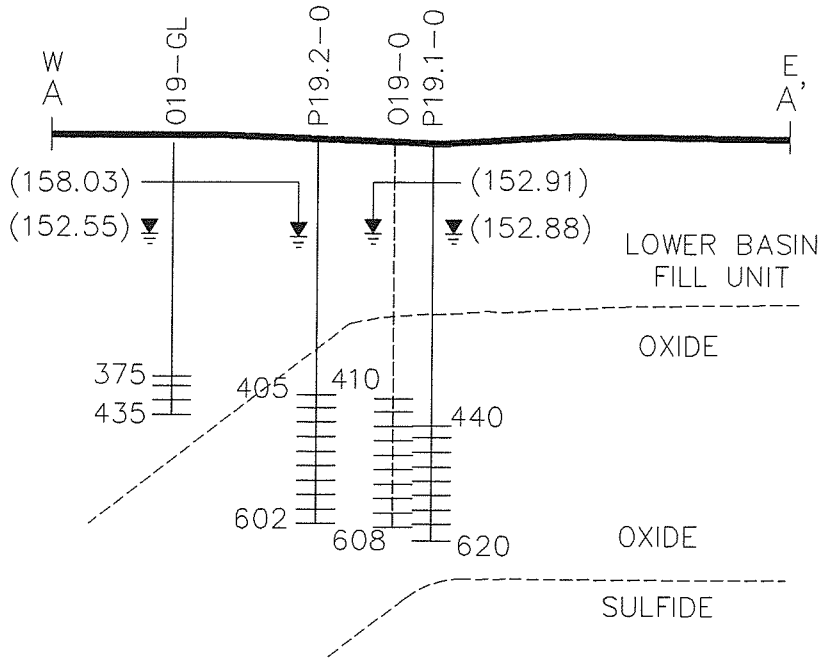

SIMPLIFIED EAST-WEST CROSS SECTION

Approximate Scale: Vertical : 1"= 300'
Horizontal: 1"= 150'

EXPLANATION

POTENTIOMETRIC SURFACE (151.00)

(SHOWN IN FEET BELOW GROUND SURFACE)

WELL PREFIXES

PUMPED WELL	P
MONITOR WELL	M
OBSERVATION WELL	O

WELL SUFFIXES (AQUIFER COMPONENT SCREEN)

BASIN FILL	GU
BASIN FILL	GL
OXIDE BEDROCK	O
SULFIDE BEDROCK	S

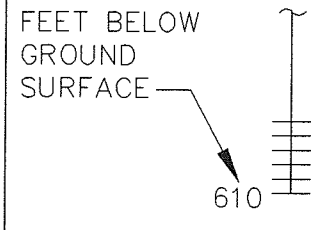

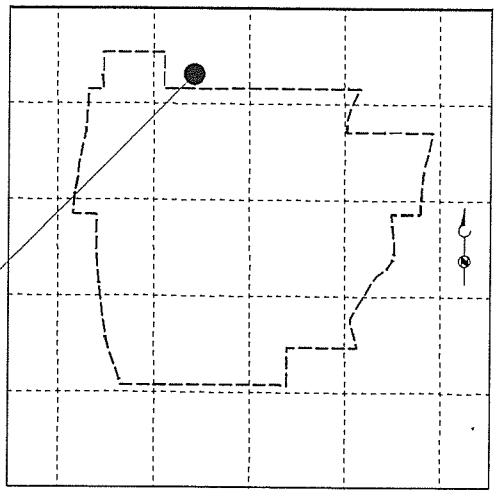

WELL LOCATION MAP

Approximate Scale: 1"= 2000'

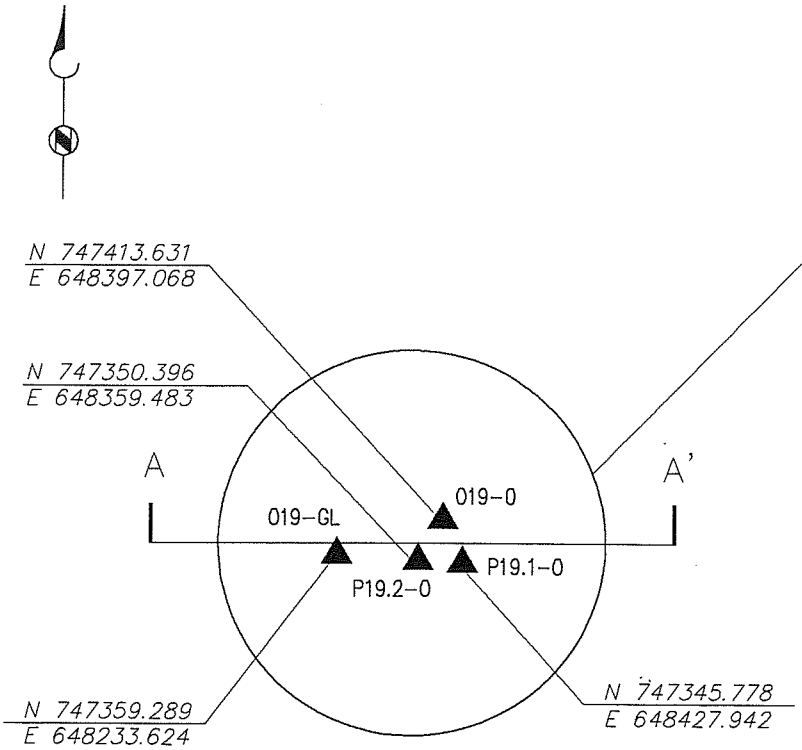

WELL PLAN VIEW

Approximate Scale: 1"= 300'

BROWN AND CALDWELL

Figure E-7 (II)
LOCATION SUMMARY
AQUIFER TEST
CLUSTER 19

MAGMA COPPER COMPANY
Florence, Arizona

E-7.2 12-01-95 DanH

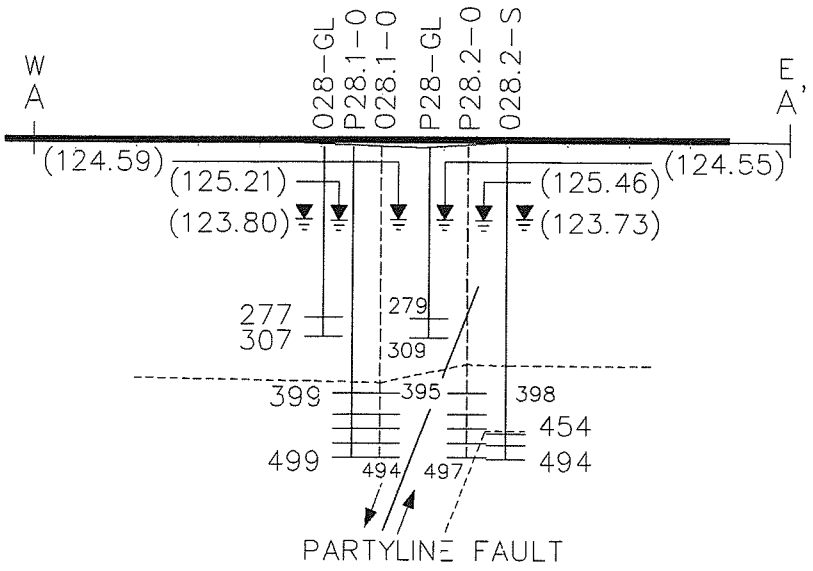

NOTE:
WELLS 028.1-0 AND P28.2-0 ARE SCREENED ACROSS FAULT ZONE.

SIMPLIFIED EAST-WEST CROSS SECTION

Approximate Scale: Vertical : 1"= 300'
Horizontal: 1"= 150'

EXPLANATION

POTENTIOMETRIC SURFACE (151.00)

(SHOWN IN FEET BELOW GROUND SURFACE)

WELL PREFIXES

PUMPED WELL	P
MONITOR WELL	M
OBSERVATION WELL	O

WELL SUFFIXES (AQUIFER COMPONENT SCREEN)

BASIN FILL	GU
BASIN FILL	GL
OXIDE BEDROCK	O
SULFIDE BEDROCK	S

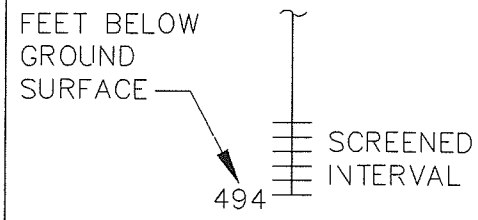

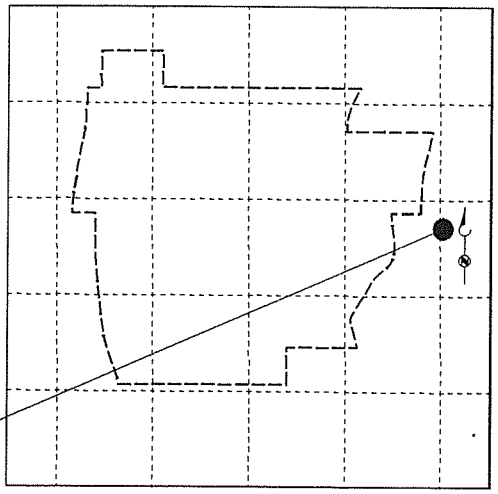

WELL LOCATION MAP

Approximate Scale: 1"= 2000'

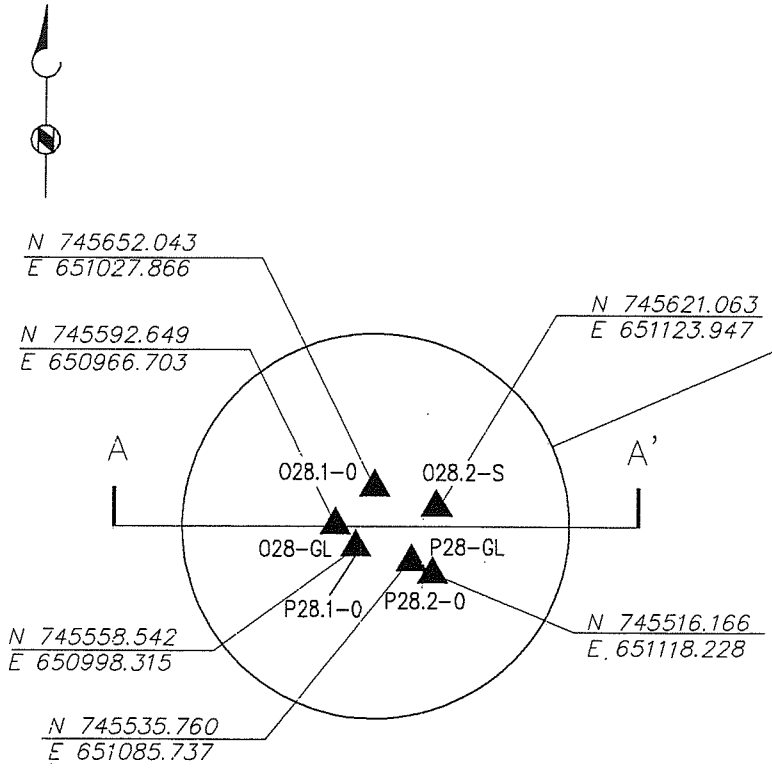

WELL PLAN VIEW

Approximate Scale: 1"= 300'

BROWN AND CALDWELL

Figure E-8 (II)
LOCATION SUMMARY
AQUIFER TEST
CLUSTER 28

MAGMA COPPER COMPANY
Florence, Arizona

E-8_2 12-01-95 DanH

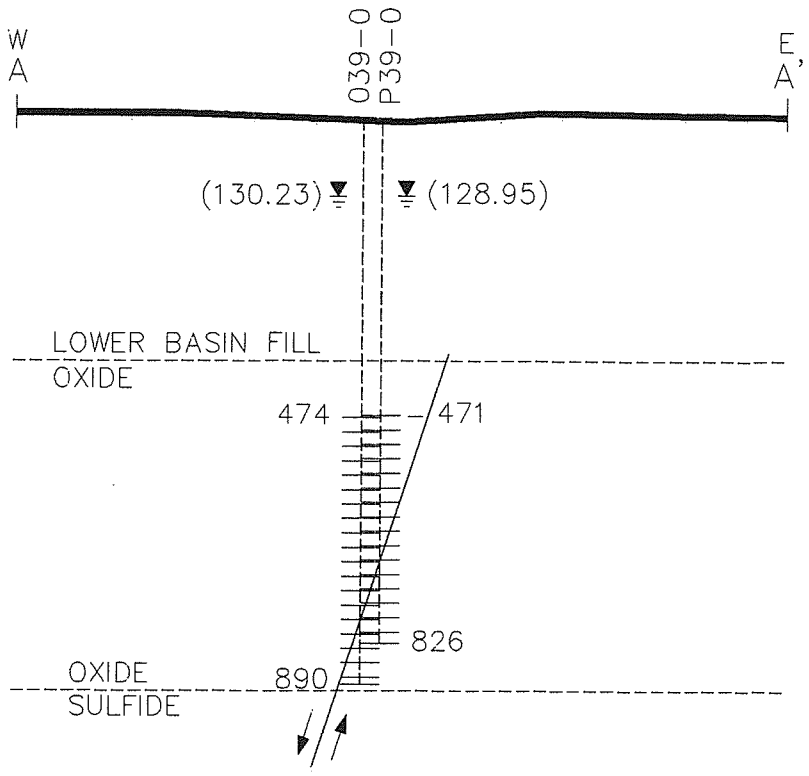

EXPLANATION

POTENTIOMETRIC SURFACE (151.00)

(SHOWN IN FEET BELOW GROUND SURFACE)

WELL PREFIXES	
PUMPED WELL	P
MONITOR WELL	M
OBSERVATION WELL	O

WELL SUFFIXES (AQUIFER COMPONENT SCREEN)	
BASIN FILL	GU
BASIN FILL	GL
OXIDE BEDROCK	O
SULFIDE BEDROCK	S

FEET BELOW GROUND SURFACE

610

SCREENED INTERVAL

SIMPLIFIED EAST-WEST CROSS SECTION

Approximate Scale: Vertical : 1"= 300'
Horizontal: 1"= 150'

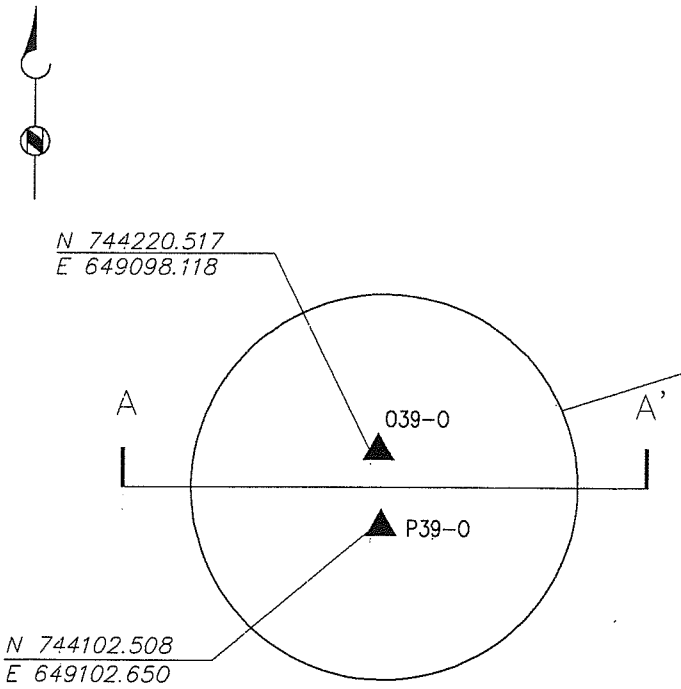

WELL PLAN VIEW

Approximate Scale: 1"= 300'

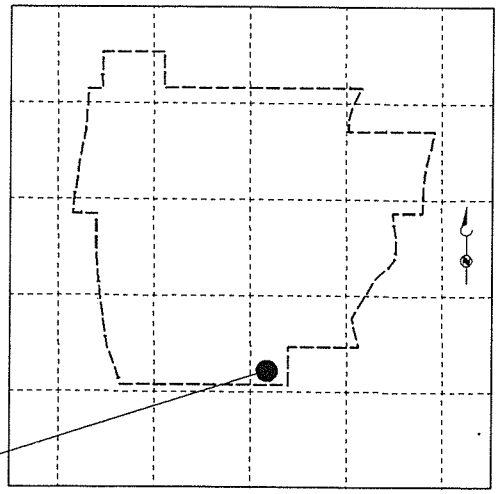

WELL LOCATION MAP

Approximate Scale: 1"= 2000'

Figure E-9 (II)
LOCATION SUMMARY
AQUIFER TEST
CLUSTER 39

BROWN AND CALDWELL

MAGMA COPPER COMPANY
Florence, Arizona

E-9_2 12-01-95 DanH

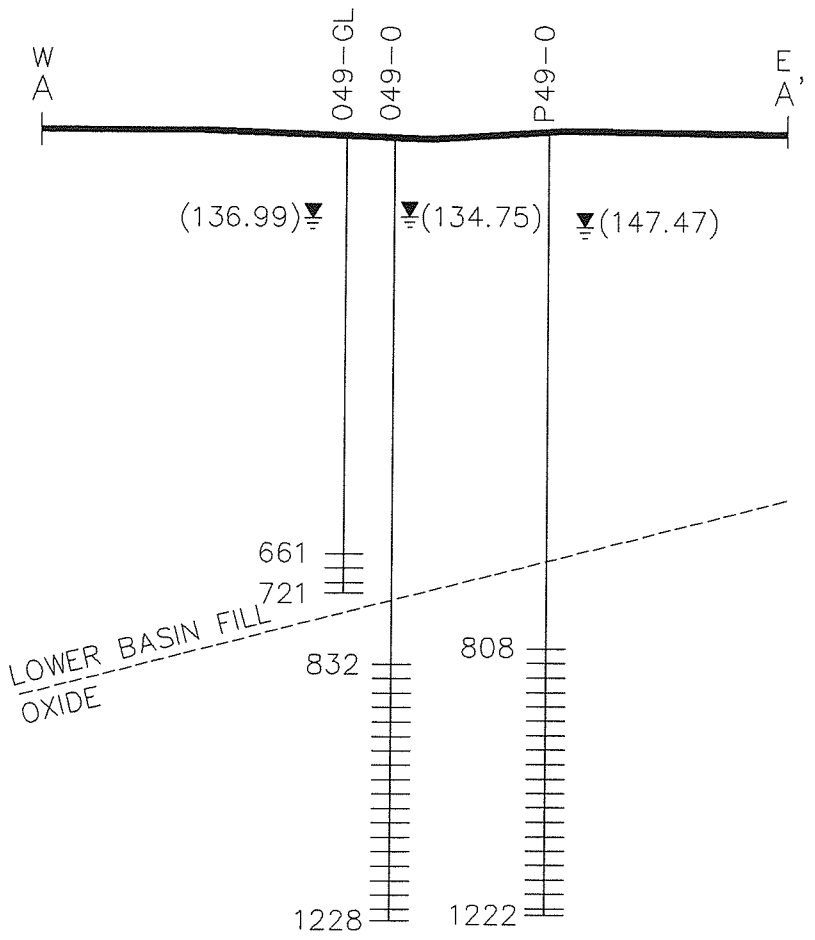

SIMPLIFIED EAST-WEST CROSS SECTION

Approximate Scale: Vertical : 1"= 300'
Horizontal: 1"= 150'

EXPLANATION

POTENTIOMETRIC SURFACE (151.00)

(SHOWN IN FEET BELOW GROUND SURFACE)

WELL PREFIXES

PUMPED WELL	P
MONITOR WELL	M
OBSERVATION WELL	O

WELL SUFFIXES (AQUIFER COMPONENT SCREEN)

BASIN FILL	GU
BASIN FILL	GL
OXIDE BEDROCK	O
SULFIDE BEDROCK	S

FEET BELOW GROUND SURFACE — 890 — SCREENED INTERVAL

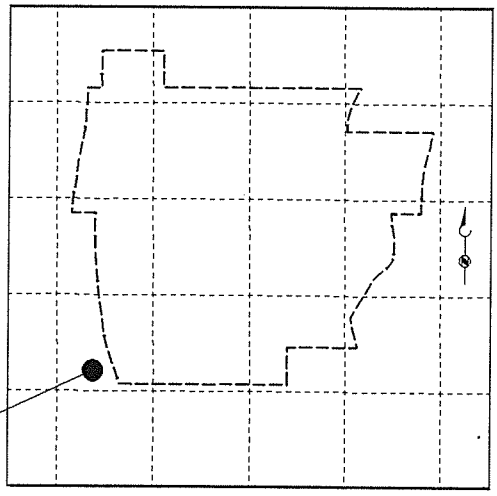

WELL LOCATION MAP

Approximate Scale: 1"= 2000'

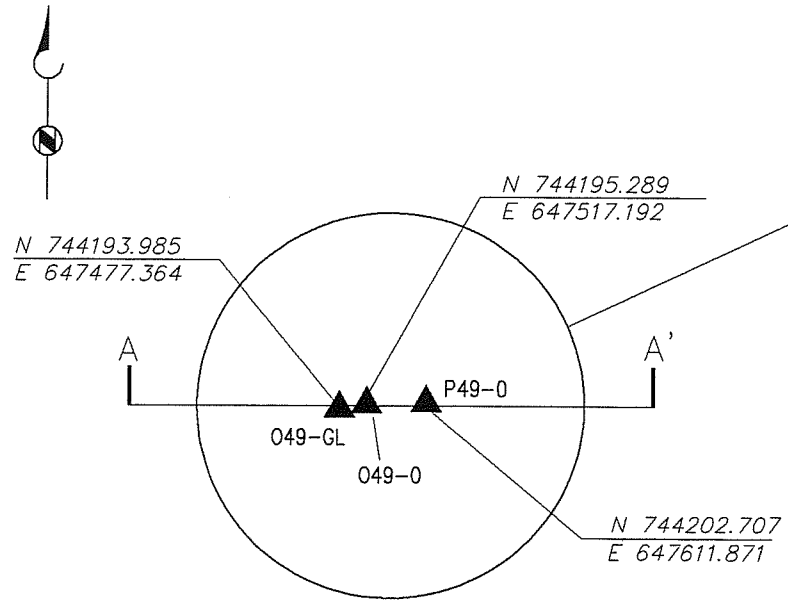

WELL PLAN VIEW

Approximate Scale: 1"= 300'

BROWN AND CALDWELL

Figure E-10 (II)
LOCATION SUMMARY
AQUIFER TEST
CLUSTER 49

MAGMA COPPER COMPANY
Florence, Arizona

E-10_2 12-01-95 DanH

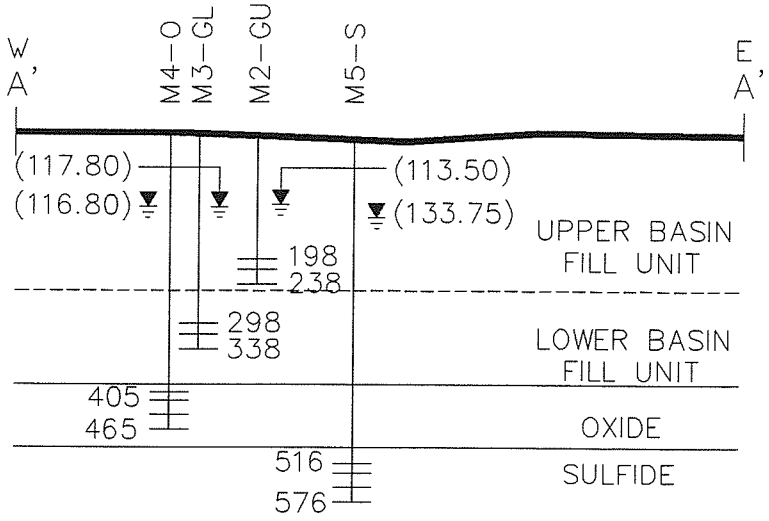

SIMPLIFIED EAST-WEST CROSS SECTION

Approximate Scale: Vertical : 1"= 300'
Horizontal: 1"= 150'

EXPLANATION

POTENTIOMETRIC SURFACE (151.00)

(SHOWN IN FEET BELOW GROUND SURFACE)

WELL PREFIXES

PUMPED WELL	P
MONITOR WELL	M
OBSERVATION WELL	□

WELL SUFFIXES (AQUIFER COMPONENT SCREEN)

BASIN FILL	GU
BASIN FILL	GL
OXIDE BEDROCK	□
SULFIDE BEDROCK	S

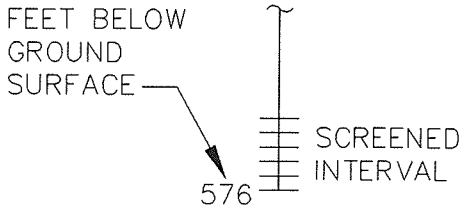

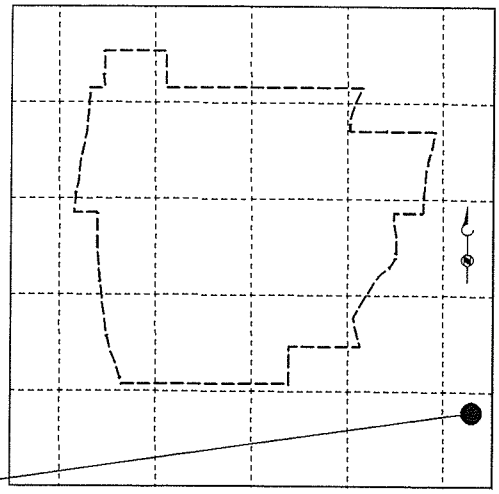

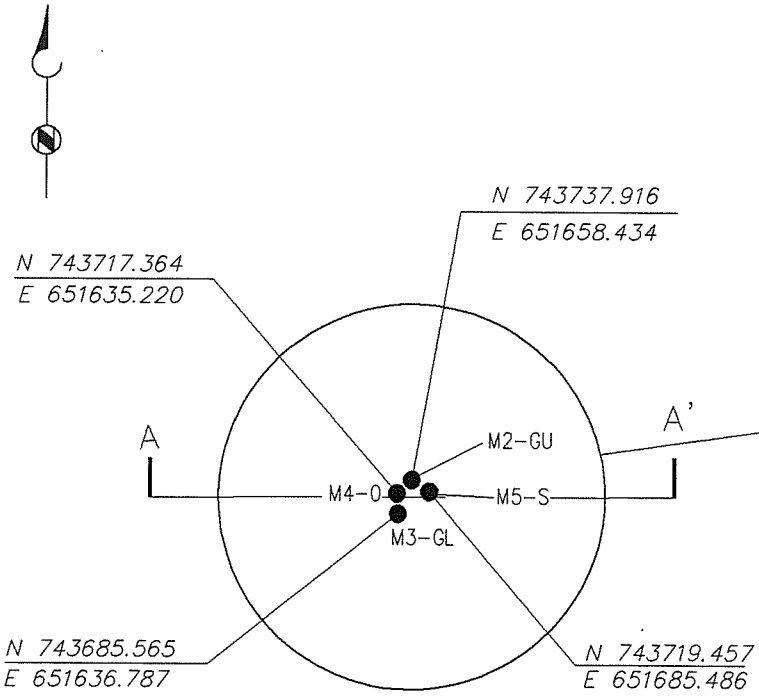

WELL PLAN VIEW

Approximate Scale: 1"= 300'

WELL LOCATION MAP

Approximate Scale: 1"= 2000'

Figure E-11 (II)
LOCATION SUMMARY
SOUTHEAST MONITORING WELL CLUSTER

MAGMA COPPER COMPANY
Florence, Arizona

BROWN AND CALDWELL

E-11_2 12-01-95 DonH

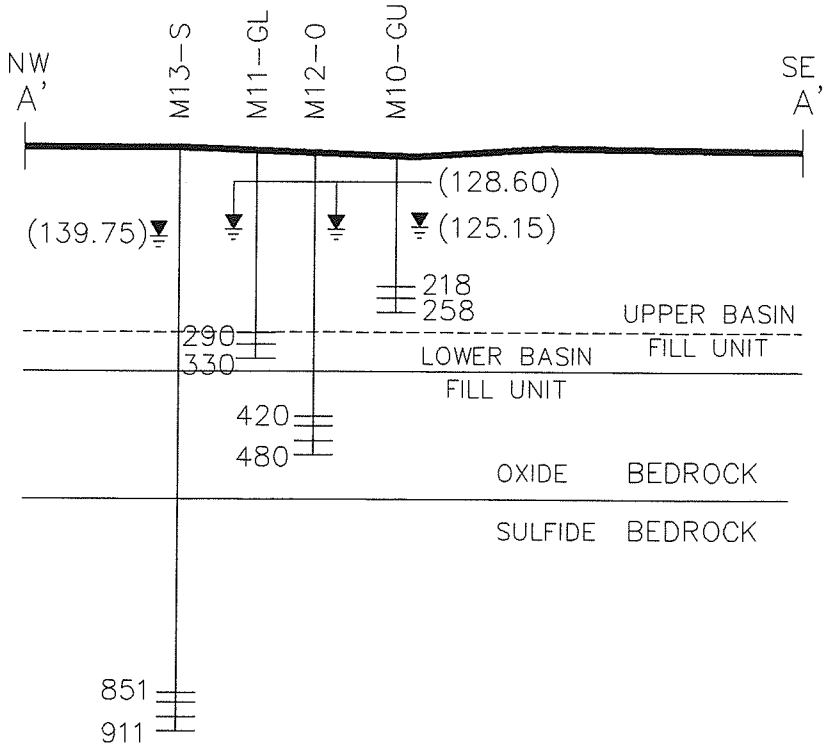

SIMPLIFIED NORTHWEST-SOUTHEAST CROSS SECTION

Approximate Scale: Vertical : 1"= 300'
Horizontal: 1"= 150'

EXPLANATION

POTENTIOMETRIC SURFACE	(151.00)
(SHOWN IN FEET BELOW GROUND SURFACE)	

WELL PREFIXES

PUMPED WELL	P
MONITOR WELL	M
OBSERVATION WELL	O

WELL SUFFIXES (AQUIFER COMPONENT SCREEN)

BASIN FILL	GU
BASIN FILL	GL
OXIDE BEDROCK	O
SULFIDE BEDROCK	S

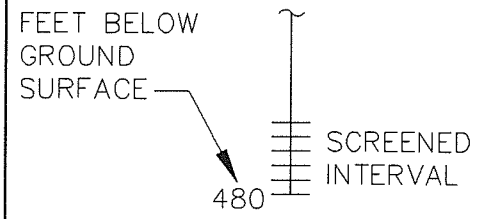

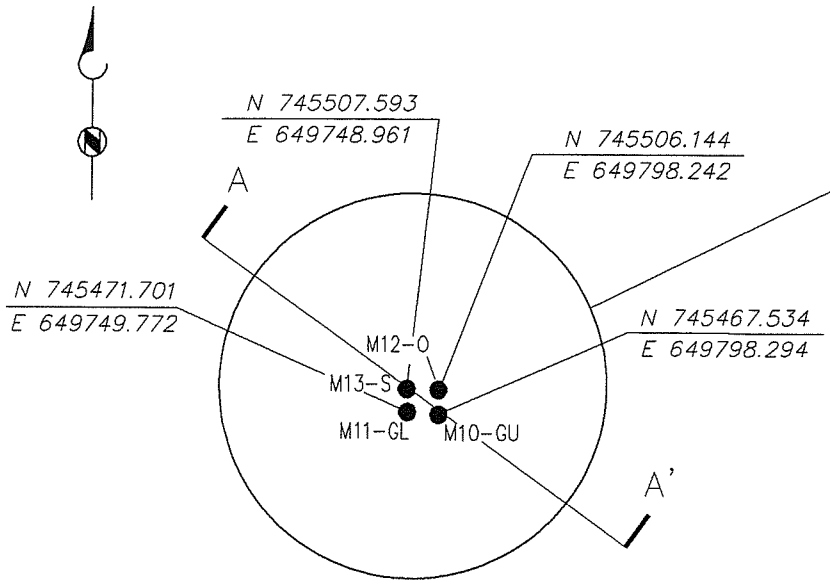

WELL PLAN VIEW

Approximate Scale: 1"= 300'

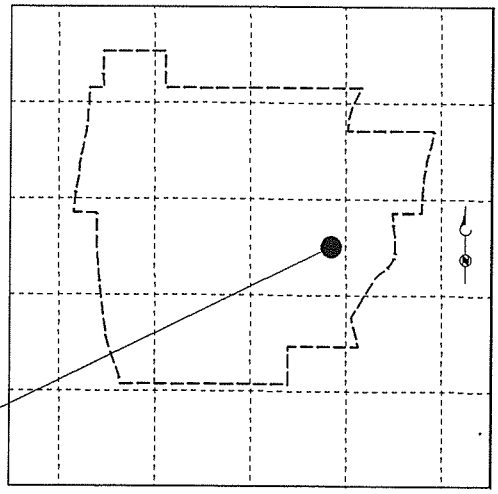

WELL LOCATION MAP

Approximate Scale: 1"= 2000'

Figure E-12 (II)
LOCATION SUMMARY
MIDDLE MONITORING WELL CLUSTER

BROWN AND CALDWELL

MAGMA COPPER COMPANY
Florence, Arizona

E-12_2 12-01-95 DonH

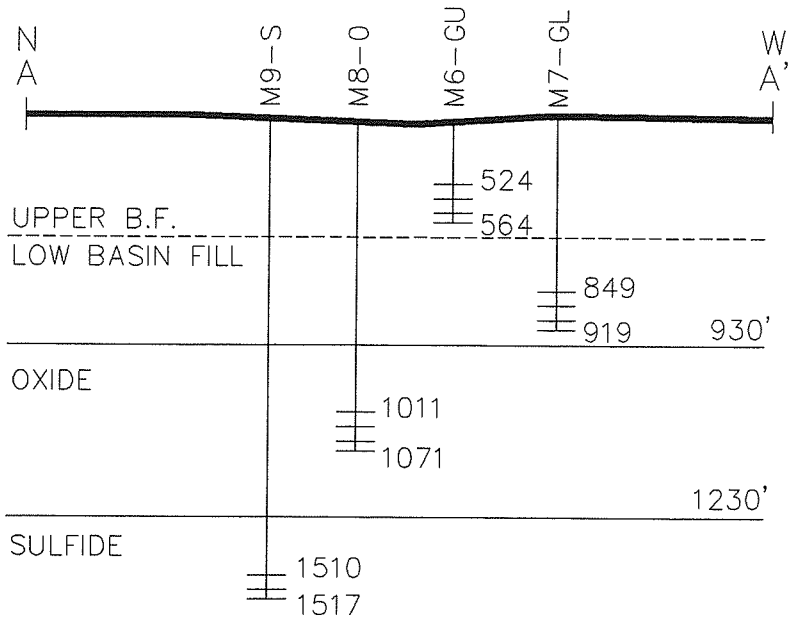

SIMPLIFIED NORTH-WEST CROSS SECTION

Approximate Scale: Vertical : 1"= 300'
Horizontal: 1"= 150'

EXPLANATION

POTENTIOMETRIC SURFACE (151.00)

(SHOWN IN FEET BELOW GROUND SURFACE)

WELL PREFIXES

PUMPED WELL	P
MONITOR WELL	M
OBSERVATION WELL	O

WELL SUFFIXES (AQUIFER COMPONENT SCREEN)

BASIN FILL	GU
BASIN FILL	GL
OXIDE BEDROCK	O
SULFIDE BEDROCK	S

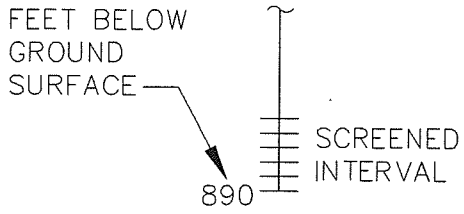

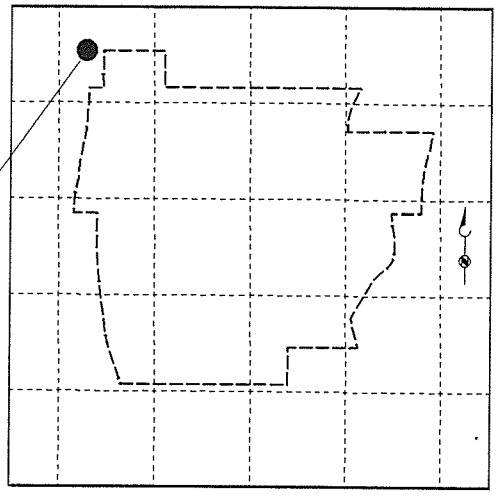

WELL LOCATION MAP

Approximate Scale: 1"= 2000'

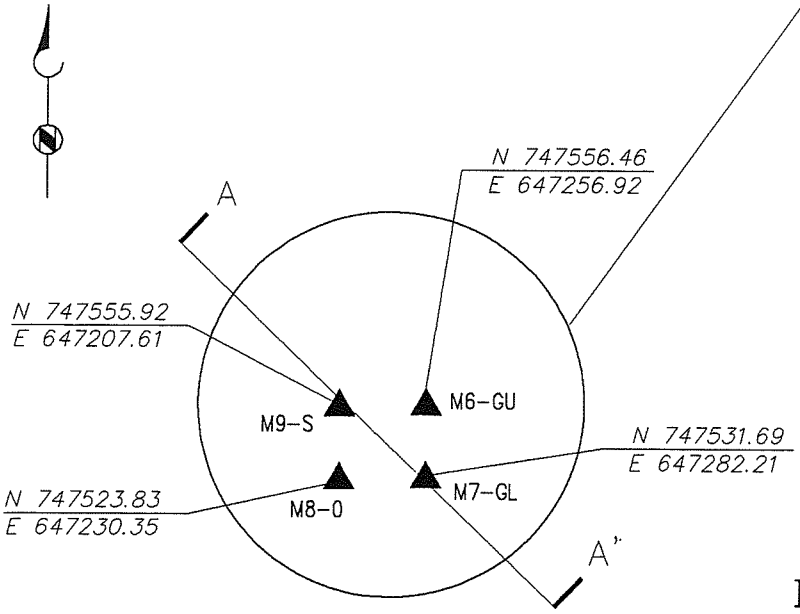

WELL PLAN VIEW

Approximate Scale: 1"= 300'

BROWN AND CALDWELL

Figure E-13 (II)

LOCATION SUMMARY NORTHWEST MONITORING WELL CLUSTER

MAGMA COPPER COMPANY
Florence, Arizona

E-13_2 12-01-95 DanH

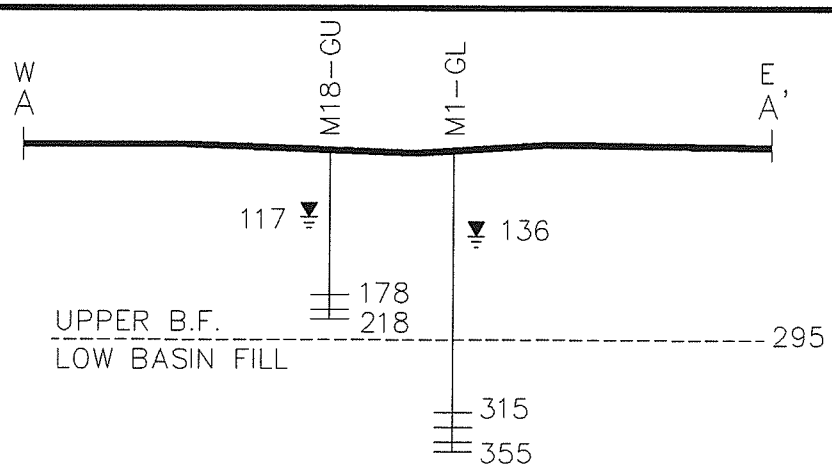

SIMPLIFIED EAST-WEST CROSS SECTION

Approximate Scale: Vertical : 1"= 300'
Horizontal: 1"= 150'

EXPLANATION

POTENTIOMETRIC SURFACE (151.00)

(SHOWN IN FEET BELOW GROUND SURFACE)

WELL PREFIXES

PUMPED WELL	P
MONITOR WELL	M
OBSERVATION WELL	O

WELL SUFFIXES (AQUIFER COMPONENT SCREEN)

BASIN FILL	GU
BASIN FILL	GL
OXIDE BEDROCK	O
SULFIDE BEDROCK	S

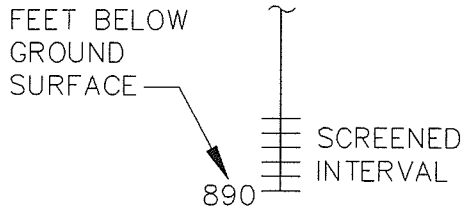

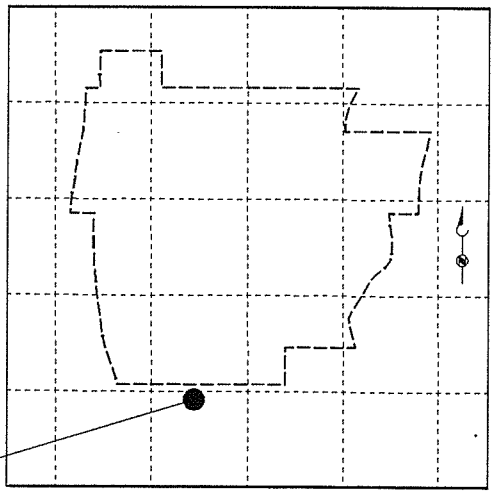

WELL LOCATION MAP

Approximate Scale: 1"= 2000'

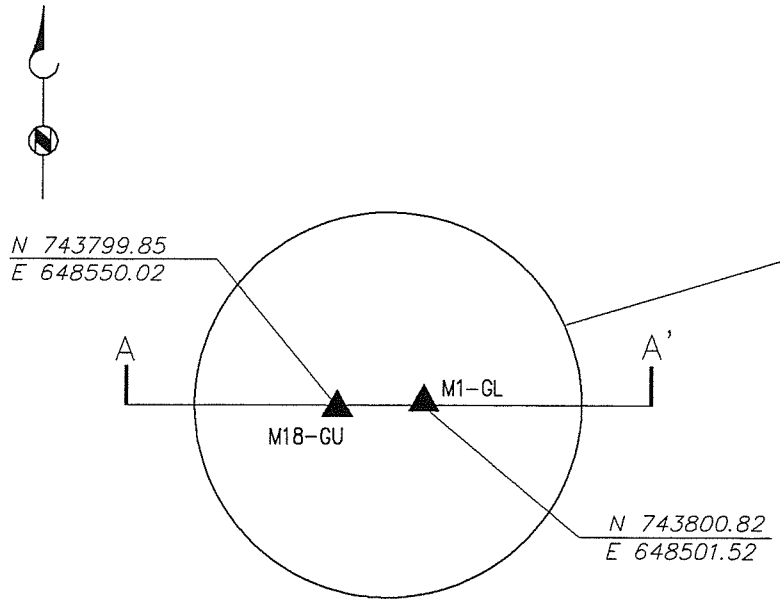

WELL PLAN VIEW

Approximate Scale: 1"= 300'

BROWN AND CALDWELL

Figure E-14 (II)

LOCATION SUMMARY MONITORING WELL CLUSTER 1 & 18

MAGMA COPPER COMPANY
Florence, Arizona

E-14_2 12-01-95 DanH

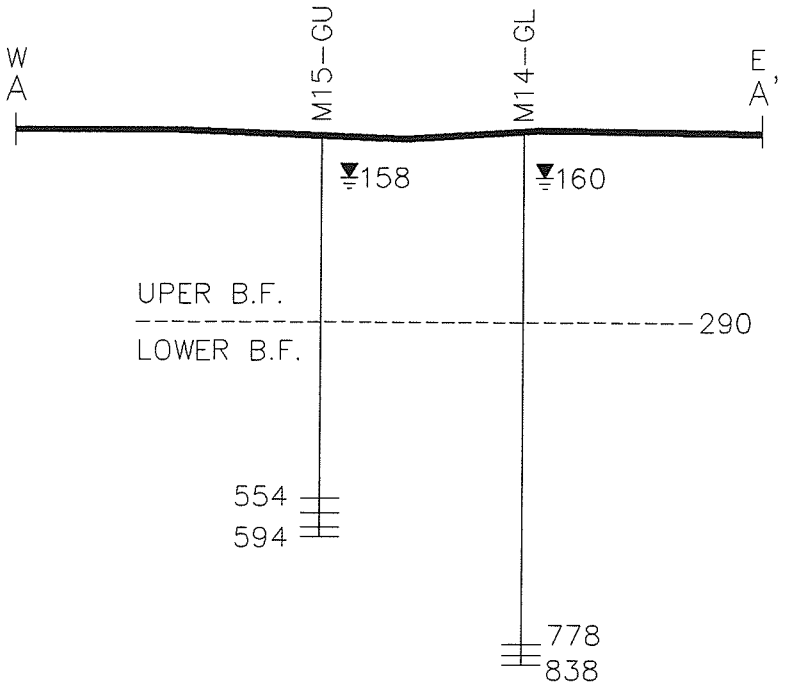

SIMPLIFIED EAST-WEST CROSS SECTION

Approximate Scale: Vertical : 1"= 300'
Horizontal: 1"= 150'

EXPLANATION

POTENTIOMETRIC SURFACE (151.00)

(SHOWN IN FEET BELOW GROUND SURFACE)

WELL PREFIXES

PUMPED WELL	P
MONITOR WELL	M
OBSERVATION WELL	O

WELL SUFFIXES (AQUIFER COMPONENT SCREEN)

BASIN FILL	GU
BASIN FILL	GL
OXIDE BEDROCK	O
SULFIDE BEDROCK	S

FEET BELOW GROUND SURFACE — 890 — SCREENED INTERVAL

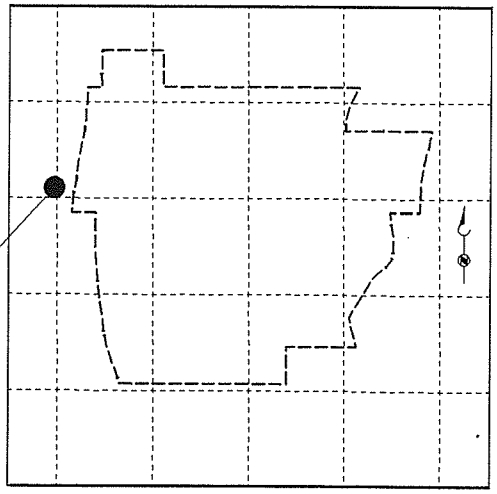

WELL LOCATION MAP

Approximate Scale: 1"= 2000'

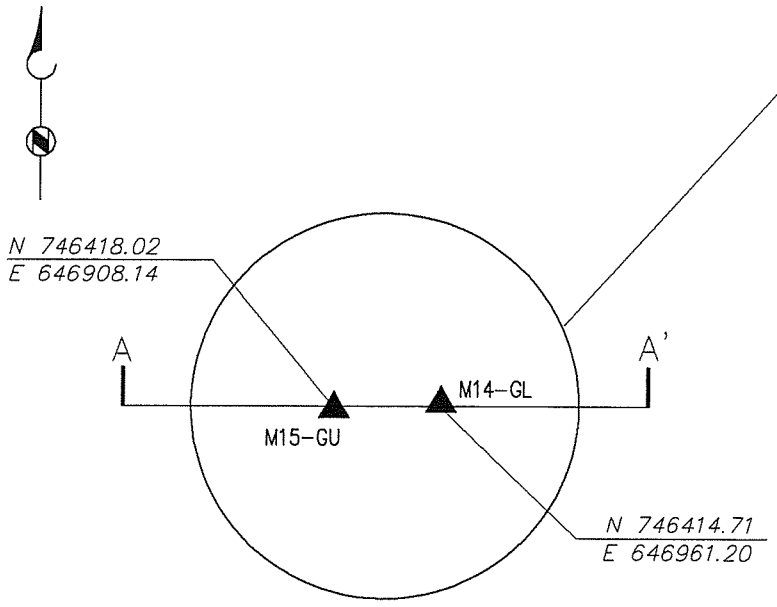

WELL PLAN VIEW

Approximate Scale: 1"= 300'

Figure E-15 (II)

LOCATION SUMMARY MONITORING WELL CLUSTER 14 & 15

BROWN AND CALDWELL

MAGMA COPPER COMPANY
Florence, Arizona

E-15_2 12-01-95 DonH

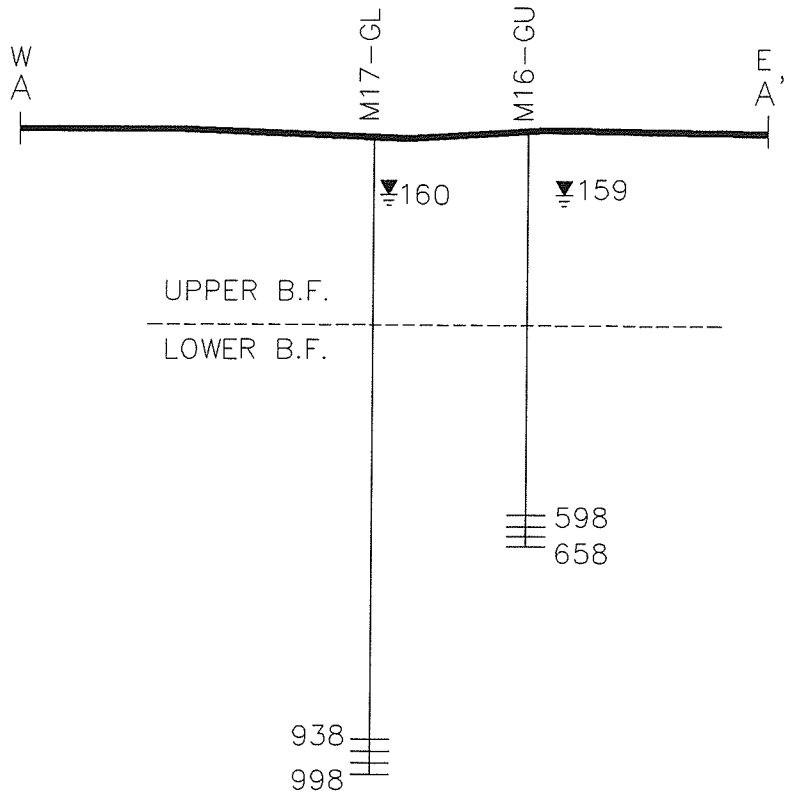

SIMPLIFIED EAST-WEST CROSS SECTION

Approximate Scale: Vertical : 1"= 300'
Horizontal: 1"= 150'

EXPLANATION

POTENTIAMENTRIC SURFACE (151.00)

(SHOWN IN FEET BELOW GROUND SURFACE)

WELL PREFIXES	
PUMPED WELL	P
MONITOR WELL	M
OBSERVATION WELL	O

WELL SUFFIXES (AQUIFER COMPONENT SCREEN)	
BASIN FILL	GU
BASIN FILL	GL
OXIDE BEDROCK	O
SULFIDE BEDROCK	S

FEET BELOW GROUND SURFACE — 890 — SCREENED INTERVAL

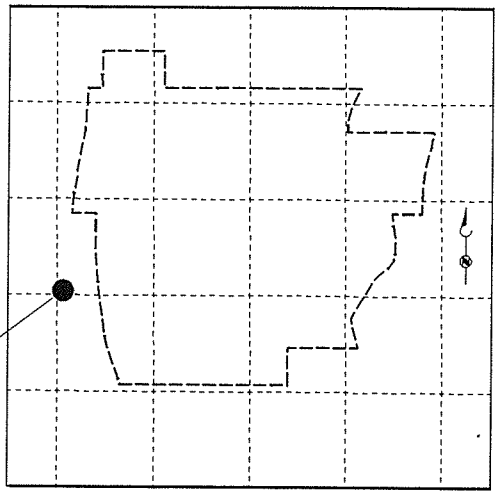

WELL LOCATION MAP

Approximate Scale: 1"= 2000'

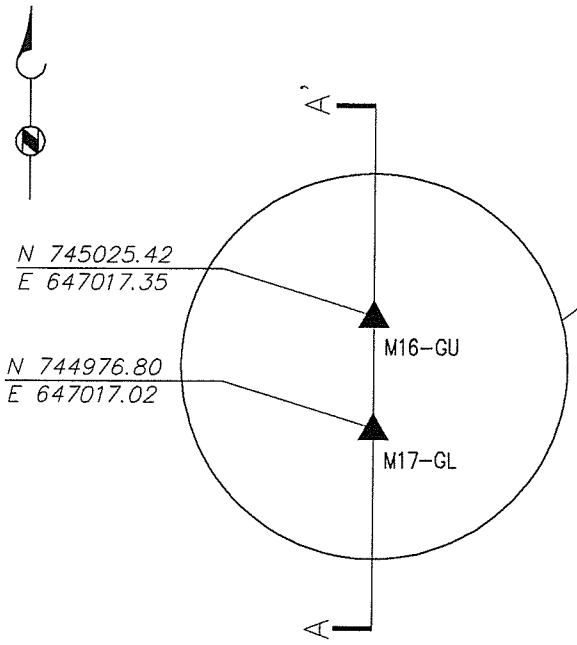

WELL PLAN VIEW

Approximate Scale: 1"= 300'

BROWN AND CALDWELL

Figure E-16 (II)
LOCATION SUMMARY
AQUIFER TEST
CLUSTER 16/17

MAGMA COPPER COMPANY
Florence, Arizona

E-16_2 12-01-95 DanH

Golder Associates Inc.

4730 N. Oracle Road
Suite 210
Tucson, AZ USA 85705
Telephone (520) 888-8818
Facsimile (520) 888-8817

Data Report
for
Initial Interpretation of the Hydraulic Tests at the Florence Mine Site

for

Magma Copper Company
Aquifer Protection Permit
Florence In Situ Leaching Project

Prepared for:

Magma Copper Company
Resource and Development Group
7400 N. Oracle Road, Suite 162
Tucson, Arizona 85704

Prepared by:

Golder Associates Inc.
4700 N. Oracle Road, Suite 210
Tucson, Arizona 85704

Distribution:
2 Copies - John Kline, Magma Copper Company
2 Copies - Dan Ramey, Magma Copper Company
2 Copies - Steve Mellon, Brown and Caldwell
2 Copies - Golder Associates

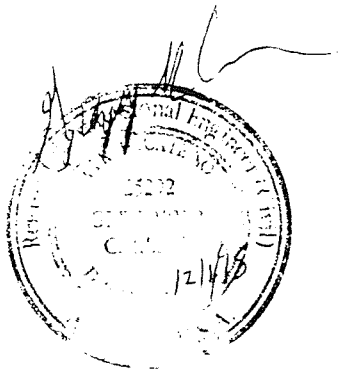

November 1995

Golder Associates

TABLE OF CONTENTS

1.0 INTRODUCTION 1

1.1 Background 1

2.0 THEORY AND METHODS OF INTERPRETATION 3

2.1 Analysis of Recovery Period 3

2.2 Analysis of Drawdown Period 5

2.3 Theoretical Background 6

2.3.1 Rock and Fluid Properties 7

2.3.1.1 Porosity and Compressibility 7

2.3.1.2 Wellbore Storage 9

2.3.1.3 Permeability and Hydraulic Conductivity 10

2.3.1.4 Hydraulic Head 12

2.4 Assumptions and Governing Equation 12

2.5 Interpretation Models 16

2.5.1 Inner Boundary 20

2.5.1.1 Wellbore Storage and Skin 20

2.5.1.2 Fracture Flow 22

2.5.2 Formation Flow Behavior 24

2.5.2.1 Homogeneous 24

2.5.2.2 Dual Porosity 25

2.5.3 Outer Boundary 28

2.5.3.1 Infinite Lateral Extent 28

2.6 Well Test Analysis 28

2.6.1 Constant Rate Tests 29

2.6.2 Straight Line Analysis Methods 30

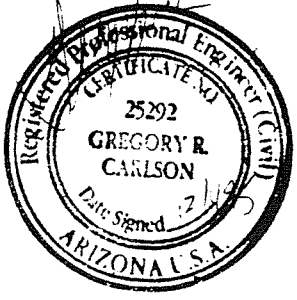

2.6.3 Type Curve Matching and Automatic Regression 32
2.6.4 Theory of Type Curve Matching 33
2.6.5 Dimensionless Type Curves 35
2.6.6 Derivative Type Curves 37
3.0 TEST INTERPRETATION RESULTS 40
4.0 DISCUSSION 59
5.0 REFERENCES 61
6.0 NOMENCLATURE 63

LIST OF TABLES AND FIGURES

TABLES

Table 1, Summary of Available Hydraulic Test Data
Table 2, Preliminary Hydraulic Conductivity Estimates

FIGURE

PAGE

Figure 1, Theoretical Flow Periods 18

Appendix A, **FlowDim™ Analysis Summaries**

Figure 1A, M1-GL A1
Figure 2A, M3-GL A2
Figure 3A, M14-GL A3
Figure 4A, M14-GL (3-D) A4
Figure 5A, M15-GU A5
Figure 6A, M18-GL A6
Figure 7A, P39-O A7
Figure 8A, O39-O A8

Figure 9A, OB7-1 A9
Figure 10A, O12-O A10
Figure 11A, O28-GL A11
Figure 12A, O28.1-O A12

Figure 13A, PW2-1 A13
Figure 14A, M3-GL A14
Figure 15A, PW4-1 A15
Figure 16A, M4-O A16
Figure 17A, PW7-1 A17
Figure 18A, P8-GU A18
Figure 19A, P12-O A19
Figure 20A, P13.1-O A20
Figure 21A, P13.2-O (3-D) A21
Figure 22A, P15-O A22
Figure 23A, P19-O A23
Figure 24A, P19-O (3-D) A24
Figure 25A. P19.1-O A25
Figure 26A. P19.1-O (3-D) A26

FIGURE		PAGE
Figure 27A,	P19.2-O	A27
Figure 28A,	P19.2-O (3-D)	A28
Figure 29A,	P28-GL	A29
Figure 30A,	P28.1-O	A30
Figure 31A,	P28.1-O (Test #2)	A31
Figure 32A,	P28.2-O (Test #2)	A32
Figure 33A,	P28.2-O	A33
Figure 34A,	P49-O (3-D)	A34

Appendix B, **Log-log Plots of Well Reponse Data and Modeled Response**

Figure 1B,	M1-GL	B1
Figure 2B,	M3-GL	B2
Figure 3B,	M14-GL	B3
Figure 4B,	M14-GL (3-D)	B4
Figure 5B,	M15-GU	B5
Figure 6B,	M18-GL	B6
Figure 7B,	P39-O	B7
Figure 8B,	O39-O	B8
Figure 9B,	OB7-1	B9
Figure 10B,	O12-O	B10
Figure 11B,	O28-GL	B11
Figure 12B,	O28.1-O	B12
Figure 13B,	PW2-1	B13
Figure 14B,	M3-GL	B14
Figure 15B,	PW4-1	B15
Figure 16B,	M4-O	B16
Figure 17B,	PW7-1	B17
Figure 18B,	P8-GU	B18
Figure 19B,	P12-O	B19
Figure 20B,	P13.1-O	B20
Figure 21B,	P13.2-O (3-D)	B21
Figure 22B,	P15-O	B22
Figure 23B,	P19-O	B23
Figure 24B,	P19-O (3-D)	B24
Figure 25B,	P19.1-O	B25
Figure 26B,	P19.1-O (3-D)	B26
Figure 27B,	P19.2-O	B27

FIGURE		PAGE
Figure 28B,	P19.2-O (3-D)	B28
Figure 29B,	P28-GL	B29
Figure 30B,	P28.1-O (Test #1)	B30
Figure 31B,	P28.1-O (Test #2)	B31
Figure 32B,	P28.2-O (Test #2)	B32
Figure 33B,	P28.2-O	B33
Figure 34B,	P49-O (3-D)	B34

Appendix C; **Test Analysis Reports**

Figure 1C,	M1-GL	C1
Figure 2C,	M3-GL	C2
Figure 3C,	M14-GL	C3
Figure 4C,	M14-GL (3-D)	C4
Figure 5C,	M15-GU	C5
Figure 6C,	M18-GL	C6
Figure 7C,	P39-O	C7
Figure 8C,	O39-O	C8
Figure 9C,	OB7-1	C9
Figure 10C,	O12-O	C10
Figure 11C,	O28-GL	C11
Figure 12C,	O28.1-O	C12
Figure 13C,	PW2-1	C13
Figure 14C,	M3-GL	C14
Figure 15C,	PW4-1	C15
Figure 16C,	M4-O	C16
Figure 17C,	PW7-1	C17
Figure 18C,	P8-GU	C18
Figure 19C,	P12-O	C19
Figure 20C,	P13.1-O	C20
Figure 21C,	P13.2-O (3-D)	C21
Figure 22C,	P15-O	C22
Figure 23C,	P19-O	C23
Figure 24C,	P19-O (3-D)	C24
Figure 25C,	P19.1-O	C25
Figure 26C,	P19.1-O (3-D)	C26
Figure 27C,	P19.2-O	C27
Figure 28C,	P19.2-O (3-D)	C28

FIGURE		PAGE
Figure 29C,	P28-GL	C29
Figure 30C,	P28.1-O (Test #1)	C30
Figure 31C,	P28.1-O (Test #2)	C31
Figure 32C,	P28.2-O (Test #2)	C32
Figure 33C,	P28.2-O	C33
Figure 34C,	P49-O (3-D)	C34

1.0 INTRODUCTION

This report presents the results of the interpretation of hydraulic tests in the area of Magma Copper Company's (Magma) proposed in-situ mining project near Florence, Arizona. The purpose of this report is to provide a technical basis for hydraulic parameter estimation for site characterization in support of state and federal environmental review and permitting requirements.

This report has been prepared as a technical appendix to the Aquifer Protection Permit (APP) Application document prepared by Brown and Caldwell (1995). As such, only hydrogeologic information pertinent to test data interpretation is discussed in this report. The interested reader is directed to the above reference for additional detail.

The analyses presented in this report are based on standard methods developed in the oil and gas industry. These methods are applied to data collected and provided by Brown and Caldwell. Interpretation of the field data is performed with the FLOWDIM™ software of Golder Associates.

This report is divided into three major sections. Chapter 2 presents the mathematical foundation for the well test analysis. A brief discussion of each test and application of this theory to the aquifer test at the Florence Site is presented in Chapter 3. Tables and graphical representation of these analyses are provided in Appendixes A through C. The field data used in these analyses are included in electronic format in the attached diskette.

1.1 Background

Magma has undertaken field studies to characterize the hydrogeologic conditions near its proposed in-situ mining site in the Poston Butte porphyry copper deposit. The proposed mine site is located in the Basin and Range Physiographic Province of southern Arizona, in the Eloy Sub-basin of the Pinal Active Management Area (AMA), and is about 1 mile southwest of Poston Butte and 2 miles

northwest of the Town of Florence, Arizona.

The rock units in the study area range in age from Precambrian to Quaternary. The floodplain alluvium is Quaternary in age and consists mainly of unconsolidated silt, sand, gravel and boulders. The Cenozoic basin fill deposits have been divided into three major units; the Upper (UBFU), Middle (MBFU) and the Lower (LBFU) Basin Fill Units. The UBFU is composed of unconsolidated to weakly cemented, interbedded clay, silt, sand gravel and boulders. The thickness of the UBFU ranges from 200 to about 500 feet in the vicinity of the mine site. The MBFU is a discontinuous layer composed by silt and clay that varies in thickness from zero to about 80 feet. Weakly to moderately cemented sand, silt and clay constitute the lower unit (LBFU). The thickness of this latter unit varies from less than 50 feet on the east to about 800 feet to the west of the mine site. The bedrock complex consists of quartz monzonite and granodiorite porphyry, and diabase, basalt and other volcanic rocks.

Magma has retained Brown and Caldwell of Phoenix, Arizona to prepare the APP application for the Florence in-situ project. As part of this APP-site characterization effort, Brown and Caldwell has installed forty six (46) monitoring wells and seventeen (17) test wells around the site. Eight (8) of these wells are completed within the UBF Unit, seventeen (17) within the LBF Unit and thirty eight (38) within the bedrock complex. To date, Brown and Caldwell has conducted twenty five (25) aquifer tests which include monitoring wells as well as test boreholes. Magma requested that Golder Associates assist Brown and Caldwell with the design and interpretation of the hydraulic tests required as part of the APP process. Nineteen (19) aquifer test locations were selected for interpretation. These locations cover the range of typical hydrogeologic conditions observed at the site. The following sections present an overview of the theory and methods of interpretation, and the analytical results for a portion of these aquifer tests.

2.0 THEORY AND METHODS OF INTERPRETATION

Well testing provides a means of acquiring knowledge of the properties of hydrogeological formations. In the process of a well test, a known signal (usually a change in flow rate) is applied to the formation and the resulting output signal or response is measured (usually in terms of a change in pressure). Well test interpretation is therefore an inverse problem in that the formation parameters are inferred by comparing a simulated model response to the measured response. The formation parameters are derived by adjusting the flow model parameters to obtain a simulation response that matches the measured data. Clearly, there can be significant ambiguity and non-uniqueness involved in this process, as more than one flow model with different physical assumptions and attributes may match the data. In most situations this can be minimized by careful validation of the selected model using other data.

The overall methodology for the detailed well test analysis of the Florence Project data was as follows:

- the data set was divided into its major components, such as the drawdown period and the shut-in or recovery period;
- appropriate parts were then analyzed separately, with different methods of analysis for flow periods and shut-in periods;
- the analyses of the different periods were checked for consistency.

2.1 Analysis of Recovery Period

The analysis of recovery (shut-in) periods is usually based on the assumption that the shut-in period corresponds to an event of zero flow rate following a fixed period of known finite, constant flow

rate. If the flow rate prior to the shut-in period is variable, then this flow history can be included in the analysis by using the superposition of a number of different but constant flow rates of different durations.

The next step in an hydraulic test analysis involves the selection of an appropriate flow model. these models are generally divided into three basic components.

- inner boundary conditions (i.e., wellbore storage and skin effects, and fracture flow effects);
- formation flow component (i.e., homogeneous formation, dual porosity, and composite model);.
- outer boundary conditions (i.e., infinite extent condition, no flow or constant pressure conditions).

In practice, recognition of a suitable model is performed using diagnostic plots. The data are plotted in different coordinate systems (such as, log-log plots, semi-log Horner plots, etc.) to help the analyst identify the appropriate model from the shape of the data. One key diagnostic plot is the derivative plot where the derivative of the pressure with respect to the natural logarithm of elapsed time is plotted against the log of time. The pressure derivative is extremely sensitive to the shape of the pressure data and as such constitutes the most useful tool for diagnostic purposes. For example, a horizontal line on a derivative plot (presented in a log-log scale) indicates infinite-acting radial flow behavior.

Data from shut-in periods are examined in both log-log and semi-log diagnostic plots. This approach allows the analyst to review the characteristics of the shut-in period. For example, when the effects of the pre-test injection/extraction flows during drilling are significant, the shut-in pressure data reach a peak before starting to decline at late time. This form of data is referred to as a 'rollover' and

can be easily diagnosed on the log-log and semi-log plots. The log-log and the semi-log diagnostic plots are also used to fit selected portions of the shut-in data with appropriate straight lines and obtain initial estimates of formation parameters.

After the flow model has been selected, the quality of the fit of the data with the model response (called 'type curves') is adjusted by using automated regression methods. During this stage of the analysis, the entire data from the selected shut-in period is considered. However, during the final regression stages, emphasis is always placed on the fit of the type curves to specific portions of the data. Judgment of the relative goodness of fit to specific portions of the shut-in data comprises one of the most important aspects of the automated data fitting procedure. Once a suitable and consistent fit of the data is obtained to the type curves, the fit is reviewed for final refinement. The entire measured data set from the shut-in period generated using the best flow model parameters derived from the shut-in analysis is displayed in a cartesian plot.

After the flow model has been selected and a consistent set of analysis results obtained, a sensitivity analysis could be conducted. This exercise is designed to quantify the likely uncertainty in the estimated hydraulic conductivity. When carried out, it helps to determine the range of the parameter within which a reasonably good fit is retained between the model response and the data. The ranges of this parameter therefore reflect uncertainty in the analysis.

2.2 Analysis of Drawdown Period

If a sufficient hydraulic head change is achieved during the drawdown period, the available data were analyzed as a constant discharge test. Otherwise, the data were not use in the interpretation.

In an analysis of the main flow period, the source signal is assumed to be in the form of an instantaneous pressure change from undisturbed in-situ conditions. The data for this flow period is the measured hydraulic head decrease during the test resulting from fluid extraction from the

formation. The analysis used a simple set of type curves which correspond to a single interpretation model :

- inner boundary condition: wellbore storage and skin;
- formation: homogeneous; and
- outer boundary condition: infinite lateral extent.

Only one of two parameter sets can be determined from this analysis: hydraulic conductivity and wellbore skin (the static water level being an input parameter for this analysis) or hydraulic conductivity and storativity. The best fit of the data to the type curves therefore corresponds to finding the optimum set of the two output parameters.

The following section (Section 2.3) describes the general theory underlying hydraulic test analysis. Section 2.4 presents the governing equations and related assumptions. The parameters for various flow models are discussed in Section 2.5. Section 2.6 outlines general methods that are applied to the analysis of hydraulic tests. The reader interested in the specific methodology of detailed test interpretation is therefore directed to Section 2.6.

2.3 Theoretical Background

The purpose of this discussion is to provide a summary of the mathematical and physical background of the aspects of well test analysis that are relevant to the Florence Site. The presentation is divided into three parts:

Part one defines the basic rock and fluid parameters used in the analysis of transient well tests (Section 2.3.1). The second part presents the 'diffusion equation' that governs the flow in porous

media, identifies its underlying assumptions, and describes some special solutions (Section 2.4). Data analyses of Florence hydraulic tests are based on various solutions of the diffusion equation. Finally, the third part describes the interpretation models that have been applied to analyze the Florence hydraulic test data (Section 2.6).

Aspects of theoretical well testing have been documented in numerous papers and textbooks, both in the petroleum engineering and the groundwater literature. The interested reader is directed to the following summarizing references: Kruseman and de Ridder (1991) and Dawson and Istok (1991) for theoretical aspects of pump test analyses written mainly for the 'hydrogeology audience' and Earlougher (1977), Streltsova (1988), Horne (1990) and Sabet (1991) targeted mainly at the 'petroleum formation evaluation audience.'

2.3.1 Rock and Fluid Properties

2.3.1.1 Porosity and Compressibility

Fluid properties such as water compressibility, density, viscosity, and in some cases the thermal expansion coefficient, have to be estimated prior to analysis of the test data. Formation compressibility and porosity must be known (or a reasonable value assumed) in order to analyze transient tests and to obtain estimates for the skin coefficient.

Rock porosity, ϕ, is defined as the ratio of the void volume to the total bulk volume. For analysis of fluid movement the effective porosity of the rock is used. It represents the interconnected volume of pores available for fluid transport. For the Florence hydraulic tests, it was assumed that the average porosity of the Oxide and unconsolidated alluvial sediments is 0.05 and 0.10 respectively. Fractured reservoir rocks can be represented as comprising of two overlapping continua with different porosities. One is the intergranular matrix porosity and the other is the porosity created by the void spaces of fractures. These two types of porosity are called primary and secondary porosity

respectively. The total porosity (or total effective porosity) of the double-porosity system is the sum of the primary and secondary porosities. Laboratory measurements on various types of fractured rock have shown that the fracture porosity is usually significantly less than the matrix porosity (von Golf-Racht, 1982)

The isothermal compressibility of water (and rock) is generally defined as:

$$c = \frac{1}{V}\frac{dV}{dP}\Big|_T \qquad 2.1$$

where the derivative is taken under the condition of constant temperature. In Eq. 2.1, V is the total volume of a given mass of material, and dV is the instantaneous change in volume induced by an instantaneous change in pressure dP.

The total compressibility of the rock-fluid system with 100% water saturation is made up of two components;

$$c_T = c_W + c_R \qquad 2.2$$

where:

c_T	=	total compressibility	Pa^{-1}
c_W	=	compressibility of water	Pa^{-1}
c_R	=	compressibility of rock	Pa^{-1}

Total compressibility was assumed equal to 5.4×10^{-4} Pa^{-1} for the analyses of the aquifer tests at the Florence site. Water compressibility data are readily available as a function of salinity, temperature and pressure. The correct estimation of the rock compressibility, however, is difficult. Data in the

literature cited in Belanger et al. (1989) give a possible range of the fractured rock compressibility as 2.0×10^{-9} kPa^{-1} to 2.0×10^{-5} kPa^{-1}.

Specific storage, S_S, of a saturated confined aquifer is defined as the volume of water that a unit volume of aquifer releases from storage under a unit decline in hydraulic head. This parameter depends directly on the ϕc_T product (Earlougher, 1977):

$$S_S = \phi c_T (\rho g) \qquad m^{-1} \qquad 2.3$$

where:

ρ	=	density of water	kg/m^3
g	=	acceleration of gravity	ms^{-2}.

2.3.1.2 Wellbore Storage

Another form of compressibility, of the fluid inside the borehole, is wellbore storage. During a hydraulic test, wellbore storage causes the downhole flow rate to change more slowly than the surface flow rate. The borehole storage is equal to the change in the volume of fluid in the wellbore, per unit change in the downhole pressure. The wellbore storage coefficient is defined by

$$C = \frac{\Delta V}{\Delta P} \qquad m^3 Pa^{-1} \qquad 2.4$$

noting that ΔV refers to the change in volume of fluid inside the wellbore, and ΔP refers to the change in the downhole (borehole) pressure.

In a wellbore with a changing fluid level (for example during a constant rate pumping period) the wellbore storage coefficient is given by:

$$C = \frac{\pi r_t^2}{\rho g} \qquad 2.5$$

where:

πr_t^2 = volume of tubing per unit length

ρg = change in pressure per unit length

When the fluid level is fixed (for example during a shut-in period) the wellbore storage coefficient is given by

$$C = \pi r_W^2 h\, c_{WW} = V_W c_{WW} \qquad 2.6$$

where V_W is the test section volume (h is the test section length and r_W the wellbore radius) and c_{WW} is the compressibility of the water in the wellbore. The wellbore storage coefficient varies by orders of magnitude depending on the mode of storage within a test. For example, assuming ρg = 10 kPa/m, h = 50 m, r_W = 0.079 m, r_t = 0.035 m and $c_{WW} = 4 \times 10^{-7}$ kPa^{-1}, values of C from equations 2.5 and 2.6 are calculated to be 3.8×10^{-4} m^3/kPa and 3.9×10^{-7} m^3/kPa, respectively.

2.3.1.3 Permeability and Hydraulic Conductivity

The estimation of hydraulic conductivity was the primary objective of the aquifer testing at the Florence site. This parameter is related to both the fluid and fluid transmitting characteristics of the formation. This relationship can be illustrated through the well-known Darcy equation:

$$q = -K\frac{dH}{dL} \qquad 2.7$$

where:

q	=	Darcy flux	ms^{-1},
K	=	hydraulic conductivity	ms^{-1},
dH/dL	=	hydraulic gradient	*unitless*,
H	=	hydraulic head	*m*,
L	=	length or distance	*m*.

The Darcy flux assumes that flow occurs over the entire flow area. In other words, it is a macroscopic velocity. Darcy's law holds only for laminar flow.

The same equation can be expressed in terms of intrinsic permeability (k) which represents the conductance that the rock offers to fluid flow:

$$q = -\frac{k}{\mu}\frac{dP}{dL} \qquad 2.8$$

where:

P	=	pressure	*Pa*,
μ	=	dynamic viscosity	*Pa-s*,
k	=	intrinsic permeability	m^2.

Intrinsic permeability is defined for a single fluid flowing through the rock and represents a transmissive property of only the rock system. Equating Eq. 2.8 with Eq. 2.7 and including the head-

pressure correlation, results in an equation relating hydraulic conductivity and intrinsic permeability:

$$K = \frac{k}{\mu} \rho g \qquad 2.9$$

2.3.1.4 Hydraulic Head

The hydraulic head is expressed in terms of the pressure (P) and an elevation (Z) relative to a known datum. It can be thought of as a column of fluid of length H with a specific density ρ, assuming an atmospheric pressure of P_{atm}, and acceleration of gravity g,

$$H = \frac{P - P_{atm}}{\rho g} - Z \qquad 2.10$$

2.4 Assumptions and Governing Equation

The general well test analysis approach is based on solutions to the diffusion equation (also known, in the petroleum literature, as the diffusivity equation) for various sets of initial and boundary conditions. There are two common ways of presenting these solutions:

a) Hydraulic head, hydraulic conductivity and storage, or

b) Pressure, permeability, porosity, compressibility and fluid viscosity.

When expressed in terms of pressure, the diffusion equation is (see, for example, Lee, 1982):

$$\frac{\partial^2 P}{\partial r^2} + \frac{1}{r}\frac{\partial P}{\partial r} = \frac{\phi \mu c_t}{k}\frac{\partial P}{\partial t} \qquad 2.11$$

where:

r	=	radial distance	*m*,
t	=	time	*s*.

This equation is a linear parabolic partial differential equation, that is derived using the following assumptions (Horne, 1990):

a) Darcy's Law applies;
b) Porosity, permeability, viscosity and rock compressibility are constant;
c) Fluid compressibility is small and constant;
d) Pressure gradients in the formation are small;
e) Flow is single phase;
f) Gravity and thermal effects are negligible;
g) Permeability is isotropic; and
h) Only horizontal radial flow is considered.

The solutions of the diffusion equation are usually given in terms of dimensionless parameters. The dimensionless variables lead to both a simplification and generalization of the mathematics (Dake, 1978). Moreover, with dimensionless variables, the solutions are invariant in form, irrespective of the units system used. The dimensionless pressure, P_D, is a solution to Eq. 2.11 for specific initial and boundary conditions. In the case of the constant surface flow rate (q), the pressure at any point in the formation penetrated by the well is described by the generalized solution below (Earlougher, 1977):

$$P_i - P(r,t) = \frac{qB\mu}{2\pi kh}[P_D(t_D, r_D, C_D, \omega, \lambda, ...) + s] \quad 2.12$$

where B is the formation volume factor, equal to a volume of fluid at well pressure and temperature normalized to standard surface conditions (B is considered to be unity during the analyses of the Florence data). The variables t_D and r_D are the dimensionless time and radius, respectively; C_D is the dimensionless wellbore storage. The other parameters are defined in the Nomenclature section (Section 6.0).

The physical pressure drop is equal to a dimensionless pressure drop times a scaling factor. The scaling factor depends only on flow rate and reservoir properties. The concept applies in general, even for complex situations. It is this generality that makes the dimensionless solution approach useful. P_D is a function of time, location, system geometry and other variables (Earlougher, 1977).

The dimensionless time, t_D, in Eq. 2.12 is defined by:

$$t_D = \frac{kt}{\phi\mu c_t r_W^2} \quad 2.13$$

where r_W is the radius of the well. The definitions for the dimensionless radius and the dimensionless wellbore storage are:

$$r_D = \frac{r}{r_W} \quad 2.14$$

and,

$$C_D = \frac{C}{2\pi\phi c_t r_W^2 h} \quad 2.15$$

Equations 2.13 through 2.15 are expressed in a consistent set of units. In the simple case of steady state radial flow, P_D is equal to ln (r_e/r_w), where r_e is the radius of the circular constant pressure boundary, and Eq. 2.12 becomes the well known steady-state radial form of Darcy's Equation (Earlougher, 1977), or the Thiem Equation (see Section 2.1.1 of Kruseman and de Ridder, 1991). For transient flow, P_D is always a function of dimensionless time (Eq. 2.13), dimensionless radius (Eq. 2.14), and other parameters related to the flow geometry (Earlougher, 1977). Dimensionless pressure can be applied easily, and results in simple general equations that apply to any sort of reservoir properties. It is easily adapted to mathematical manipulation and superposition so that more complex systems can be considered.

In order to account for tests that do not have a constant flow rate (the assumption used to derive Eq. 2.12), the superposition technique is applied. This approach makes it possible to describe a variable rate event (including a shut-in, which is an event with a zero surface flow rate) using a number of constant rate events. The variable rate superposition has been described in detail in well testing literature (Earlougher, 1977; Lee, 1982; Horne, 1990).

The principle of superposition holds for systems that can be described mathematically as 'linear systems' (Horne, 1990). Since most well test solutions are derived from linear diffusive flow equations with linear boundary conditions, the principle of superposition is applicable for most of the standard response functions. The superposition theorem simply states that the sum of individual solutions of a linear flow equation is also a solution of that equation (Drake, 1978). For a variable rate event, the principle of superposition in time can be used to describe the flow response, using a series of constant rate solutions. If a variable rate event is separated (discretized) into 'n' constant rate flow periods, a solution for the n^{th} flow period can be found by solving the diffusivity equation for each flow rate individually and superposing the solutions according to the following equation (Gringarten, 1979; Bourdet et al., 1989):

$$P_D = \sum_{i=1}^{n-1} \frac{q_i - q_{i-1}}{q_{n-1} - q_n} \left[P_D\left(\sum_{j=1}^{n-1} \Delta t_{jD}\right) - P_D\left(\sum_{j=1}^{n-1} \Delta t_{jD} + \Delta t_D\right)\right] + P_D(\Delta t_D) \qquad 2.16$$

where each of the 'n' flow periods has a flow rate of q_i ($q_i \geq 0$) and a duration of Δt_i with Δt being the elapsed time in the 'n^{th}' flow sequence. The subscript 'D' for the time refers to dimensionless time, which is proportional to real time and is given by Eq 2.13.

2.5 Interpretation Models

Type curve matching for pumping test data was first introduced by Theis (1935) for interpreting crosshole responses in homogeneous aquifers. Since then, type curve matching has become one of the most common tools in the interpretation of well test data, both in petroleum and groundwater areas. A type curve is a graphical representation of the theoretical response during a test of an interpretation model that represents the well and the formation being tested. A type curve is therefore specific to the type of test for a given flow system. The type curve analysis of well test data essentially consists of selecting a type curve that can adequately describe the actual response of the wellbore and the formation during the test.

Type curves, therefore, include the entire dynamic behavior of an interpretation model during a test; in other words, type curves include all the individual 'flow regimes' of an interpretation model. 'Flow regimes' are but characteristic features for the various components of an interpretation model. The individual components of an interpretation model dominate the well test response at different times. These responses are broadly divided into three groups: early time, middle time, and late time (Earlougher, 1977).

As a given test starts, the pressure transients generated by the test move away from the generator (ie. the source/sink well) and into the formation. At early time, the pressure signals are dominated by features in the flow system close to the source - such as wellbore storage and skin, presence o

fractures intersecting the source, etc. As the test progresses, the pressure transients move farther away from the source and the test section pressure response reflects the transmission of pressure through each of the significant features in the flow system in succession. The development of the individual flow regimes in the pressure responses does not occur in discreet steps but are separated by 'transition periods' in which the influences of parameters characterizing the two regimes are combined. After the early time effects are over, the pressure response is indicative of larger scale conditions in the formation. During this phase of the pressure response, features such as double porosity, homogeneous behavior, etc. dominate the pressure response. As the test duration increases, the pressure response reflects the formation conditions farther away from the borehole and features such as boundary effects may affect the pressure response. Until the boundary effects are 'seen' by the pressure signals, the formation effectively responds as if it were of 'infinite lateral extent'.

Type curves combine all the flow regimes, including the transition periods, for specific interpretation models. Well test interpretation models are used to define the complete theoretical flow system and the characteristics of the interpretation models are divided into these distinct periods:

1. Inner Boundary (wellbore storage, fracture flow etc.);
2. Formation Flow Behavior (homogeneity, dual porosity etc.); and
3. Outer Boundary (infinite acting, constant pressure etc.).

These periods are illustrated in Figure 1 for pressure and pressure derivative curves. The first period represents the inner boundary condition of the interpretation model and governs the early time response of the model. The formation flow behavior is the flow regime when the pressure response at the pumping well is dominated by formation flow parameters. The outer boundary condition, as the name implies, characterizes the late-time effects.

In an idealized data set the pressure or pressure derivative will have a recognizable shape which can be related to what is happening in the formation. When analyzing well test data it is now common practice to plot the pressure derivative (derivative of pressure change with respect to the natural

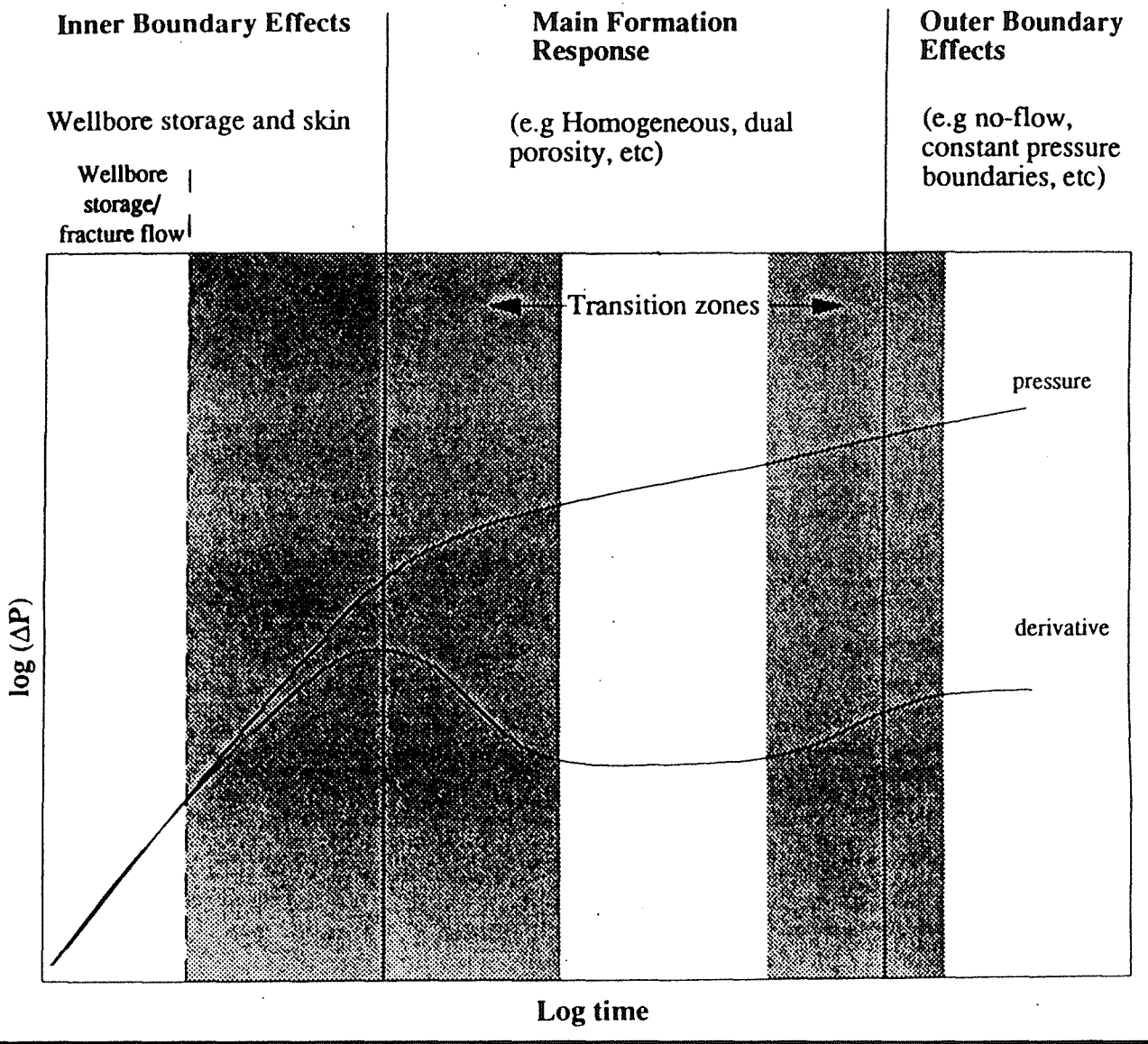

CLIENT/PROJECT					TITLE
Magma Florence			Golder Associates Tucson, Arizona		FIGURE 1
DRAWN AMG	CHECKED AGG	REVIEWED AGG	DATE NOV 1995	SCALE NO SCALE	JOB NO. 953-2908	Hydraulic Test Interpretation - Flow Periods

logarithm of time) in addition to the pressure because it is easier to recognize the characteristic shapes of the test periods on the pressure derivative (Bourdet et al, 1983; Bourdet et al, 1989). Examination of pressure derivative plots allows the analyst to determine the extent of each of the three periods and, from diagnostic curve shapes, identify different types of formation response and boundary effects. The following interpretation models are available in Golder's FLOWDIM™ code:

Inner Boundary Conditions:

a) Wellbore storage and skin;

b) Infinite conductivity or uniform flux fracture; and

b) Finite conductivity fracture.

Formation Flow Behavior:

a) Homogeneous -standard 'porous medium' flow;

b) Dual porosity -fractures in a less permeable matrix; and

c) Fractional Dimension -fracture controlled flow with "imperfect" connections.

Outer Boundary Conditions:

I) Single boundary -constant pressure or no flow.

The following sections discuss only the interpretation models and parameters, which are applied to the analyses of the Florence data. The models are:

- Inner Boundary -Wellbore storage and Skin, and Fractures;
- Formation Flow -Homogeneous and Dual Porosity; and
- Outer Boundary -Infinite Acting.

Different sets of constitutive parameters are used to represent each of the components of the well test interpretation models. The parameters are:

C:	wellbore storage;
h:	total thickness of the formation (equals the test section length, for a 'fully penetrating well' assumption);
k:	formation permeability;
k_f:	fracture permeability in a double porosity system;
k_{fw}:	permeability of finite conductivity fracture;
s:	skin factor;
w:	fracture width;
x_f:	fracture half length;
ω:	interporosity storativity ratio; and
λ:	interporosity flow coefficient.

These components of the interpretation models are described in the following sections.

2.5.1 Inner Boundary

2.5.1.1 Wellbore Storage and Skin

The wellbore storage effect prevents the downhole flow rate from instantaneously following the surface flow rate in the case of constant rate tests. This affects the early-time transient pressure response to a considerable extent. The wellbore storage effect can mask the formation response in tests of very low permeability formations. Wellbore storage is characterized by a wellbore storage constant, C, which is the change in wellbore fluid volume with pressure. For a well filled with a single phase fluid occupying a fixed volume V_w, this constant is given by Eq. 2.6. For a well with a changing liquid level (open tubing flow) the wellbore storage constant is given by Eq. 2.5.

To account for the wellbore storage effect in the solutions of Eq. 2.11, a dimensionless wellbore storage constant C_D was introduced (Eq. 2.15) and P_D becomes a function of t_D, C_D and s, together

with other system parameters.

It is important to note that the compressibility on Eq. 2.6 is that of the fluid in the wellbore. In fractured formations, the actual wellbore storage values can exceed those computed with Eq. 2.6 because part of the storage is due to the volume of fractures in communication with the wellbore. The difference can be a factor of 10 to 100 depending on borehole conditions (Ostrowski and Kloska, 1989). Other effects, such as tool compliance or tool induced injections, can also increase the apparent wellbore storage and cause the wellbore storage constant to be higher than calculated.

Another important dimensionless variable is the skin factor (s) which quantifies the near-borehole flow conditions. Skin factors estimated from transient testing include all features that affect the efficiency of fluid flow into the wellbore. The skin factor represents a steady sate dimensionless pressure drop at the well face in addition to the normal transient pressure drop in the formation. The additional pressure drop is assumed to occur in an infinitesimally thin "skin zone" (van Everdingen, 1953). The additional pressure drop can be the result of local permeability alteration (for example, caused by plugging of flow paths by fines in the drilling fluid, etc.). This pressure drop could also be caused by deviation from purely 2-D radial flow near the well (for example, caused by a fracture near the well giving rise to more linear than cylindrical symmetry flow at early time); this is also called 'pseudo-skin' (Earlougher, 1977). The skin factor is related to this additional pressure drop by the following equation (Earlougher, 1977):

$$s = \frac{2\pi kh}{qB\mu}\,\Delta P_s \qquad 2.17$$

where Δp_s, is the additional pressure drop in the skin zone. A more physically realistic concept of skin is obtained by assuming that the skin effect is due to an altered zone of radius r_S with a skin zone hydraulic conductivity (K_S); for such a case the skin effect can be calculated from the following equation (Earlougher, 1977):

$$s = [\frac{K}{K_s} - 1] \ln[\frac{r_s}{r_w}] \quad (unitless) \qquad 2.18$$

It can be seen from this equation that when the skin zone hydraulic conductivity (K_S) is higher than the formation hydraulic conductivity (K) the skin effect is negative. There is clearly a practical limit to how large the magnitude of skin can become; for the Florence tests, skin coefficients typically vary between -7.5 and 12.0.

Pseudo-skins result from situations such as partial penetration of the water bearing formations, turbulent flow, multiphase effects, and fractures intersecting the wellbore. The important difference between mechanical skins and pseudo-skins is that the pseudo-skins penetrate the formation, creating transient pressure drops that become stable only some time after the beginning of flow in the well (Dowell Schlumberger, 1985). The total skin effect is the combination of the mechanical and all pseudo-skins.

2.5.1.2 Fracture Flow

When the borehole penetrates a single fracture, the early time pressure response is determined by wellbore storage and the flow behavior within the fracture. Two different kinds of fractures are considered, an infinite conductivity fracture and a finite conductivity fracture. In both these models, the flow is assumed to take place from the formation to the fracture and from the fracture into the wellbore. For the infinite conductivity fracture, a negligible pressure drop is assumed to occur within the fracture itself. For this model, the flow goes through two flow regimes:

a) Linear flow towards the fracture from the formation, and then
b) A global radial flow in the formation.

These two successive flow regimes are also shown by a 'uniform flux' fracture (Earlougher, 1977;

Horne, 1990). A uniform flux fracture is a fully penetrating vertical fracture with a uniform flow into the fracture along its length. Both the infinite conductivity and the uniform flux fracture models are based on the following assumption:

a) There is no wellbore storage;
b) The fracture is vertical and fully penetrating;
c) Pressure within the fracture and the borehole is the same at all points;
d) The fracture is characterized by a half-length (x_f); and
e) The fracture is in a homogeneous aquifer.

Analysis using these models yields an estimate of:

x_f = Fracture half-length

In a finite conductivity fracture model, pressure drop is allowed to take place within the fracture. For a finite conductivity fracture, the flow goes through three regimes:

a) Linear flow within the fracture;
b) Linear flow toward the fracture and within the fracture (bilinear flow); and
c) Global radial flow.

In this case, the flow is determined by the fracture half length as in the case of the infinite conductivity fracture and also by the product of fracture permeability and fracture width. Fracture permeability is not a parameter for the case of an infinite conductivity fracture model, since it is considered to be infinitely large. Analysis with the finite conductivity vertical fracture yields estimates for:

x_f = Fracture half-length

k_{fw} = Fracture permeability

None of the Florence tests analyzed so far have shown a response that could be associated to either of these models. In other words, all of the tests analyzed to date have hydraulic responses typical of porous media flow.

2.5.2 Formation Flow Behavior

Many theoretical models have been developed to describe the flow of fluids through different types of formations in the subsurface. Flow models have been developed to account for a multitude of heterogeneous formation behaviors. These models have increased in complexity in line with the increased computational and graphical display powers of desktop computers. To discuss all the models and combinations of models currently available is beyond the scope of this report. Therefore, only the models that are or might be potentially useful for the analyses of the Florence data are discussed here, namely; homogeneous and dual porosity flow models.

2.5.2.1 Homogeneous

The homogeneous model is the simplest formation flow model. It describes flow through the pore spaces of a homogeneous isotropic formation. Analysis with this model in FLOWDIM™ yields estimates of:

k = permeability; and
s = skin.

This flow model is typically combined with the wellbore storage and skin (Inner boundary) and infinite acting (Outer boundary) models to produce the theoretical model of the simplest formation

response.

2.5.2.2 Dual Porosity

A different method of analysis is applied to fractured formations in which flow occurs through both the matrix and through a network of fractures. To analyze tests conducted in these formations, a dual porosity flow model was developed by Warren and Root (1963). They showed that a model which included two fracture related parameters, in addition to permeability and skin, could be used to describe the pressure-time behavior of a fractured formation. These additional parameters represent the storativity ratio of the fractures and the matrix, and the ratio of the matrix permeability to the fracture permeability. It should be noted that the dual porosity model may also be used to represent flow in a fracture system, where relatively low conductivity and less well connected 'background fractures' can be equated with the 'matrix' and more dominant transmissive features with the 'fractures.'

The dual porosity models available in the well testing literature are characterized by the way flow in the more permeable flow conduits (i.e., the fractures) interacts with that in the less permeable flow medium (i.e. the matrix). There are two types of dual porosity models available within FLOWDIM™ depending on the different types of interporosity flow:

a) Restricted Interporosity Flow: In this model there is a skin between the more permeable medium (the fissures) and the less permeable medium (the matrix blocks) which restricts flow; and

b) Unrestricted Interporosity Flow: In this model there is no impediment to flow between the two media and the less permeable medium is assumed to be shaped either like slabs or spheres.

Analysis using the dual porosity model in FLOWDIM™ yields estimates of:

k_f	=	permeability of the more permeable medium;
s	=	skin factor of the well;
s_f	=	skin factor between fissures and the matrix;
ω	=	interporosity storativity ratio; and
λ	=	interporosity flow coefficient.

The definitions of permeability and skin are similar to those in Section 2.3.1.3 and 2.5.1.1. The modifications necessary to fit them into the dual porosity model are noted below. The first of the parameters specific to the dual porosity model, interporosity storativity ratio 'ω', is defined by:

$$\omega = \frac{(\phi c_t)_f}{(\phi c_t)_f + (\phi c_t)_m} \qquad 2.19$$

This relationship characterizes the relative storage capacity of the two media, fracture and matrix (characterized by subscripts 'f' and 'm' respectively). The interporosity flow coefficient 'λ', characterizes the ability of the matrix to flow into the fractures and is defined by:

$$\lambda = \alpha \frac{k_m}{k_f} r_w^2 \qquad 2.20$$

where α is a geometrical factor which depends on the shape of the matrix block. For spherical matrix blocks of radius r_m,

$$\alpha = \frac{15}{r_m^2} \qquad 2.21$$

and for horizontal slab matrix blocks of thickness h_m.

$$\alpha = \frac{12}{h_m^2} \qquad 2.22$$

The theory of the Warren and Root model (Warren and Root, 1963) is extensively discussed in the well test literature (Earlougher, 1977; Streltsova, 1988; Horne, 1990; Sabet, 1991). Therefore, only practical aspects and the physical meaning of the dual-porosity flow parameters are discussed below.

The interporosity storativity ratio, ω, represents the ratio between storage capacity of the fracture network and the total storage capacity of the formation. A value of ω close to zero corresponds to a formation with a very small fracture storage capacity; $\omega = 1$ represents a reservoir with a single dominant flow medium. Small values of ω (<0.1) typically reflect the small storage capacity of fractures relative to the much larger storage capacity of the rock matrix.

The interporosity flow coefficient, λ, represents the dimensionless interporosity flow capacity which depends, primarily, on the ratio of the matrix permeability to the fracture permeability, k_m/k_f. For a given block shape factor α, small λ values correspond to a large contrast between fracture and matrix block permeability. A permeability ratio equal to 1 represents a single porosity (homogeneous) reservoir.

Alternatively, if k_m/k_f is known (e.g. k_m from laboratory tests and k_f from hydraulic testing), it is possible to estimate the characteristics of the fractures. High α values mean large contact surface and consequently smaller matrix blocks (high fracture density). A low value of α corresponds to a smaller contact surface, large matrix blocks and consequently low fracture density.

To date, none of the Florence hydraulic test responses have shown a dual-porosity behavior.

2.5.3 Outer Boundary

2.5.3.1 Infinite Lateral Extent

The model that simulates an infinite acting formation response requires no additional parameters. In this model there is no outer boundary response different from the formation flow response.

2.6 Well Test Analysis

Pressure transient testing has been a subject of extensive work both in the field of groundwater hydrogeology and in the oil industry for the past forty years. Over this period better measuring devices have become available, providing more reliable field data and this, together with the advent of powerful desktop computers, has given rise to the development of more sophisticated interpretation techniques.

In general, transient well tests can be separated into three basic types based on the nature of the source signal:

a) constant rate;
b) constant pressure; and
c) slug and pulse tests.

For constant rate and constant pressure tests, the surface rate and the surface pressure, respectively, are kept constant during the testing period. A slug test is initiated by an instantaneous pressure change (withdraw or injection) and then the groundwater is allowed to flow to the open borehole and to return to initial conditions. A pulse test is very similar to a slug test, the only difference is that the interval is shut-in so that the fluid volume is kept constant. The hydraulic tests conducted at the Florence site are constant rate type tests.

Depending on the type of test, different analysis methods have been developed and documented in numerous papers and manuals. The interested reader is directed to the following summarizing references: Earlougher (1977), Gringarten (1979), Lee (1982), and Bourdet et al. (1983 and 1989) for the analysis of constant rate tests, including multi-rate and shut-in tests; Grisak et al. (1985) for the analysis of wellbore storage dominated pulse and slug, where practical and theoretical aspects of testing in low permeability formations are also discussed; and Pickens et al. (1987) present some interesting practical considerations on interpretation of hydraulic tests in low permeability formations. For detailed descriptions of the various well test analysis methods currently in use, the interested reader is referred to the following additional references: Streltsova (1988), Sabet (1991) and Dawson and Istok (1991).

The purpose of this section is to present some aspects of the test analysis methods that are found to be important for interpretation of the Florence test data. The only tests that will be described in detail are the constant rate tests since these are the type of tests used at the Florence site.

The principles governing the test analysis can be considered as a special pattern recognition problem (Gringarten, 1986). In a well test, a known signal (e.g. pumping rate) is applied to an unknown system and the response of that system (e.g. the change in water pressure) is measured during the test. This type of problem is known as the 'inverse problem.' Its solution involves finding a well defined theoretical system, whose response to the same input signal is as close as possible to that of the actual flow system. Normally this solution is not unique, but with reasonable assumptions and information from other sources like geophysical and geological data, in most cases it is possible to give at least a confined range of solutions.

2.6.1 Constant Rate Tests

The analysis methods for a constant rate test can be divided into two general classes:

a) Straight line analysis methods; and

b) Type curve matching.

After plotting the data in specific coordinate systems, straight lines can be fitted to specific segments of the data set and reservoir parameters determined from the slope and intercept of these lines. This approach requires the data to be divided into discrete sections representing the near wellbore, formation, and outer boundary responses. Each section is then analyzed separately.

The type curve matching approach considers the data as a continuous record. In this approach the data is matched to type curves that represent pressure response models for different combinations of formation and boundary conditions. The type curves are represented in terms of the dimensionless parameters which were introduced in Section 2.4. The formation parameters are calculated from the match points between the measured data and the type curves. These two methods are discussed in more detail in the sections that follow.

2.6.2 Straight Line Analysis Methods

A commonly used method of obtaining reservoir parameters is by straight line analysis. In this approach, pressure data is plotted on specialized plots, e.g. versus log(t), and straight lines fitted to specific portions of the data are used to derive formation parameters. The theory behind straight line methods, especially semilog Horner and MDH has been extensively described in the literature (Earlougher, 1977). Therefore only the application of this method will be discussed here.

Straight lines fitted to the early time portion of the data can be used to obtain estimates of the wellbore storage (pressure versus time or log pressure versus log time) or near well fracture flow parameters (pressure vs. $t^{1/2}$ or $t^{1/4}$). Straight line fits to semilog plots (pressure versus log time), or log (Horner time) can be used to obtain estimates of wellbore storage, skin, permeability and initial pressure; Horner time is defined later in this section. Straight lines fitted to multiple periods of

pseudo radial flow can also be used to identify a dual porosity response and estimate the appropriate flow parameters (λ and ω, see nomenclature).

Straight line analysis methods can also be applied to data presented on log-log plots. A horizontal line fitted to a pseudo radial flow portion of the pressure derivative will provide an estimate of the formation permeability, similar to the Horner approach. Distances to outer boundaries and the existence of multiple boundaries can also be estimated by fitting lines to the log-log plot.

The necessary condition for application of the straight line approach to determine initial hydraulic head and hydraulic conductivity is that the aquifer must be 'infinite acting.' This means that the pressure response must extend beyond the influence of wellbore storage and skin effects and into a period of pseudo-radial flow. In the case of heterogeneous behavior, the total system response must be obtained for the method to be applied. When these conditions are met, the basic reservoir parameters (e.g. hydraulic conductivity) can be derived. The straight line method was in many cases not applicable to the Florence test data, even for the estimation of basic formation parameters, because many of the hydraulic tests are strongly affected by pumping in nearby irrigation wells, rendering the pseudo-radial flow period difficult to identify.

Nonetheless, the basic ideas of the straight line analysis are presented here for the benefit of the reader. A special application of this method is the case of the analysis of a shut-in period after a constant rate flow period. According to the superposition principle, the solution for this case is (Horne, 1990):

$$P_D = P_D [t_{pD} + \Delta t_D] - P_D [\Delta t_D] \qquad 2.23$$

where t_{pD} is the dimensionless flow period duration and Δt_D is the dimensionless elapsed time from the start of the shut-in. The dimensionless pressure (P_D) and the dimensionless time are defined in Section 2.5.2. For infinite acting radial flow during both the flow period and the shut-in, Eq. 2.23

leads to the following solution for the source well in a homogeneous reservoir:

$$P(\Delta t) = P_i - \frac{qB\mu}{4\pi kh} \ln \frac{t_P + \Delta t}{\Delta t} \qquad 2.24$$

Therefore when the pressure is plotted against the natural logarithm of $(t_P + \Delta t)/\Delta t$, where t_P is the flow period duration and Δt is the shut-in time, the data will show a straight line with a slope of

$$m = \frac{qB\mu}{4\pi kh} \qquad 2.25$$

during a period of infinite acting radial flow. The pressure axis intercept represents the initial formation pressure (P_i) or equivalently the static water level. Such a plot is known as a Horner plot and $(t_p + \Delta t)/\Delta t$ is referred to as Horner time which is a dimensionless quantity. For a multiple rate transient test this method can be generalized by plotting (Gringarten et al., 1980):

$$P(\Delta t) \; vs. \; \frac{1}{|q_{n-1} - q_n|} \left[\sum_{i=1}^{n-1} (q_i - q_{i-1}) \log \left[\sum_{j=1}^{n-1} \Delta t_j + \Delta t \right] - (q_{n-1} - q_n) \log \Delta t \right] \qquad 2.26$$

where Δt_j is the duration of each constant rate event. In Eq, 2.26 the time/rate function is referred to as the superposition function, and the plot is known as a generalized Horner plot.

2.6.3 Type Curve Matching and Automatic Regression

A transient well test generally comprises an input impulse (e.g. a change in flow rate) which is imposed on the test interval, and the recorded response (e.g. a change in pressure). The nature and

shape of the response is governed by test geometry parameters (interval volume, flow rate, etc.), fluid parameters (viscosity, compressibility, etc), and formation flow parameters (permeability, porosity, etc.). Some of these are known directly or can be measured either in-situ during the test or in laboratory tests. However, some of the parameters which control the formation response cannot be measured directly and must be inferred from the test response. An analytical mathematical model of the dependence of the formation response on the formation flow parameters can be developed and solved. Then by matching the measured test response to the model response it can be inferred that the model parameters have the same values as the actual reservoir parameters. This process is known as 'Type Curve Matching.'

2.6.4 Theory of Type Curve Matching

We will consider the single constant rate case to present the basic theory of type curve matching. For a constant rate case, the dimensionless pressure is defined as (Horne, 1990):

$$P_D = \frac{2\pi kh}{qB\mu}(P_i - P) = A\,\Delta P \qquad 2.27$$

where A is a function of k, h, q, B, and μ.

Re-arranging Eq.'s 2.13 and 2.27, we get:

$$\frac{t_D}{C_D} = B\left(\frac{\Delta t}{C}\right) \qquad 2.28$$

where B is a function of k, h, and μ. Or in logarithmic terms:

$$Log P_D = Log \Delta P + Log A \qquad 2.29$$

$$Log(\frac{t_D}{C_D}) = Log \Delta t + Log(\frac{B}{C}) \qquad 2.30$$

The combination of the dimensionless time and wellbore storage is a way to reduce the number of independent variables and make the type curves easier to distinguish from each other. Since, by definition, the dimensionless pressure and time/storage are linear functions of actual pressure and time, the log of actual pressure change will differ from the log of the dimensionless pressure drop by a constant amount. The same is also true for the log of actual time. Thus when the appropriate interpretation model has been selected, the actual pressure vs. (time) curve and the theoretical curve P_D vs. (T_D/C_D) have identical shapes, but are shifted with respect to one and other when plotted on the same log-log scale.

The objective of this type curve analysis is to evaluate the amount of shift between the two sets of curves. When the actual data is matched to the theoretical curve on the log-log axes, a match point is selected and the reservoir parameters obtained by rearranging and substituting P_D and ΔP, and (T_D/c_D) and Δt into the above equations as follows:

$$[\frac{P_D}{\Delta P}] matchpoint = A \Rightarrow permeability \qquad 2.31$$

$$[\frac{t_D/C_D}{\Delta t}] matchpoint = (B/C) + permeability \Rightarrow wellbore\ storage \qquad 2.32$$

Originally P_D was plotted versus t_D on a series of distinct curves for welbore storage/skin and infinite acting radial flow (Agarwal et al., 1970). Manipulation of the dimensionless pressure equation, created a combined storage and skin variable, C_De^{2s} that could be used to generate a series of type curves (Gringarten, 1979) for different C_De^{2s} values. The skin factor is obtained by substitution of the calculated dimensionless storage into the C_De^{2s} value obtained from the type curve that gives the best match, and the corresponding C_De^{2s} appropriate to that curve. Other type curves have been developed for fractured reservoirs (see, for example, Bourdet and Gringarten, 1980) and for formations with composite behavior.

For further details of the theoretical aspects of type curve matching, the interested reader is referred to Gringarten (1987), Chapter 4 of Sabet (1991), and Section 3.3 of Earlougher (1977).

2.6.5 Dimensionless Type Curves

The solutions to the analytical models can be expressed as a series of dimensionless variables (Section 2.5.1). These dimensionless variables are important because they simplify the formation response models by representing the transient test parameters in terms of model parameters which remain fixed during the test, thus reducing the total number of unknowns which need to be considered. They also have the additional advantage of providing model solutions that are independent of units. The definition of these dimensionless variables assumes that the test parameters (flow rate, interval volume), the fluid parameters (viscosity, compressibility), and the reservoir parameters (permeability, compressibility, porosity, and reservoir thickness) all remain constant throughout the test.

Theoretical models of reservoir behavior can be presented as a family of dimensionless type curves, expressed in terms of dimensionless pressure (P_D), that are a function of t_D and other dimensionless variables. Each curve in the family is characterized by dimensionless variables that depend on the particular model. These parameters are defined as the product of a measured parameter (e.g. pressure

or time change) and parameters characterizing the reservoir (porosity, permeability, etc.).

The type curves used for the analysis of a pumped withdrawal test in a formation are called drawdown type curves and are defined as:

$$P_D = P_D[(\Delta t)_D] \qquad 2.33$$

The actual data for type curve analysis are defined as:

$$\Delta P = P_i - P(\Delta t) \qquad 2.34$$

The change in pressure (ΔP) is plotted against the change in time (Δt) where Δt is the elapsed time since the start of the pumping sequence, and ΔP is the corresponding pressure reading.

Interpretation models can be obtained by a combination of the appropriate component (inner boundary, formation behavior, and outer boundary) models which have been developed. Their dimensionless solutions are superposed (in space and time) to obtain the type curves required for analysis. Type curves have been published for most of the common reservoir configurations (e.g. homogeneous, dual porosity, etc).

The drawdown type curves are not strictly valid for analyzing flow periods (drawdowns or build-ups) after the first drawdown. For each drawdown type curve there exists a 'family' of build-up type curves that depend on the production period, t_p. The corresponding theoretical build-up type curve is obtained from the appropriate drawdown curve by superposition as follows (Gringarten et al., 1980):

$$(P_D)_{BU} = P_D(T_{pD}) - P_D(t_{pD} + \Delta t_D) + P_D(\Delta t_D) \qquad 2.35$$

The build-up type curves must be calculated for each test, because they depend upon the test conditions. For a multi rate (MR) flow test the type curve can be expressed by Eq. 2.16 in Section 2.5.

2.6.6 Derivative Type Curves

A relatively recent innovation (Bourdet et al., 1983), made much easier with the introduction of computer aided techniques, is to plot the derivative of P_D with respect to ln (t_D/C_D) on the same axes as the P_D vs. T_D/C_D. The derivative is useful as a diagnostic plot when trying to determine the different flow regimes that may occur during the test. The advantage of the derivative plot is that it is able to display in a single graph many separate characteristics that would otherwise require different plots.

During pure wellbore storage (Earlougher, 1977) showed that:

$$P_D = \frac{t_D}{C} \qquad 2.36$$

then taking the derivative

$$\frac{dP_D}{d(\frac{t_D}{C_D})} = P_D' = 1 \qquad 2.37$$

During infinite acting radial flow (which does not show a characteristic response on a log-log scale) in a homogeneous formation (Bourdet et al., 1983):

$$P_D = 0.5[\ln(\frac{t_D}{C_D}) + 0.80907 + \ln(C_D e^{2s})] \quad 2.38$$

then taking the derivative

$$\frac{dP_D}{d(\frac{t_D}{C_D})} = P_D' = 0.5/(\frac{t_D}{C_D}) \quad 2.39$$

Therefore, both at early and late times, all P_D' behaviors are identical and independent of the C_De^{2s} values. At early time, all the curves merge into a straight line corresponding to $P_D' = 1$. At late time the curves merge into a single straight line of slope = -1, corresponding to $P_D' = 0.5/(t_D/C_D)$. Between these two asymptotes, each of the C_De^{2s} curves exhibit a specific shape. It is more useful however, to plot the type curves as P_D' (t_D/C_D) versus (t_D/C_D). This is a better choice of axes because the pressure and time axes are now consistent with the dimensioless pressure axes described earlier.

At early time, the type curves follow a unit slope log-log straight line. When infinite acting radial flow is reached, the derivative curves become horizontal at P_D' $(t_D/C_D) = 0.5$. Between these two asymptotes, the type curves and derivatives are distinctly different for the combined 'family' of C_de^{2s} curves. This makes it easier to correctly identify the correct C_de^{2s} curve corresponding to the data. The derivative shape also provides an improved diagnostic tool for other formation models such as dual porosity, composite, fracture flow, and outer boundary responses.

Modern well test analysis has been greatly enhanced by the introduction of the pressure derivative type curves. The advent of computer aided interpretation has made calculation of the derivative of real data relatively straightforward. The advantage of the derivative plot is that it is able to display in a single graph many separate characteristics of the flow system that would otherwise require different plots (Horne, 1990). The power of the pressure derivative arises from the fact that it magnifies the differences in shapes between the various flow regimes that can be present during a

given flow period, thereby enhancing the diagnostic capabilities of the analyst by a significant amount (Gringarten, 1986).

The interpretation method implemented in FLOWDIM, a Golder Associates proprietary software, takes full advantage of the derivative approach as discussed above. Test interpretation of the aquifer tests in the Florence study area were conducted using this software. The following section presents a brief discussion of the interpretation of each test.

3.0 TEST INTERPRETATION RESULTS

This section provides a brief description of the conditions during each aquifer test, general comments on the quality of the data, and results from the analytical interpretation. One critical piece of information during any hydraulic test program is the location of nearby active wells and their pumping rates and duration of pumping periods. In the case of the Florence aquifer tests, a precise discharge rate history for nearby agricultural wells is, in general, not available. Complete interpretation of the affected aquifer tests is not possible without this information, and the resulting estimated hydraulic conductivity may be inaccurate.

In some cases, boundary effects and abrupt changes in the pumped well discharge rate complicated the interpretation of the drawdown and recovery data, not to mention the effect of nearby agricultural wells. To the extent permitted by the data, an attempt was made to discern amongst effects produced by geological controls and those produced by the cycling of nearby agricultural wells. Information about the hydraulic tests conducted to date is summarized in Table 1 (See Appendix A). Also shown in this table are the name designations of the wells participating in a given test, starting and ending date of the test, and available information regarding geologic formation, screen location, drawdown and discharge data.

Table 2 (See Appendix A) presents a summary of the hydraulic conductivity estimates resulting from our interpretation. Also included in this table is the name of the formation penetrated by the particular well(s), and comments and qualifiers on the conductivity estimates. The available data are classified into three different categories; fair, acceptable and good. A fair data set is one that is interpretable but the estimated hydraulic conductivity should be used with caution. An acceptable data set represents a test with some uncertainty and usually results in an underestimate of the formation hydraulic parameters. A good data set results in a hydraulic conductivity that is deemed as a close representation of the formation conductivity.

The following table is considered useful for the understanding of subsequent section ans is therefore

included in the text. The table provides an abbreviated summary of the estimate hydraulic

Well Identification	Active/Observation	K (feet/day)
Basin Fill Deposits		
M1-GL	Active	17.3
M3-GL	Active	15.9
M14-GL	Active	1.7
M14-GL3d	Active	0.1
M15-GU	Active	2.6
M18-GL	Active	19.6
P28-GL	Active	8.3
O28-GL	Observation (P28-GL)	23.2
M3-GL	Observation (M4-O)	14.8
P8-GU	Active	61.3
Oxide		
M4-O	Active	0.6
PW2-1	Active	1.4
PW4-1	Active	3.8
PW7-1	Active	0.2
OB7-1	Observation (PW7-1)	0.1
P12-O	Active	0.4
O12-O	Observation (P12-O)	0.6
P19.1-O	Active	0.3
P19-O	Observation (P19.1-O)	0.2
P19.2-O	Observation (P19.1-O)	0.2
P19.1-O3d	Active	1.00E-02
P19-O3d	Observation (P19.1-O)	2.39E-04
P19.2-O3d	Observation (P19.1-O)	1.99E-04
P39-O	Active	0.3
O39-O	Observation (P39-O)	0.3
P28.1-O	Active	7.7
P28.1-O (2)	Active	3.6
P28.2 -O	Observation (P28.1-O)	2.7
P28.2-O	Active	3.1
O28.1-O	Observation (P28.2-O)	3.0
P13.1-O	Active	0.3
P49-O3d	Active/Recovery Data	7.75E-03
P15-O	Active	0.5

conductivity presented in Table 2 in Appendix A. This abbreviated table divides wells into those testing the Basin Fill Units, and those testing the mineralized bedrock.

As seen from this table, the hydraulic conductivity for the Basin Fill Units vary from 1.7 to 61.3 feet per day (ft/day), whereas that for the quartz monzonite and the granodiorite porphyry vary from 0.1 to 7.7 ft/day (with exception of the 3-D analyses). The maximum conductivity value for the Basin Fill units was derived from a test in the Upper Unit. The smaller variation in the hydraulic conductivity suggest a greater degree of heterogeneity than that of the mineralized bedrock.

Appendix A contains a summary sheet for each test interpretation, including a calculation of hydraulic conductivity in feet per minute (ft/min), feet/day (ft/day), meter per second (m/sec), and centimeter per second (cm/sec), as well as the estimated value of the skin factor. Appendix B presents the log-log plots of the type curve selected for the analysis, and observed drawdown versus time. Appendix C includes report forms from the FLOWDIM interpretation for each test. This form contains the well name, type of test, and date of the test. Well geometry information, such as well radius, interval length, formation tested, total depth, as well as discharge rate and test duration are also included in this form. In addition, this form presents also the model assumptions and numerical values for hydraulic parameters.

The following paragraphs offer a cursory description of test conditions and hydraulic conductivity estimates for each test. The first few tests are discussed in detail to provide the reader with a basis for understanding the remaining tests presented in Appendix A through C. Detailed discussion for unique and interesting tests is given as warranted by test response.

Aquifer Test on M1-GL

This constant rate test involved a single well with a discharge of 10 gallons per minute (gpm). Well M1-GL is a monitoring borehole completed within the lower basin fill unit (LBFU). Nearby agricultural wells BIA-9 and BIA-10B were reported to be active during the test. The test response shows a slight "recovery" of the hydraulic head during the test. This effect is responsible for the decrease in drawdown (circles) in the late time data presented in Figure 1B in Appendix B. Final

recovery of the hydraulic head resulted in a water elevation higher than the elevation reported at the beginning of the test; indicating that the observed hydraulic head response is a superposition of more than one stress on the aquifer (namely; the transient effects from wells BIA-9 and BIA-10B).

The log-log plot presented in Figure 1B shows both the drawdown data and its derivative with respect to the natural log of time (triangles) versus time, and the dimensionless type curve that was selected for interpretation of this test. In this particular case the selected type curve corresponds to a two-dimensional (notice the asymptotic approach to $p_D' = 0.5$), homogeneous flow model, with a C_De^{2s} parameter equal to 2×10^{8} . This value, in turn, results in a skin coefficient of 3.3 (see summary interpretation in Figure 1A in Appendix A) indicating some possible formation clogging near the well face. Figure 1B shows the transient effects produced by nearby pumping, and that the match between the data and the type curve is poor. The pressure derivative of the data shows a large amount of random variation in late time, making it difficult to better assess the hydraulic parameters. The hydraulic conductivity estimate is 17.3 ft/day. It is our opinion that this conductivity value most likely overestimates the actual conductivity of the formation in that the observed drawdown appears to be affected by a recovery trend that limits its final magnitude. The effect of nearby pumping (recovery) may be responsible for the extremely small estimate of the storage coefficient (8.4×10^{-9}).

Aquifer Test on M3-GL

Aquifer test on monitoring well M3-GL (Figure 14B) involved wells M2-GU, M4-O and M5-S as observation points. Average discharge from M3-GL during this test was reported at 10 gpm. Well M3-GL is completed in the Lower Basin Fill Unit, while M2-GU and M4-O are completed in the Upper Basin Fill Unit (UBFU) and the oxide unit, respectively. Irrigation Well ENGLAND #3 was on during the test but no information regarding its pumping rate is available. Observation wells M2-GU and M5-S showed recovery 100 minutes into the test. The hydraulic response for wells M2-GU and M4-O is minimal and quite erratic. This small response between M2-GU and M3-GL may indicate a limited hydraulic connection between the lower and Upper Basin Fill Unit in this area of

the site. After shut in of well M3-GL, observation wells M2-GU and M4-O showed a slight recovery and then began to drop off again which may be the result of cycling of agricultural pumping. The hydraulic response of well M5-S appears completely independent of pumping on well M3-GL. Due to the above conditions, the hydraulic responses from the observation wells were considered not suitable for interpretation.

Data interpretation for this test was accomplished by means of a 2-D, homogeneous model (as indicated by the approach of the derivative of $p_D = 0.5$) with a $C_D e^{2s}$ parameter equal to 1×10^{6} (Figure 14B). The skin parameter was estimated to be 1.16 (Figure 14A); indicating slight formation clogging near the well face. The overall fit of the drawdown data and the selected type curve is relatively good up to about 10 hours into the test. However, the pressure derivative data deviates sharply from the type curve just after about 0.1 hour into the test. The estimated hydraulic conductivity for the Lower Basin Fill Unit is 15.9 ft/day with a storage coefficient of 3×10^{-7}. The deviation of the data from the derivative and this small storage coefficient may be an effect produced by pumping from ENGLAND #3 well.

Aquifer Test on M14-GL

Well M14-GL was tested under a constant discharge of about 10 gpm. This well is completed within the Lower Basin Fill Unit (LBFU). Well M15-GU, in the Upper Basin Fill Unit, serves as an observation well. Irrigation Wells BIA-9 and BIA-10B were on during the test but no information is available regarding their pumping rate history. Additionally, M1-GL was pumping during testing. Very little drawdown was seen in the observation well (M15-GU). However, a sharp increase in hydraulic head was observed at about 1,000 minutes after pumping in M14-GL ceased. Recovery in the pumping well went beyond initial reported static water level. It is suspected that one or both of the pumping agricultural wells may be responsible for these effects. Field data from the observation well was not considered suitable for interpretation.

Two interpretation models were applied to the drawdown data from well M14-GL. First, a 2-D, homogeneous model (Figure 3A) was used to match the field data. It was seen (Figure 3B) that only the early data ($t < 50$ min) closely approximated both the pressure and pressure derivative of the 2-D type curve. At later times, the derivative of the field data deviated sharply from the type curve. As discussed in Section 2.6, this type of deviation is characteristic of a 3-D flow regime. Analyses of these data using a 3-D model (Figures 4A and 4B) shows that the overall fit to both pressure and pressure derivative improved significantly. Given the relatively short length of the screened interval as compared to the thickness of the Lower Basin Fill Unit in that location, it is not surprising that the test response suggests 3-D flow (typical of a partially penetrating well). Hydraulic conductivity estimates from these two different models are reported in Table 2 as well as in Figures 3C and 4C. The resulting conductivity estimates are 1.7 and 0.1 ft/day for the 2-D and 3-D models respectively. Although the 3-D type-curve better represents this field data, it is recommended, for the sake of conservatism, that numerical simulation of flow and transport be conducted with the larger hydraulic conductivity estimate. As will be discussed later for some of the other tests, 3-D conductivity estimates are typically smaller than corresponding 2-D estimates.

Aquifer Test on M15-GU

This constant rate test involved a single pumping well (M15-GU) discharging at 10 gpm from the upper consolidated unit (UBFU) and one observation well (M14-GL) which was completed in the Lower Basin Fill Unit (LBFU). Irrigation Wells BIA-9 and BIA-10B were on during the test but no information is available regarding their pumping rate history. The pumping well recovery rose above the static water level. It may be that one or both of the irrigation wells were shut off during testing, causing these effects. Due to the above effects the data form the observation well were not considered suitable for interpretation. Only the data for M15-GU was analyzed.

The selected type curve for the pumping well data (M15-GU) corresponds to a 2-D, homogeneous flow model, with a C_De^{2s} parameter equal to 10 (see Figure 5C). This value, in turn, results in a skin

coefficient of 6.6 indicating (Figure 5A), perhaps, some formation clogging near the well face. As shown in the log-log plot (Figure 5B), the match between the data and the type curve is good. The hydraulic conductivity estimate is 2.6 ft/day. The estimate for the storage coefficient is 1.1×10^{-11} which is clearly too small and another indication of the difficulty involved in modeling marginal data.

Aquifer Test on M18-GU

This constant rate test involved a single pumping well (M18-GU) with a discharge of 10 gpm from the Upper Basin Fill Unit (UBFU). This was a short duration test with no observation wells. The data set is fair for interpretation.

The selected type curve for the pumping well data (M18-GU) corresponds to a 2-D, homogeneous flow model, with a C_De^{2s} parameter equal to 1.0×10^{15} . This value, in turn, results in a skin coefficient of 11.4 (Figure 6A) indicating significant formation clogging near the well face. As shown in the log-log plot (Figure 6B), the match between the data and the type curve is good. The hydraulic conductivity estimate is 19.6 ft/day. The estimate for the storage coefficient is 8.7×10^{-16} which is clearly much too small and another indication of only a fair data set.

Aquifer Test on P39-O

This constant rate test involved a single pumping well (P39-O) with a discharge of 55 gpm pumping from the oxide zone. It had a single observation well (O39-O) which was also completed in the oxide zone. The data appears to be good and suitable for analysis.

The selected type curve for the pumping well data (P39-O) corresponds to a 2-D, homogeneous flow model, with a C_De^{2s} parameter equal to 100. This value, in turn, results in a skin coefficient of -1.8 (Figure 7A). As shown in the log-log plot (Figure 7B), the match between the data and the type curve is good. The hydraulic conductivity estimate is 0.3 ft/day and the estimate for the storage coefficient is 9.6×10^{-4}.

The selected type curve for the observation well data (O39-O) corresponds to a 2-D, homogeneous flow model, with a C_De^{2s} parameter equal to 2.0. As shown in this log-log plot (Figure 8B), the match between the data and the type curve is good. The hydraulic conductivity estimate is 0.3 ft/day and the estimate for the storage coefficient is 4.3×10^{-4} (Figure 8C).

Aquifer Test on PW7-1

This constant rate test involved a single pumping well (PW7-1) with a discharge of 38 gpm from the oxide zone. Observation wells OB7-1 and OB-1 are also completed in the oxide zone. Observation well O3-GL straddles the interface between the basin fill deposits and the oxide. Irrigation wells BIA-10B and WW-3 were on during testing and appear to have had some effect on the data as shown by early recovery in these wells. However, data sets from PW7-1 and OB7-1 appear acceptable and suitable for analysis.

The selected type curve for the pumping well data (PW7-1) corresponds to a 2-D, homogeneous flow model, with a C_De^{2s} parameter equal to 100. This value, in turn, results in a skin coefficient of -2.1 (Figure 17A) which indicates enhanced hydraulic conductivity near the well. As shown in the log-log plot (Figure 17B), and in spite of the transient effects produced by nearby pumping, the match between the data and the type curve is good. The hydraulic conductivity estimate is 0.2 ft/day and the estimate for the storage coefficient is 1.8×10^{-3} (Figure 17C).

The selected type curve for the observation well data (OB7-1) corresponds to a 2-D, homogeneous

flow model. As shown in this log-log plot (Figure 9B), and due to the transient effects produced by nearby pumping, the match between the data and the type curve is fair. The hydraulic conductivity estimate is 0.1 ft/day and the estimate for the storage coefficient is 1.3×10^{-4} (Figure 9C).

Aquifer Test on P12-O

This constant rate test involved a single pumping well (P12-O) with a discharge of 64 gpm from the oxide zone. Observation well O12-O was also completed in the oxide zone whereas observation well O12-GL was completed within the LBFU. The data appear to show multiple pumping well effects. Drawdown increased at approximately 500 minutes into the test, recovery was observed at 3,000 minutes, additional drawdown was seen at 7,000 minutes, and more recovery was observed at approximately 9,000 minutes. Large drawdown variations were also recorded the observation wells. Due to the above effects, this test is considered marginal for interpretation, and only the first 3,000 minutes of data from wells P12-O and O12-O were used.

The selected type curve for the pumping well data (P12-O) corresponds to a 2-D, homogeneous flow model, with a C_De^{2s} parameter equal to 3.0. This value, in turn, results in a skin coefficient of -4.3 which indicates enhanced hydraulic conductivity near the well. This enhanced conductivity could be natural, as resulting from nearby fractures, or it could be due to the drilling and well development process. As shown in the log-log plot (Figure 19B), the match between the data and the type curve is fair. The hydraulic conductivity estimate is 0.4 ft/day and the estimate for the storage coefficient is 4.2×10^{-1}.

The selected type curve for observation well data (O12-O) corresponds to a 2-D, homogeneous flow model. As shown in this log-log plot (Figure 10B), the match between the data and the type curve is fair. The hydraulic conductivity estimate is 0.6 ft/day and the estimate for the storage coefficient is 2.2×10^{-3}.

Aquifer Test on P28-GL

This constant rate test involved a single pumping well (P28-GL) with a discharge of 75 gpm from the Lower Basin Fill Unit (LBFU). Observation well O28-GL was completed in the Lower Basin Fill Unit (LBFU) and observation wells P28.1-O, P28.2-O and O28.1-O were completed in the oxide zone. Observation well O28.2-S was completed in the sulfide zone. Irrigation Wells BIA-9 and BIA-10B were on during the test but no information is available regarding their pumping rate history. Additionally ENGLAND #3 and WW-3 were on briefly for sampling toward the beginning of the test, and P8-GU was also pumping during this test. The test results appear good and suitable for analysis, however, only data from P28-O and O29-GL were interpreted.

The selected type curve for the pumping well data (P28-GL) corresponds to a 2-D, homogeneous flow model, with a C_De^{2s} parameter equal to 1.0×10^6 . This value, in turn, results in a skin coefficient of 1.3 which may indicate some formation damage near the well face. As shown in the log-log plot (Figure 29B), and in spite of the transient effects produced by nearby pumping, the match between the data and the type curve is good. The hydraulic conductivity estimate is 8.3 ft/day and the estimate for the storage coefficient is 3.4×10^{-7}.

The selected type curve for the observation well data (O28-GL) corresponds to a 2-D, homogeneous flow model, with a C_De^{2s} parameter equal to 2.0. As shown in this log-log plot (Figure 11B), and in spite of the transient effects produced by nearby pumping, the match between the data and the type curve is fair. The hydraulic conductivity estimate is 23.2 ft/day. The estimate for the storage coefficient is 2.7×10^{-5}.

Aquifer Test on P28.2-O

This constant rate test involved a single pumping well (P28.2-O) with a discharge of 77 gpm pumping from the oxide zone. Observation wells P28-GL and O28-GL were completed in the Lower

Basin Fill Unit (LBFU), observation well O28.1-O and P28.1-O were completed in the oxide zone. and observation well O28.2-S was completed in the sulfide zone. Irrigation Wells BIA-9 and BIA10-B were on during the test but no information is available regarding their pumping rate history. These wells did affect the data in all observation wells as evidenced by decrease in the drawdown at later time in all observation wells. Also, the recovery in the pumping well went beyond static water level, indicating that the observations in the pumping well are not ideal for interpretation. However, overall, the test is judged to be acceptable for interpretation.

The selected type curve for the pumping well data (P28.2-O) corresponds to a 2-D, homogeneous flow model, with a C_De^{2s} parameter equal to 10. This value, in turn, results in a skin coefficient of -6.5 which indicates enhanced hydraulic conductivity near the well. This enhanced conductivity could result from nearby fractures, or it could be due to the drilling and well development process. As shown in the log-log plot (Figure 33B), and due to the transient effects produced by nearby pumping, the match between the data and the type curve is only fair. The hydraulic conductivity estimate is 3.1 ft/day. The estimate for the storage coefficient turns out to be 3.8 which is clearly unreasonable (S is a dimensionless quantity smaller than one). This unreasonable storage coefficient estimate results, most likely, from a data set affected by pumping from wells BIA-9 and BIA 10-B. The resulting storativity estimates are, therefore, not reliable.

The selected type curve for the observation well data (O28.1-O) corresponds to a 2-D, homogeneous flow model, with a C_De^{2s} parameter equal to 2.0. As shown in this log-log plot (Figure 12B), and in spite of the transient effects produced by nearby pumping, the match between the data and the type curve is acceptable. The hydraulic conductivity estimate is 3.0 ft/day. The estimate for the storage coefficient is 1.1×10^{-3} (a much better result than was obtained from the pumping well).

Aquifer Test on PW2-1

This constant rate test involved a single pumping well (PW2-1) and one observation well OB2-1,

both on the oxide unit. Only the drawdown data for PW2-1 was analyzed; however, the observation well data appear suitable for analysis.

The selected type curve for the pumping well data (PW2-1) corresponds to a 2-D, homogeneous flow model, with a C_De^{2s} parameter equal to 2.0×10^8. The estimated skin coefficient is 4.3 indicating, perhaps, some formation clogging near the well face. As shown in the log-log plot (Figure 13B), the match between the data and the type curve is good. The hydraulic conductivity estimate is 1.4 ft/day. Interestingly, the estimated storage coefficient (3.2×10^{-9}) seems too small compared to that computed for other tests on the oxide unit.

Aquifer Test on PW4-1 (Test 1)

This constant rate test involved a single pumping well (PW4-1) and one observation well OB4-1. Only the drawdown data for PW4-1 was analyzed; however, the observation data appear to be good and suitable for analysis.

The selected type curve for the pumping well data (PW4-1) corresponds to a 2-D, homogeneous flow model, with a C_De^{2s} parameter equal to 2.0×10^8 which results in a skin coefficient of 4.6 indicating (Figure 15A), perhaps, some formation clogging near the well face. As shown in the log-log plot (Figure 15B), the match between the data and the type curve is good. The hydraulic conductivity estimate is 3.8 ft/day, however the estimate for the storage coefficient seems to small (2.5×10^{-9}).

Aquifer Test on M4-O

The aquifer test on monitoring well M4-O involved wells M2-GU, M3-GL and M5-S as observation points. Average discharge from M4-O during this test was reported at 15 gpm. Irrigation Well

ENGLAND #3 was on during the test but no information is available regarding its pumping rate history. Little or no drawdown was seen in any of the observation wells. However, at about 550 minutes into the test, the hydraulic head in all the wells shows a sharp decrease. After turning the pump off in well M4-O, the observation wells in the unconsolidated unit showed some partial recovery and then, at about 1,900 minutes, show a sharp drawdown. The hydraulic connection between the oxide unit and the overlain unconsolidated units seems limited at this location. Observation well M5-S (completed in the sulfide unit) did not show any drawdown, but instead recovered throughout the test indicating a very limited connection to the oxide unit. Due to these conditions, the test response from the observation wells M2-GU and M5-S was not considered suitable for interpretation.

FLOWDIM interpretation for the pumping well results in a fair match (Figure 16B) between the homogeneous 2-D model ($C_De^{2s} = 2 \times 10^8$) and the field data. The hydraulic conductivity estimate is 0.6 ft/day, with a skin factor of 3.8. The hydraulic conductivity is, however, deemed an underestimation of the actual formation conductivity due to the effect of pumping well ENGLAND #3.

Interpretation of observation well M3-GL used a 2-D model and resulted in a permeability estimate of 14.8 ft/day, and storativity of 8.8×10^{-2}. The match to the selected type curve is presented in Figure 2B.

Aquifer Test on P8-GU

This aquifer test involved a single pumping well (P8-GU) with a discharge of 85 gpm from the Upper Basin Fill Unit (UBFU). Four observations wells (P8.1-O, P8.2-O, O8-O, and O8-GL) were monitored. Irrigation wells BIA-9 and BIA-10B were on during the test but no information is available regarding their pumping rate history. Additionally, irrigation well WW-3 was turned on briefly for sampling toward the beginning of testing, and P28-GL was also pumped during testing. These wells did affect the measurements in the observation wells as evidenced by their lack of

recovery when the pumping in P8-GU was stopped at about 3200 minutes into the test. Also, the recovery in the pumping well did not reach static water level, indicating that the observations in the pumping well are only fair for interpretation.

Field data interpretation was attempted with a type curve for the drawdown data (P8-GU) corresponding to a 2-D, homogeneous flow model, with a C_De^{2s} parameter equal to 1.0×10^6. This value, in turn, results in a skin coefficient of 0.9 indicating, perhaps, only minor formation clogging near the well face. As shown in the log-log plot (Figure 18B), the match between the data and the type curve is fair. The hydraulic conductivity estimate is 61.3 ft/day and the estimate for the storage coefficient is 3.2×10^{-6}.

Aquifer Test on P13.1-O

This constant rate test involved a single pumping well (P13.1-O) with a discharge of 46 gpm. All irrigation wells are reported to be off during the test. Observation well P13-GL data shows some irregularity, but the pumping well and observation well P13.2-O appear suitable for analysis. Observation well O13-O showed no response during this test.

The selected type curve corresponds to a 2-D, homogeneous flow model, with a C_De^{2s} parameter equal to 1×10^6. This value, in turn, results in a skin coefficient of -3.4 which indicates enhanced hydraulic conductivity near the well. This enhanced conductivity could be the result of natural fractures or it might be due to the drilling and well development process. As shown in the log-log plot (Figure 20B), there is a good match between the data and the type curve so results of this test are judged to be good. The hydraulic conductivity estimate is 0.3 ft/day which is a typical value for the oxide zone and the storage coefficient estimate is 4.7×10^{-7}.

The hydraulic response for observation well P13.2-O shows a strong 3-D component (Figure 21B). Analyses of these data result in a hydraulic conductivity of 1.3×10^{-4} ft/day and a storativity of 7.0

$x10^{-7}$.

Aquifer Test on P15-O

This constant rate test involved a single pumping well (P15-O) with a discharge of 60 gpm. However, irrigation Wells BIA-9 and BIA-10B were on during the test but no information is available regarding their pumping rates. These wells did affect observation wells (P15-GL and O15-O) as evidenced by the sudden change in drawdown near the end of the test. The sudden change in drawdown is superimposed upon the drawdown due to P15-O and is difficult to separate. These irregularities indicate that the observation wells are not suitable for interpretation. The pumping well is suitable, however.

The selected type curve corresponds to a 2-D, homogeneous flow model, with a C_De^{2s} parameter equal to 1×10^2. This value, in turn, results in a skin coefficient of -5.0 which indicates enhanced hydraulic conductivity near the well. As shown in the log-log plot (Figure 22B), there is a fair match between the data and the type curve so results of this test are judged to be acceptable when considering the complications introduced by additional pumping wells (BIA-9 and BIA-10B). The hydraulic conductivity estimate is 0.5 ft/day which is a typical value for the oxide zone and the storage coefficient estimate is 1.3×10^{-2}.

Aquifer Test on P19.1-O

This constant rate test involved a single pumping well (P19.1-O) with a discharge of 24 gpm pumping from the oxide zone. Observation wells P19-O and P19.2-O were also completed in the oxide zone. Two additional observations wells were also monitored during this test (O19-GL and well 138). The data from these two wells were strongly affected by pumping in irrigation wells BIA-10B and WW-3. However, the data sets for the oxide wells appear acceptable for analysis.

The selected type curve for the pumping well data (P19.1-O) corresponds to a 2-D, homogeneous flow model, with a C_De^{2s} parameter equal to 2.0×10^{8} . This value, in turn, results in a skin coefficient of 5.1 indicating some formation damage or clogging near the well face. As shown in the log-log plot (Figure 25B), the match between the data and the type curve is acceptable. The hydraulic conductivity estimate is 0.3 ft/day and the estimate for the storage coefficient is 6.2×10^{-10}.

The selected type curve for observation well data (P19-O) corresponds to a 2-D, homogeneous flow model, with a C_De^{2s} parameter equal to 3.0. As shown in this log-log plot (Figure 23B), the match between the data and the type curve is good. The hydraulic conductivity estimate is 0.2 ft/day and the estimate for the storage coefficient is 7.7×10^{-4}.

The selected type curve for observation well data (P19.2-O) corresponds to a 2-D, homogeneous flow model, with a C_De^{2s} parameter equal to 2.0. As shown in this log-log plot (Figure 27B), the match between the data and the type curve is fair. The hydraulic conductivity estimate is 0.2 ft/day and the estimate for the storage coefficient is 1.5×10^{-4}.

The above analyses show that the data deviates strongly from the 2-D flow model. Therefore, these data were reinterpreted using a 3-D model. For this interpretation, the selected type curve for the pumping well data.(P19.1-O) corresponds a C_De^{2s} parameter equal to 10. As shown in the log-log plot (Figure 26B), the match between the data and the type curve is slightly better than that obtained with the 2-D model. The estimated skin coefficient is -3.3 which indicates enhanced hydraulic conductivity near the well as opposed to the formation clogging indicated by the 2-D interpretation. The hydraulic conductivity estimate is 0.01 ft/day and the estimate for the storage coefficient is 5.6×10^{-3}.

The selected 3-D type curve for observation well data (P19-O) corresponds a C_De^{2s} parameter equal to 3.0. As shown in this log-log plot (Figure 24B), the match between the data and the type curve is only slightly better than that obtained with the 2-D model. The hydraulic conductivity estimate is 2.4×10^{-4} ft/day and the estimate for the storage coefficient is 1.4×10^{-6}.

The selected 3-D type curve for observation well data (P19.2-O) corresponds a C_De^{2s} parameter equal to 3.0. As shown in this log-log plot (Figure 28B), the match between the data and the type curve is acceptable. The hydraulic conductivity estimate is 2.0×10^{-4} ft/day and the estimate for the storage coefficient is 3.4×10^{-7}.

Aquifer Test on P28.1-O (Test #1)

This constant rate test involved a single pumping well (P28.1-O) with a discharge of 28 gpm from the oxide zone. Observation wells P28-GL and O28-GL were completed in the Lower Basin Fill Unit (LBFU) and observation wells P28.2-O and O28.1-O were completed in the oxide zone. Irrigation Well England #3 was on during the test but no information is available regarding its pumping rate history. Also, the recovery in the pumping well went beyond static water level. Test interpretation included only the data set from the pumping well.

The selected type curve for the pumping well data (P28.1-O) corresponds to a 2-D, homogeneous flow model, with a C_De^{2s} parameter equal to 10. This value, in turn, results in a skin coefficient of -6.7 which indicates enhanced hydraulic conductivity near the well. This enhanced conductivity could be natural, as resulting from nearby fractures, or it could be due to the drilling and well development process. As shown in the log-log plot (Figure 30B), and due to the transient effects produced by nearby pumping, the match between the data and the type curve is only fair. The hydraulic conductivity estimate is 7.7 ft/day. The estimate for the storage coefficient is 5.2 which is clearly unreasonable (S is a dimensionless quantity smaller than one). This impossible storage coefficient estimate results from a data set affected by pumping from irrigation well England #3. This data set is hard to match with a type curve.

Aquifer Test on P28.1-O (Test #2)

This constant rate test involved a single pumping well (P28.1-O) with a discharge of 86 gpm from the oxide zone. Observation wells P28-GL and O28-GL were completed in the Lower Basin Fill Unit (LBFU) and observation wells P28.2-O and O28.1-O were completed in the oxide zone. Irrigation Well BIA-9 was on during testing, as was well P8.1-O. However, the data appear well-behaved and suitable for analysis.

The selected type curve for the pumping well data (P28.1-O) corresponds to a 2-D, homogeneous flow model, with a C_De^{2s} parameter equal to 10. This value, in turn, results in a skin coefficient of -4.2 which indicates enhanced hydraulic conductivity near the well. This enhanced conductivity could be natural, as resulting from nearby fractures, or it could be due to the drilling and well development process. As shown in the log-log plot (Figure 31B), and in spite of the transient effects produced by nearby pumping, the match between the data and the type curve is good. The hydraulic conductivity estimate is 3.6 ft/day and the estimate for the storage coefficient is 3.4×10^{-2}.

The selected type curve for the observation well data (P28.2-O) corresponds to a 2-D, homogeneous flow model, with a C_De^{2s} parameter equal to 2.0. As shown in this log-log plot (Figure 32B), and in spite of the transient effects produced by nearby pumping, the match between the data and the type curve is good. The hydraulic conductivity estimate is 2.7 ft/day. The estimate for the storage coefficient is 2.9×10^{-4}.

Aquifer Test on P49-O

The aquifer test conducted on well P49-O consisted of a constant discharge of about 40 gpm. Two observation wells were monitored during this test; well O49-O, completed in the oxide unit, and well O49-GL completed in the Lower Basin Fill Unit. More than 180 ft of drawdown in the pumping well rendered the pressure transducer dry. Pressure response on the observation wells was relatively clean, with well O49-O showing a drawdown of about 95 ft, and a drawdown in the basin fill well of about 0.5 ft. No other wells were reported in operation during this test, so the quality of the data

is good. As mentioned before, only partial data was collected during drawdown in the pumping well. so the hydraulic conductivity for this test was estimated from the shut in data.

The log-log plot (Figure 34B) for this test shows that a 3-D model represents the observed data quite well. A type-curve parameter C_De^{2s} of 0.3 produces and estimated hydraulic conductivity value of 7.8×10^{-3} ft/day and a skin coefficient of -7.7. The estimated storage coefficient is however surprisingly high (0.8). The reason for this extreme value is not apparent at this time.

4.0 DISCUSSION

The hydraulic conductivity estimates from aquifer tests in the basin fill are quite variable, ranging from 0.1 to 61.3 ft/day and, as expected, they are about an order of magnitude larger than the hydraulic conductivity estimates for the oxide zone. The majority of hydraulic conductivity estimates in the Basin Fill and oxide zone are reasonable. A large variation in storativity is observed and some of these estimates are unrealistically small. The smallest values are usually derived from interpretation of pumping well data. As commonly found in most filed tests, and also indicated by the Florence data, test analyses in observation wells tend to give more reasonable storativity estimates than analyses of pumping well data.

Analyses of many of the tests described above show the effects from multiple pumping wells with unknown pumping rate history. It is our opinion that further analyses of these tests would be better accomplished by inverse techniques that use available drawdown data to simultaneously estimate the unknown flow rate history in the agricultural wells and the aquifer parameters. Golder Associates has initiated work to accomplish these analyses. The actual effect of additional pumping from wells in the vicinity of a test on the magnitude of the estimated hydraulic parameters is not well understood. It would depend on whether a particular well is pumping or shut in after some period of pumping. When a nearby well is pumping, the estimates would more likely underestimate the actual aquifer parameters. The true effect needs, however, to be evaluated through analytical studies that simulate typical conditions observed in the field.

Several of the hydraulic responses for the tests analyzed in this report seem to be better interpreted by assuming a 3-D flow geometry. However, the estimated hydraulic conductivity and storativity obtained through the 3-D analysis are two or three orders of magnitude smaller than those obtained from the traditional 2-D radial flow model. The reason for the smaller hydraulic parameters is clear when one considers the area available for flow under each of these models. Under the 2-D radial flow model this area increases as a linear function of the distance from the pumping well, whereas for the 3-D model, it increases with the square of this distance.

In terms of predicting the producing capacity of a well, the distinction between alternative flow geometries is not crucial. However, for evaluation of transport of solutes through the aquifer this distinction becomes extremely relevant. It is important to notice, however, that for the simulation of solute transport in the context of the APP process, use of the 2-D hydraulic parameters results in conservative estimates of solute migration. By using a "reduced" area for solute transport (interaction) one would necessarily overestimate the potential migration of solutes. It is recommended that numerical simulations of flow and transport be carried out with the 2-D hydraulic parameter estimates.

Of paramount importance for the in-situ operation and for environmental protection, is the distinction between porous media flow and that resulting from discrete features. So far, the available field data indicate that flow at the Florence Site can safely be simulated with a porous media approach such as that built within numerical flow models like MODFLOW.

Golder Associates will continue interpreting the available hydraulic test data to support potential needs for the APP process and future mining needs. The next phase of aquifer test interpretation will concentrate on data from observation wells using inverse procedures as briefly described above. The three-dimensional model does not seem to fit the data sets any better than the two-dimensional model. Again, for the sake of conservatism, and due to the large uncertainty in the interpretation of these tests, it is recommended that the values obtained from the 2-D model be used for subsequent numerical simulations.

5.0 REFERENCES

Belanger, D.W., Freeze, G.A., Lolcama, J.L., and Pickens, J.F., 1989, *Interpretation of Hydraulic Testing in Crystalline Rock at the Leuggern Borehole*, NAGRA Technischer Bericht 87-19.

Bourdet, D., Whittle, T.M., Douglas, A.A., and Pirard, Y.M., 1983, *A New Set of Type Curves Simplifies Well Test Analysis*, World Oil, May 1983, pp.95-1-6.

Bourdet, D., Ayoub, J.A., and Pirard, Y.M., 1989, *Use of Pressure Derivative in Well-Test Interpretation, SPE Formation Evaluation*, June 1989, pp. 293-302.

Dake, L.P., 1978, *Fundamentals of Reservoir Engineering*, Chapter 7, Elsevier, Amsterdam, 1978.

Dawson, K.J. and Istok, J.D., 1991, *Aquifer Testing: Design and Analysis of Pumping and Slug Tests*, Lewis Publishers, Michigan, 1991.

Dowell Schlumberger, 1985, *Well Test Manual*, Internal Edition, 1985.

Earlougher, R.C. Jr., 1977, *Advances in Well Test Analysis*, Monograph 5 of the Henry L. Doherty Series, Society of Petroleum Engineers of AIME, New York, Second Edition, 1977.

Gringarten, A.C., 1979, *A Comparison Between Different Skin and Wellbore Storage Type Curves for Early-Time Transient Analysis*, SPE Paper No. 8205, 1979.

Gringarten, A.C., Bourdet, D., Fjare, D.S., and Viturat, D., 1980, *Horner Type-Curve Analysis*, SPE Paper NO. 8291, Sept. 1980.

Gringarten, A.C., 1986, *Computer-Aided Well Test Analysis*, SPE Paper No. 14099, March 1986.

Gringarten, A.C., 1987, *Type Curve Analysis: What it Can and Cannot Do*, Journal of Petroleum Technology, January 1987, pp. 11-13.

Grisak, G.E., Pickens, J.F., Balanger, D.W., and Avis, J.D., 1985, *Hydrogeologic Testing of Crystalline Rocks During the Nagra Deep Drilling Program*, Nagra Technischer Bericht 85-08.

Horne, R.N., 1990, *Modern Well Test Analysis: A Computer Aided Approach*, Petroway, Palo Alto, California, 1990.

Kruseman, G.P. and de Ridder, N.A., 1991, *Analysis and Evaluation of Pumping Test Data*, Second Edition (Reprinted), International Institute for Land Reclamation and Improvement (ILRI) Publication 47, Wageningen, The Netherlands, 1991.

Lee, J., 1982, *Well Testing*, First Printing, Society of Petroleum Engineers of AIME, New York, 1982.

Ostrowski, L.P. and Kloska, M.B., 1989, *Final Interpretation of Hydraulic Testing at the Siblingen Borehole*, Nagra/CISRA Technical Report 89-10, Baden, Switzerland, Sept., 1989.

Pickens, J.F., Grisak, G.E., Avis, J.D., Belanger, D.W., and Thury, M., 1987, *Analysis and Interpretation of Borehole Hydraulic Tests in Deep Boreholes: Principles, Model Development and Applications*, Water Resources Research, Vol. 23, No. 7, 1987, pp. 1341-1375.

Sabet, M.A., 1991, *Well Test Analysis*, Gulf Publishing Company, Houston, Texas, 1991.

Streltsova, T.D., 1988, *Well Testing in Heterogeneous Formations*, Exxon Monograph, John Wiley & Sons, New York, 1988.

Theis, C.V., 1935, *The Relation Between the Lowering of the Piezometric Surface and the Rate and Duration of Discharge of a Well Using Groundwater Storage*, Transactions of the American Geophysical Union, Vol. 16, 1935, pp. 519-524.

van Everdingen, A.F., 1953, *The Skin Effect and its Influence on the Productive Capacity of a Well*, Transactions of AIME, Vol. 198, 1953, pp. 171-176.

van Golf-Racht, T.D., 1982, *Fundamentals of Fractured Reservoir Engineering*, Developments in Petroleum Science 12, Elsevier Publishing Company, Amsterdam, The Netherlands, 1982.

Warren, J.E. and Root, P.J., 1963, *The Behaviour of Naturally Fractured Reservoirs*, Society of Petroleum Engineers Journal, Sept. 1963, pp. 245-255.

6.0 NOMENCLATURE

Symbol		Unit
B	formation volume factors	-
c_r	rock compressibility	Pa^{-1}
c_t	total compressibility	Pa^{-1}
c_w	water compressibility	Pa^{-1}
c_{ww}	water compressibility in wellbore	Pa^{-1}
C	wellbore storage coefficient	m^3/Pa
C_D	dimensionless wellbore storage coefficient	-
d_i	distance to boundary "I"	m
g	acceleration due to gravity	ms^{-2}
h	test section length	m
h_m	thickness of matrix blocks	m
H	head	m
k	intrinsic permeability (1 milli Darcy = 10^{-15} m^2)	m^2
k_f	fracture permeability (in a double porosity system)	m^2
k_{fD}	dimensionless fracture permeability	-
k_{fw}	fracture permeability	m^2
k_m	matrix permeability	m^2
$(kh/\mu)_{1,2}$	mobility ratio	-
K	hydraulic conductivity	ms^{-1}
K_s	hydraulic conductivity of the skin zone	ms^{-1}
l	linear distance	m
m	meters	m
P	pressure	Pa
P_{atm}	atmospheric pressure	Pa
P_D	dimensionless pressure	-
q	flow rate	m^3/day
q_i	the i^{th} constant rate flow period	m^3/s
r	radial distance	m
r_D	dimensionless radius	-
r_e	radius of circular constant pressure boundary	m
r_l	radius of the composite discontinuity	m
r_w	wellbore radius	m
r_{we}	effective well radius	m
s	skin factor of the well	-
s_f	skin factor between the fractures and the matrix	-
S	formation storage (storativity)	-
S_S	specific storage	m^{-1}

NOMENCLATURE - *continued*

Symbol		Unit
t	time	s
t_m	thickness of the matrix blocks	m
t_p	flow period duration	s
t_{pD}	dimensionless flow period duration	-
t_D	dimensionless time	-
V	volume of fluid	m^3
V_w	test section volume	m^3
x_f	fracture half-length	m
Z	elevation	m
α	dual porosity block geometry scale factor	-
ϕ	porosity	fraction
ϕ_f	fracture porosity	fraction
ϕ_m	matrix porosity	fraction
$(\phi c_t h)_{1/2}$	storativity ratio	-
λ	interporosity flow coefficient	-
μ	dynamic viscosity	Pa-s
ω	interporosity storativity ratio	-
ρ	density	$Kg\ m^{-3}$
Δt	time change	s
Δt_I	duration of the i^{th} constant rate event	s

Table 1 Summary of Available Hydraulic Test Data

Active Well	Observation Wells	Start Date	End Date	Well Location	Screen Location	Drawdown Data	Rate Data	Summary Sheet
M1-GL		11-Aug	13-Aug	X	X	X	X	X
	none							
M2-GU		25-Jul	26-Jul	X	X	X	X	X
	M3-GL			X	X	X		X
	M4-O			X	X	X		X
	M5-S			X	?	X		X
M3-GL		26-Jul	27-Jul	X	X	X	X	X
	M2-GU			X	X	X		X
	M4-O			X	X	X		X
	M5-S			X	X	X		X
M4-O		28-Jul	29-Jul	X	X	X	X	X
	M2-GU			X	X	X		X
	M3-GL			X	X	X		X
	M5-S			X	?	X		X
M10-GU		25-Jul	26-Jul	X	X	X	X	X
	M11-GL			X	X	X		X
	M12-O			X	X	X		X
	M13-S			X	X	X		X
M11-GL		29-Jul	30-Jul	X	X	X	X	X
	M10-GU			X	X	X		X
	M12-O			X	X	X		X
	M13-S			X	X	X		X
M12-O		31-Jul	1-Aug	X	X	X	X	X
	M10-GU			X	X	X		X
	M11-GL			X	X	X		X
	M13-S			X	?	X		X
M14-GL		11-Aug	13-Aug	X	X	X	X	X
	M15-GU			X	X	X		X
M15-GU		8-Aug	11-Aug	X	X	X	X	X
	M14-GL			X	X	X		X
M18-GU		8-Aug	11-Aug	X	X	X	X	X
	none							
PW2-1		8-Mar	?	X	X	X	X	N/A
	OB2-1			X	X			
PW3-1		24-Mar	1-Apr	X	X	X	?	N/A
	OB3-1			X	X	X		
PW4-1	(Test 1)	19-May	?	X	X	X	X	N/A
	OB4-1			X	X	X		
PW4-1	(Test 2)	23-May	31-May	X	X	X	X	N/A
	OB4-1			X	X			
P5-O		18-Oct	24 Oct	X	X	X	X	X
	O5.1-O			X	X	X		X
	O5.2-O			X	X	X		X
P5-O-MOD		18-Oct	24 Oct	X	X	X	X	X
	O5.1-O			X	X	X		X
	O5.2-O			X	X	X		X

Table 1 Summary of Available Hydraulic Test Data

Active Well	Observation Wells	Start Date	End Date	Well Location	Screen Location	Drawdown Data	Rate Data	Summary Sheet
PW7-1		16-Jun	21-Jun	X	X	X	X	N/A
	OB7-1			X	X	X		
	O3-GL			X	X	X		
	OB-1			X	X	X		
P8.2-O		?	?	X	X	?	X	?
	P8-GL			X	X	?		
	P8.1-O			X	X	?		
	O8-O			X	X	?		
	O8-GL			X	X	?		
P8.1-O		8-Sep-95	11-Sep	X	X	X	X	X
	P8-GU			X	X	X		X
	P8.2-O			X	X	X		X
	O8-O			X	X	X		X
	O8-GU			X	X	X		X
P8-GU		18-Sep	22-Sep	X	X	X	X	X
	P8.1-O			X	X	X		X
	P8.2-O			X	X	X		X
	O8-O			X	X	X		X
	O8-GU			X	X	X		X
P12-O		1-Jun	7-Jun	X	X	X	X	X
	O12-O			X	X	X		X
	O12-GL			X	X	X		X
P13.1-O		9-Oct	16-Oct	X	X	X	X	X
	P13-GL			X	X	X		X
	P13.2-O			X	X	X		X
	O13-O			X	X	X		X
P15-O		29-Sep	5-Oct	X	X	X	X	X
	P15-GL			X	X	X		X
	O15-O			X	X	X		X
	WW3			?	?	?		X
	BIA-9			?	?	?		X
P19.1-O		3-Jul	6-Jul	X	X	X	X	N/A
	P19-O			X	X	X		
	P19.2-O			X	X	X		
	O19-GL			X	X	X		
	138			X	X	X		
P28-GL		20-Sep	25-Sep	X	X	X	X	X
	P28.1-O			X	X	No Data		
	P28.2-O			X	X	X		X
	O28-GL			X	X	X		X
	O28.1-O			X	X	X		X
	O28.2-S			X	X	X		X
P28.1-O		15-Aug	18-Aug	X	X	X	X	X
(Test 1)	P28.2-O			X	X	X		X
	P28-GL			X	X	X		X
	O28-GL			X	X	X		X
	O28.1-O			X	X	X		X
	O28.2-S			X	X	No Data		

Table 1 Summary of Available Hydraulic Test Data

Active Well	Observation Wells	Start Date	End Date	Well Location	Screen Location	Drawdown Data	Rate Data	Summary Sheet
P28.1-O		8-Sep	11-Sep	X	X	X	X	X
(Test 2)	P28.2-O			X	X	X		X
	P28-GL			X	X	X		X
	O28-GL			X	X	X		X
	O28.1-O			X	X	X		X
	O28.2-S			X	X	No Data		
P28.2-O		2-Oct	5-Oct	X	X	X	X	X
	P28-GL			X	X	X		X
	P28.1-O			X	X	X		X
	O28.1-O			X	X	X		X
	O28-GL			X	X	X		X
	O28.2-O			X	X	X		X
P39-O		19-May	20-May	X	X	X	X	X
	O39-O			X	X	X		X
P49-O		11-Oct	16-Oct	X	X	X	X	X
	O49-O			X	X	X		X
	O49-GL			X	X	X		X

Table 2. Hydraulic Conductivity Estimates

Well	Active/Observation	K (feet/day)	Screened Formation	Comments
M1-GL	Active	17.3	LBFU	(1), (2); Acceptable
M3-GL	Active	15.9	LBFU	(1), (3); Acceptable
M14-GL	Active	1.7	LBFU	(1), (2); Acceptable
M14-GL3d	Active	0.1	LBFU	(1), (2); Acceptable
M15-GU	Active	2.6	LBFU	(1), (2), (3); Acceptable
M18-GL	Active	19.6	LBFU	(1); Fair
P28-GL	Active	8.3	LBFU	(1), (3); Acceptable
O28-GL	Observation (P28-GL)	23.2	LBFU	(1), (3); Acceptable
M3-GL	Observation (M4-O)	14.8	LBFU	(1), (3); Acceptable
P8-GU	Active	61.3	UBFU	(1), (2), (3); Fair
M4-O	Active	0.6	Oxide	(1), (3); Acceptable
PW2-1	Active	1.4	Oxide	Good
PW4-1	Active	3.8	Oxide	Good
PW7-1	Active	0.2	Oxide	(1), (3); Acceptable
OB7-1	Observation (PW7-1)	0.1	Oxide	(1), (3); Acceptable
P12-O	Active	0.4	Oxide	(1), (2), (3); Fair
O12-O	Observation (P12-O)	0.6	Oxide	(1), (2), (3); Fair
P19.1-O	Active	0.3	Oxide	(1), (2), (3); Acceptable
P19-O	Observation (P19.1-O)	0.2	Oxide	(1), (2), (3); Acceptable
P19.2-O	Observation (P19.1-O)	0.2	Oxide	(1), (2), (3); Fair
P19.1-O3d	Active	1.00E-02	Oxide	(1), (2), (3); Acceptable
P19-O3d	Observation (P19.1-O)	2.39E-04	Oxide	(1), (2), (3); Acceptable
P19.2-O3d	Observation (P19.1-O)	1.99E-04	Oxide	(1), (2), (3); Acceptable
P39-O	Active	0.3	Oxide	Good
O39-O	Observation (P39-O)	0.3	Oxide	Good
P28.1-O	Active	7.7	Oxide	(1), (3); Fair
P28.1-O (2)	Active	3.6	Oxide	(1); Good
P28.2 -O	Observation (P28.1-O)	2.7	Oxide	(1); Good
P28.2-O	Active	3.1	Oxide	(1), (3); Fair
O28.1-O	Observation (P28.2-O)	3.0	Oxide	(1), (3); Acceptable
P13.1-O	Active	0.3	Oxide	Good
				Obs. Well shows 3-D behavior
P49-O3d	Active/Recovery Data	7.75E-03	Oxide	Good, Clear 3-D behavior
P15-O	Active	0.5	Oxide	(1),(3); Acceptable

(1) Other wells were pumping during this test at an unknown rate
(2) Data indicates recovery over the initial "static" water table
(3) Observation wells show effects of recovery or drawdown produced by other wells

Qualifiers	Description
Good	The reported K value is a good indication of the formation hydraulic conductivity
Acceptable	The reported K value is most likely an under-estimation of the formation conductivity
Fair	The reported K value has a large uncertainty due to conditions during test

APPENDIX A

FlowDim Analysis File : **m1-gld.dat**

	Parameter		Units
r_w	Well radius	**0.064**	m
μ	Groundwater viscosity	**1.00E-03**	Pa s
ρ	Groundwater density	**1.00E+03**	kg/m^3
c_t	Total compressibility	**5.40E-10**	1/Pa
ϕ	Porosity of formation	**10.00**	%
C	Wellbore storage	**4.35E-06**	m^3/Pa
h	Length of aquifer tested	**12.19**	m

Skin Factor Calculation

Assuming formation storativity, the skin factor (s) can be calculated from the following equation.

$$s = \frac{\ln (C_D e^{2s} 2 \pi \phi c_t h r_w^2 / C)}{2}$$

Match Point Parameters From Analysis

$C_D e^{2s}$	2.0000E+08
P (kPa)	7.5335E-01
T (hr)	3.9350E+02

Results

T(m^2/sec)	K (feet/min)	K (ft/day)	K (m/s)	K (cm/s)	Skin
7.43E-04	**1.20E-02**	**17.29**	**6.10E-05**	**6.10E-03**	**3.32**

FlowDim Analysis File : **m3gloddb.fd1**

	Parameter		Units
r_w	Well radius	**0.064**	m
μ	Groundwater viscosity	**1.000E-03**	Pa s
ρ	Groundwater density	**1.000E+03**	kg/m^3
c_t	Total compressibility	**5.400E-10**	1/Pa
ϕ	Porosity of formation	**5.00**	%
C	Wellbore storage	**N/A**	m^3/Pa
h	Length of aquifer tested	**18.29**	m

Skin Factor Calculation

Assuming formation storativity, the skin factor (s) can be calculated from the following equation.

$$s = \frac{\ln (C_D e^{2s} 2 \pi \phi c_t h r_w^2 / C)}{2}$$

Match Point Parameters From Analysis

$C_D e^{2s}$	N/A
P (kPa)	6.4470E-01
T (hr)	4.1462E-01

Results

$T(m^2/sec)$	K (feet/min)	K(feet/dat)	K (m/s)	K (cm/s)	Skin
9.53E-04	**1.03E-02**	**14.77**	**5.21E-05**	**5.21E-03**	#########

FlowDim Analysis File : **m14-gld.dat**

	Parameter		Units
r_w	Well radius	**0.064**	m
μ	Groundwater viscosity	**1.00E-03**	Pa s
ρ	Groundwater density	**1.00E+03**	kg/m^3
c_t	Total compressibility	**5.40E-10**	1/Pa
ϕ	Porosity of formation	**10.00**	%
C	Wellbore storage	**2.35E-06**	m^3/Pa
h	Length of aquifer tested	**18.29**	m

Skin Factor Calculation

Assuming formation storativity, the skin factor (s) can be calculated from the following equation.

$$s = \frac{\ln (C_D e^{2s} 2 \pi \phi c_t h r_w^2 / C)}{2}$$

Match Point Parameters From Analysis

$C_D e^{2s}$	1.0000E+06
P (kPa)	1.1410E-01
T (hr)	1.1015E+02

Results

$T(m^2/sec)$	K (feet/min)	K (ft/day)	K (m/s)	K (cm/s)	Skin
1.12E-04	**1.21E-03**	**1.74**	**6.15E-06**	**6.15E-04**	**1.18**

FlowDim Analysis File : **m14gld3d.dat**

	Parameter		Units
r_w	Well radius	**0.064**	m
μ	Groundwater viscosity	**1.00E-03**	Pa s
ρ	Groundwater density	**1.00E+03**	kg/m^3
c_t	Total compressibility	**5.40E-10**	1/Pa
ϕ	Porosity of formation	**10.00**	%
C	Wellbore storage	**2.22E-06**	m^3/Pa
h	Length of aquifer tested	**18.29**	m

Skin Factor Calculation

Assuming formation storativity, the skin factor (s) can be calculated from the following equation.

$$s = \frac{\ln (C_D e^{2s} \, 2 \pi \phi \, c_t \, h \, r_w^2 / C)}{2}$$

Match Point Parameters From Analysis

$C_D e^{2s}$	1.0000E+01
P (kPa)	1.0766E-02
T (hr)	1.1022E+01

Results

T(m^2/sec)	K (feet/min)	K (ft/day)	K (m/s)	K (cm/s)	Skin
5.31E-06	**5.71E-05**	**0.08**	**2.90E-07**	**2.90E-05**	**-4.54**

FlowDim Analysis File : **m15-gud.dat**

	Parameter		Units
r_w	Well radius	**0.064**	m
μ	Groundwater viscosity	**1.00E-03**	Pa s
ρ	Groundwater density	**1.00E+03**	kg/m^3
c_t	Total compressibility	**5.40E-10**	1/Pa
ϕ	Porosity of formation	**10.00**	%
C	Wellbore storage	**2.78E-07**	m^3/Pa
h	Length of aquifer tested	**12.19**	m

Skin Factor Calculation

Assuming formation storativity, the skin factor (s) can be calculated from the following equation.

$$s = \frac{\ln (C_D e^{2s} \, 2 \pi \phi \, c_t \, h \, r_w^2 / C)}{2}$$

Match Point Parameters From Analysis

$C_D e^{2s}$	1.0000E+10
P (kPa)	1.1287E-01
T (hr)	9.2222E+02

Results

$T(m^2/sec)$	K (feet/min)	K (ft/day)	K (m/s)	K (cm/s)	Skin
1.11E-04	**1.80E-03**	**2.59**	**9.14E-06**	**9.14E-04**	**6.65**

FlowDim Analysis File : **m18-gud.dat**

	Parameter		Units
r_w	Well radius	0.064	m
μ	Groundwater viscosity	1.00E-03	Pa s
ρ	Groundwater density	1.00E+03	kg/m^3
c_t	Total compressibility	5.40E-10	1/Pa
ϕ	Porosity of formation	10.00	%
C	Wellbore storage	2.25E-06	m^3/Pa
h	Length of aquifer tested	12.19	m

Skin Factor Calculation

Assuming formation storativity, the skin factor (s) can be calculated from the following equation.

$$s = \frac{\ln (C_D e^{2s} 2 \pi \phi c_t h r_w^2 / C)}{2}$$

Match Point Parameters From Analysis

$C_D e^{2s}$	1.0000E+15
P (kPa)	8.5570E-01
T (hr)	8.6654E+02

Results

T(m^2/sec)	K (feet/min)	K (ft/day)	K (m/s)	K (cm/s)	Skin
8.44E-04	**1.36E-02**	**19.64**	**6.93E-05**	**6.93E-03**	**11.36**

FlowDim Analysis File : **mf39pwpd.dat**

	Parameter		Units
r_w	Well radius	0.130	m
μ	Groundwater viscosity	1.00E-03	Pa s
ρ	Groundwater density	1.00E+03	kg/m^3
c_t	Total compressibility	5.40E-10	1/Pa
ϕ	Porosity of formation	5.00	%
C	Wellbore storage	1.04E-06	m^3/Pa
h	Length of aquifer tested	108.20	m

Skin Factor Calculation

Assuming formation storativity, the skin factor (s) can be calculated from the following equation.

$$s = \frac{\ln (C_D e^{2s} 2 \pi \phi c_t h r_w^2 / C)}{2}$$

Match Point Parameters From Analysis

$C_D e^{2s}$	1.0000E+02
P (kPa)	2.0728E-02
T (hr)	2.4897E+02

Results

$T(m^2/sec)$	K (feet/min)	K (ft/day)	K (m/s)	K (cm/s)	Skin
1.12E-04	**2.04E-04**	**0.29**	**1.04E-06**	**1.04E-04**	**-1.76**

FlowDim Analysis File : **mf39owpd.dat**

	Parameter		Units
r_w	Well radius	**0.127**	m
μ	Groundwater viscosity	**1.00E-03**	Pa s
ρ	Groundwater density	**1.00E+03**	kg/m^3
c_t	Total compressibility	**5.40E-10**	1/Pa
ϕ	Porosity of formation	**50.00**	%
C	Wellbore storage	**NA**	m^3/Pa
h	Length of aquifer tested	**126.80**	m

Skin Factor Calculation

Assuming formation storativity, the skin factor (s) can be calculated from the following equation.

$$s = \frac{\ln (C_D e^{2s} \, 2 \pi \phi \, c_t \, h \, r_w^2 / C)}{2}$$

Match Point Parameters From Analysis

$C_D e^{2s}$	2.0000E+00
P (kPa)	2.6738E-02
T (hr)	9.3173E-01

Results

$T(m^2/sec)$	K (feet/min)	K (ft/day)	K (m/s)	K (cm/s)	Skin
1.44E-04	**2.24E-04**	**0.32**	**1.14E-06**	**1.14E-04**	#########

FlowDim Analysis File : **ob7-1dda.fd1**

	Parameter		Units
r_w	Well radius	**0.076**	m
μ	Groundwater viscosity	**1.000E-03**	Pa s
ρ	Groundwater density	**1.000E+03**	kg/m^3
c_t	Total compressibility	**5.400E-10**	1/Pa
ϕ	Porosity of formation	**5.00**	%
C	Wellbore storage	**N/A**	m^3/Pa
h	Length of aquifer tested	**103.63**	m

Skin Factor Calculation

Assuming formation storativity, the skin factor (s) can be calculated from the following equation.

$$s = \frac{\ln (C_D e^{2s} 2 \pi \phi c_t h r_w^2 / C)}{2}$$

Match Point Parameters From Analysis

$C_D e^{2s}$	N/A
P (kPa)	1.2560E-02
T (hr)	5.7458E+00

Results

$T(m^2/sec)$	K (feet/min)	K(feet/dat)	K (m/s)	K (cm/s)	Skin
4.95E-05	**9.40E-05**	**0.14**	**4.78E-07**	**4.78E-05**	#########

FlowDim Analysis File : **012-oddc.fd1**

	Parameter		Units
r_w	Well radius	**0.051**	m
μ	Groundwater viscosity	**1.000E-03**	Pa s
ρ	Groundwater density	**1.000E+03**	kg/m^3
c_t	Total compressibility	**5.400E-10**	1/Pa
ϕ	Porosity of formation	**5.00**	%
C	Wellbore storage	**N/A**	m^3/Pa
h	Length of aquifer tested	**152.40**	m

Skin Factor Calculation

Assuming formation storativity, the skin factor (s) can be calculated from the following equation.

$$s = \frac{\ln (C_D e^{2s} \, 2 \pi \phi \, c_t \, h \, r_w^2 / C)}{2}$$

Match Point Parameters From Analysis

$C_D e^{2s}$	N/A
P (kPa)	5.0164E-02
T (hr)	1.0792E+00

Results

$T(m^2/sec)$	K (feet/min)	K(feet/dat)	K (m/s)	K (cm/s)	Skin
3.21E-04	**4.15E-04**	**0.60**	**2.11E-06**	**2.11E-04**	#########

FlowDim Analysis File : **o28-gld.dat**

	Parameter		Units
r_w	Well radius	**0.051**	m
μ	Groundwater viscosity	**1.00E-03**	Pa s
ρ	Groundwater density	**1.00E+03**	kg/m^3
c_t	Total compressibility	**5.40E-10**	1/Pa
ϕ	Porosity of formation	**10.00**	%
C	Wellbore storage	**NA**	m^3/Pa
h	Length of aquifer tested	**9.14**	m

Skin Factor Calculation

Assuming formation storativity, the skin factor (s) can be calculated from the following equation.

$$s = \frac{\ln (C_D e^{2s} 2 \pi \phi c_t h r_w^2 / C)}{2}$$

Match Point Parameters From Analysis

$C_D e^{2s}$	2.0000E+00
P (kPa)	1.0130E-01
T (hr)	6.1809E+01

Results

$T(m^2/sec)$	K (feet/min)	K (ft/day)	K (m/s)	K (cm/s)	Skin
7.49E-04	**1.61E-02**	**23.22**	**8.19E-05**	**8.19E-03**	#########

FlowDim Analysis File : **o281-od.dat**

	Parameter		Units
r_w	Well radius	**0.051**	m
μ	Groundwater viscosity	**1.00E-03**	Pa s
ρ	Groundwater density	**1.00E+03**	kg/m^3
c_t	Total compressibility	**5.40E-10**	1/Pa
ϕ	Porosity of formation	**5.00**	%
C	Wellbore storage	**NA**	m^3/Pa
h	Length of aquifer tested	**30.48**	m

Skin Factor Calculation

Assuming formation storativity, the skin factor (s) can be calculated from the following equation.

$$s = \frac{\ln (C_D e^{2s} 2 \pi \phi c_t h r_w^2 / C)}{2}$$

Match Point Parameters From Analysis

$C_D e^{2s}$	2.0000E+00
P_{DM}	4.2352E-02
T_{DM}	4.3542E-01

Results

T(m^2/sec)	K (feet/min)	K (ft/day)	K (m/s)	K (cm/s)	Skin
3.17E-04	**2.05E-03**	**2.95**	**1.04E-05**	**1.04E-03**	#########

FlowDim Analysis File : **pw2-1d.dat**

	Parameter		Units
r_w	Well radius	**0.076**	m
μ	Groundwater viscosity	**1.00E-03**	Pa s
ρ	Groundwater density	**1.00E+03**	kg/m^3
c_t	Total compressibility	**5.40E-10**	1/Pa
ϕ	Porosity of formation	**5.00**	%
C	Wellbore storage	**2.36E-06**	m^3/Pa
h	Length of aquifer tested	**67.06**	m

Skin Factor Calculation

Assuming formation storativity, the skin factor (s) can be calculated from the following equation.

$$s = \frac{\ln (C_D e^{2s} 2 \pi \phi c_t h r_w^2 / C)}{2}$$

Match Point Parameters From Analysis

$C_D e^{2s}$	2.0000E+08
P (kPa)	6.5031E-02
T (hr)	3.1235E+02

Results

$T(m^2/sec)$	K (feet/min)	K (ft/day)	K (m/s)	K (cm/s)	Skin
3.20E-04	**9.41E-04**	**1.35**	**4.78E-06**	**4.78E-04**	**4.31**

FlowDim Analysis File : **pm3-glda.fd1**

	Parameter		Units
r_w	Well radius	**0.064**	m
μ	Groundwater viscosity	**1.00E-03**	Pa s
ρ	Groundwater density	**1.00E+03**	kg/m^3
c_t	Total compressibility	**5.40E-10**	1/Pa
ϕ	Porosity of formation	**10.00**	%
C	Wellbore storage	**8.16E-07**	m^3/Pa
h	Length of aquifer tested	**12.19**	m

Skin Factor Calculation

Assuming formation storativity, the skin factor (s) can be calculated from the following equation.

$$s = \frac{\ln (C_D e^{2s} \, 2 \pi \phi \, c_t \, h \, r_w^2 / C)}{2}$$

Match Point Parameters From Analysis

$C_D e^{2s}$	1.0000E+06
P (kPa)	6.9300E-01
T (hr)	1.9300E+03

Results

$T(m^2/sec)$	K (feet/min)	K (ft/day)	K (m/s)	K (cm/s)	Skin
6.83E-04	**1.10E-02**	**15.88**	**5.60E-05**	**5.60E-03**	**1.51**

FlowDim Analysis File : **pw4-1.dat**

	Parameter		Units
r_w	Well radius	**0.076**	m
μ	Groundwater viscosity	**1.00E-03**	Pa s
ρ	Groundwater density	**1.00E+03**	kg/m^3
c_t	Total compressibility	**5.40E-10**	1/Pa
ϕ	Porosity of formation	**5.00**	%
C	Wellbore storage	**1.87E-06**	m^3/Pa
h	Length of aquifer tested	**103.63**	m

Skin Factor Calculation

Assuming formation storativity, the skin factor (s) can be calculated from the following equation.

$$s = \frac{\ln (C_D e^{2s} \, 2 \pi \phi \, c_t \, h \, r_w^{\,2} / C)}{2}$$

Match Point Parameters From Analysis

$C_D e^{2s}$	2.0000E+08
P (kPa)	1.9640E-01
T (hr)	1.6933E+03

Results

$T(m^2/sec)$	K (feet/min)	K (ft/day)	K (m/s)	K (cm/s)	Skin
1.37E-03	**2.61E-03**	**3.76**	**1.33E-05**	**1.33E-03**	**4.65**

FlowDim Analysis File : **pm4-od.fd1**

	Parameter		Units
r_w	Well radius	**0.06**	m
μ	Groundwater viscosity	**1.00E-03**	Pa s
ρ	Groundwater density	**1.00E+03**	kg/m^3
c_t	Total compressibility	**5.40E-10**	1/Pa
ϕ	Porosity of formation	**5.00**	%
C	Wellbore storage	**1.38E-06**	m^3/Pa
h	Length of aquifer tested	**18.29**	m

Skin Factor Calculation

Assuming formation storativity, the skin factor (s) can be calculated from the following equation.

$$s = \frac{\ln (C_D e^{2s} 2 \pi \phi c_t h r_w^2 / C)}{2}$$

Match Point Parameters From Analysis

$C_D e^{2s}$	2.0000E+08
P (kPa)	2.4300E-02
T (hr)	6.0000E+01

Results

$T(m^2/sec)$	K (feet/min)	K (feet/day)	K (m/s)	K (cm/s)	Skin
3.59E-05	**3.86E-04**	**0.56**	**1.96E-06**	**1.96E-04**	**3.75**

FlowDim Analysis File : **PW7-1dda.fd1**

	Parameter		Units
r_w	Well radius	**0.076**	m
μ	Groundwater viscosity	**1.000E-03**	Pa s
ρ	Groundwater density	**1.000E+03**	kg/m^3
c_t	Total compressibility	**5.400E-10**	1/Pa
ϕ	Porosity of formation	**5.00**	%
C	Wellbore storage	**6.871E-07**	m^3/Pa
h	Length of aquifer tested	**103.63**	m

Skin Factor Calculation

Assuming formation storativity, the skin factor (s) can be calculated from the following equation.

$$s = \frac{\ln (C_D e^{2s} \, 2 \pi \phi \, c_t \, h \, r_w^2 / C)}{2}$$

Match Point Parameters From Analysis

$C_D e^{2s}$	1.0000E+02
P (kPa)	2.1298E-02
T (hr)	2.8162E+02

Results

$T(m^2/sec)$	K (feet/min)	K (feet/day)	K (m/s)	K (cm/s)	Skin
8.40E-05	**1.59E-04**	**0.23**	**8.10E-07**	**8.10E-05**	**-2.10**

FlowDim Analysis File : **p8-gud.dat**

	Parameter		Units
r_w	Well radius	**0.076**	m
μ	Groundwater viscosity	**1.00E-03**	Pa s
ρ	Groundwater density	**1.00E+03**	kg/m^3
c_t	Total compressibility	**5.40E-10**	1/Pa
ϕ	Porosity of formation	**10.00**	%
C	Wellbore storage	**1.19E-05**	m^3/Pa
h	Length of aquifer tested	**36.58**	m

Skin Factor Calculation

Assuming formation storativity, the skin factor (s) can be calculated from the following equation.

$$s = \frac{\ln (C_D e^{2s} 2 \pi \phi c_t h r_w^2 / C)}{2}$$

Match Point Parameters From Analysis

$C_D e^{2s}$	1.0000E+06
P (kPa)	9.0703E-01
T (hr)	1.5374E+03

Results

$T(m^2/sec)$	K (feet/min)	K (ft/day)	K (m/s)	K (cm/s)	Skin
7.91E-03	**4.26E-02**	**61.31**	**2.16E-04**	**2.16E-02**	**0.90**

FlowDim Analysis File : **P12-oddc.fd1**

	Parameter		Units
r_w	Well radius	**0.076**	m
μ	Groundwater viscosity	**1.000E-03**	Pa s
ρ	Groundwater density	**1.000E+03**	kg/m^3
c_t	Total compressibility	**5.400E-10**	1/Pa
ϕ	Porosity of formation	**10.00**	%
C	Wellbore storage	**4.640E-06**	m^3/Pa
h	Length of aquifer tested	**152.40**	m

Skin Factor Calculation

Assuming formation storativity, the skin factor (s) can be calculated from the following equation.

$$s = \frac{\ln (C_D e^{2s} \, 2 \pi \phi \, c_t \, h \, r_w^2 / C)}{2}$$

Match Point Parameters From Analysis

$C_D e^{2s}$	3.0000E+00
P (kPa)	3.1823E-02
T (hr)	1.0126E+02

Results

$T(m^2/sec)$	K (feet/min)	K (feet/day)	K (m/s)	K (cm/s)	Skin
2.04E-04	**2.63E-04**	**0.38**	**1.34E-06**	**1.34E-04**	**-4.27**

FlowDim Analysis File : **P131od.dat**

	Parameter		Units
r_w	Well radius	0.076	m
μ	Groundwater viscosity	1.00E-03	Pa s
ρ	Groundwater density	1.00E+03	kg/m^3
c_t	Total compressibility	5.40E-10	1/Pa
ϕ	Porosity of formation	0.05	%
C	Wellbore storage	1.75E-03	m^3/Pa
h	Length of aquifer tested	206.35	m

Skin Factor Calculation

Assuming formation storativity, the skin factor (s) can be calculated from the following equation.

$$s = \frac{\ln (C_D e^{2s} 2 \pi \phi c_t h r_w^2 / C)}{2}$$

Match Point Parameters From Analysis

$C_D e^{2s}$	1.0000E+06
P (kPa)	4.2200E-02
T (hr)	2.5150E+02

Results

$T(m^2/sec)$	K (feet/min)	K (ft/day)	K (m/s)	K (cm/s)	Skin
1.91E-04	1.82E-04	0.26	9.26E-07	9.26E-05	-3.38

FlowDim Analysis File : **P132od3d.dat**

	Parameter		Units
r_w	Well radius	**0.076**	m
μ	Groundwater viscosity	**1.00E-03**	Pa s
ρ	Groundwater density	**1.00E+03**	kg/m^3
c_t	Total compressibility	**5.40E-10**	1/Pa
ϕ	Porosity of formation	**0.05**	%
C	Wellbore storage	**N/A**	m^3/Pa
h	Length of aquifer tested	**182.27**	m

Skin Factor Calculation

Assuming formation storativity, the skin factor (s) can be calculated from the following equation.

$$s = \frac{\ln (C_D e^{2s} 2 \pi \phi c_t h r_w^2 / C)}{2}$$

Match Point Parameters From Analysis

$C_D e^{2s}$	N/A
P (kPa)	3.6000E-05
T (hr)	4.2500E-01

Results

T(m^2/sec)	K (feet/min)	K (ft/day)	K (m/s)	K (cm/s)	Skin
8.18E-08	**8.84E-08**	**1.27E-04**	**4.49E-10**	**4.49E-08**	#########

FlowDim Analysis File : **P150d.dat**

	Parameter		Units
r_w	Well radius	**0.076**	m
μ	Groundwater viscosity	**1.00E-03**	Pa s
ρ	Groundwater density	**1.00E+03**	kg/m^3
c_t	Total compressibility	**5.40E-10**	1/Pa
ϕ	Porosity of formation	**0.05**	%
C	Wellbore storage	**4.94E-06**	m^3/Pa
h	Length of aquifer tested	**219.46**	m

Skin Factor Calculation

Assuming formation storativity, the skin factor (s) can be calculated from the following equation.

$$s = \frac{\ln (C_D e^{2s} \, 2 \pi \phi \, c_t \, h \, r_w^2 / C)}{2}$$

Match Point Parameters From Analysis

$C_D e^{2s}$	1.0000E+02
P (kPa)	6.6100E-02
T (hr)	1.7940E+02

Results

$T(m^2/sec)$	K (feet/min)	K (ft/day)	K (m/s)	K (cm/s)	Skin
3.84E-04	**3.44E-04**	**0.50**	**1.75E-06**	**1.75E-04**	**-5.02**

FlowDim Analysis File : **p19-od.dat**

	Parameter		Units
r_w	Well radius	**0.076**	m
μ	Groundwater viscosity	**1.00E-03**	Pa s
ρ	Groundwater density	**1.00E+03**	kg/m^3
c_t	Total compressibility	**5.40E-10**	1/Pa
ϕ	Porosity of formation	**5.00**	%
C	Wellbore storage	**NA**	m^3/Pa
h	Length of aquifer tested	**60.35**	m

Skin Factor Calculation

Assuming formation storativity, the skin factor (s) can be calculated from the following equation.

$$s = \frac{\ln (C_D e^{2s} \, 2 \pi \phi \, c_t \, h \, r_w^2 / C)}{2}$$

Match Point Parameters From Analysis

$C_D e^{2s}$	3.0000E+00
P (kPa)	1.8917E-02
T (hr)	3.7000E-01

Results

$T(m^2/sec)$	K (feet/min)	K (ft/day)	K (m/s)	K (cm/s)	Skin
4.10E-05	**1.34E-04**	**0.19**	**6.80E-07**	**6.80E-05**	#########

FlowDim Analysis File : **p19-od3d.dat**

	Parameter		Units
r_w	Well radius	**0.076**	m
μ	Groundwater viscosity	**1.00E-03**	Pa s
ρ	Groundwater density	**1.00E+03**	kg/m^3
c_t	Total compressibility	**5.40E-10**	1/Pa
ϕ	Porosity of formation	**5.00**	%
C	Wellbore storage	**NA**	m^3/Pa
h	Length of aquifer tested	**60.35**	m

Skin Factor Calculation

Assuming formation storativity, the skin factor (s) can be calculated from the following equation.

$$s = \frac{\ln (C_D e^{2s} 2 \pi \phi c_t h r_w^2 / C)}{2}$$

Match Point Parameters From Analysis

$C_D e^{2s}$	3.0000E+00
P (kPa)	4.6825E-05
T (hr)	2.4582E-01

Results

$T(m^2/sec)$	K (feet/min)	K (ft/day)	K (m/s)	K (cm/s)	Skin
5.08E-08	**1.66E-07**	**0.00**	**8.41E-10**	**8.41E-08**	#########

FlowDim Analysis File : **p191-od.dat**

	Parameter		Units
r_w	Well radius	**0.076**	m
μ	Groundwater viscosity	**1.00E-03**	Pa s
ρ	Groundwater density	**1.00E+03**	kg/m^3
c_t	Total compressibility	**5.40E-10**	1/Pa
ϕ	Porosity of formation	**5.00**	%
C	Wellbore storage	**4.58E-07**	m^3/Pa
h	Length of aquifer tested	**60.35**	m

Skin Factor Calculation

Assuming formation storativity, the skin factor (s) can be calculated from the following equation.

$$s = \frac{\ln (C_D e^{2s} 2 \pi \phi c_t h r_w^2 / C)}{2}$$

Match Point Parameters From Analysis

$C_D e^{2s}$	2.0000E+08
P (kPa)	2.9442E-02
T (hr)	3.2135E+02

Results

T(m^2/sec)	K (feet/min)	K (ft/day)	K (m/s)	K (cm/s)	Skin
6.39E-05	**2.08E-04**	**0.30**	**1.06E-06**	**1.06E-04**	**5.08**

FlowDim Analysis File : **p191od3d.dat**

	Parameter		Units
r_w	Well radius	0.076	m
μ	Groundwater viscosity	1.00E-03	Pa s
ρ	Groundwater density	1.00E+03	kg/m^3
c_t	Total compressibility	5.40E-10	1/Pa
ϕ	Porosity of formation	5.00	%
C	Wellbore storage	4.19E-07	m^3/Pa
h	Length of aquifer tested	60.35	m

Skin Factor Calculation

Assuming formation storativity, the skin factor (s) can be calculated from the following equation.

$$s = \frac{\ln (C_D e^{2s} \, 2 \pi \phi \, c_t \, h \, r_w^2 / C)}{2}$$

Match Point Parameters From Analysis

$C_D e^{2s}$	1.0000E+01
P (kPa)	2.1754E-03
T (hr)	2.5952E+01

Results

$T(m^2/sec)$	K (feet/min)	K (ft/day)	K (m/s)	K (cm/s)	Skin
2.36E-06	**7.70E-06**	**0.01**	**3.91E-08**	**3.91E-06**	**-3.28**

FlowDim Analysis File : **p192-od.dat**

	Parameter		Units
r_w	Well radius	**0.051**	m
μ	Groundwater viscosity	**1.00E-03**	Pa s
ρ	Groundwater density	**1.00E+03**	kg/m^3
c_t	Total compressibility	**5.40E-10**	1/Pa
ϕ	Porosity of formation	**5.00**	%
C	Wellbore storage	**NA**	m^3/Pa
h	Length of aquifer tested	**60.35**	m

Skin Factor Calculation

Assuming formation storativity, the skin factor (s) can be calculated from the following equation.

$$s = \frac{\ln (C_D e^{2s} \, 2 \pi \phi \, c_t \, h \, r_w^2 / C)}{2}$$

Match Point Parameters From Analysis

$C_D e^{2s}$	2.0000E+00
P (kPa)	1.4484E-02
T (hr)	1.7103E+00

Results

$T(m^2/sec)$	K (feet/min)	K (ft/day)	K (m/s)	K (cm/s)	Skin
3.14E-05	**1.02E-04**	**0.15**	**5.20E-07**	**5.20E-05**	#########

FlowDim Analysis File : **p192od3d.dat**

	Parameter		Units
r_w	Well radius	**0.051**	m
μ	Groundwater viscosity	**1.00E-03**	Pa s
ρ	Groundwater density	**1.00E+03**	kg/m^3
c_t	Total compressibility	**5.40E-10**	1/Pa
ϕ	Porosity of formation	**5.00**	%
C	Wellbore storage	**NA**	m^3/Pa
h	Length of aquifer tested	**60.35**	m

Skin Factor Calculation

Assuming formation storativity, the skin factor (s) can be calculated from the following equation.

$$s = \frac{\ln (C_D e^{2s} 2 \pi \phi c_t h r_w^2 / C)}{2}$$

Match Point Parameters From Analysis

$C_D e^{2s}$	3.0000E+00
P (kPa)	3.8942E-05
T (hr)	1.0011E+00

Results

$T(m^2/sec)$	K (feet/min)	K (ft/day)	K (m/s)	K (cm/s)	Skin
4.22E-08	**1.38E-07**	**0.00**	**7.00E-10**	**7.00E-08**	#########

FlowDim Analysis File : **p28-gld.dat**

	Parameter		Units
r_w	Well radius	**0.064**	m
μ	Groundwater viscosity	**1.00E-03**	Pa s
ρ	Groundwater density	**1.00E+03**	kg/m^3
c_t	Total compressibility	**5.40E-10**	1/Pa
ϕ	Porosity of formation	**10.00**	%
C	Wellbore storage	**8.71E-07**	m^3/Pa
h	Length of aquifer tested	**9.14**	m

Skin Factor Calculation

Assuming formation storativity, the skin factor (s) can be calculated from the following equation.

$$s = \frac{\ln (C_D e^{2s} \, 2 \pi \phi \, c_t \, h \, r_w^2 / C)}{2}$$

Match Point Parameters From Analysis

$C_D e^{2s}$	1.0000E+06
P (kPa)	3.6017E-02
T (hr)	7.0454E+02

Results

$T(m^2/sec)$	K (feet/min)	K (ft/day)	K (m/s)	K (cm/s)	Skin
2.66E-04	**5.73E-03**	**8.26**	**2.91E-05**	**2.91E-03**	**1.33**

FlowDim Analysis File : **p281-oad.dat**

	Parameter		Units
r_w	Well radius	0.067	m
μ	Groundwater viscosity	1.00E-03	Pa s
ρ	Groundwater density	1.00E+03	kg/m^3
c_t	Total compressibility	5.40E-10	1/Pa
ϕ	Porosity of formation	5.00	%
C	Wellbore storage	1.50E-04	m^3/Pa
h	Length of aquifer tested	30.48	m

Skin Factor Calculation

Assuming formation storativity, the skin factor (s) can be calculated from the following equation.

$$s = \frac{\ln (C_D e^{2s} 2 \pi \phi c_t h r_w^2 / C)}{2}$$

Match Point Parameters From Analysis

$C_D e^{2s}$	1.0000E+01
P (kPa)	2.8879E-01
T (hr)	1.2647E+01

Results

$T(m^2/sec)$	K (feet/min)	K (ft/day)	K (m/s)	K (cm/s)	Skin
8.25E-04	**5.33E-03**	**7.68**	**2.71E-05**	**2.71E-03**	**-6.69**

FlowDim Analysis File : **p281-obd.dat**

	Parameter		Units
r_w	Well radius	**0.076**	m
μ	Groundwater viscosity	**1.00E-03**	Pa s
ρ	Groundwater density	**1.00E+03**	kg/m^3
c_t	Total compressibility	**5.40E-10**	1/Pa
ϕ	Porosity of formation	**5.00**	%
C	Wellbore storage	**1.28E-06**	m^3/Pa
h	Length of aquifer tested	**30.48**	m

Skin Factor Calculation

Assuming formation storativity, the skin factor (s) can be calculated from the following equation.

$$s = \frac{\ln (C_D e^{2s} \, 2 \pi \phi \, c_t \, h \, r_w^2 / C)}{2}$$

Match Point Parameters From Analysis

$C_D e^{2s}$	1.0000E+01
P (kPa)	4.6017E-02
T (hr)	6.9315E+02

Results

T(m^2/sec)	K (feet/min)	K (ft/day)	K (m/s)	K (cm/s)	Skin
3.86E-04	**2.49E-03**	**3.59**	**1.26E-05**	**1.26E-03**	**-4.18**

FlowDim Analysis File : **p282-obd.dat**

	Parameter		Units
r_w	Well radius	**0.051**	m
μ	Groundwater viscosity	**1.00E-03**	Pa s
ρ	Groundwater density	**1.00E+03**	kg/m^3
c_t	Total compressibility	**5.40E-10**	1/Pa
ϕ	Porosity of formation	**5.00**	%
C	Wellbore storage	**NA**	m^3/Pa
h	Length of aquifer tested	**30.18**	m

Skin Factor Calculation

Assuming formation storativity, the skin factor (s) can be calculated from the following equation.

$$s = \frac{\ln (C_D e^{2s} \, 2 \pi \phi \, c_t \, h \, r_w^2 / C)}{2}$$

Match Point Parameters From Analysis

$C_D e^{2s}$	2.0000E+00
P (kPa)	3.3963E-02
T (hr)	3.9303E+00

Results

$T(m^2/sec)$	K (feet/min)	K (ft/day)	K (m/s)	K (cm/s)	Skin
2.84E-04	**1.86E-03**	**2.67**	**9.43E-06**	**9.43E-04**	#########

FlowDim Analysis File : **p282-od.dat**

	Parameter		Units
r_w	Well radius	**0.076**	m
μ	Groundwater viscosity	**1.00E-03**	Pa s
ρ	Groundwater density	**1.00E+03**	kg/m^3
c_t	Total compressibility	**5.40E-10**	1/Pa
ϕ	Porosity of formation	**5.00**	%
C	Wellbore storage	**1.41E-04**	m^3/Pa
h	Length of aquifer tested	**30.18**	m

Skin Factor Calculation

Assuming formation storativity, the skin factor (s) can be calculated from the following equation.

$$s = \frac{\ln (C_D e^{2s} 2 \pi \phi c_t h r_w^2 / C)}{2}$$

Match Point Parameters From Analysis

$C_D e^{2s}$	1.0000E+01
P (kPa)	4.4105E-02
T (hr)	5.4115E+00

Results

$T(m^2/sec)$	K (feet/min)	K (ft/day)	K (m/s)	K (cm/s)	Skin
3.30E-04	**2.15E-03**	**3.10**	**1.09E-05**	**1.09E-03**	**-6.53**

FlowDim Analysis File : **P49Od.dat**

	Parameter		Units
r_w	Well radius	**0.076**	m
μ	Groundwater viscosity	**1.00E-03**	Pa s
ρ	Groundwater density	**1.00E+03**	kg/m^3
c_t	Total compressibility	**5.40E-10**	1/Pa
ϕ	Porosity of formation	**0.05**	%
C	Wellbore storage	**1.78E-06**	m^3/Pa
h	Length of aquifer tested	**126.19**	m

Skin Factor Calculation

Assuming formation storativity, the skin factor (s) can be calculated from the following equation.

$$s = \frac{\ln (C_D e^{2s} \, 2 \pi \phi \, c_t \, h \, r_w^2 / C)}{2}$$

Match Point Parameters From Analysis

$C_D e^{2s}$	3.0000E-01
P (kPa)	1.7500E-03
T (hr)	8.9400E+00

Results

$T(m^2/sec)$	K (feet/min)	K (ft/day)	K (m/s)	K (cm/s)	Skin
3.45E-06	**5.38E-06**	**7.75E-03**	**2.73E-08**	**2.73E-06**	**-7.69**

APPENDIX B

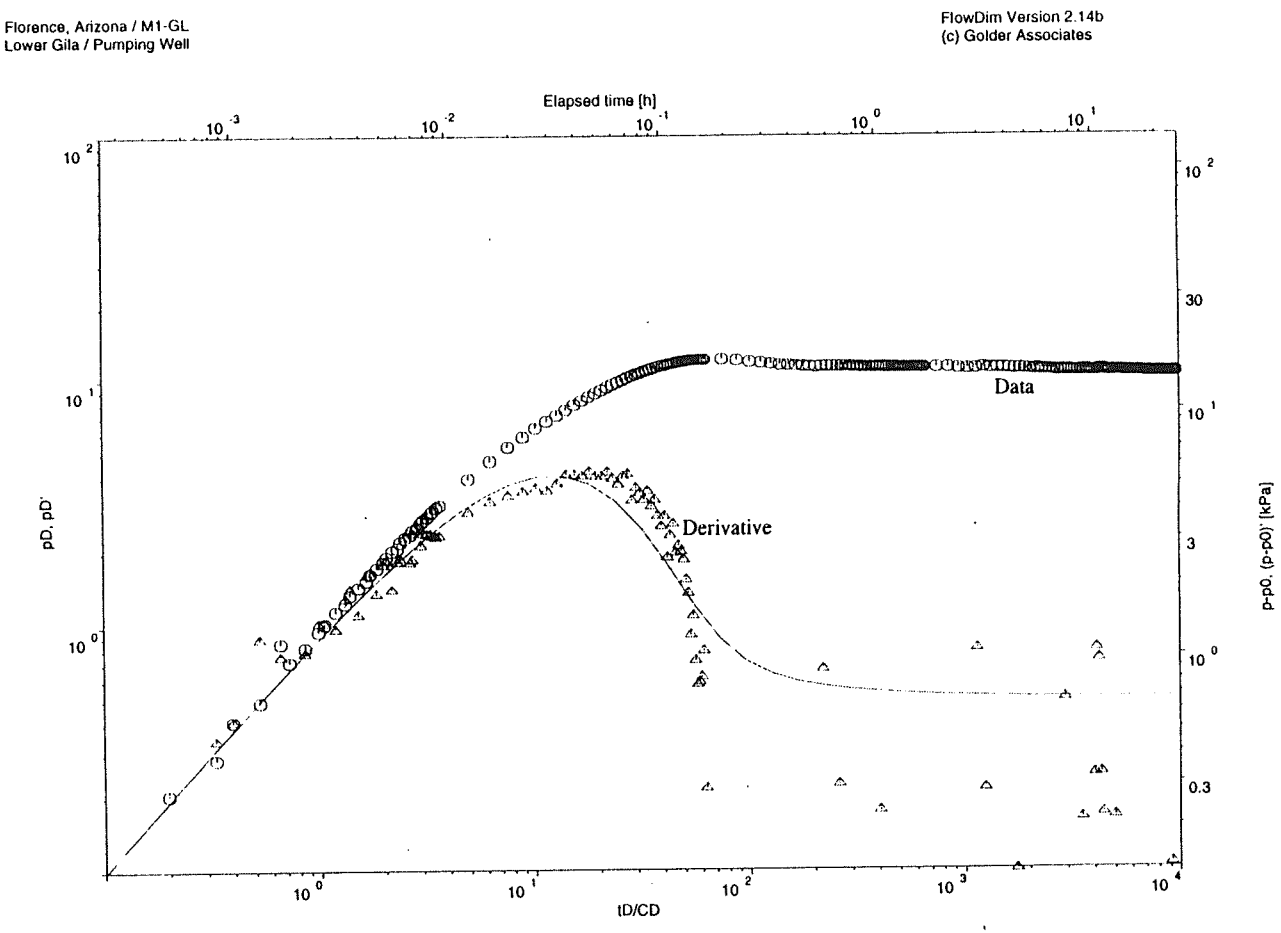

FLOW MODEL : Homogeneous
BOUNDARY CONDITIONS: Constant rate
WELL TYPE : Source
SUPERPOSITION TYPE : No superposition
PLOT TYPE : Log-log

C=	4.35E-06	m3/Pa
T=	7.43E-04	m2/s
S=	8.43E-09	-
s=	0.00E+00	-
n=	2.00E+00	-

Figure 1B

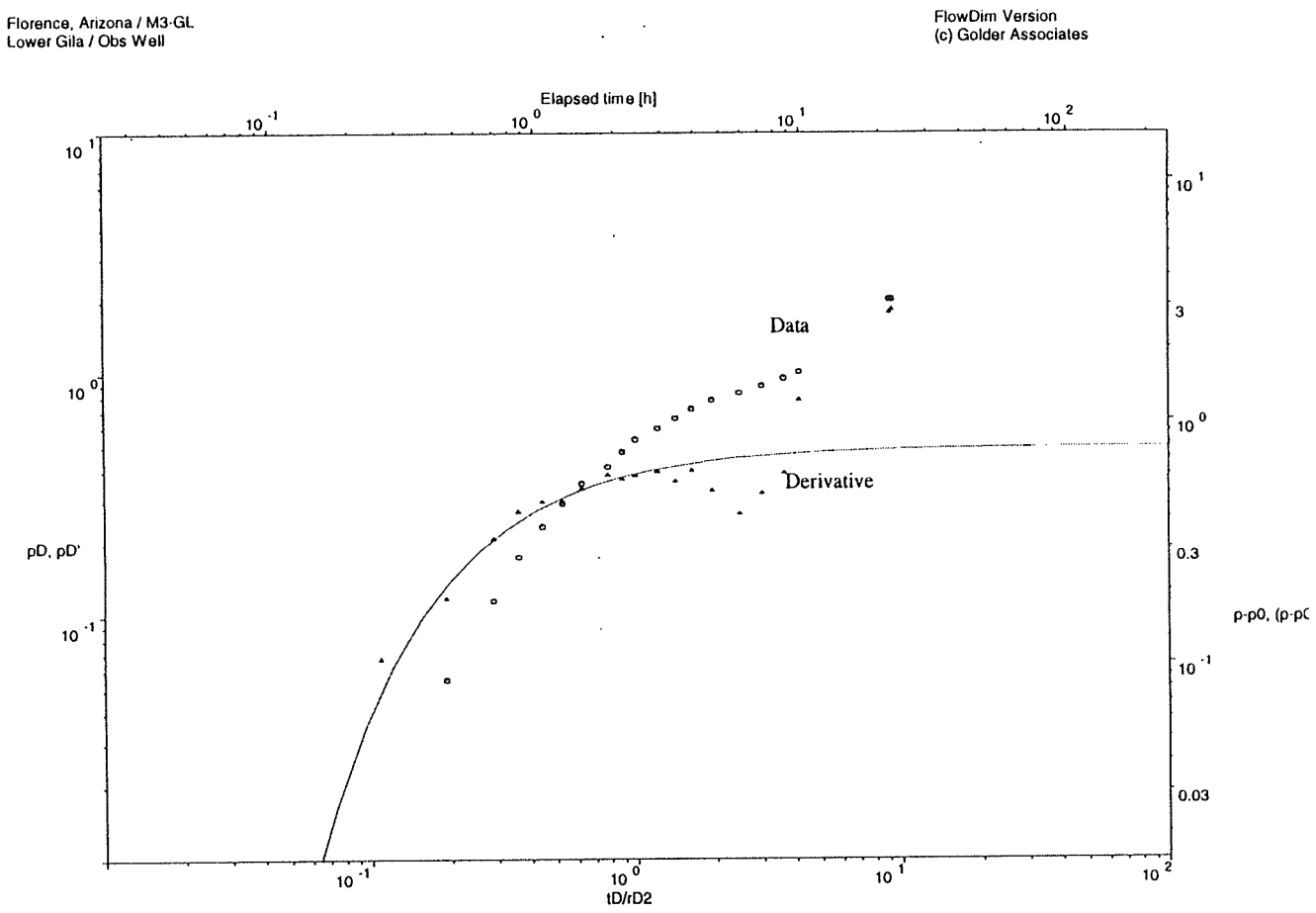

FLOW MODEL :
BOUNDARY CONDITIONS: Constant rate
WELL TYPE :
SUPERPOSITION TYPE : No superposition
PLOT TYPE : Log-

T=	9.53E-04	m2/s
S=	8.78E-02	-
rD=	1.53E+02	-
n=	2.00E+00	-

Figure 2B

Golder Associates

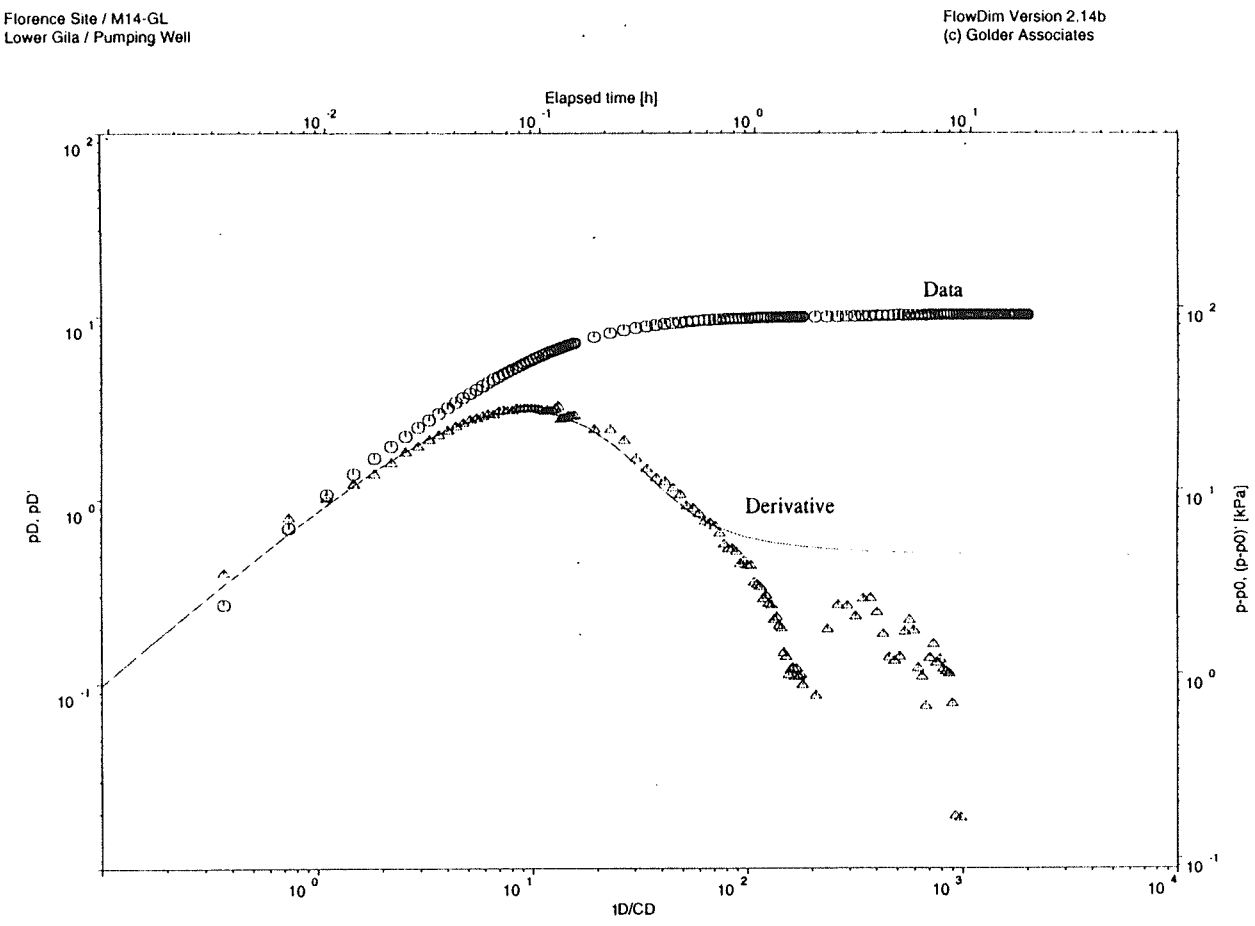

FLOW MODEL : Homogeneous
BOUNDARY CONDITIONS: Constant rate
WELL TYPE : Source
SUPERPOSITION TYPE : No superposition
PLOT TYPE : Log-log

C=	2.35E-06	m3/Pa
T=	1.12E-04	m2/s
S=	9.11E-07	-
s=	0.00E+00	-
n=	2.00E+00	-

Figure 3B

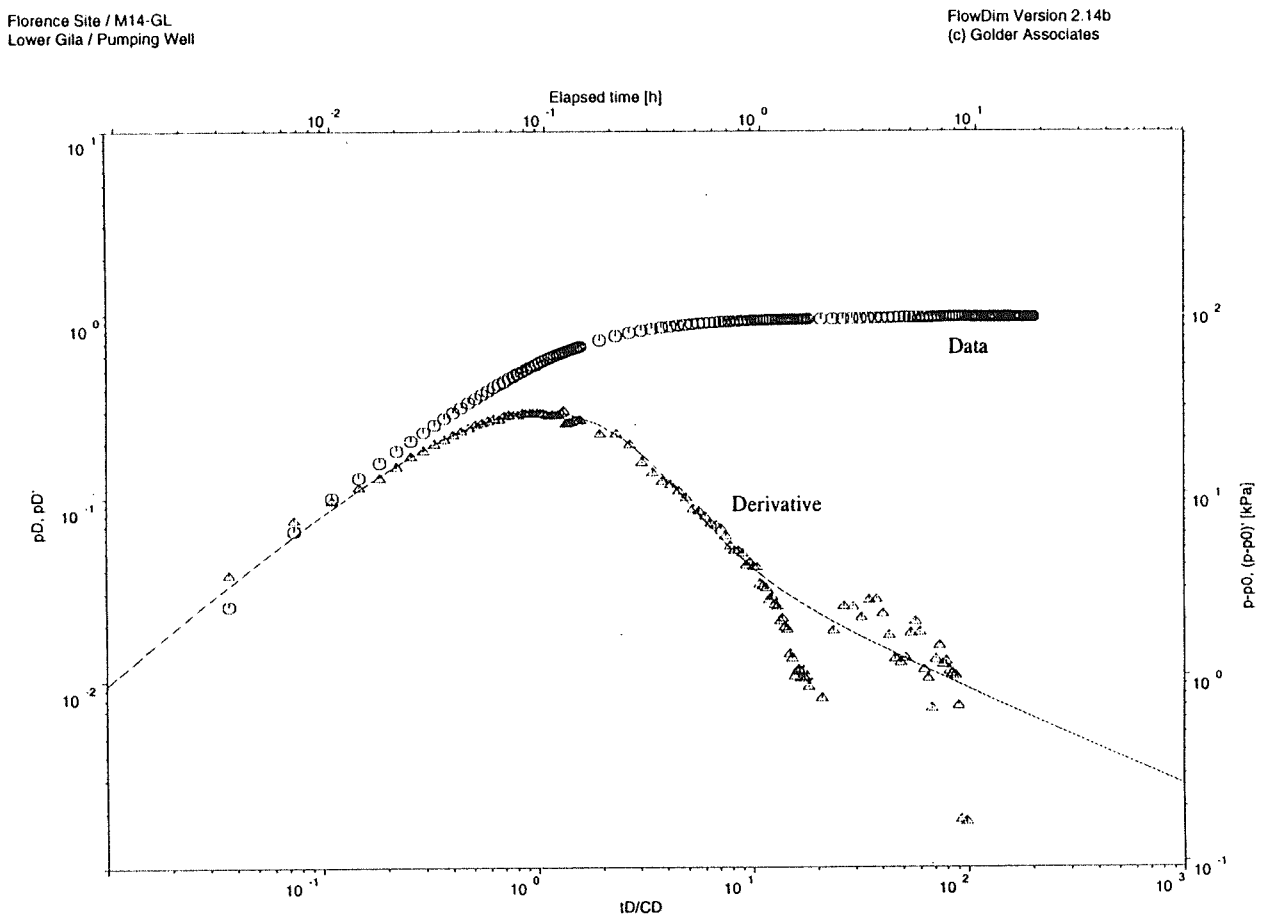

FLOW MODEL : Homogeneous
BOUNDARY CONDITIONS: Constant rate
WELL TYPE : Source
SUPERPOSITION TYPE : No superposition
PLOT TYPE : Log-log

C=	2.22E-06	m3/Pa
T=	5.31E-06	m2/s
S=	4.30E-02	-
s=	0.00E+00	-
n=	3.00E+00	-

Figure 4B

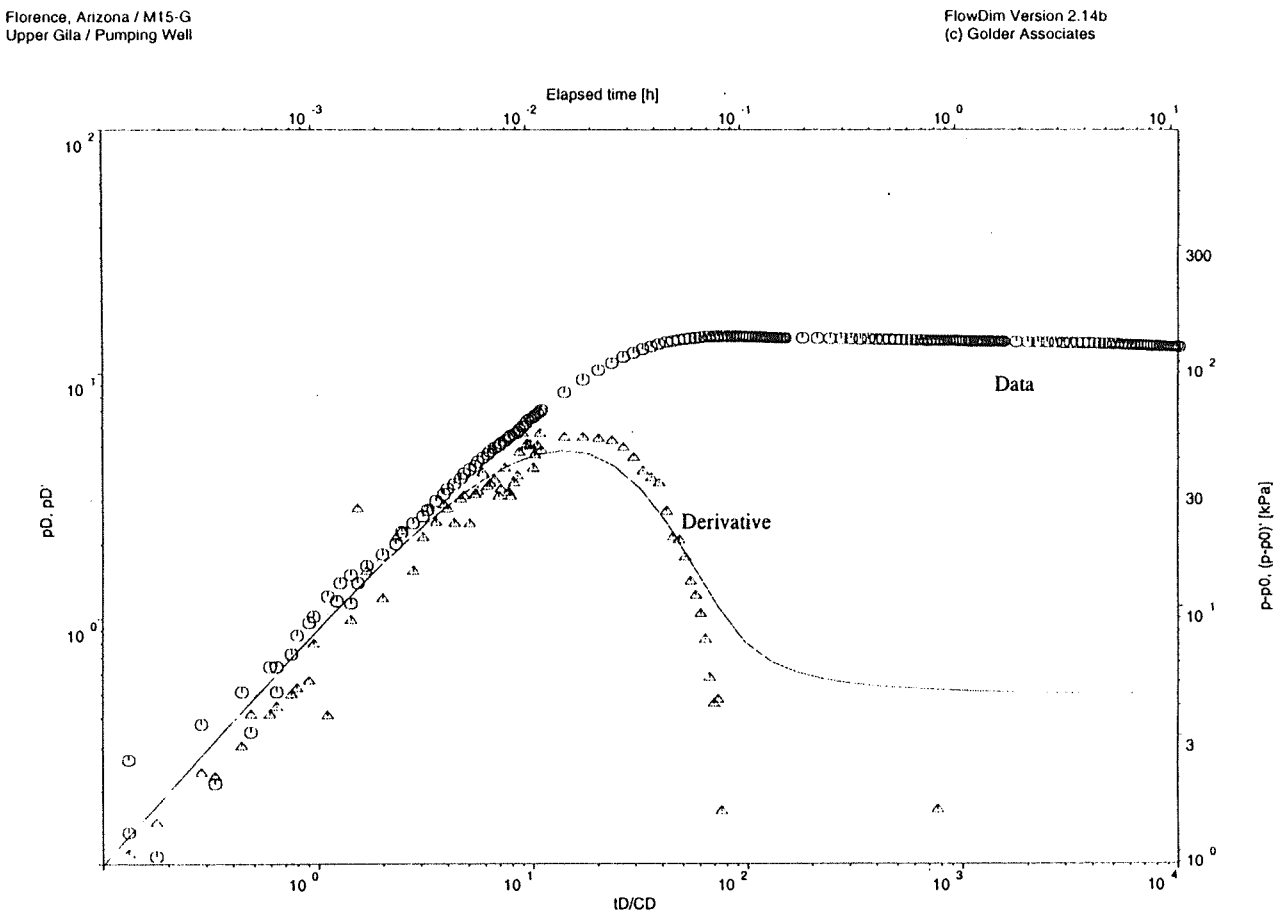

FLOW MODEL : Homogeneous
BOUNDARY CONDITIONS: Constant rate
WELL TYPE : Source
SUPERPOSITION TYPE : No superposition
PLOT TYPE : Log-log

C=	2.78E-07	m3/Pa
T=	1.11E-04	m2/s
S=	1.08E-11	-
s=	0.00E+00	-
n=	2.00E+00	-

Figure 5B

Golder Associates

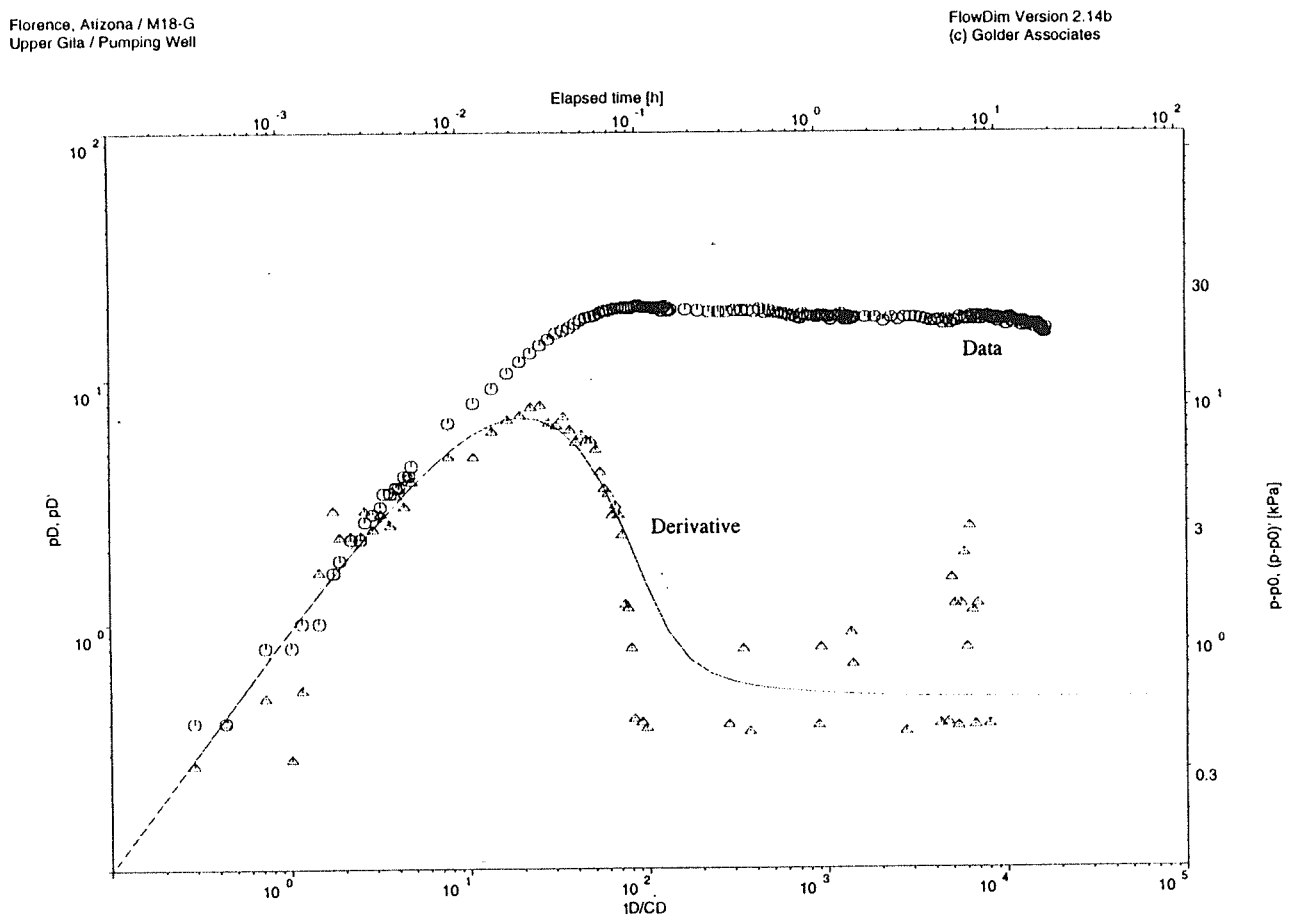

FLOW MODEL : Homogeneous
BOUNDARY CONDITIONS: Constant rate
WELL TYPE : Source
SUPERPOSITION TYPE : No superposition
PLOT TYPE : Log-log

C=	2.25E-06	m3/Pa
T=	8.44E-04	m2/s
S=	8.70E-16	-
s=	0.00E+00	-
n=	2.00E+00	-

Figure 6B

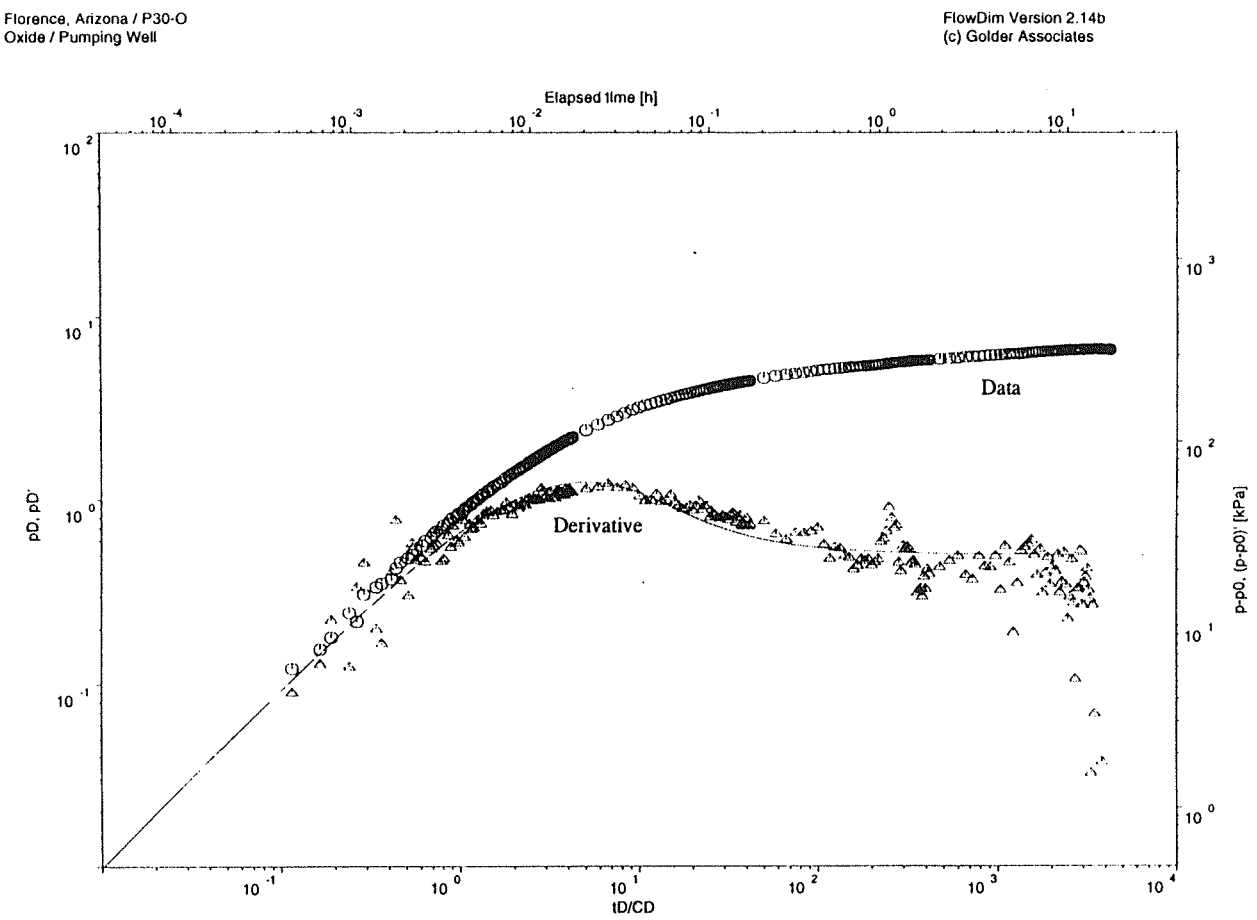

FLOW MODEL : Homogeneous
BOUNDARY CONDITIONS: Constant rate
WELL TYPE : Source
SUPERPOSITION TYPE : No superposition
PLOT TYPE : Log-log

C=	1.04E-06	m3/Pa
T=	1.12E-04	m2/s
S=	9.60E-04	-
s=	0.00E+00	-
n=	2.00E+00	-

Figure 7B

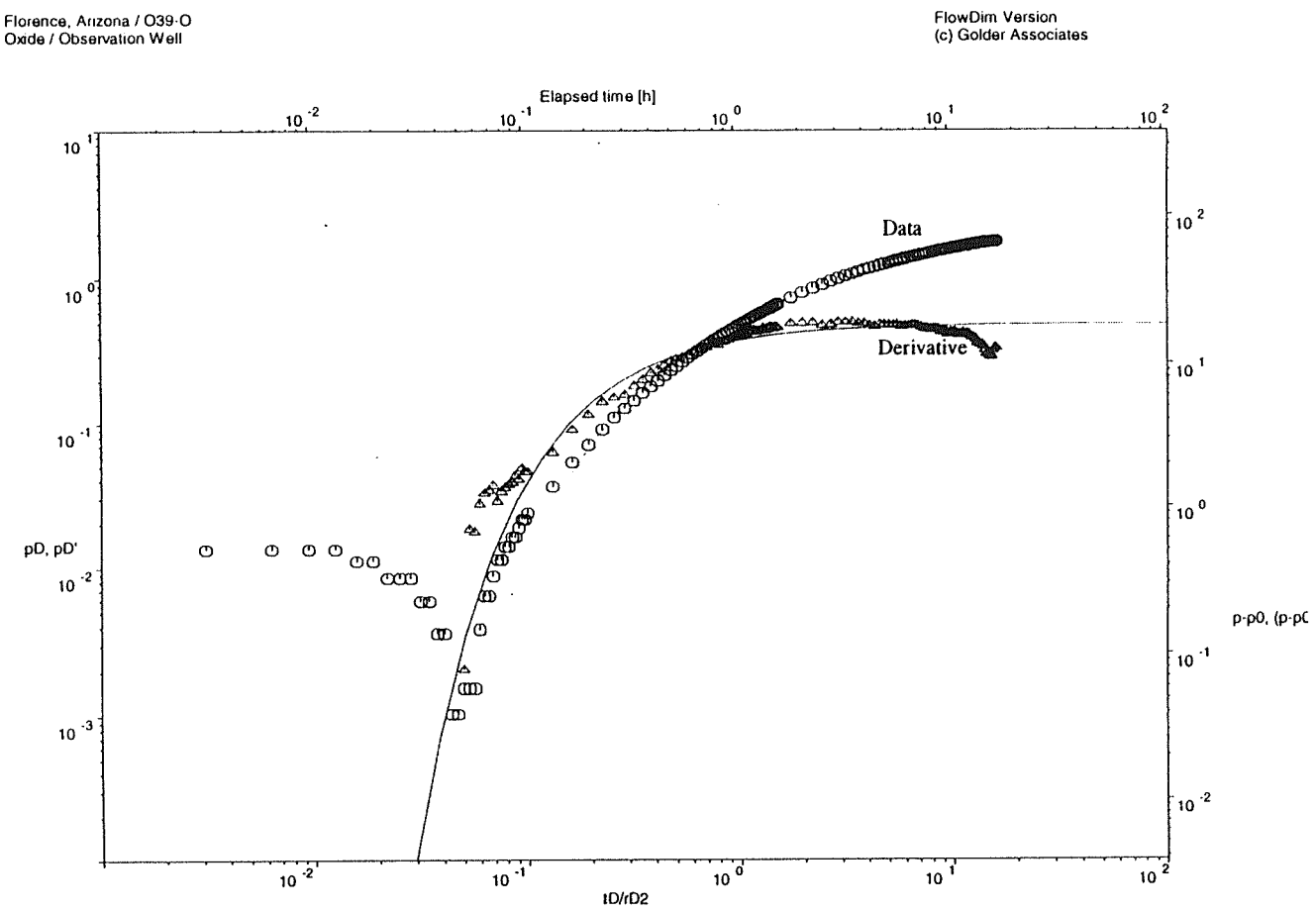

FLOW MODEL :
BOUNDARY CONDITIONS: Constant rate
WELL TYPE :
SUPERPOSITION TYPE : No superposition
PLOT TYPE : Log-

T=	1.45E-04	m2/s
S=	4.32E-04	-
rD=	2.83E+02	-
n=	2.00E+00	-

Figure 8B

Florence, Arizona / OB7-1
Oxide / Observation Well

FlowDim Version 2.14b
(c) Golder Associates

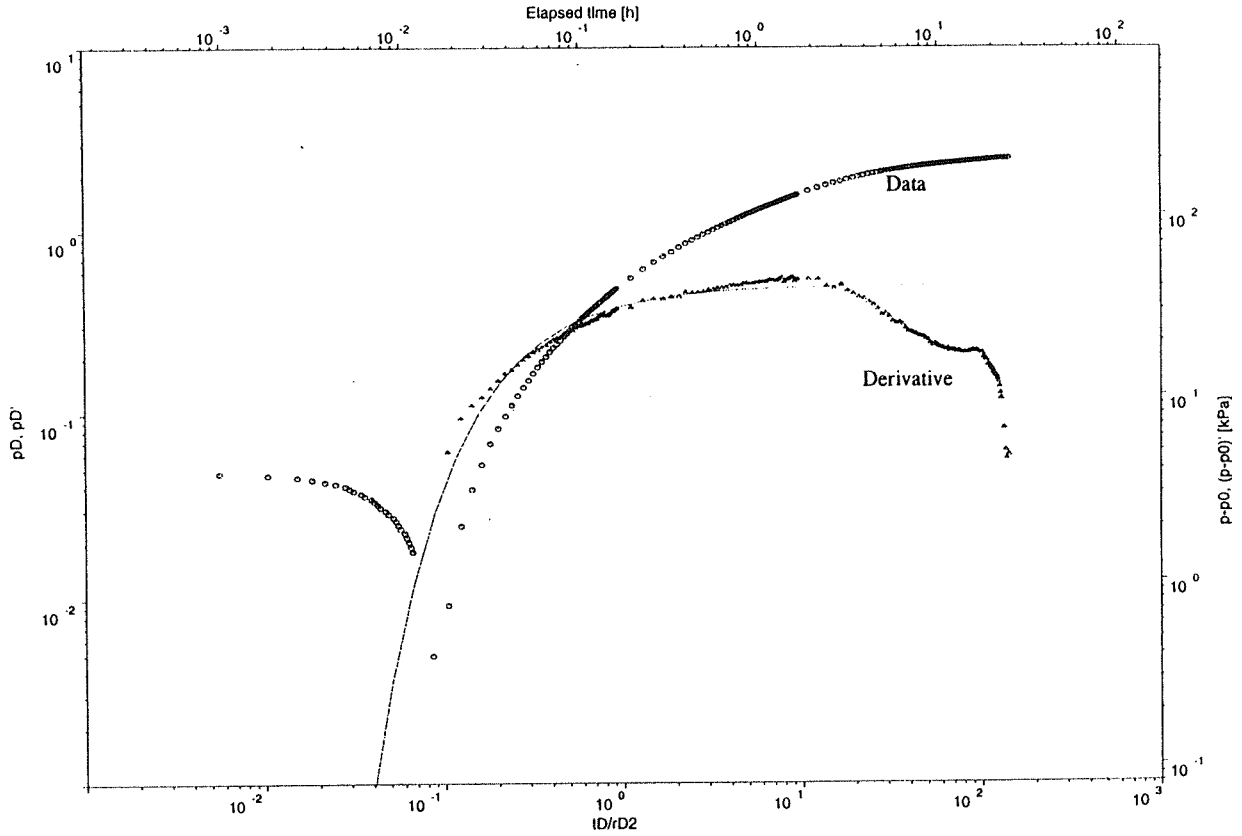

FLOW MODEL : Homogeneous
BOUNDARY CONDITIONS: Constant rate
WELL TYPE : Observation
SUPERPOSITION TYPE : No superposition
PLOT TYPE : Log-log

T=	4.95E-05	m2/s
S=	1.33E-04	-
rD=	2.01E+02	-
n=	2.00E+00	-

Figure 9B

Golder Associates

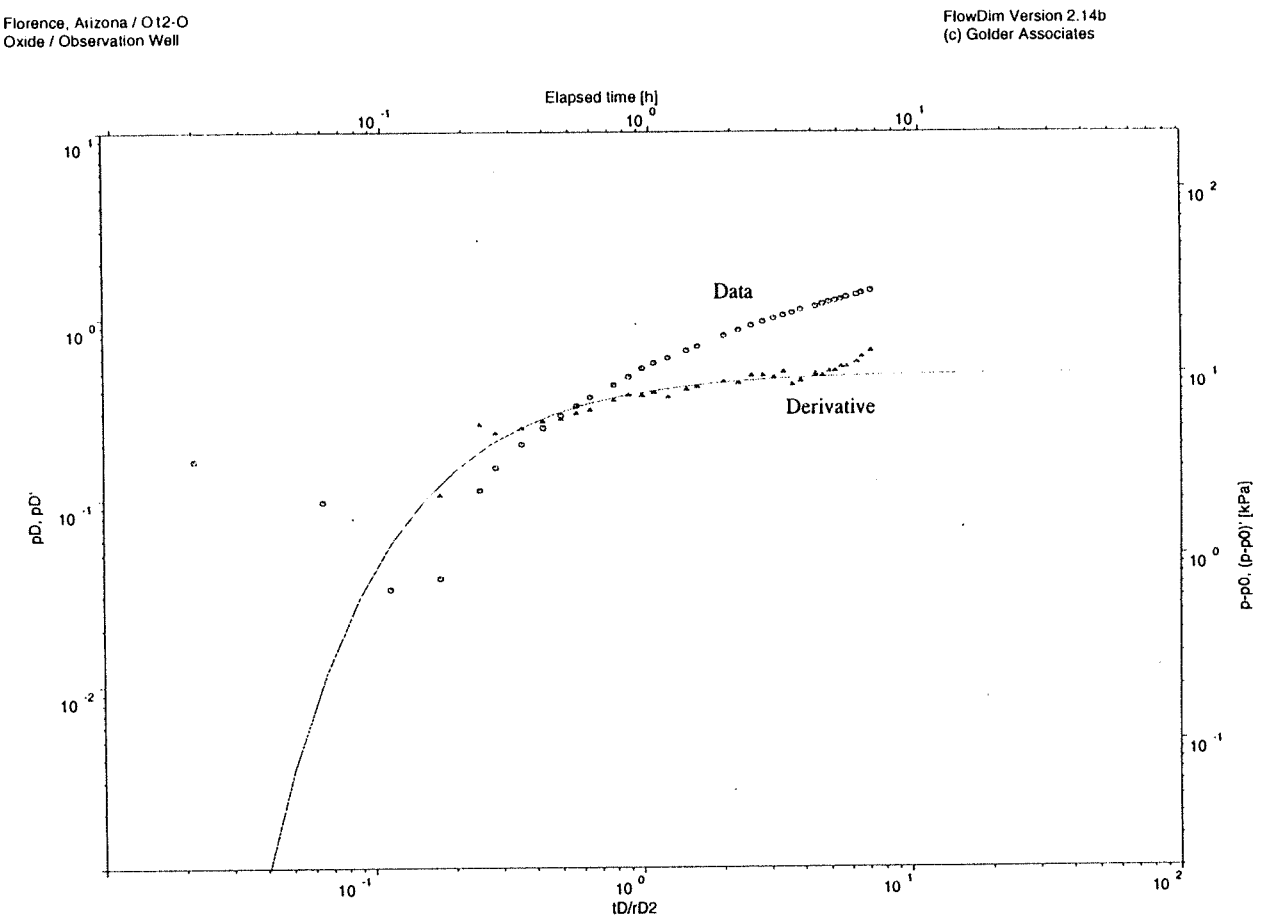

FLOW MODEL : Homogeneous
BOUNDARY CONDITIONS: Constant rate
WELL TYPE : Observation
SUPERPOSITION TYPE : No superposition
PLOT TYPE : Log-log

T=	3.21E-04	m2/s
S=	2.24E-03	-
rD=	2.87E+02	-
n=	2.00E+00	-

Figure 10B

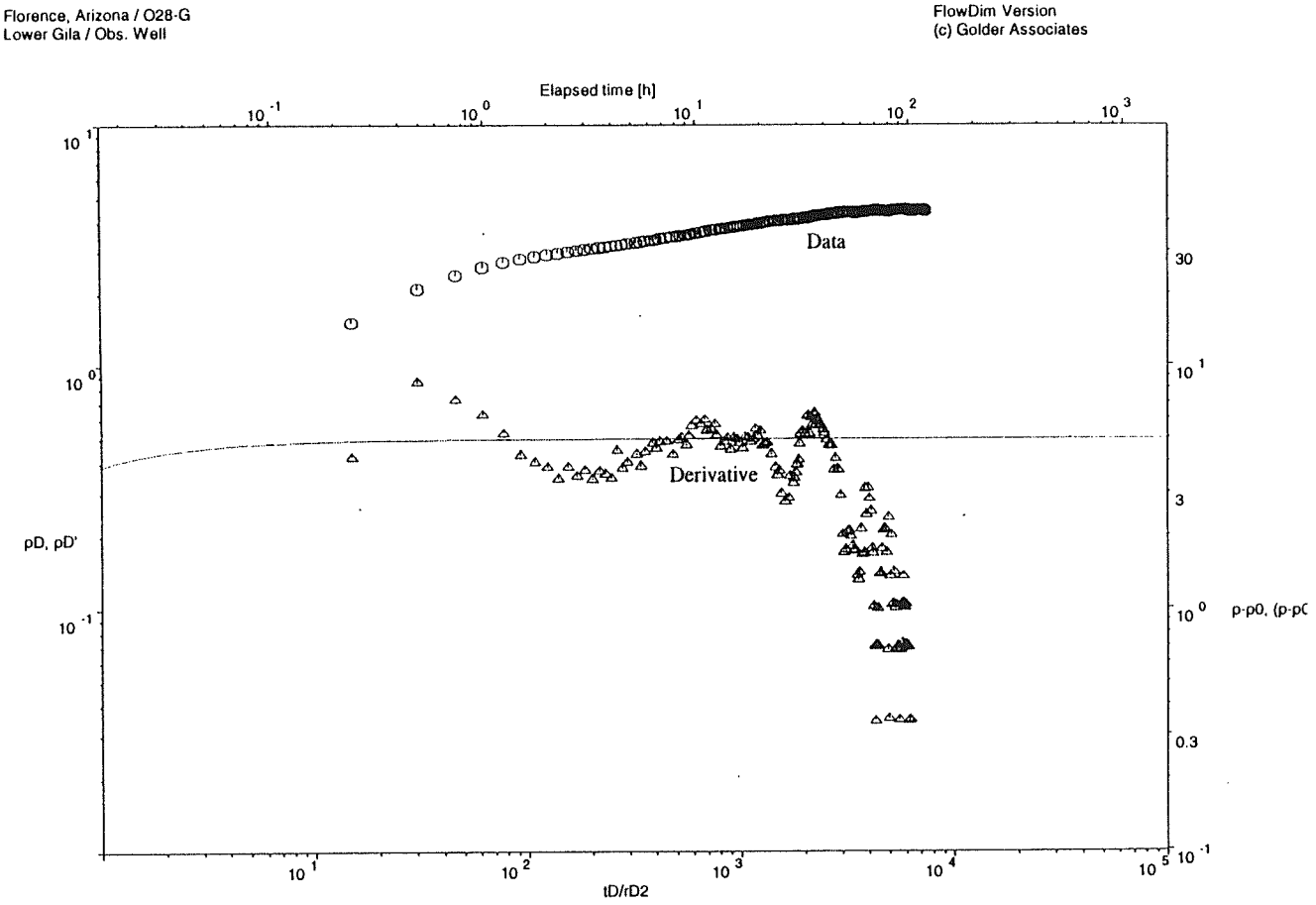

FLOW MODEL :
BOUNDARY CONDITIONS: Constant rate
WELL TYPE :
SUPERPOSITION TYPE : No superposition
PLOT TYPE : Log-

T=	7.49E-04	m2/s
S=	2.70E-05	-
rD=	7.92E+02	-
n=	2.00E+00	-

Figure 11B

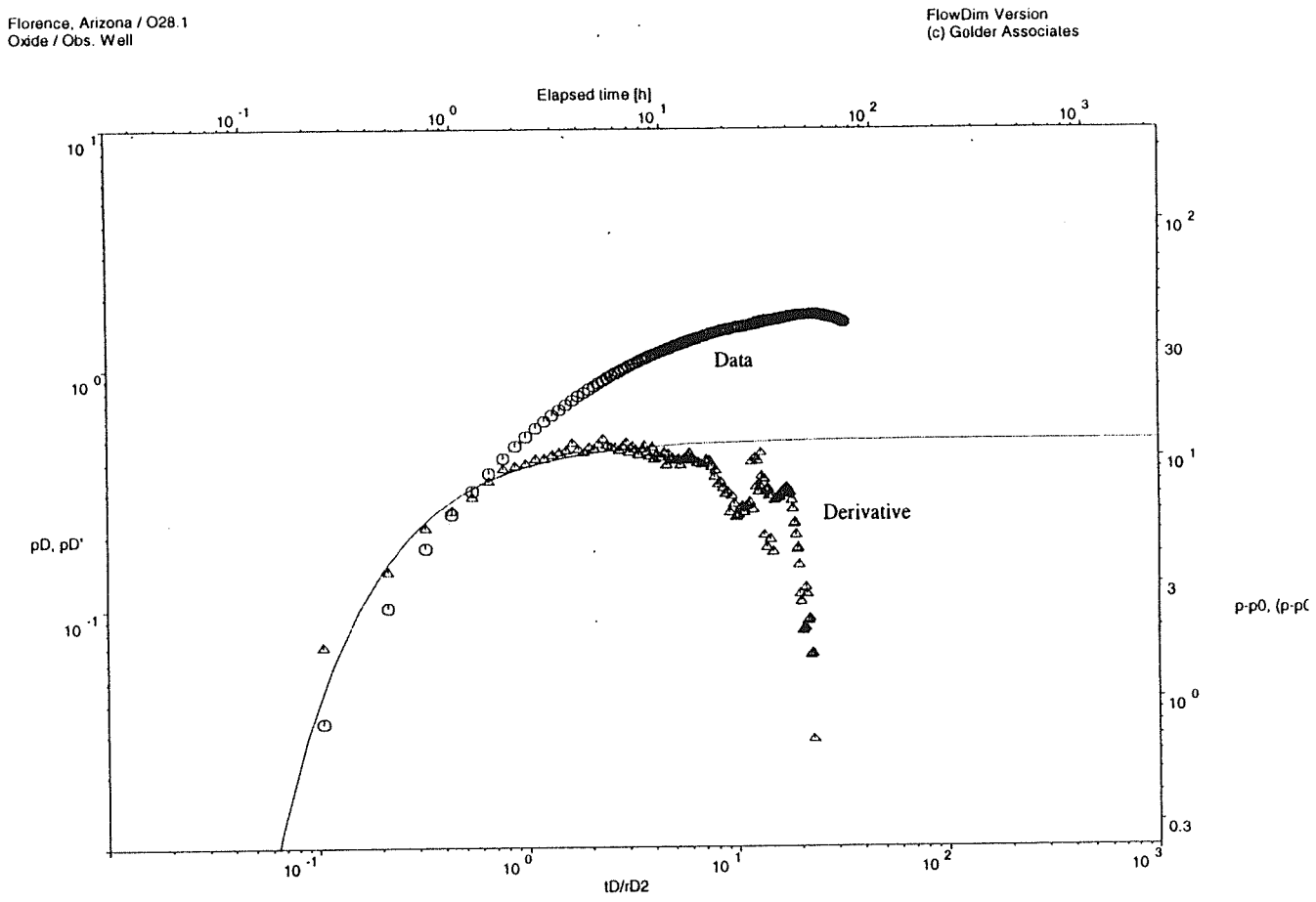

Figure 12B

Golder Associates

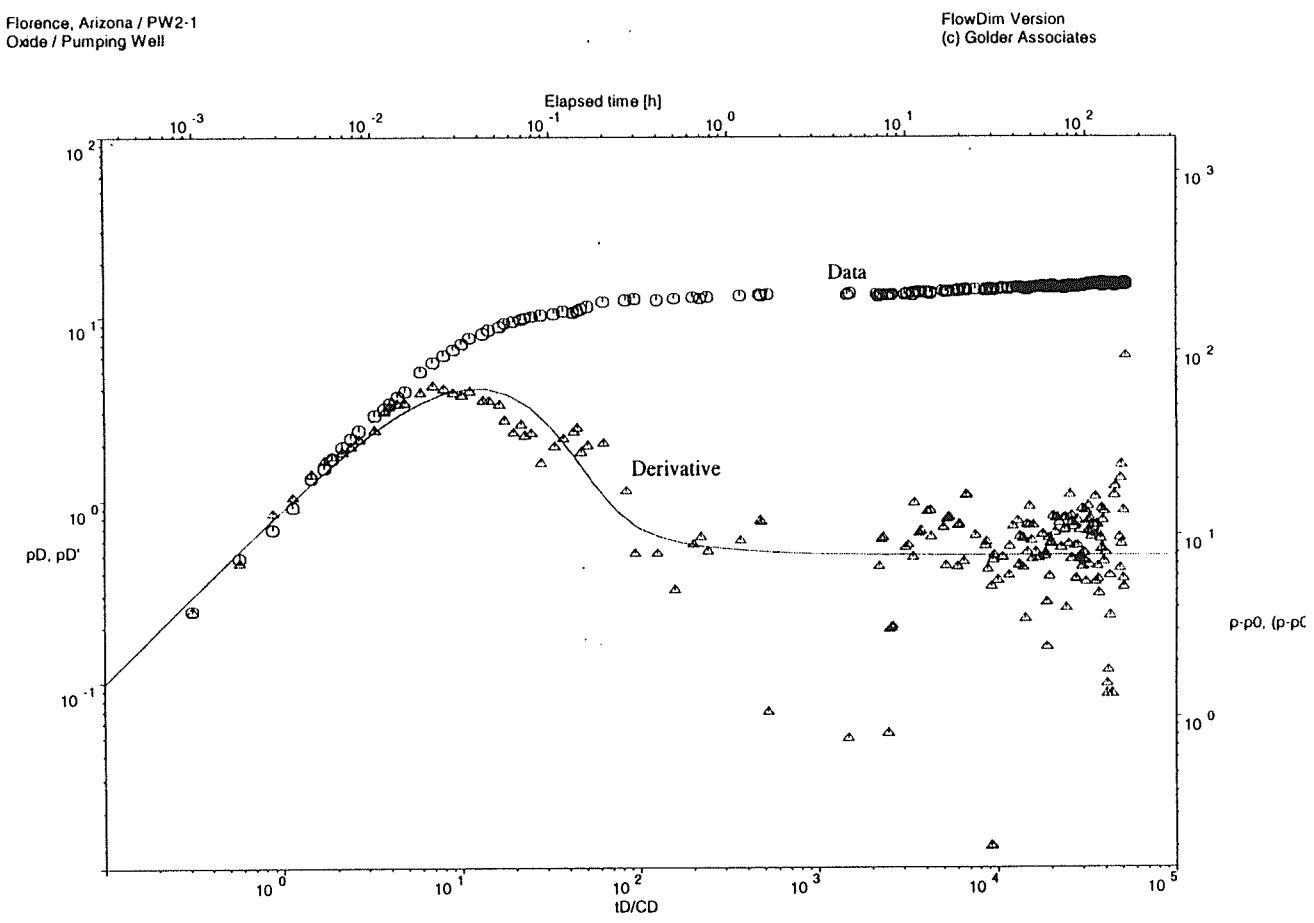

FLOW MODEL :
BOUNDARY CONDITIONS: Constant rate
WELL TYPE :
SUPERPOSITION TYPE : No superposition
PLOT TYPE : Log-

C=	2.36E-06	m3/Pa
T=	3.20E-04	m2/s
S=	3.18E-09	-
s=	0.00E+00	-
n=	2.00E+00	-

Figure 13B

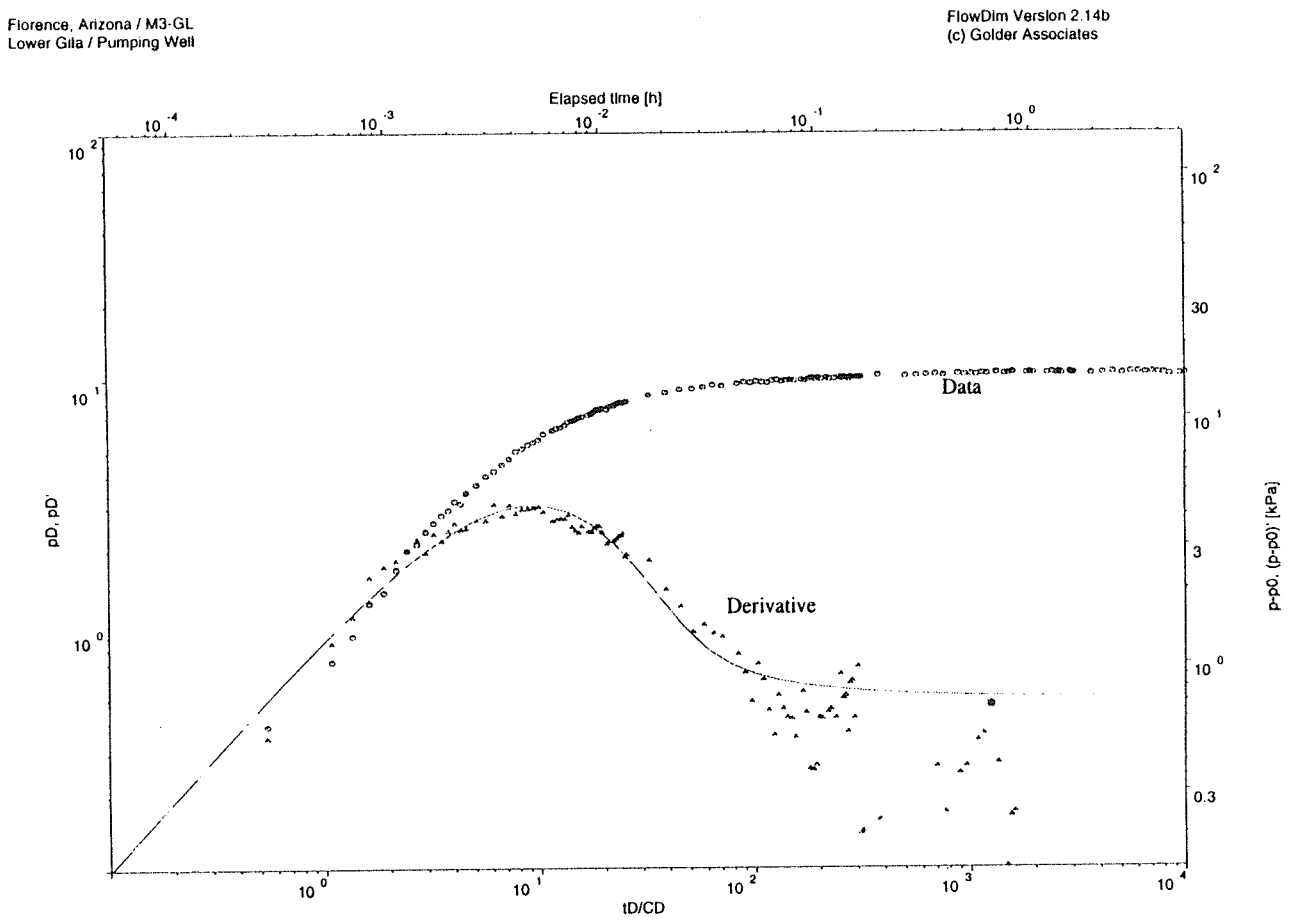

FLOW MODEL : Homogeneous
BOUNDARY CONDITIONS: Constant rate
WELL TYPE : Source
SUPERPOSITION TYPE : No superposition
PLOT TYPE : Log-log

C=	8.16E-07	m3/Pa
T=	6.83E-04	m2/s
S=	3.16E-07	-
s=	0.00E+00	-
n=	2.00E+00	-

Figure 14B

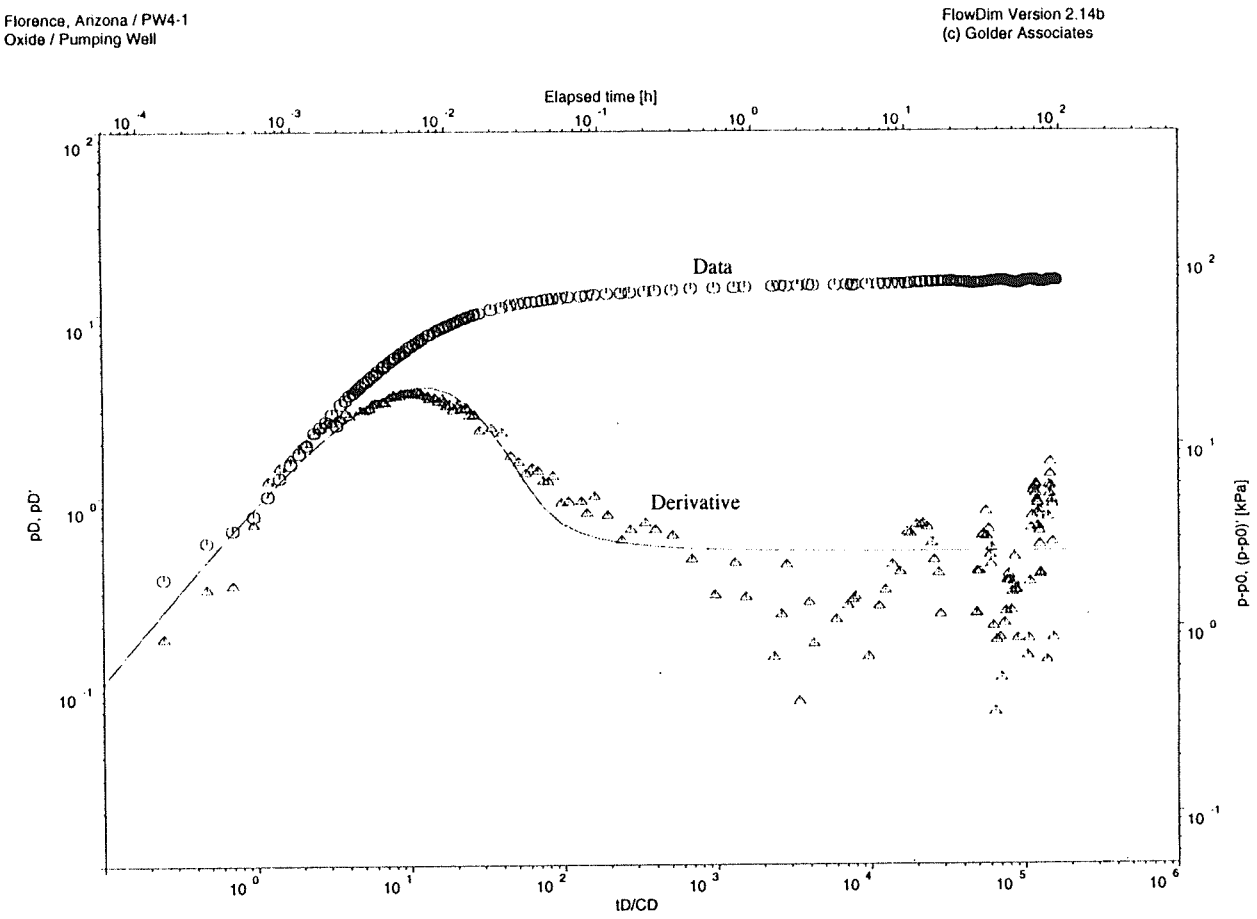

FLOW MODEL : Homogeneous
BOUNDARY CONDITIONS: Constant rate
WELL TYPE : Source
SUPERPOSITION TYPE : No superposition
PLOT TYPE : Log-log

C=	1.87E-06	m3/Pa
T=	1.37E-03	m2/s
S=	2.52E-09	-
s=	0.00E+00	-
n=	2.00E+00	-

Figure 15B

Golder Associates

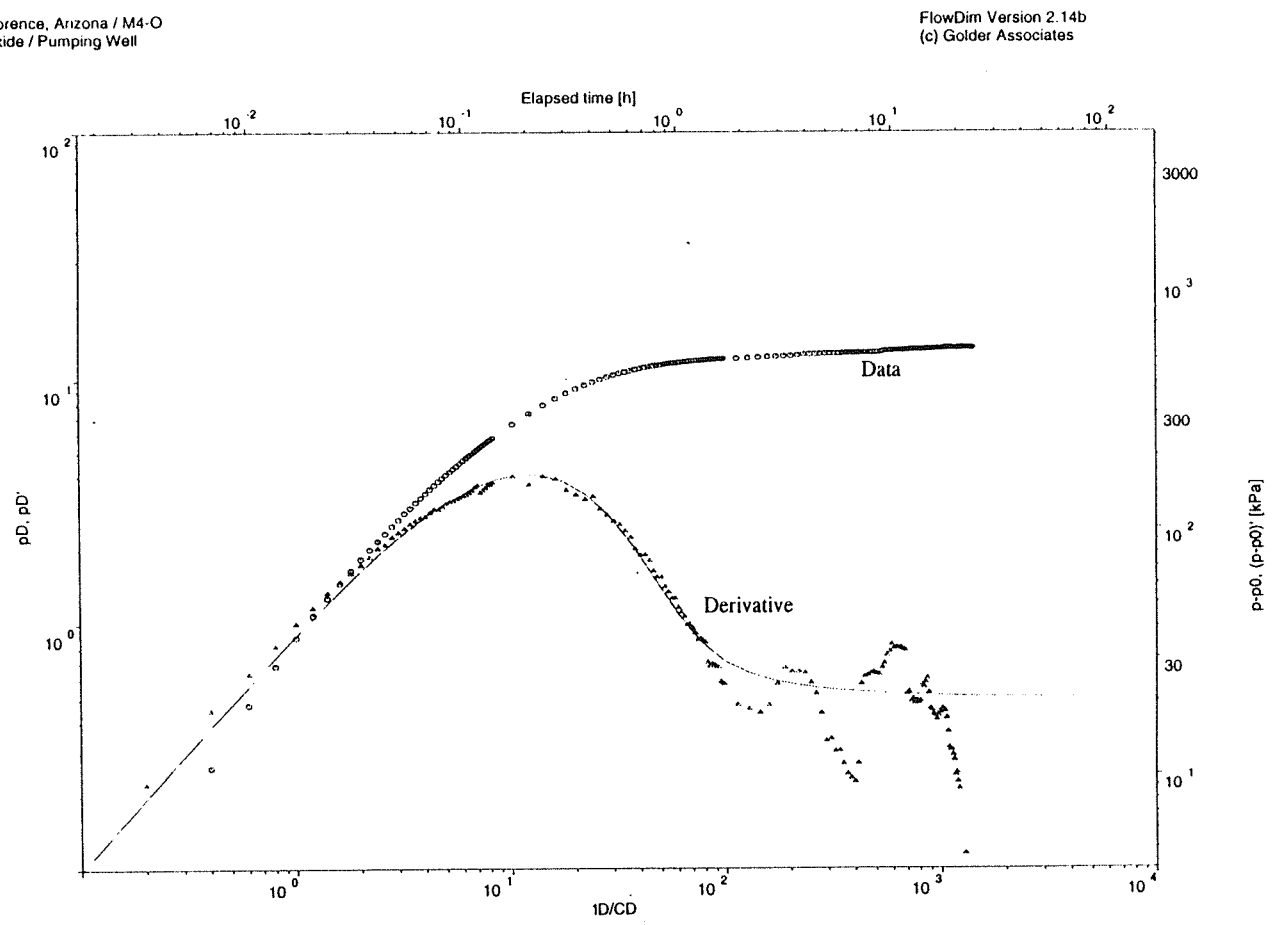

FLOW MODEL : Homogeneous
BOUNDARY CONDITIONS: Constant rate
WELL TYPE : Source
SUPERPOSITION TYPE : No superposition
PLOT TYPE : Log-log

C=	1.38E-06	m3/Pa
T=	3.59E-05	m2/s
S=	2.68E-09	-
s=	0.00E+00	-
n=	2.00E+00	-

Figure 16B

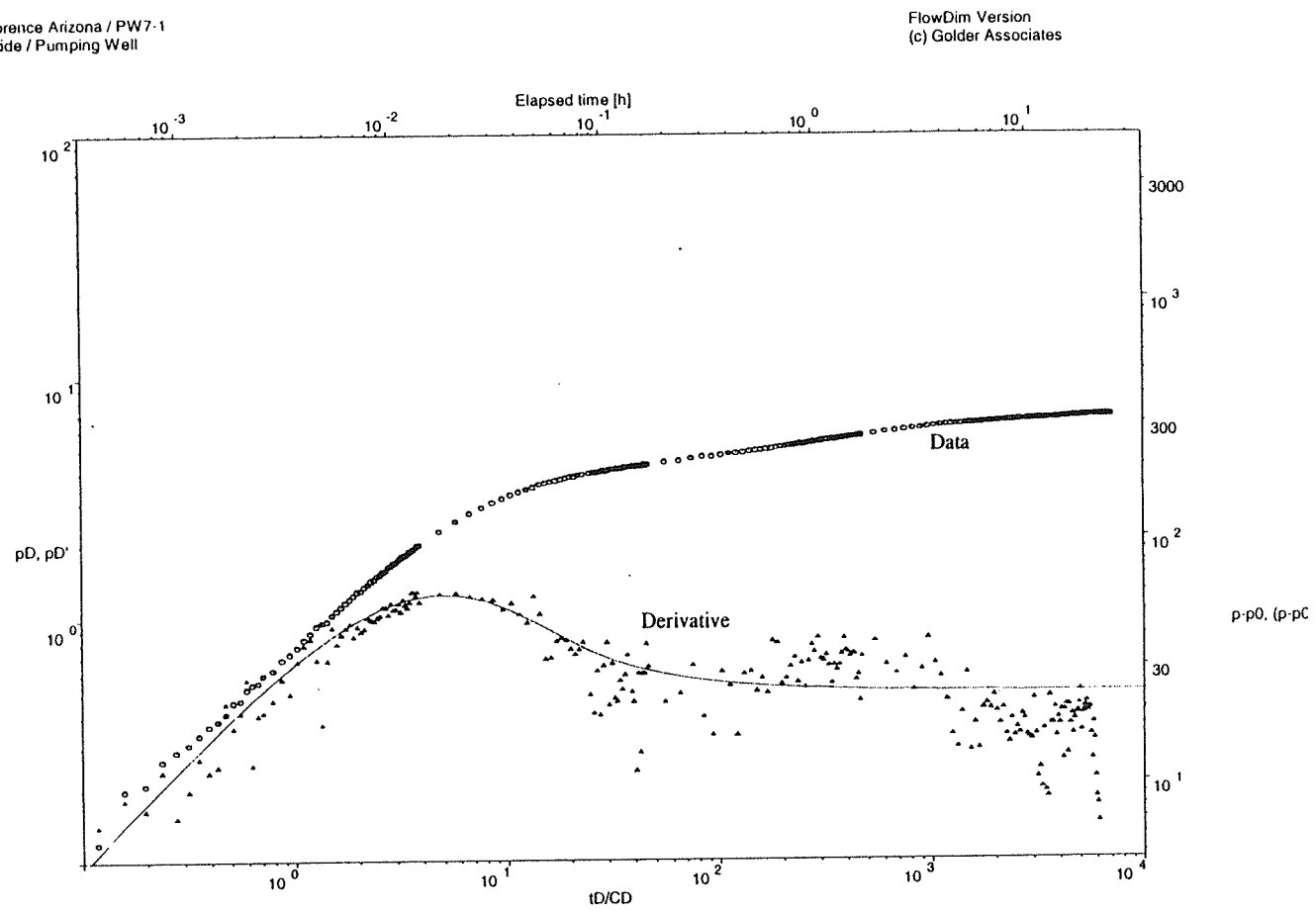

FLOW MODEL :
BOUNDARY CONDITIONS: Constant rate
WELL TYPE :
SUPERPOSITION TYPE : No superposition
PLOT TYPE : Log-

C=	6.87E-07	m3/Pa
T=	8.40E-05	m2/s
S=	1.85E-03	-
s=	0.00E+00	-
n=	2.00E+00	-

Figure 17B

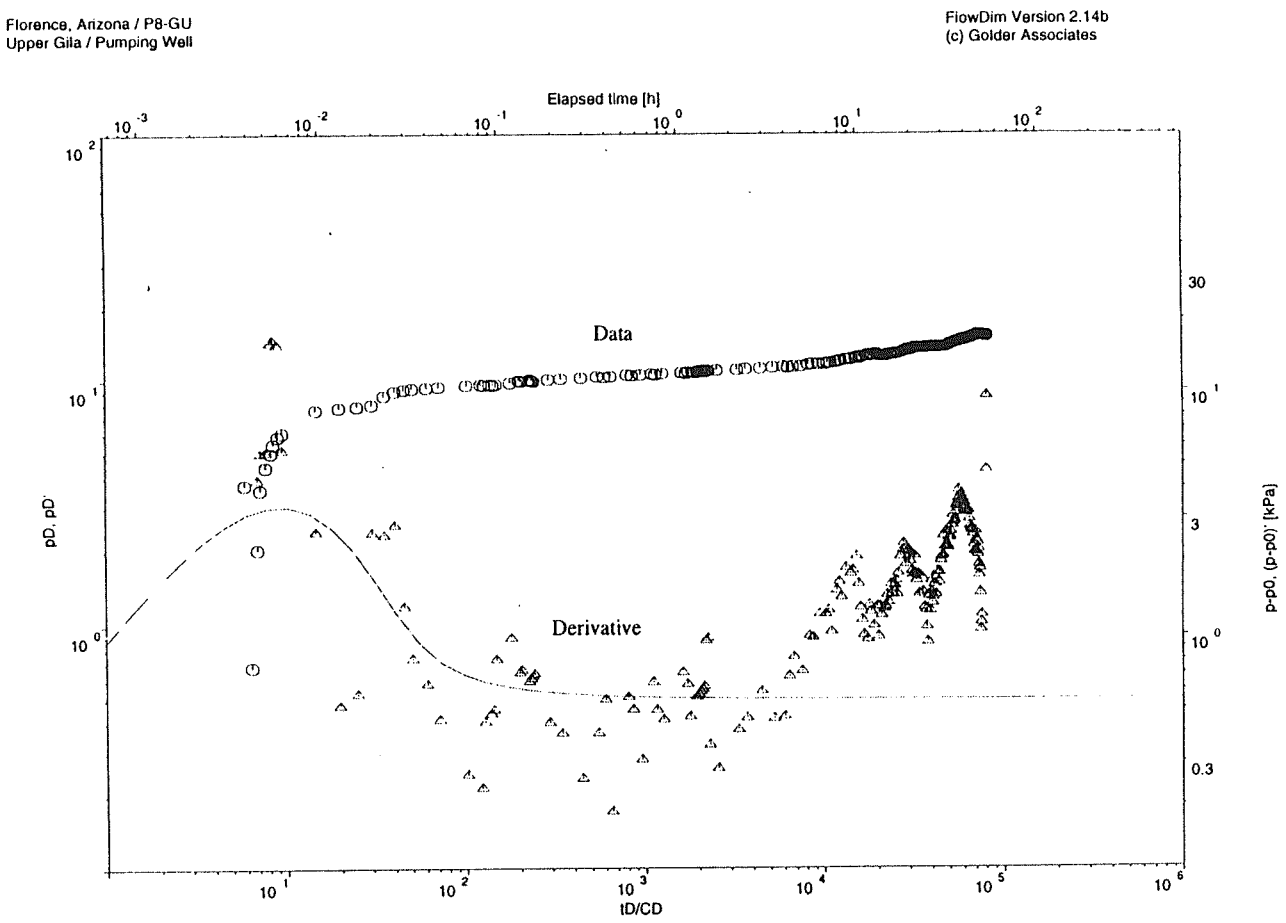

FLOW MODEL : Homogeneous
BOUNDARY CONDITIONS: Constant rate
WELL TYPE : Source
SUPERPOSITION TYPE : No superposition
PLOT TYPE : Log-log

C=	1.19E-05	m3/Pa
T=	7.91E-03	m2/s
S=	3.19E-06	-
s=	0.00E+00	-
n=	2.00E+00	-

Figure 18B

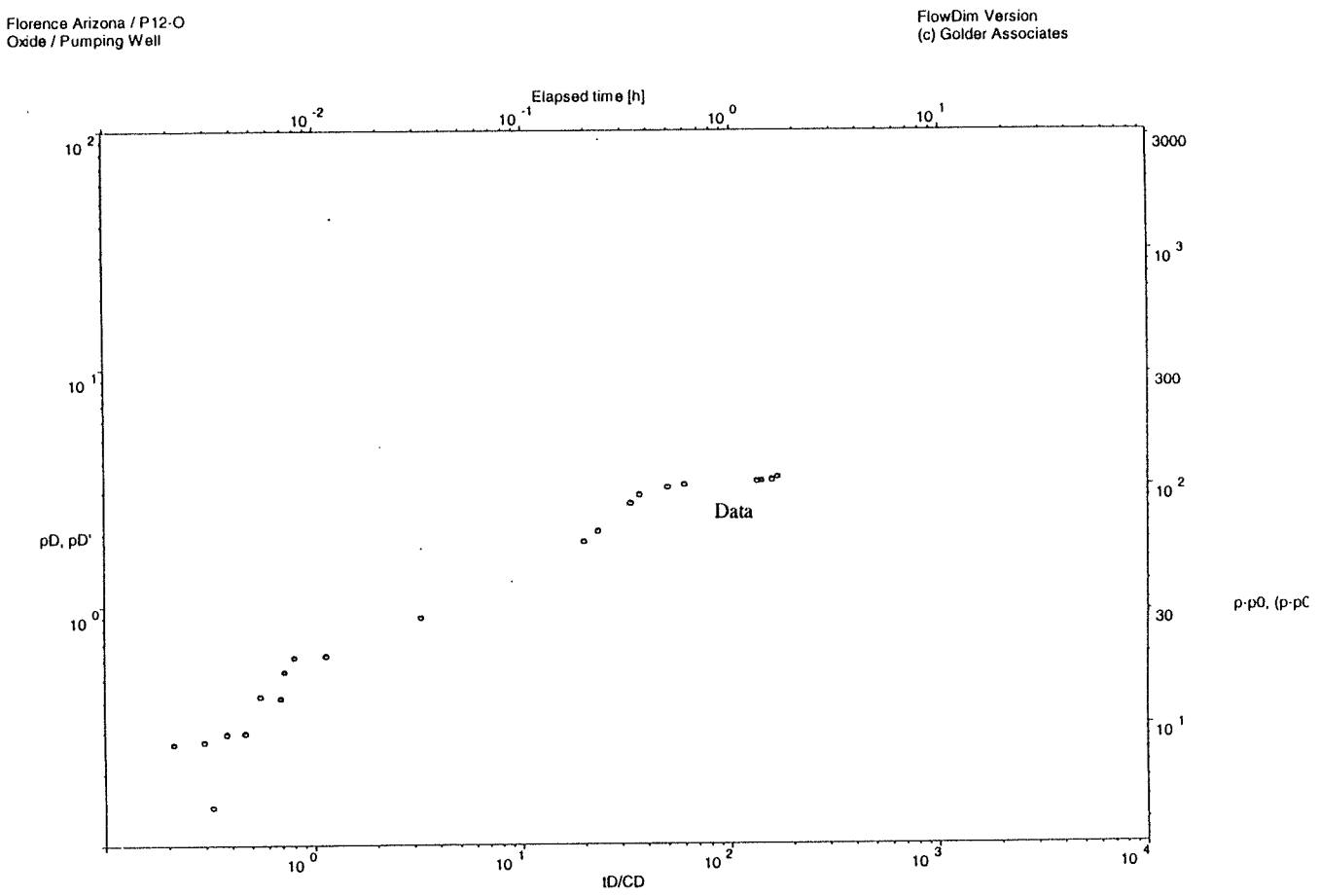

FLOW MODEL :
BOUNDARY CONDITIONS: Constant rate
WELL TYPE :
SUPERPOSITION TYPE : No superposition
PLOT TYPE : Log-

C=	4.64E-06	m3/Pa
T=	2.04E-04	m2/s
S=	4.16E-01	-
s=	0.00E+00	-
n=	2.00E+00	-

Figure 19B

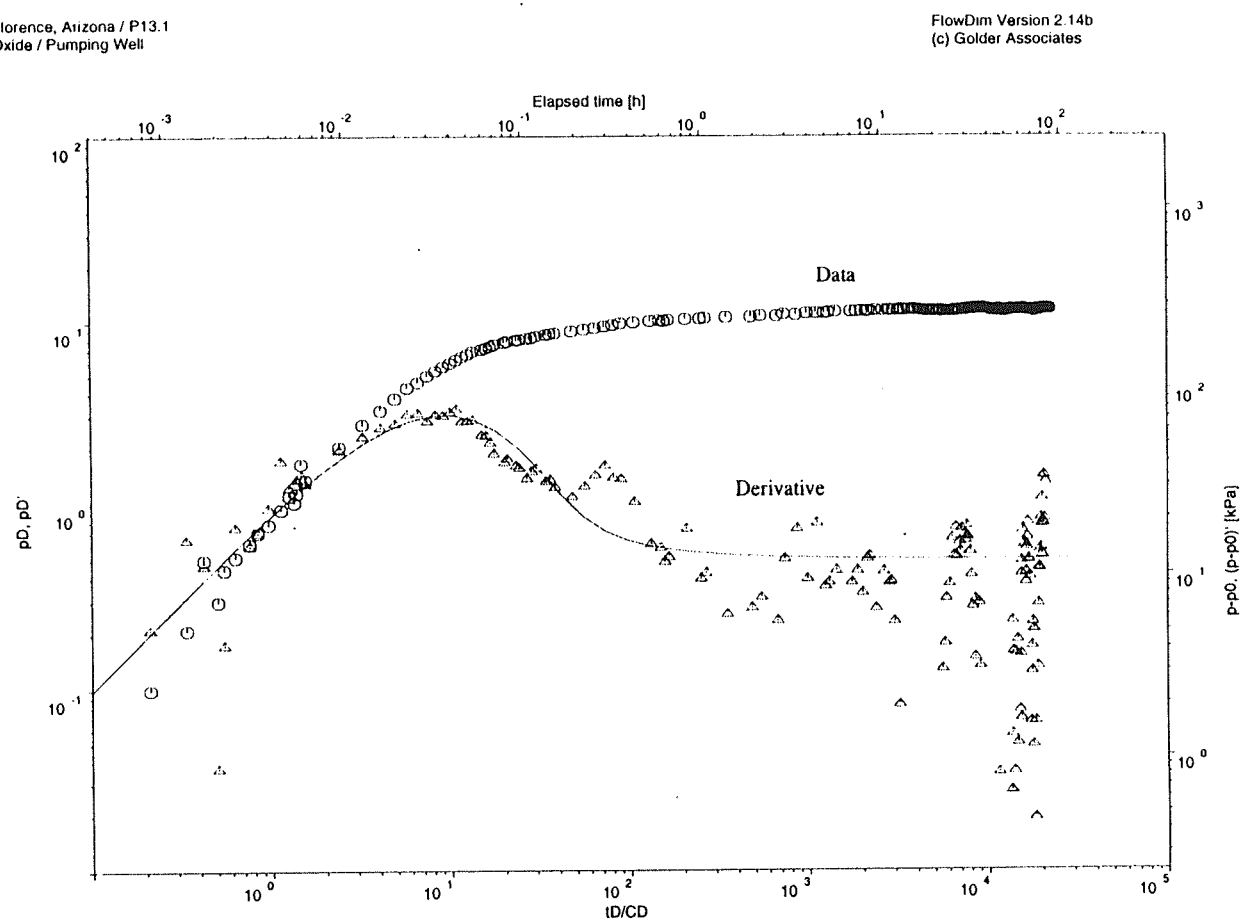

FLOW MODEL : Homogeneous
BOUNDARY CONDITIONS: Constant rate
WELL TYPE : Source
SUPERPOSITION TYPE : No superposition
PLOT TYPE : Log-log

C=	1.75E-06	m3/Pa
T=	1.91E-04	m2/s
S=	4.72E-07	-
s=	0.00E+00	-
n=	2.00E+00	-

Figure 20B

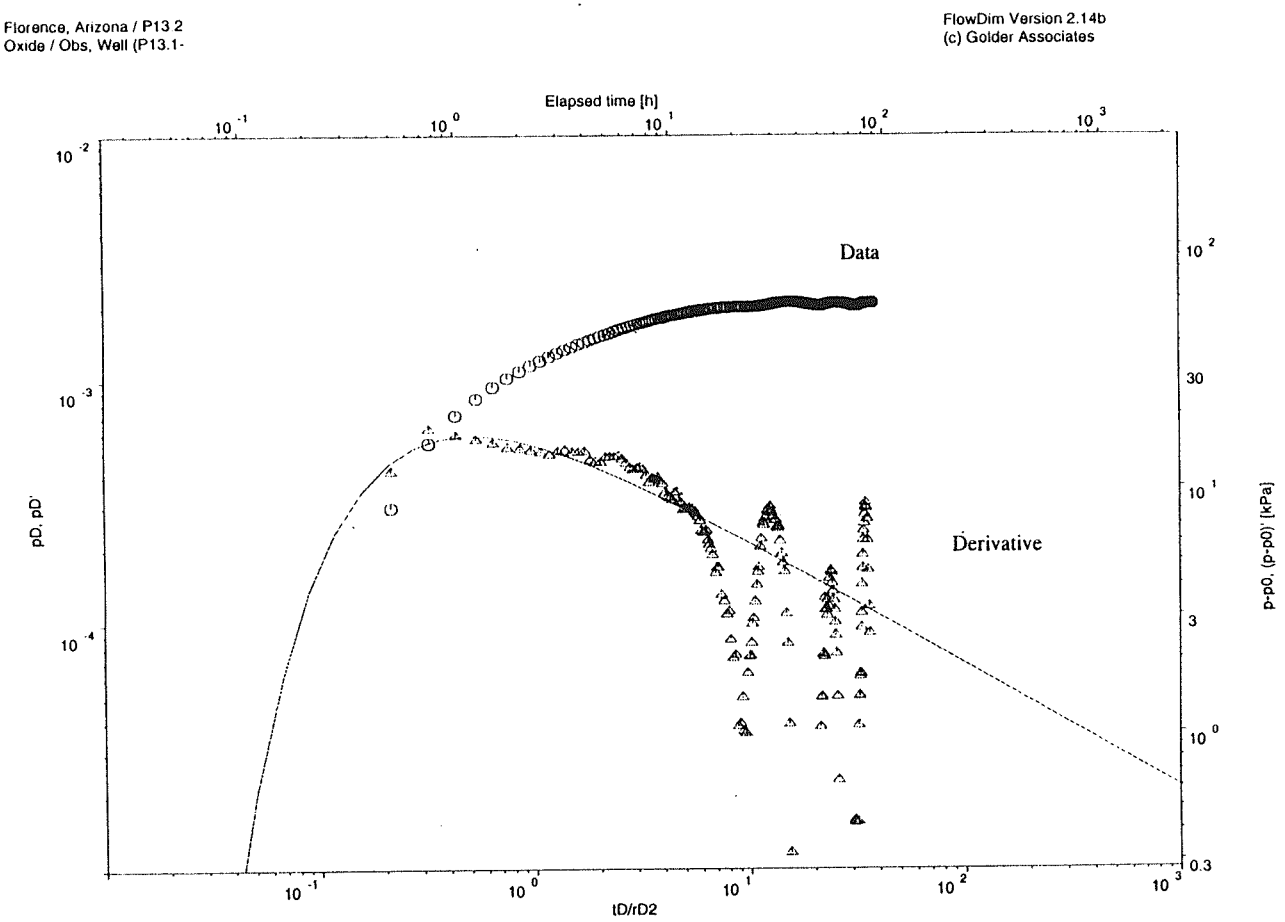

FLOW MODEL : Homogeneous
BOUNDARY CONDITIONS: Constant rate
WELL TYPE : Observation
SUPERPOSITION TYPE : No superposition
PLOT TYPE : Log-log

T=	8.18E-08	m2/s
S=	7.04E-07	-
rD=	4.12E+02	-
n=	3.00E+00	-

Figure 21B

Golder Associates

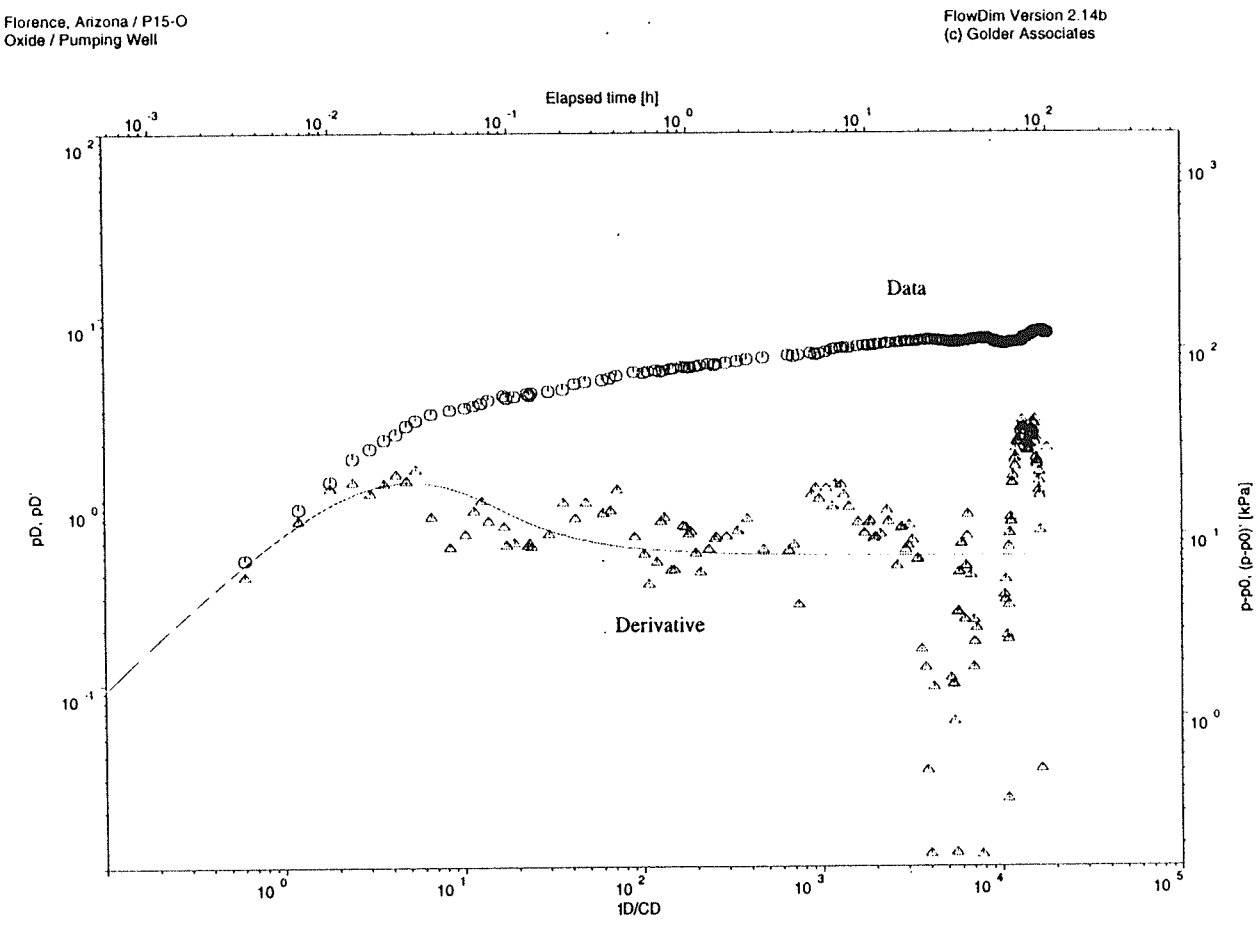

FLOW MODEL : Homogeneous
BOUNDARY CONDITIONS: Constant rate
WELL TYPE : Source
SUPERPOSITION TYPE : No superposition
PLOT TYPE : Log-log

C=	4.94E-06	m3/Pa
T=	3.84E-04	m2/s
S=	1.33E-02	-
s=	0.00E+00	-
n=	2.00E+00	-

Figure 22B

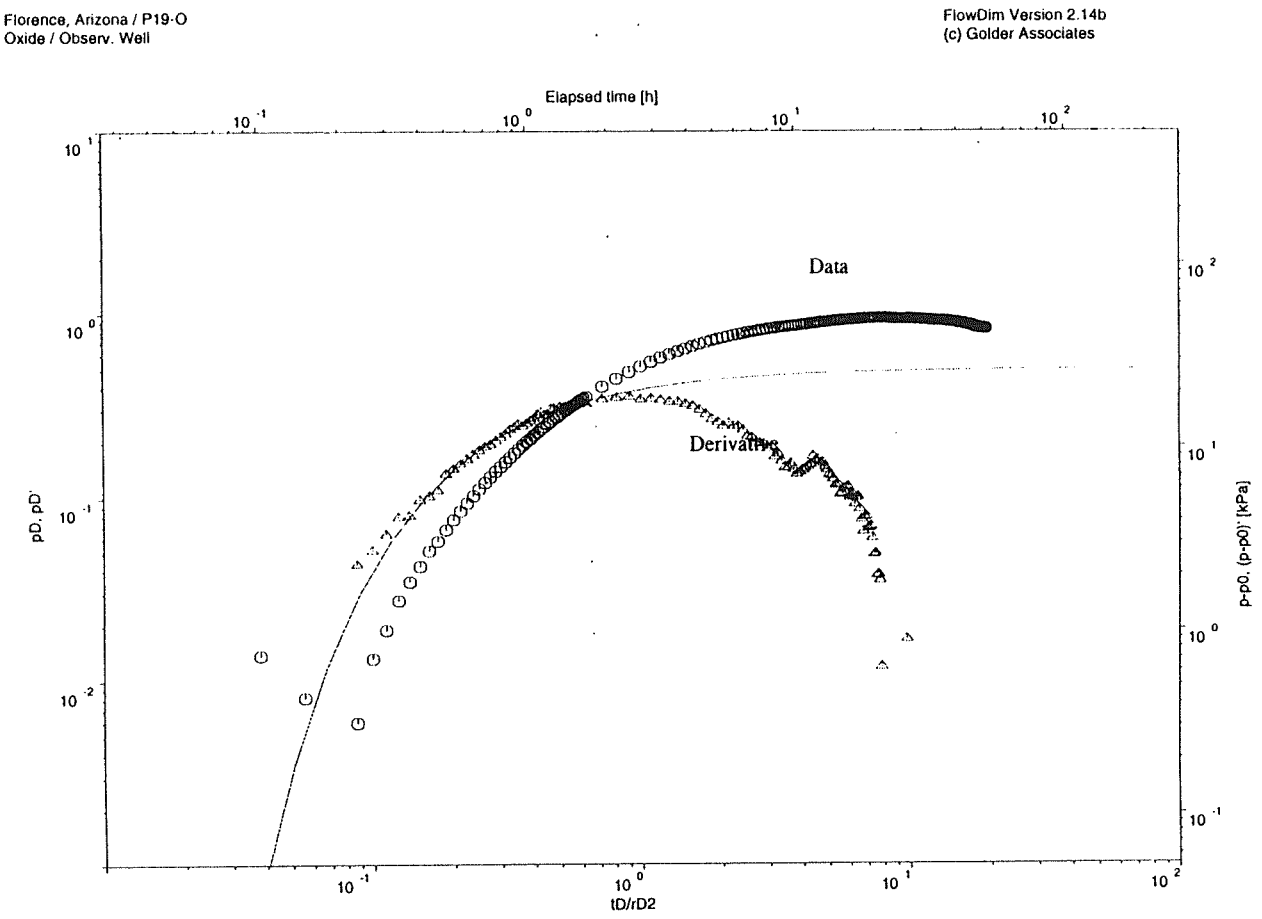
Florence, Arizona / P19-O
Oxide / Observ. Well
FlowDim Version 2.14b
(c) Golder Associates
Elapsed time [h]
Data
Derivative
pD, pD'
p-p0, (p-p0)' [kPa]
tD/rD2
FLOW MODEL : Homogeneous
BOUNDARY CONDITIONS: Constant rate
WELL TYPE : Observation
SUPERPOSITION TYPE : No superposition
PLOT TYPE : Log-log
T= 4.10E-05 m2/s
S= 7.66E-04 -
rD= 2.98E+02 -
n= 2.00E+00 -

Figure 23B

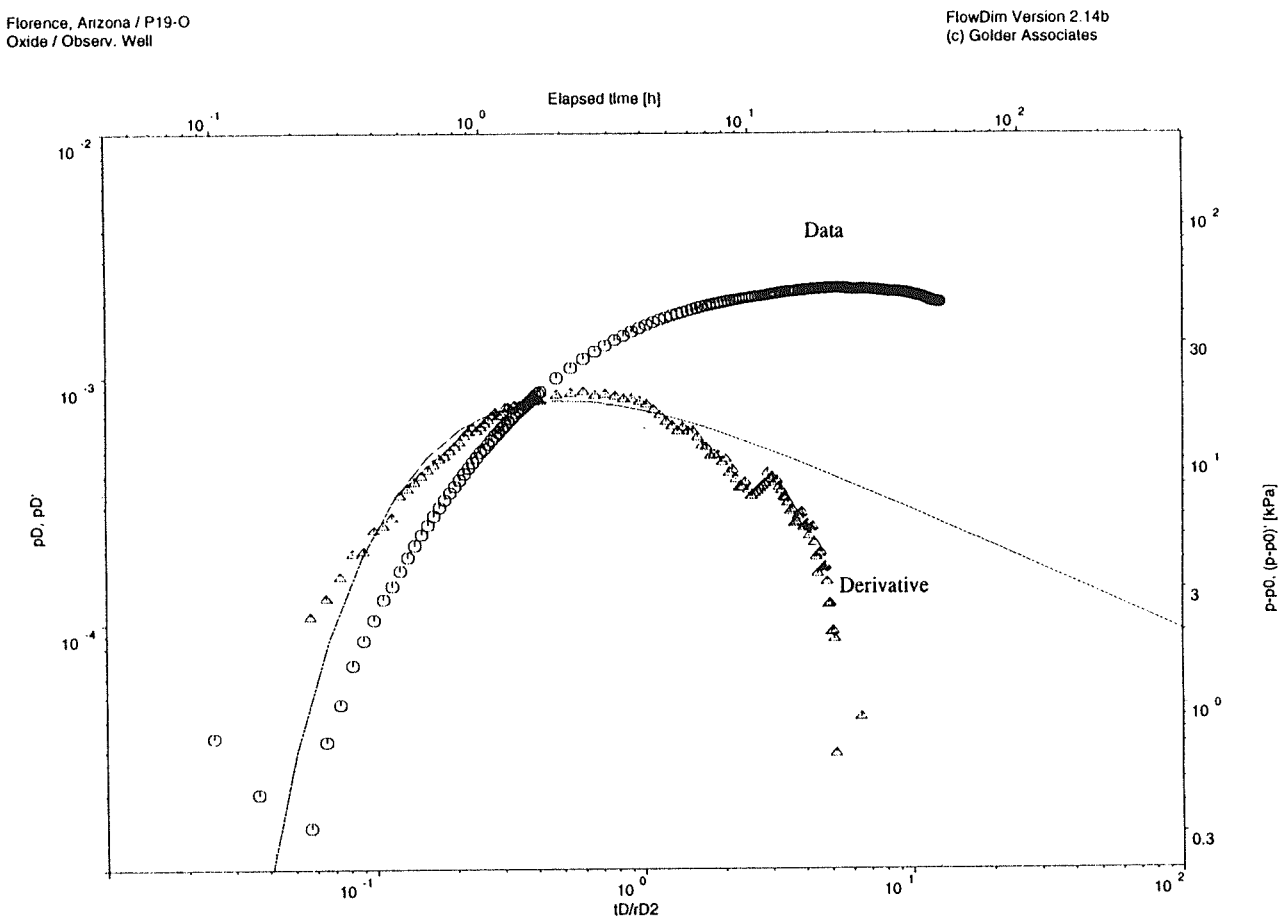
Florence, Arizona / P19-O
Oxide / Observ. Well
FlowDim Version 2.14b
(c) Golder Associates
Elapsed time [h]
Data
Derivative
pD, pD'
p-p0, (p-p0)' [kPa]
tD/rD2
FLOW MODEL : Homogeneous
BOUNDARY CONDITIONS: Constant rate
WELL TYPE : Observation
SUPERPOSITION TYPE : No superposition
PLOT TYPE : Log-log
T= 5.08E-08 m2/s
S= 1.44E-06 -
rD= 2.98E+02 -
n= 3.00E+00 -

Figure 24B

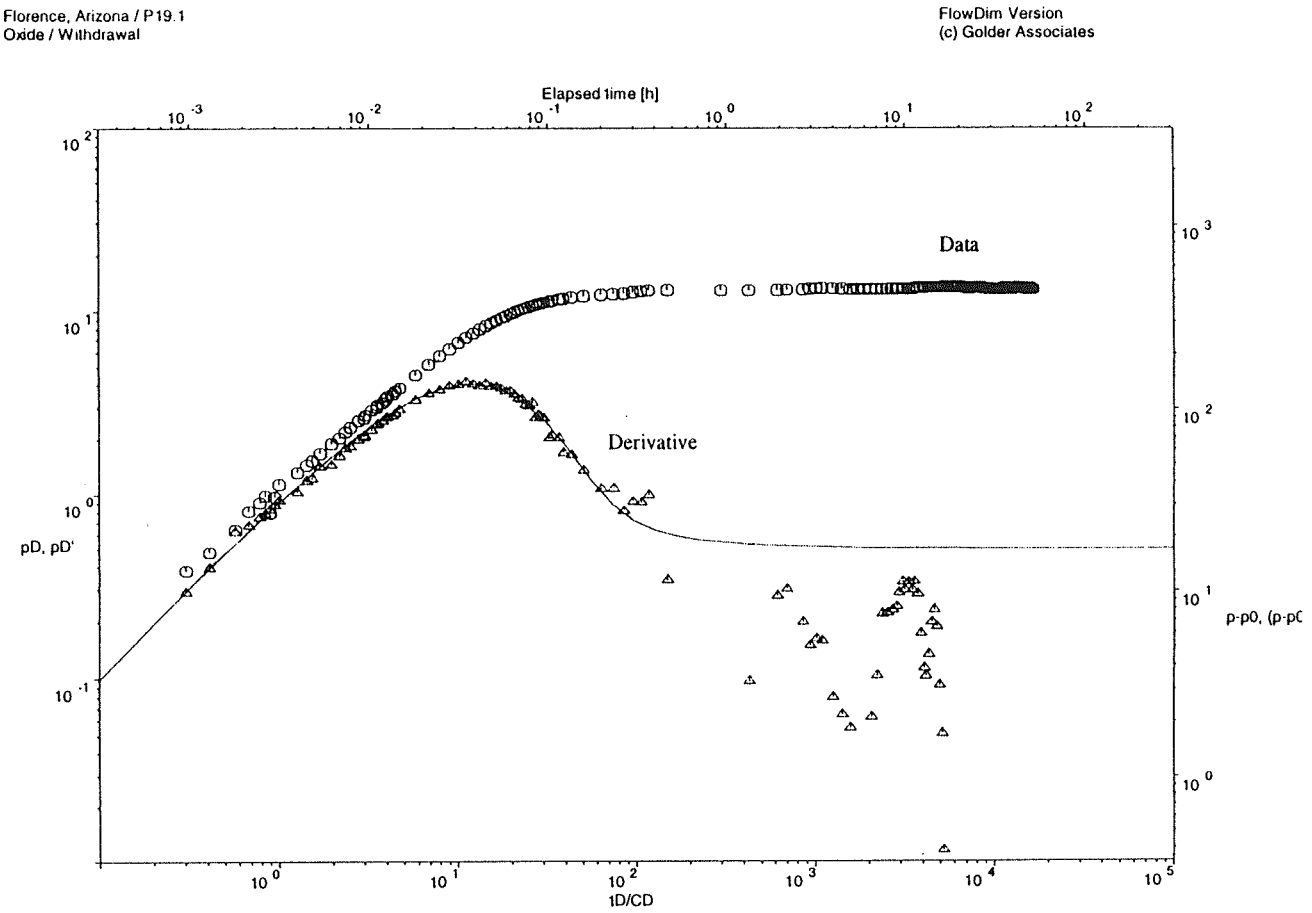

FLOW MODEL :
BOUNDARY CONDITIONS: Constant rate
WELL TYPE :
SUPERPOSITION TYPE : No superposition
PLOT TYPE : Log-

C=	4.58E-07	m3/Pa
T=	6.39E-05	m2/s
S=	6.16E-10	-
s=	0.00E+00	-
n=	2.00E+00	-

Figure 25B

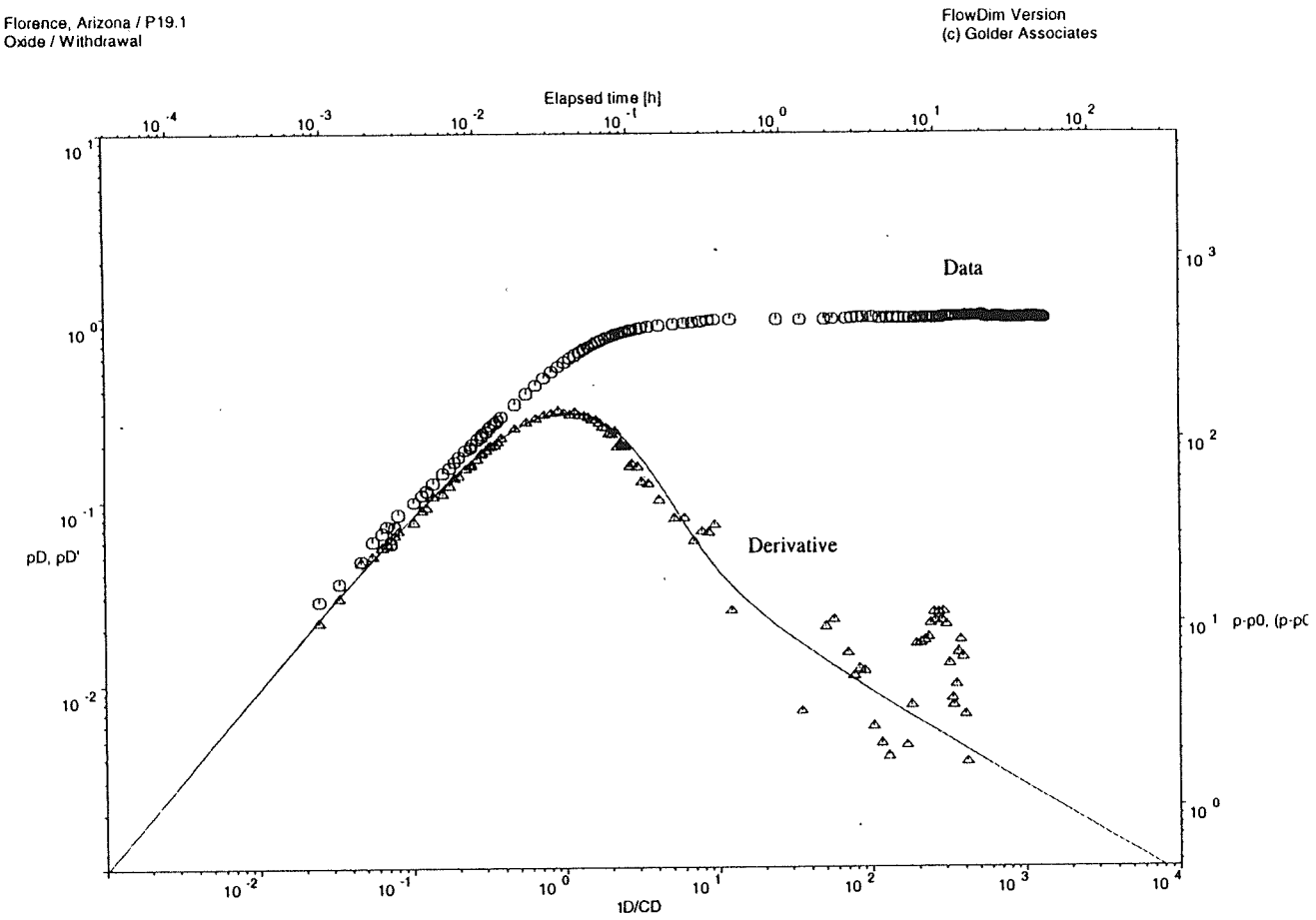

FLOW MODEL :
BOUNDARY CONDITIONS: Constant rate
WELL TYPE :
SUPERPOSITION TYPE : No superposition
PLOT TYPE : Log-

C=	4.19E-07	m3/Pa
T=	2.36E-06	m2/s
S=	5.64E-03	-
s=	0.00E+00	-
n=	3.00E+00	-

Figure 26B

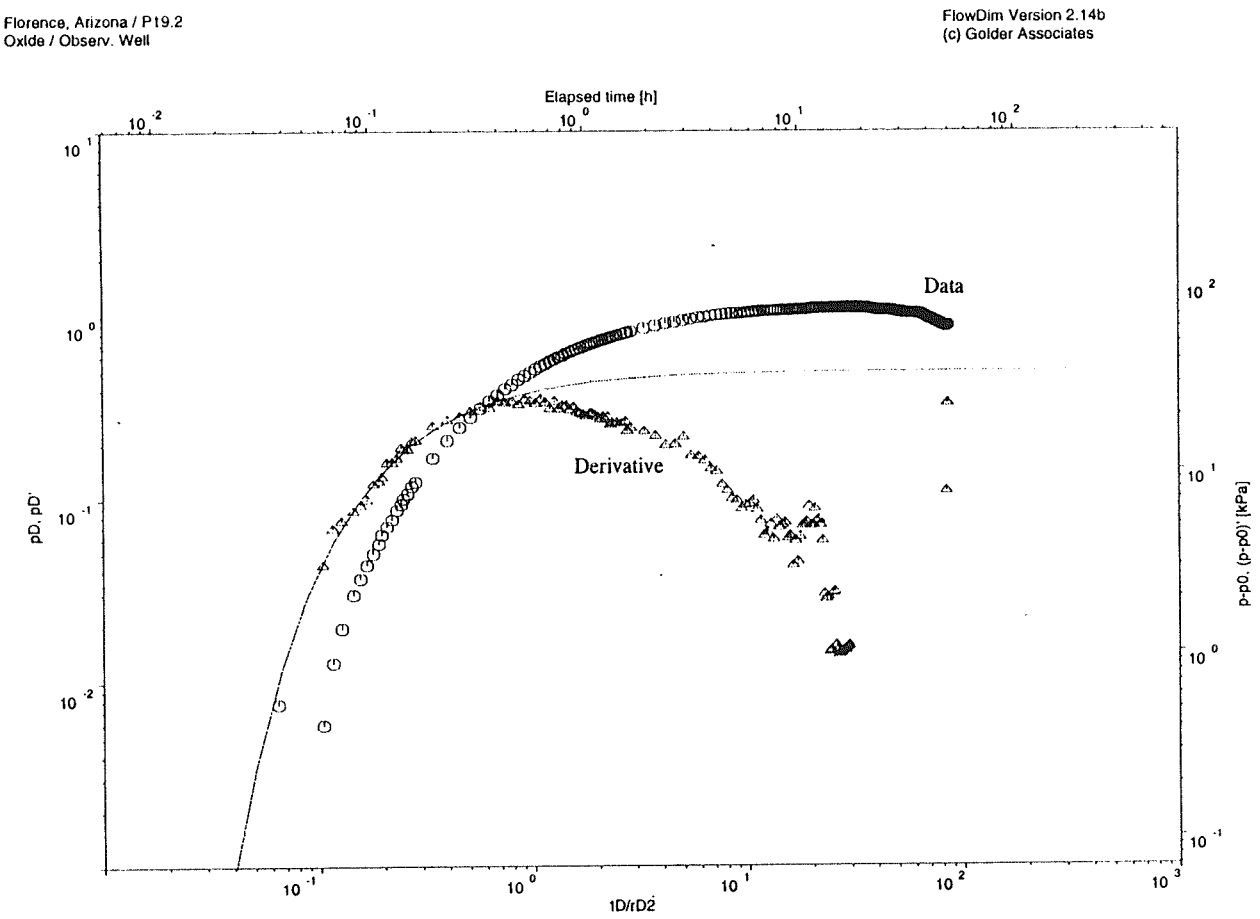

FLOW MODEL : Homogeneous
BOUNDARY CONDITIONS: Constant rate
WELL TYPE : Observation
SUPERPOSITION TYPE : No superposition
PLOT TYPE : Log-log

T=	3.14E-05	m2/s
S=	1.47E-04	-
rD=	2.68E+02	-
n=	2.00E+00	-

Figure 27B

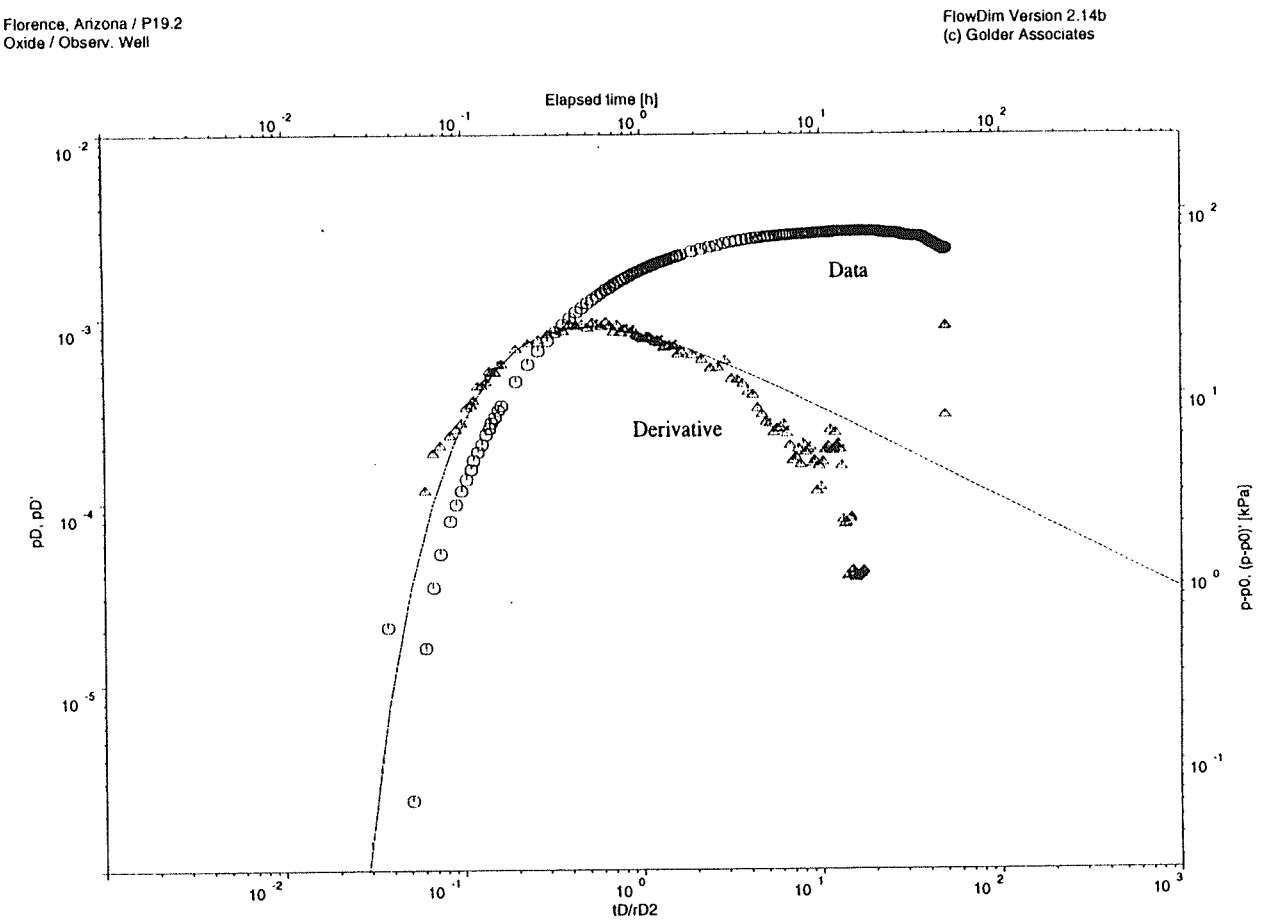

FLOW MODEL : Homogeneous
BOUNDARY CONDITIONS: Constant rate
WELL TYPE : Observation
SUPERPOSITION TYPE : No superposition
PLOT TYPE : Log-log

T=	4.22E-08	m2/s
S=	3.38E-07	-
rD=	2.68E+02	-
n=	3.00E+00	-

Figure 28B

Florence, Arizona / P28-G
Lower Gila / Pumping Well

FlowDim Version 2.14b
(c) Golder Associates

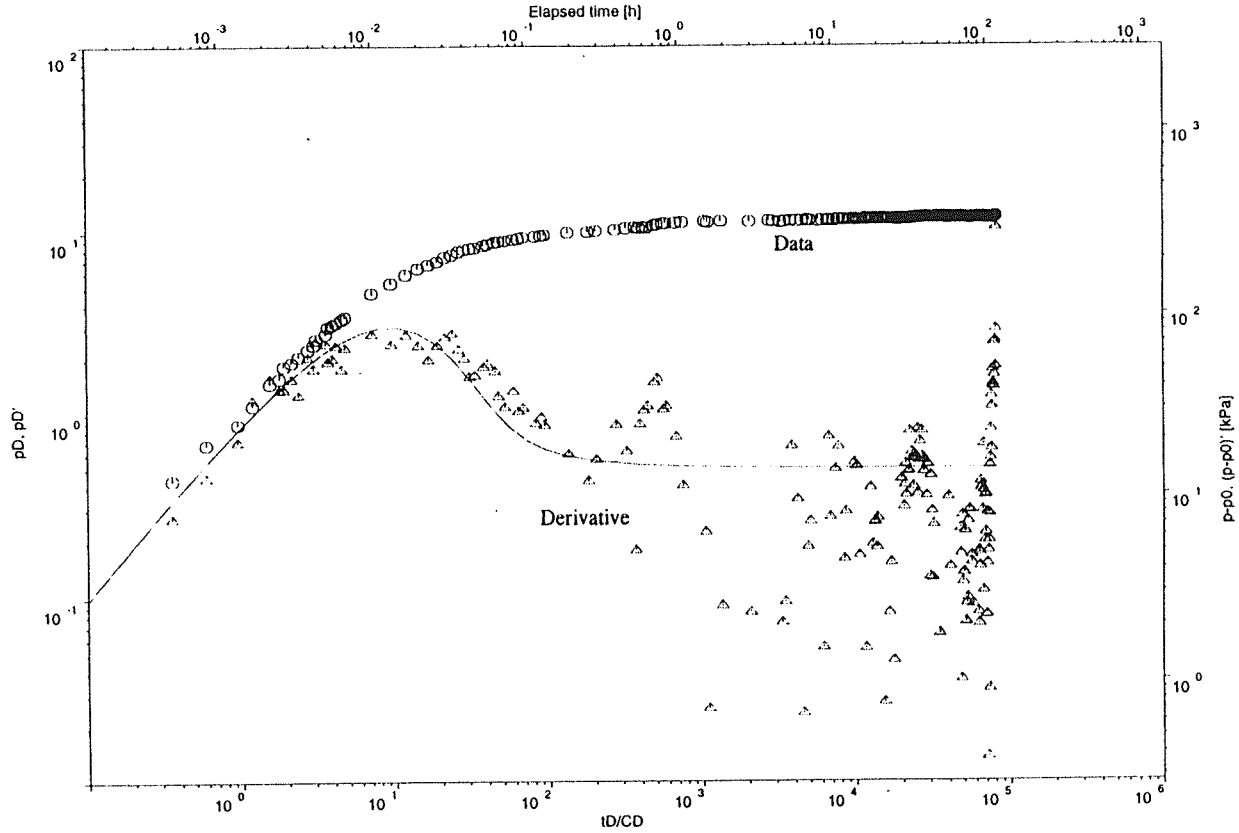

FLOW MODEL : Homogeneous
BOUNDARY CONDITIONS: Constant rate
WELL TYPE : Source
SUPERPOSITION TYPE : No superposition
PLOT TYPE : Log-log

C=	8.71E-07	m3/Pa
T=	2.66E-04	m2/s
S=	3.37E-07	-
s=	0.00E+00	-
n=	2.00E+00	-

Figure 29B

Golder Associates

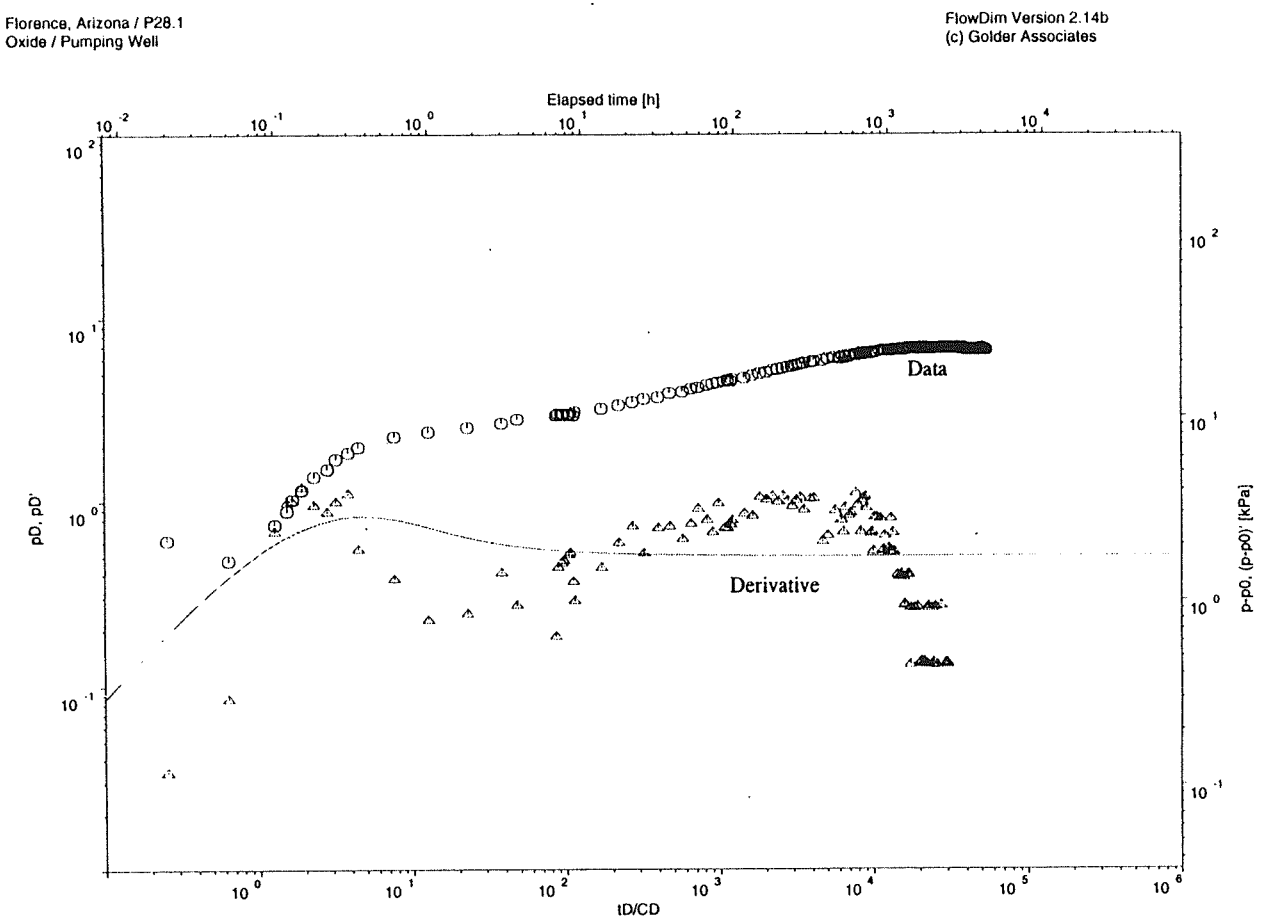

FLOW MODEL : Homogeneous
BOUNDARY CONDITIONS: Constant rate
WELL TYPE : Source
SUPERPOSITION TYPE : No superposition
PLOT TYPE : Log-log

C=	1.50E-04	m3/Pa
T=	8.25E-04	m2/s
S=	5.20E+00	-
s=	0.00E+00	-
n=	2.00E+00	-

Figure 30B

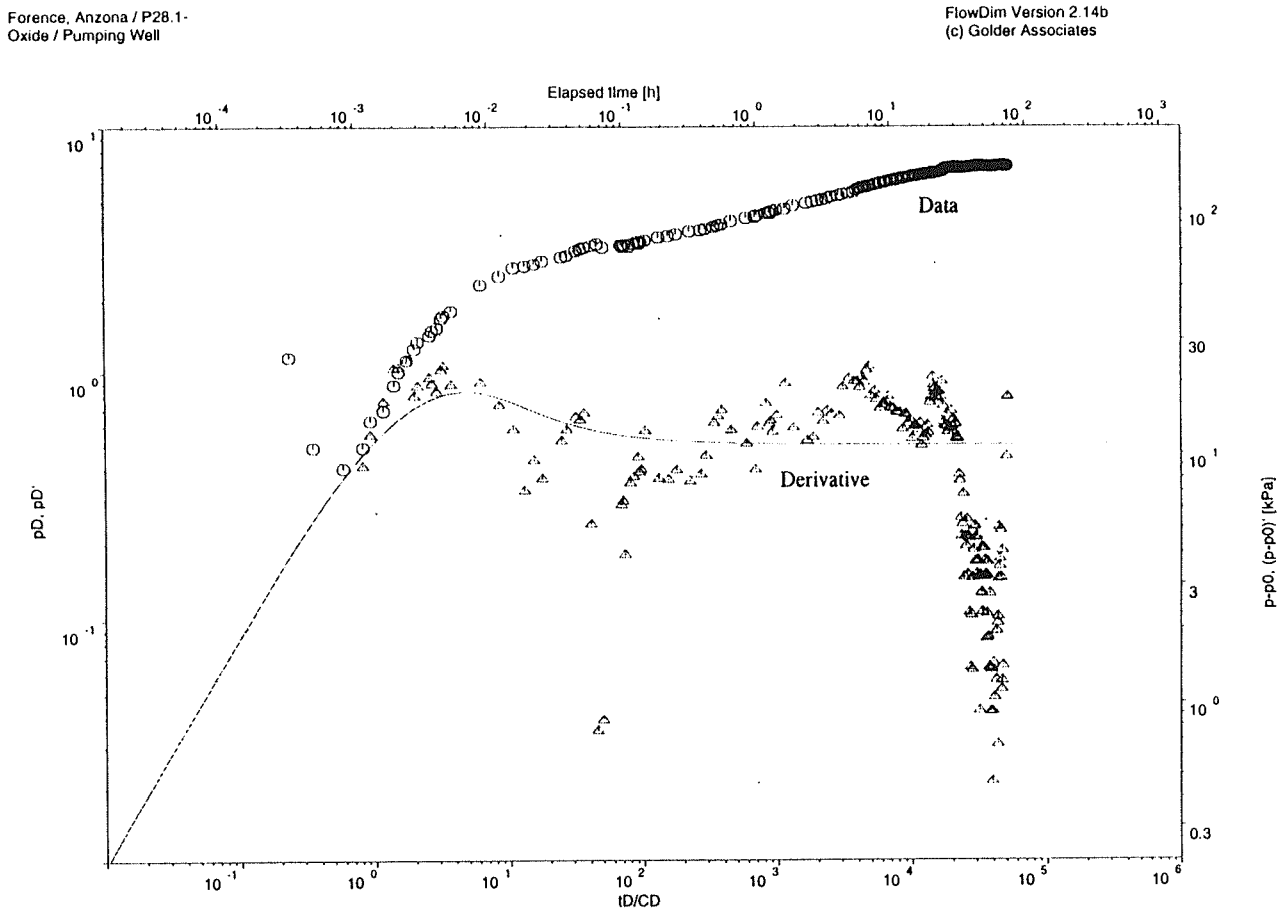

FLOW MODEL : Homogeneous
BOUNDARY CONDITIONS: Constant rate
WELL TYPE : Source
SUPERPOSITION TYPE : No superposition
PLOT TYPE : Log-log

C=	1.28E-06	m3/Pa
T=	3.86E-04	m2/s
S=	3.45E-02	-
s=	0.00E+00	-
n=	2.00E+00	-

Figure 31B

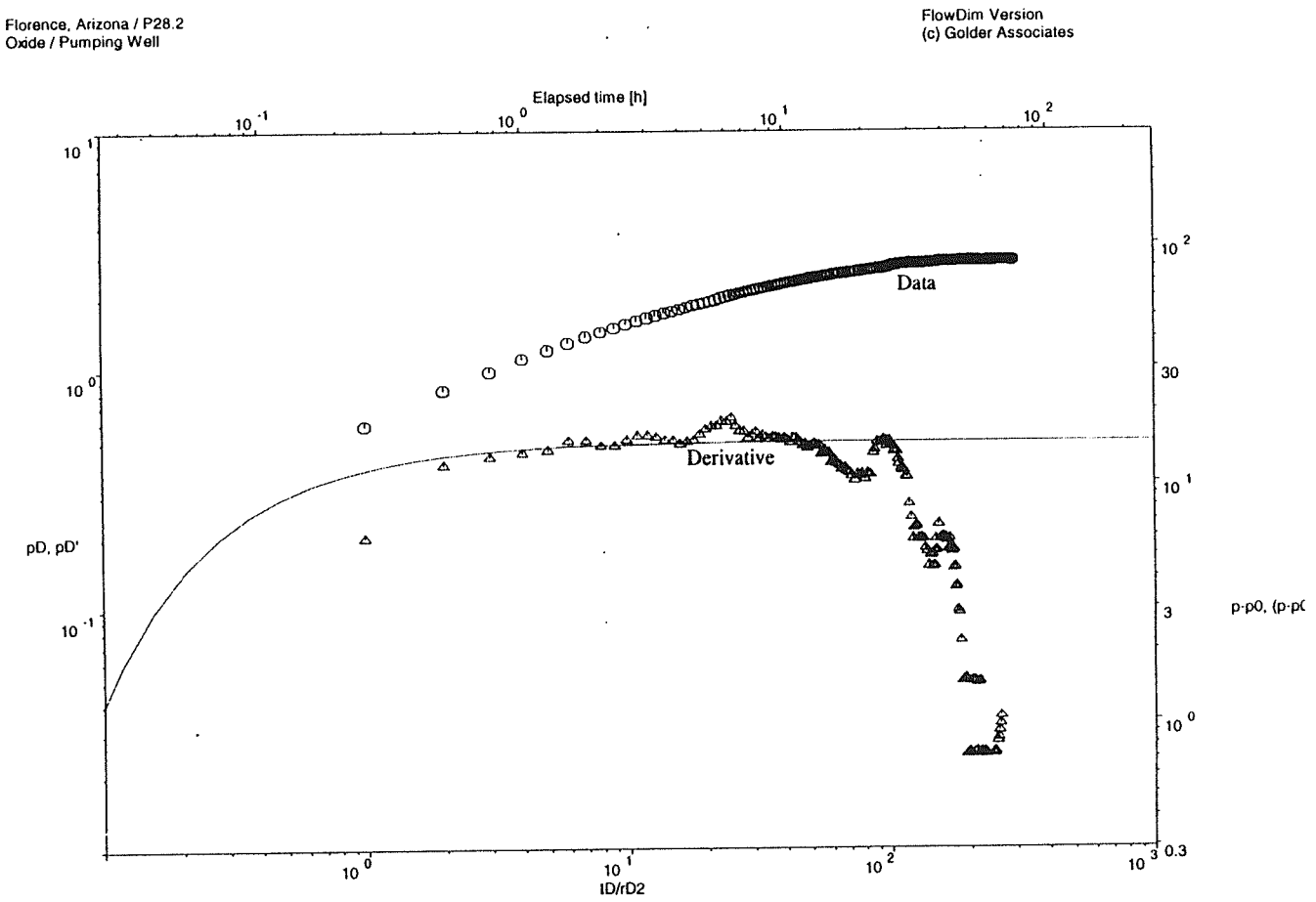

FLOW MODEL :
BOUNDARY CONDITIONS: Constant rate
WELL TYPE :
SUPERPOSITION TYPE : No superposition
PLOT TYPE : Log-

T=	2.84E-04	m2/s
S=	2.91E-04	-
rD=	5.89E+02	-
n=	2.00E+00	-

Figure 32B

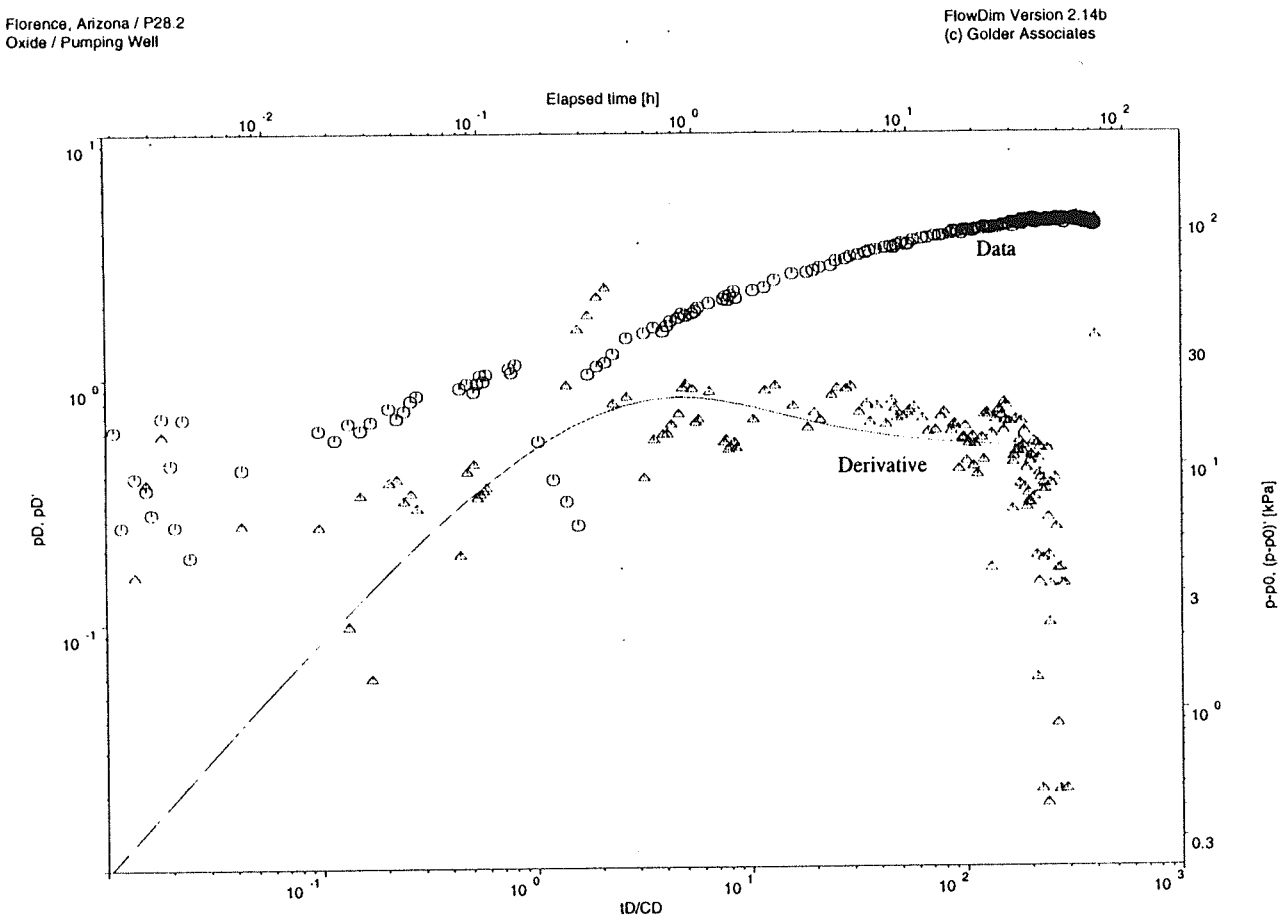

FLOW MODEL : Homogeneous
BOUNDARY CONDITIONS: Constant rate
WELL TYPE : Source
SUPERPOSITION TYPE : No superposition
PLOT TYPE : Log-log

C=	1.41E-04	m3/Pa
T=	3.30E-04	m2/s
S=	3.78E+00	-
s=	0.00E+00	-
n=	2.00E+00	-

Figure 33B

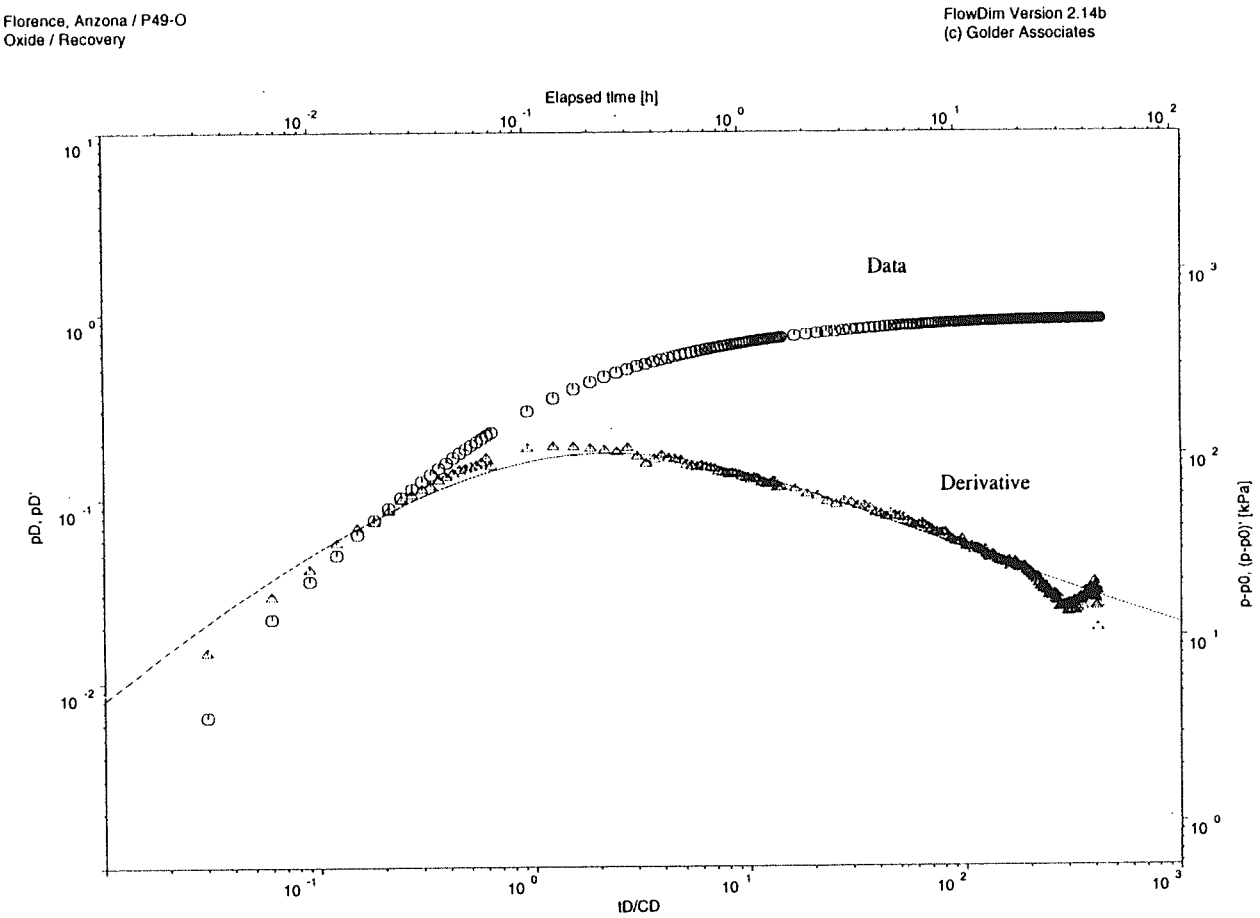

FLOW MODEL : Homogeneous
BOUNDARY CONDITIONS: Constant rate
WELL TYPE : Source
SUPERPOSITION TYPE : Build-up TC
PLOT TYPE : Log-log

C=	1.78E-06	m3/Pa
T=	3.45E-06	m2/s
S=	7.99E-01	-
s=	0.00E+00	-
n=	3.00E+00	-

Figure 34B

APPENDIX C

TEST ANALYSIS REPORT 16.11.1995

Identification

Site name	Florence, Arizona
Well name	M1-GL
Interval name	Lower Gila
Event name	Pumping Well
Test date	11 - 13 Aug. 1995
Input file name	m1-gld.rec

Well parameters

Well depth	[m brp]	1.2802E+02
Reference point elevation	[m asl]	0.0000E+00
Wellbore radius	[m]	6.3500E-02
Interval length	[m]	1.2190E+01

Testparameter

Flow rate	[l/min]	3.7900E+01
Test duration	[h]	2.4458E+01

Fluid and formation parameters

Viscosity	[Pa s]	1.0000E-03
Total compressibility	[1/Pa]	5.4000E-10
Porosity	[-]	1.0000E-01

Model assumptions

Flow model	Homogeneous
Boundary conditions	Constant rate
Well type	Source
Superposition type	Drawdown

Results of analysis

Transmissibility	[m3]	7.5775E-11
Transmissivity	[m2/s]	7.4335E-04
Storage	[m/Pa]	8.5961E-13
Storativity	[-]	8.4327E-09
Wellbore storage	[m3/Pa]	4.3535E-06
Skin (assumed)	[-]	0.0000E+00
Inner shell flow dimension	[-]	2.0000E+00
Time match	[1/h]	3.9350E+02
Pressure match	[1/kPa]	7.5335E-01

Comments

FlowDim V2.14b Copyright (c) Golder Associates 1994

TEST ANALYSIS REPORT 29.10.1995

Identification		
Site name		Florence, Arizona
Well name		M3-GL
Interval name		Lower Gila
Event name		Observation Well (M4-O)
Test date		28 - 29 July, 1995
Input file name		m3gloddb.fdl

Well parameters		
Well depth	[m bgl]	1.5545E+02
Wellbore radius	[m]	6.3500E-02
Interval length	[m]	1.8290E+01
Distance to active well	[m]	9.7100E+00
Active wellbore radius	[m]	6.3500E+02

Testparameter		
Flow rate	[l/min]	5.6780E+01
Test duration	[h]	2.2171E+01

Fluid and formation parameters		
Viscosity	[Pa s]	1.0000E-03
Total compressibility	[1/Pa]	5.4000E-10
Porosity	[-]	5.0000E-02

Model assumptions	
Flow model	Homogeneous
Boundary conditions	Constant rate
Well type	Observation
Superposition type	Drawdown

Results of analysis		
Transmissibility	[m3]	9.7150E-11
Transmissivity	[m2/s]	9.5304E-04
Storage	[m/Pa]	8.9465E-06
Storativity	[-]	8.7765E-02
Inner shell flow dimension	[-]	2.0000E+00
Dimensionles obs. point distance	[-]	1.5291E+02
Time match	[1/h]	4.1462E-01
Pressure match	[1/kPa]	6.4470E-01

Comments

FlowDim V2.14b Copyright (c) Golder Associates 1994

TEST ANALYSIS REPORT 16.11.1995

Identification

Site name	Florence Site
Well name	M14-GL
Interval name	Lower Gila
Event name	Pumping Well
Test date	11 - 12 Aug. 1995
Input file name	m14-gld.rec

Well parameters

Well depth	[m brp]	2.8956E+02
Reference point elevation	[m asl]	0.0000E+00
Wellbore radius	[m]	6.3500E-02
Interval length	[m]	1.8290E+01

Testparameter

Flow rate	[l/min]	3.7850E+01
Test duration	[h]	1.8180E+01

Fluid and formation parameters

Viscosity	[Pa s]	1.0000E-03
Total compressibility	[1/Pa]	5.4000E-10
Porosity	[-]	1.0000E-01

Model assumptions

Flow model	Homogeneous
Boundary conditions	Constant rate
Well type	Source
Superposition type	Drawdown

Results of analysis

Transmissibility	[m3]	1.1462E-11
Transmissivity	[m2/s]	1.1244E-04
Storage	[m/Pa]	9.2897E-11
Storativity	[-]	9.1132E-07
Wellbore storage	[m3/Pa]	2.3524E-06
Skin (assumed)	[-]	0.0000E+00
Inner shell flow dimension	[-]	2.0000E+00
Time match	[1/h]	1.1015E+02
Pressure match	[1/kPa]	1.1410E-01

Comments

FlowDim V2.14b Copyright (c) Golder Associates 1994

TEST ANALYSIS REPORT 16.11.1995

Identification

Site name	Florence Site
Well name	M14-GL
Interval name	Lower Gila
Event name	Pumping Well
Test date	11 - 12 Aug. 1995
Input file name	m14gld3d.rec

Well parameters

Well depth	[m brp]	2.8956E+02
Reference point elevation	[m asl]	0.0000E+00
Wellbore radius	[m]	6.3500E-02
Interval length	[m]	1.8290E+01

Testparameter

Flow rate	[l/min]	3.7850E+01
Test duration	[h]	1.8180E+01

Fluid and formation parameters

Viscosity	[Pa s]	1.0000E-03
Total compressibility	[1/Pa]	5.4000E-10
Porosity	[-]	1.0000E-01

Model assumptions

Flow model	Homogeneous
Boundary conditions	Constant rate
Well type	Source
Superposition type	Drawdown

Results of analysis

Transmissibility	[m3]	5.4085E-13
Transmissivity	[m2/s]	5.3057E-06
Storage	[m/Pa]	4.3810E-06
Storativity	[-]	4.2977E-02
Wellbore storage	[m3/Pa]	2.2182E-06
Skin (assumed)	[-]	0.0000E+00
Inner shell flow dimension	[-]	3.0000E+00
Time match	[1/h]	1.1022E+01
Pressure match	[1/kPa]	1.0766E-02

Comments

FlowDim V2.14b Copyright (c) Golder Associates 1994

TEST ANALYSIS REPORT 16.11.1995

Identification	
Site name	Florence, Arizona
Well name	M15-GU
Interval name	Upper Gila
Event name	Pumping Well
Test date	8 - 9 Aug. 1995
Input file name	m15-gud.rec

Well parameters		
Well depth	[m brp]	1.9202E+02
Reference point elevation	[m asl]	0.0000E+00
Wellbore radius	[m]	6.3500E-02
Interval length	[m]	1.2190E+01

Testparameter		
Flow rate	[l/min]	3.7900E+01
Test duration	[h]	1.6695E+01

Fluid and formation parameters		
Viscosity	[Pa s]	1.0000E-03
Total compressibility	[1/Pa]	5.4000E-10
Porosity	[-]	1.0000E-01

Model assumptions	
Flow model	Homogeneous
Boundary conditions	Constant rate
Well type	Source
Superposition type	Drawdown

Results of analysis		
Transmissibility	[m3]	1.1353E-11
Transmissivity	[m2/s]	1.1137E-04
Storage	[m/Pa]	1.0991E-15
Storativity	[-]	1.0782E-11
Wellbore storage	[m3/Pa]	2.7832E-07
Skin (assumed)	[-]	0.0000E+00
Inner shell flow dimension	[-]	2.0000E+00
Time match	[1/h]	9.2222E+02
Pressure match	[1/kPa]	1.1287E-01

Comments

FlowDim V2.14b Copyright (c) Golder Associates 1994

TEST ANALYSIS REPORT 16.11.1995

Identification

Site name	Florence, Arizona
Well name	M18-GU
Interval name	Upper Gila
Event name	Pumping Well
Test date	8 - 11 Aug. 1995
Input file name	m18-gud.rec

Well parameters

Well depth	[m brp]	7.3150E+01
Reference point elevation	[m asl]	0.0000E+00
Wellbore radius	[m]	6.3500E-02
Interval length	[m]	1.2190E+01

Testparameter

Flow rate	[l/min]	3.7900E+01
Test duration	[h]	1.9194E+01

Fluid and formation parameters

Viscosity	[Pa s]	1.0000E-03
Total compressibility	[1/Pa]	5.4000E-10
Porosity	[-]	1.0000E-01

Model assumptions

Flow model	Homogeneous
Boundary conditions	Constant rate
Well type	Source
Superposition type	Drawdown

Results of analysis

Transmissibility	[m3]	8.6070E-11
Transmissivity	[m2/s]	8.4434E-04
Storage	[m/Pa]	8.8678E-20
Storativity	[-]	8.6993E-16
Wellbore storage	[m3/Pa]	2.2455E-06
Skin (assumed)	[-]	0.0000E+00
Inner shell flow dimension	[-]	2.0000E+00
Time match	[1/h]	8.6654E+02
Pressure match	[1/kPa]	8.5570E-01

Comments

FlowDim V2.14b Copyright (c) Golder Associates 1994

TEST ANALYSIS REPORT 15.11.1995

Identification	
Site name	Florence, Arizona
Well name	P39-O
Interval name	Oxide
Event name	Pumping Well
Test date	19 - 20 May, 1995
Input file name	mf39pwpd.rec

Well parameters		
Well depth	[m brp]	2.7890E+02
Reference point elevation	[m asl]	0.0000E+00
Wellbore radius	[m]	1.3000E-01
Interval length	[m]	1.0820E+02

Testparameter		
Flow rate	[l/min]	2.0800E+02
Test duration	[h]	1.6917E+01

Fluid and formation parameters		
Viscosity	[Pa s]	1.0000E-03
Total compressibility	[1/Pa]	5.4000E-10
Porosity	[-]	5.0000E-02

Model assumptions	
Flow model	Homogeneous
Boundary conditions	Constant rate
Well type	Source
Superposition type	Drawdown

Results of analysis		
Transmissibility	[m3]	1.1442E-11
Transmissivity	[m2/s]	1.1225E-04
Storage	[m/Pa]	9.7900E-08
Storativity	[-]	9.6040E-04
Wellbore storage	[m3/Pa]	1.0390E-06
Skin (assumed)	[-]	0.0000E+00
Inner shell flow dimension	[-]	2.0000E+00
Time match	[1/h]	2.4897E+02
Pressure match	[1/kPa]	2.0728E-02

Comments

FlowDim V2.14b Copyright (c) Golder Associates 1994

TEST ANALYSIS REPORT 15.11.1995

Identification

Site name	Florence, Arizona
Well name	O39-O
Interval name	Oxide
Event name	Observ. Well (P39-O)
Test date	19 - 20 May, 1995
Input file name	mf39owpd.rec

Well parameters

Well depth	[m brp]	2.7920E+02
Reference point elevation	[m asl]	0.0000E+00
Wellbore radius	[m]	1.2700E-01
Interval length	[m]	1.2680E+02
Distance to active well	[m]	3.6000E+01

Testparameter

Flow rate	[l/min]	2.0800E+02
Test duration	[h]	1.6857E+01

Fluid and formation parameters

Viscosity	[Pa s]	1.0000E-03
Total compressibility	[1/Pa]	5.4000E-10
Porosity	[-]	5.0000E-01

Model assumptions

Flow model	Homogeneous
Boundary conditions	Constant rate
Well type	Observation
Superposition type	Drawdown

Results of analysis

Transmissibility	[m3]	1.4760E-11
Transmissivity	[m2/s]	1.4479E-04
Storage	[m/Pa]	4.4004E-08
Storativity	[-]	4.3168E-04
Inner shell flow dimension	[-]	2.0000E+00
Dimensionles obs. point distance	[-]	2.8346E+02
Time match	[1/h]	9.3173E-01
Pressure match	[1/kPa]	2.6738E-02

Comments

FlowDim V2.14b Copyright (c) Golder Associates 1994

TEST ANALYSIS REPORT 27.10.1995

Identification

Site name	Florence, Arizona
Well name	OB7-1
Interval name	Oxide
Event name	Observation Well
Test date	16 - 21 June, 1995
Input file name	ob7-1dda.fd1

Well Parameters

Well depth	[m bgl]	2.7432E+02
Wellbore radius	[m]	7.6200E-02
Interval length	[m]	1.0363E+02
Distance to active well	[m]	1.5300E+01

Test Parameters

Flow rate	[l/min]	1.5142E+02
Test duration	[h]	2.4666E+01

Fluid and Formation Parameters

Viscosity	[Pa s]	1.0000E-03
Total compressibility	[1/Pa]	5.4000E-10
Porosity	[-]	5.0000E-02

Model assumptions

Flow model	Homogeneous
Boundary conditions	Constant rate
Well type	Observation
Superposition type	Drawdown

Results of analysis

Transmissibility	[m3]	5.0475E-12
Transmissivity	[m2/s]	4.9516E-05
Storage	[m/Pa]	1.3510E-08
Storativity	[-]	1.3253E-04
Inner shell flow dimension	[-]	2.0000E+00
Dimensionles obs. point distance	[-]	2.0079E+02
Time match	[1/h]	5.7458E+00
Pressure match	[1/kPa]	1.2560E-02
Type Curve Match	[-]	

Comments

FlowDim V2.14b Copyright (c) Golder Associates 1994

TEST ANALYSIS REPORT 27.10.1995

Identification

Site name	Florence, Arizona
Well name	O12-O
Interval name	Oxide
Event name	Observation Well
Test date	1 - 7 June, 1995
Input file name	o12-oddc.fdl

Well Parameters

Well depth	[m bgl]	2.9570E+02
Wellbore radius	[m]	5.0800E-02
Interval length	[m]	1.5240E+02
Distance to active well	[m]	2.1900E+01
Radius of active well	[m]	7.6200E-02

Test Parameters

Flow rate	[l/min]	2.4610E+02
Test duration	[h]	6.6313E+00

Fluid and Formation Parameters

Viscosity	[Pa s]	1.0000E-03
Total compressibility	[1/Pa]	5.4000E-10
Porosity	[-]	5.0000E-02

Model assumptions

Flow model	Homogeneous
Boundary conditions	Constant rate
Well type	Observation
Superposition type	Drawdown

Results of analysis

Transmissibility	[m3]	3.2764E-11
Transmissivity	[m2/s]	3.2141E-04
Storage	[m/Pa]	2.2788E-07
Storativity	[-]	2.2355E-03
Inner shell flow dimension	[-]	2.0000E+00
Dimensionles obs. point distance	[-]	2.8740E+02
Time match	[1/h]	1.0792E+00
Pressure match	[1/kPa]	5.0164E-02

Comments

FlowDim V2.14b Copyright (c) Golder Associates 1994

TEST ANALYSIS REPORT 16.11.1995

Identification

Site name	Florence, Arizona
Well name	O28-GL
Interval name	Lower Gila
Event name	Obs. Well (P28-GL)
Test date	20 - 25 Sep. 1995
Input file name	o28-gld.rec

Well parameters

Well depth	[m brp]	9.7540E+01
Reference point elevation	[m asl]	0.0000E+00
Wellbore radius	[m]	5.0800E-02
Interval length	[m]	9.1400E+00
Distance to active well	[m]	4.0220E+01

Testparameter

Flow rate	[l/min]	2.8391E+02
Test duration	[h]	1.1873E+02

Fluid and formation parameters

Viscosity	[Pa s]	1.0000E-03
Total compressibility	[1/Pa]	5.4000E-10
Porosity	[-]	1.0000E-01

Model assumptions

Flow model	Homogeneous
Boundary conditions	Constant rate
Well type	Observation
Superposition type	Drawdown

Results of analysis

Transmissibility	[m3]	7.6324E-11
Transmissivity	[m2/s]	7.4874E-04
Storage	[m/Pa]	2.7481E-09
Storativity	[-]	2.6959E-05
Inner shell flow dimension	[-]	2.0000E+00
Dimensionles obs. point distance	[-]	7.9173E+02
Time match	[1/h]	6.1809E+01
Pressure match	[1/kPa]	1.0130E-01

Comments

FlowDim V2.14b Copyright (c) Golder Associates 1994

TEST ANALYSIS REPORT 16.11.1995

Identification

Site name	Florence, Arizona
Well name	O28.1-O
Interval name	Oxide
Event name	Obs. Well (P28.2-O)
Test date	2 - 5 Oct. 1995
Input file name	o281-od.rec

Well parameters

Well depth	[m brp]	1.6154E+02
Reference point elevation	[m asl]	0.0000E+00
Wellbore radius	[m]	5.0800E-02
Interval length	[m]	3.0480E+01
Distance to active well	[m]	4.9730E+01

Testparameter

Flow rate	[l/min]	2.8770E+02
Test duration	[h]	7.3888E+01

Fluid and formation parameters

Viscosity	[Pa s]	1.0000E-03
Total compressibility	[1/Pa]	5.4000E-10
Porosity	[-]	5.0000E-02

Model assumptions

Flow model	Homogeneous
Boundary conditions	Constant rate
Well type	Observation
Superposition type	Drawdown

Results of analysis

Transmissibility	[m3]	3.2337E-11
Transmissivity	[m2/s]	3.1723E-04
Storage	[m/Pa]	1.0811E-07
Storativity	[-]	1.0605E-03
Inner shell flow dimension	[-]	2.0000E+00
Dimensionles obs. point distance	[-]	9.7894E+02
Time match	[1/h]	4.3542E-01
Pressure match	[1/kPa]	4.2352E-02

Comments

FlowDim V2.14b Copyright (c) Golder Associates 1994

TEST ANALYSIS REPORT 16.11.1995

Identification

Site name	Florence, Arizona
Well name	PW2-1
Interval name	Oxide
Event name	Pumping Well
Test date	8 Mar. 1995
Input file name	pw2-1d.rec

Well parameters

Well depth	[m brp]	1.9507E+02
Reference point elevation	[m asl]	0.0000E+00
Wellbore radius	[m]	7.6200E-02
Interval length	[m]	6.7060E+01

Testparameter

Flow rate	[l/min]	1.8927E+02
Test duration	[h]	1.6767E+02

Fluid and formation parameters

Viscosity	[Pa s]	1.0000E-03
Total compressibility	[1/Pa]	5.4000E-10
Porosity	[-]	5.0000E-02

Model assumptions

Flow model	Homogeneous
Boundary conditions	Constant rate
Well type	Source
Superposition type	Drawdown

Results of analysis

Transmissibility	[m3]	3.2665E-11
Transmissivity	[m2/s]	3.2045E-04
Storage	[m/Pa]	3.2419E-13
Storativity	[-]	3.1803E-09
Wellbore storage	[m3/Pa]	2.3643E-06
Skin (assumed)	[-]	0.0000E+00
Inner shell flow dimension	[-]	2.0000E+00
Time match	[1/h]	3.1235E+02
Pressure match	[1/kPa]	6.5031E-02

Comments

FlowDim V2.14b Copyright (c) Golder Associates 1994

TEST ANALYSIS REPORT 27.10.1995

Identification		
Site name		Florence, Arizona
Well name		M3-GL
Interval name		Lower Gila
Event name		Pumping Well
Test date		26 - 27 July, 1995
Input file name		pm3-glda.fdl

Well parameters		
Well depth	[m bgl]	1.1278E+02
Wellbore radius	[m]	6.3500E-02
Interval length	[m]	1.2190E+01

Test parameters		
Flow rate	[l/min]	3.7850E+01
Test duration	[h]	2.6919E+01

Fluid and formation parameters		
Viscosity	[Pa s]	1.0000E-03
Total compressibility	[1/Pa]	5.4000E-10
Porosity	[-]	5.0000E-02

Model assumptions	
Flow model	Homogeneous
Boundary conditions	Constant rate
Well type	Source
Superposition type	Drawdown

Results of analysis		
Transmissibility	[m3]	6.9585E-11
Transmissivity	[m2/s]	6.8263E-04
Storage	[m/Pa]	3.2211E-11
Storativity	[-]	3.1599E-07
Wellbore storage	[m3/Pa]	8.1567E-07
Skin (assumed)	[-]	0.0000E+00
Inner shell flow dimension	[-]	2.0000E+00
Time match	[1/h]	1.9287E+03
Pressure match	[1/kPa]	6.9273E-01
Type Curve Match	[-]	1.0000E+06

Comments

FlowDim V2.14b Copyright (c) Golder Associates 1994

TEST ANALYSIS REPORT 16.11.1995

Identification	
Site name	Florence, Arizona
Well name	PW4-1
Interval name	Oxide
Event name	Pumping Well
Test date	19 May, 1995
Input file name	pw4-1.rec

Well parameters		
Well depth	[m brp]	2.4384E+02
Reference point elevation	[m asl]	0.0000E+00
Wellbore radius	[m]	7.6200E-02
Interval length	[m]	1.0363E+02

Testparameter		
Flow rate	[l/min]	2.6876E+02
Test duration	[h]	9.5190E+01

Fluid and formation parameters		
Viscosity	[Pa s]	1.0000E-03
Total compressibility	[1/Pa]	5.4000E-10
Porosity	[-]	5.0000E-02

Model assumptions	
Flow model	Homogeneous
Boundary conditions	Constant rate
Well type	Source
Superposition type	Drawdown

Results of analysis		
Transmissibility	[m3]	1.4008E-10
Transmissivity	[m2/s]	1.3742E-03
Storage	[m/Pa]	2.5645E-13
Storativity	[-]	2.5158E-09
Wellbore storage	[m3/Pa]	1.8703E-06
Skin (assumed)	[-]	0.0000E+00
Inner shell flow dimension	[-]	2.0000E+00
Time match	[1/h]	1.6933E+03
Pressure match	[1/kPa]	1.9640E-01

Comments

FlowDim V2.14b Copyright (c) Golder Associates 1994

TEST ANALYSIS REPORT 27.10.1995

Identification

Site name	Florence, Arizona
Well name	M4-O
Interval name	Oxide
Event name	Pumping Well
Test date	28 - 29 July, 1995
Input file name	pm4-od.fdl

Well parameters

Well depth	[m bgl]	1.5240E+02
Wellbore radius	[m]	6.3500E-02
Interval length	[m]	1.8290E+01

Test parameters

Flow rate	[l/min]	5.6780E+01
Test duration	[h]	2.3641E+01

Fluid and formation parameters

Viscosity	[Pa s]	1.0000E-03
Total compressibility	[1/Pa]	5.4000E-10
Porosity	[-]	5.0000E-02

Model assumptions

Flow model	Homogeneous
Boundary conditions	Constant rate
Well type	Source
Superposition type	Drawdown

Results of analysis

Transmissibility	[m3]	3.6643E-12
Transmissivity	[m2/s]	3.5947E-05
Storage	[m/Pa]	2.7270E-13
Storativity	[-]	2.6752E-09
Wellbore storage	[m3/Pa]	1.3811E-06
Skin (assumed)	[-]	0.0000E+00
Inner shell flow dimension	[-]	2.0000E+00
Time match	[1/h]	5.9983E+01
Pressure match	[1/kPa]	2.4317E-02
Type Curve Match	[-]	2.0000E+08

Comments

FlowDim V2.14b Copyright (c) Golder Associates 1994

TEST ANALYSIS REPORT 26.10.1995

Identification		
Site name		Florence, Arizona
Well name		PW7-1
Interval name		Oxide
Event name		Pumping Test
Test date		16 - 21 June 1995
Input file name		pw7-1dda.fdl

Well parameters		
Well depth	[m bgl]	2.7432E+02
Wellbore radius	[m]	7.6200E-02
Interval length	[m]	1.0363E+02

Test parameter		
Flow rate	[l/min]	1.5142E+02
Test duration	[h]	2.4919E+01

Fluid and formation parameters		
Viscosity	[Pa s]	1.0000E-03
Total compressibility	[1/Pa]	5.4000E-10
Porosity	[-]	5.0000E-02

Model assumptions	
Flow model	Homogeneous
Boundary conditions	Constant rate
Well type	Source
Superposition type	Drawdown

Results of analysis		
Transmissibility	[m3]	8.5587E-12
Transmissivity	[m2/s]	8.3960E-05
Storage	[m/Pa]	1.8842E-07
Storativity	[-]	1.8484E-03
Wellbore storage	[m3/Pa]	6.8707E-07
Skin (assumed)	[-]	0.0000E+00
Inner shell flow dimension	[-]	2.0000E+00
Time match	[1/h]	2.8162E+02
Pressure match	[1/kPa]	2.1298E-02
Type Curve Match	[-]	1.0000E+02

Comments

FlowDim V2.14b Copyright (c) Golder Associates 1994

TEST ANALYSIS REPORT 16.11.1995

Identification

Site name	Florence, Arizona
Well name	P8-GU
Interval name	Upper Gila
Event name	Pumping Well
Test date	18 - 22 Sep. 1995
Input file name	p8-gud.rec

Well parameters

Well depth	[m brp]	8.2300E+01
Reference point elevation	[m asl]	0.0000E+00
Wellbore radius	[m]	7.6200E-02
Interval length	[m]	3.6580E+01

Testparameter

Flow rate	[l/min]	3.3501E+02
Test duration	[h]	5.3012E+01

Fluid and formation parameters

Viscosity	[Pa s]	1.0000E-03
Total compressibility	[1/Pa]	5.4000E-10
Porosity	[-]	1.0000E-01

Model assumptions

Flow model	Homogeneous
Boundary conditions	Constant rate
Well type	Source
Superposition type	Drawdown

Results of analysis

Transmissibility	[m3]	8.0643E-10
Transmissivity	[m2/s]	7.9111E-03
Storage	[m/Pa]	3.2522E-10
Storativity	[-]	3.1904E-06
Wellbore storage	[m3/Pa]	1.1859E-05
Skin (assumed)	[-]	0.0000E+00
Inner shell flow dimension	[-]	2.0000E+00
Time match	[1/h]	1.5374E+03
Pressure match	[1/kPa]	9.0703E-01

Comments

FlowDim V2.14b Copyright (c) Golder Associates 1994

TEST ANALYSIS REPORT 26.10.1995

Identification

Site name	Florence Arizona
Well name	P12-O
Interval name	Oxide
Event name	Pumping Test
Test date	1 - 7 June, 1995
Input file name	p12-oddc.fdt

Well parameters

Well depth	[m bgl]	1.0000E+02
Wellbore radius	[m]	7.6200E-02
Interval length	[m]	1.5240E+02

Test parameters

Flow rate	[l/min]	2.4610E+02
Test duration	[h]	1.6624E+00

Fluid and formation parameters

Viscosity	[Pa s]	1.0000E-03
Total compressibility	[1/Pa]	5.4000E-10
Porosity	[-]	1.0000E-01

Model assumptions

Flow model	Homogeneous
Boundary conditions	Constant rate
Well type	Source
Superposition type	Drawdown

Results of analysis

Transmissibility	[m3]	2.0785E-11
Transmissivity	[m2/s]	2.0390E-04
Storage	[m/Pa]	4.2419E-05
Storativity	[-]	4.1613E-01
Wellbore storage	[m3/Pa]	4.6404E-06
Skin (assumed)	[-]	0.0000E+00
Inner shell flow dimension	[-]	2.0000E+00
Time match	[1/h]	1.0126E+02
Pressure match	[1/kPa]	3.1823E-02
Type Curve parameter	[-]	3.0000E+00

Comments

FlowDim V2.14b Copyright (c) Golder Associates 1994

TEST ANALYSIS REPORT 23.11.1995

Identification

Site name	Florence, Arizona
Well name	P13.1-O
Interval name	Oxide
Event name	Pumping Well
Test date	9 - 16 Oct. 1995
Input file name	p131od.rec

Well parameters

Well depth	[m brp]	4.4958E+02
Reference point elevation	[m asl]	0.0000E+00
Wellbore radius	[m]	7.6200E-02
Interval length	[m]	2.0635E+02

Testparameter

Flow rate	[l/min]	1.7413E+02
Test duration	[h]	8.8082E+01

Fluid and formation parameters

Viscosity	[Pa s]	1.0000E-03
Total compressibility	[1/Pa]	5.4000E-10
Porosity	[-]	5.0000E-02

Model assumptions

Flow model	Homogeneous
Boundary conditions	Constant rate
Well type	Source
Superposition type	Drawdown

Results of analysis

Transmissibility	[m3]	1.9503E-11
Transmissivity	[m2/s]	1.9133E-04
Storage	[m/Pa]	4.8082E-11
Storativity	[-]	4.7168E-07
Wellbore storage	[m3/Pa]	1.7533E-06
Skin (assumed)	[-]	0.0000E+00
Inner shell flow dimension	[-]	2.0000E+00
Time match	[1/h]	2.5149E+02
Pressure match	[1/kPa]	4.2203E-02

Comments

FlowDim V2.14b Copyright (c) Golder Associates 1994

TEST ANALYSIS REPORT 24.11.1995

Identification

Site name	Florence, Arizona
Well name	P13.2-O
Interval name	Oxide
Event name	Obs, Well (P13.1-O)
Test date	9 - 16 Oct. 1995
Input file name	p132od3d.rec

Well parameters

Well depth	[m brp]	4.2672E+02
Reference point elevation	[m asl]	0.0000E+00
Wellbore radius	[m]	7.6200E-02
Interval length	[m]	1.8227E+02
Distance to active well	[m]	3.1370E+01

Testparameter

Flow rate	[l/min]	1.7413E+02
Test duration	[h]	8.8176E+01

Fluid and formation parameters

Viscosity	[Pa s]	1.0000E-03
Total compressibility	[1/Pa]	5.4000E-10
Porosity	[-]	5.0000E-02

Model assumptions

Flow model	Homogeneous
Boundary conditions	Constant rate
Well type	Observation
Superposition type	Drawdown

Results of analysis

Transmissibility	[m3]	8.3410E-15
Transmissivity	[m2/s]	8.1825E-08
Storage	[m/Pa]	7.1721E-11
Storativity	[-]	7.0358E-07
Inner shell flow dimension	[-]	3.0000E+00
Dimensionles obs. point distance	[-]	4.1168E+02
Time match	[1/h]	4.2545E-01
Pressure match	[1/kPa]	3.6089E-05

Comments

FlowDim V2.14b Copyright (c) Golder Associates 1994

TEST ANALYSIS REPORT 25.11.1995

Identification

Site name	Florence, Arizona
Well name	P15-O
Interval name	Oxide
Event name	Pumping Well
Test date	29 Sep-5 Oct. 1995
Input file name	p15od.rec

Well parameters

Well depth	[m brp]	4.2062E+02
Reference point elevation	[m asl]	0.0000E+00
Wellbore radius	[m]	7.6200E-02
Interval length	[m]	2.1946E+02

Testparameter

Flow rate	[l/min]	2.2330E+02
Test duration	[h]	1.0083E+02

Fluid and formation parameters

Viscosity	[Pa s]	1.0000E-03
Total compressibility	[1/Pa]	5.4000E-10
Porosity	[-]	5.0000E-02

Model assumptions

Flow model	Homogeneous
Boundary conditions	Constant rate
Well type	Source
Superposition type	Drawdown

Results of analysis

Transmissibility	[m3]	3.9175E-11
Transmissivity	[m2/s]	3.8431E-04
Storage	[m/Pa]	1.3542E-06
Storativity	[-]	1.3285E-02
Wellbore storage	[m3/Pa]	4.9380E-06
Skin (assumed)	[-]	0.0000E+00
Inner shell flow dimension	[-]	2.0000E+00
Time match	[1/h]	1.7936E+02
Pressure match	[1/kPa]	6.6105E-02

Comments

FlowDim V2.14b Copyright (c) Golder Associates 1994

TEST ANALYSIS REPORT 16.11.1995

Identification

Site name	Florence, Arizona
Well name	P19-O
Interval name	Oxide
Event name	Observ. Well
Test date	3 - 6 Jul. 1995
Input file name	p19-0d.rec

Well parameters

Well depth	[m brp]	2.0726E+02
Reference point elevation	[m asl]	0.0000E+00
Wellbore radius	[m]	7.6200E-02
Interval length	[m]	6.0350E+01
Distance to active well	[m]	2.2720E+01

Testparameter

Flow rate	[l/min]	8.3280E+01
Test duration	[h]	5.1266E+01

Fluid and formation parameters

Viscosity	[Pa s]	1.0000E-03
Total compressibility	[1/Pa]	5.4000E-10
Porosity	[-]	5.0000E-02

Model assumptions

Flow model	Homogeneous
Boundary conditions	Constant rate
Well type	Observation
Superposition type	Drawdown

Results of analysis

Transmissibility	[m3]	4.1810E-12
Transmissivity	[m2/s]	4.1016E-05
Storage	[m/Pa]	7.8809E-08
Storativity	[-]	7.7311E-04
Inner shell flow dimension	[-]	2.0000E+00
Dimensionles obs. point distance	[-]	2.9816E+02
Time match	[1/h]	3.7000E-01
Pressure match	[1/kPa]	1.8917E-02

Comments

FlowDim V2.14b Copyright (c) Golder Associates 1994

TEST ANALYSIS REPORT 16.11.1995

Identification

Site name	Florence, Arizona
Well name	P19-O
Interval name	Oxide
Event name	Observ. Well
Test date	3 - 6 Jul. 1995
Input file name	p19-od3d.rec

Well parameters

Well depth	[m brp]	2.0726E+02
Reference point elevation	[m asl]	0.0000E+00
Wellbore radius	[m]	7.6200E-02
Interval length	[m]	6.0350E+01
Distance to active well	[m]	2.2720E+01

Testparameter

Flow rate	[l/min]	8.3280E+01
Test duration	[h]	5.1266E+01

Fluid and formation parameters

Viscosity	[Pa s]	1.0000E-03
Total compressibility	[1/Pa]	5.4000E-10
Porosity	[-]	5.0000E-02

Model assumptions

Flow model	Homogeneous
Boundary conditions	Constant rate
Well type	Observation
Superposition type	Drawdown

Results of analysis

Transmissibility	[m3]	5.1759E-15
Transmissivity	[m2/s]	5.0775E-08
Storage	[m/Pa]	1.4684E-10
Storativity	[-]	1.4405E-06
Inner shell flow dimension	[-]	3.0000E+00
Dimensionles obs. point distance	[-]	2.9816E+02
Time match	[1/h]	2.4582E-01
Pressure match	[1/kPa]	4.6825E-05

Comments

FlowDim V2.14b Copyright (c) Golder Associates 1994

TEST ANALYSIS REPORT 16.11.1995

Identification

Site name	Florence, Arizona
Well name	P19.1-O
Interval name	Oxide
Event name	Withdrawal
Test date	3 - 6 Jul. 1995
Input file name	p191-od.rec

Well parameters

Well depth	[m brp]	2.0726E+02
Reference point elevation	[m asl]	0.0000E+00
Wellbore radius	[m]	7.6200E-02
Interval length	[m]	6.0350E+01

Testparameter

Flow rate	[l/min]	8.3300E+01
Test duration	[h]	5.1267E+01

Fluid and formation parameters

Viscosity	[Pa s]	1.0000E-03
Total compressibility	[1/Pa]	5.4000E-10
Porosity	[-]	5.0000E-02

Model assumptions

Flow model	Homogeneous
Boundary conditions	Constant rate
Well type	Source
Superposition type	Drawdown

Results of analysis

Transmissibility	[m3]	6.5087E-12
Transmissivity	[m2/s]	6.3851E-05
Storage	[m/Pa]	6.2788E-14
Storativity	[-]	6.1595E-10
Wellbore storage	[m3/Pa]	4.5791E-07
Skin (assumed)	[-]	0.0000E+00
Inner shell flow dimension	[-]	2.0000E+00
Time match	[1/h]	3.2135E+02
Pressure match	[1/kPa]	2.9442E-02

Comments

FlowDim V2.14b Copyright (c) Golder Associates 1994

TEST ANALYSIS REPORT 16.11.1995

Identification

Site name	Florence, Arizona
Well name	P19.1-O
Interval name	Oxide
Event name	Withdrawal
Test date	3 - 6 Jul. 1995
Input file name	p191od3d.rec

Well parameters

Well depth	[m brp]	2.0726E+02
Reference point elevation	[m asl]	0.0000E+00
Wellbore radius	[m]	7.6200E-02
Interval length	[m]	6.0350E+01

Testparameter

Flow rate	[l/min]	8.3300E+01
Test duration	[h]	5.1267E+01

Fluid and formation parameters

Viscosity	[Pa s]	1.0000E-03
Total compressibility	[1/Pa]	5.4000E-10
Porosity	[-]	5.0000E-02

Model assumptions

Flow model	Homogeneous
Boundary conditions	Constant rate
Well type	Source
Superposition type	Drawdown

Results of analysis

Transmissibility	[m3]	2.4052E-13
Transmissivity	[m2/s]	2.3595E-06
Storage	[m/Pa]	5.7460E-07
Storativity	[-]	5.6368E-03
Wellbore storage	[m3/Pa]	4.1894E-07
Skin (assumed)	[-]	0.0000E+00
Inner shell flow dimension	[-]	3.0000E+00
Time match	[1/h]	2.5952E+01
Pressure match	[1/kPa]	2.1754E-03

Comments

FlowDim V2.14b Copyright (c) Golder Associates 1994

TEST ANALYSIS REPORT 16.11.1995

Identification

Site name	Florence, Arizona
Well name	P19.2-O
Interval name	Oxide
Event name	Observ. Well
Test date	3 - 6 Jul. 1995
Input file name	p192-od.rec

Well parameters

Well depth	[m brp]	1.9111E+02
Reference point elevation	[m asl]	0.0000E+00
Wellbore radius	[m]	5.0800E-02
Interval length	[m]	6.0350E+01
Distance to active well	[m]	2.1200E+01

Testparameter

Flow rate	[l/min]	8.3280E+01
Test duration	[h]	4.9513E+01

Fluid and formation parameters

Viscosity	[Pa s]	1.0000E-03
Total compressibility	[1/Pa]	5.4000E-10
Porosity	[-]	5.0000E-02

Model assumptions

Flow model	Homogeneous
Boundary conditions	Constant rate
Well type	Observation
Superposition type	Drawdown

Results of analysis

Transmissibility	[m3]	3.2012E-12
Transmissivity	[m2/s]	3.1404E-05
Storage	[m/Pa]	1.4992E-08
Storativity	[-]	1.4707E-04
Inner shell flow dimension	[-]	2.0000E+00
Dimensionles obs. point distance	[-]	2.6835E+02
Time match	[1/h]	1.7103E+00
Pressure match	[1/kPa]	1.4484E-02

Comments

FlowDim V2.14b Copyright (c) Golder Associates 1994

TEST ANALYSIS REPORT 16.11.1995

Identification

Site name	Florence, Arizona
Well name	P19.2-O
Interval name	Oxide
Event name	Observ. Well
Test date	3 - 6 Jul. 1995
Input file name	p192od3d.rec

Well parameters

Well depth	[m brp]	1.9111E+02
Reference point elevation	[m asl]	0.0000E+00
Wellbore radius	[m]	5.0800E-02
Interval length	[m]	6.0350E+01
Distance to active well	[m]	2.1200E+01

Testparameter

Flow rate	[l/min]	8.3280E+01
Test duration	[h]	4.9513E+01

Fluid and formation parameters

Viscosity	[Pa s]	1.0000E-03
Total compressibility	[1/Pa]	5.4000E-10
Porosity	[-]	5.0000E-02

Model assumptions

Flow model	Homogeneous
Boundary conditions	Constant rate
Well type	Observation
Superposition type	Drawdown

Results of analysis

Transmissibility	[m3]	4.3045E-15
Transmissivity	[m2/s]	4.2228E-08
Storage	[m/Pa]	3.4441E-11
Storativity	[-]	3.3786E-07
Inner shell flow dimension	[-]	3.0000E+00
Dimensionles obs. point distance	[-]	2.6835E+02
Time match	[1/h]	1.0011E+00
Pressure match	[1/kPa]	3.8942E-05

Comments

FlowDim V2.14b Copyright (c) Golder Associates 1994

TEST ANALYSIS REPORT 16.11.1995

Identification

Site name	Florence, Arizona
Well name	P28-GL
Interval name	Lower Gila
Event name	Pumping Well
Test date	20 - 25, Sep. 1995
Input file name	p28-gld.rec

Well parameters

Well depth	[m brp]	9.7540E+01
Reference point elevation	[m asl]	0.0000E+00
Wellbore radius	[m]	6.3500E-02
Interval length	[m]	9.1400E+00

Testparameter

Flow rate	[l/min]	2.8390E+02
Test duration	[h]	1.1539E+02

Fluid and formation parameters

Viscosity	[Pa s]	1.0000E-03
Total compressibility	[1/Pa]	5.4000E-10
Porosity	[-]	1.0000E-01

Model assumptions

Flow model	Homogeneous
Boundary conditions	Constant rate
Well type	Source
Superposition type	Drawdown

Results of analysis

Transmissibility	[m3]	2.7137E-11
Transmissivity	[m2/s]	2.6622E-04
Storage	[m/Pa]	3.4388E-11
Storativity	[-]	3.3735E-07
Wellbore storage	[m3/Pa]	8.7080E-07
Skin (assumed)	[-]	0.0000E+00
Inner shell flow dimension	[-]	2.0000E+00
Time match	[1/h]	7.0454E+02
Pressure match	[1/kPa]	3.6017E-02

Comments

FlowDim V2.14b

Copyright (c) Golder Associates 1994

TEST ANALYSIS REPORT 16.11.1995

Identification		
Site name		Florence, Arizona
Well name		P28.1-O
Interval name		Oxide
Event name		Pumping Well
Test date		15 - 18 Aug, 1995
Input file name		p281-oad.rec

Well parameters		
Well depth	[m brp]	1.5850E+02
Reference point elevation	[m asl]	0.0000E+00
Wellbore radius	[m]	6.7200E-02
Interval length	[m]	3.0480E+01

Testparameter		
Flow rate	[l/min]	1.0978E+02
Test duration	[h]	4.2844E+03

Fluid and formation parameters		
Viscosity	[Pa s]	1.0000E-03
Total compressibility	[1/Pa]	5.4000E-10
Porosity	[-]	5.0000E-02

Model assumptions	
Flow model	Homogeneous
Boundary conditions	Constant rate
Well type	Source
Superposition type	Drawdown

Results of analysis		
Transmissibility	[m3]	8.4137E-11
Transmissivity	[m2/s]	8.2539E-04
Storage	[m/Pa]	5.3035E-04
Storativity	[-]	5.2027E+00
Wellbore storage	[m3/Pa]	1.5040E-04
Skin (assumed)	[-]	0.0000E+00
Inner shell flow dimension	[-]	2.0000E+00
Time match	[1/h]	1.2647E+01
Pressure match	[1/kPa]	2.8879E-01

Comments

FlowDim V2.14b Copyright (c) Golder Associates 1994

TEST ANALYSIS REPORT 15.11.1995

Identification	
Site name	Forence, Arizona
Well name	P28.1-O
Interval name	Oxide
Event name	Pumping Well
Test date	8 - 11 Sep, 1995
Input file name	p281-obd.rec

Well parameters		
Well depth	[m brp]	1.5850E+02
Reference point elevation	[m asl]	0.0000E+00
Wellbore radius	[m]	7.6200E-02
Interval length	[m]	3.0480E+01

Testparameter		
Flow rate	[l/min]	3.2180E+02
Test duration	[h]	7.4053E+01

Fluid and formation parameters		
Viscosity	[Pa s]	1.0000E-03
Total compressibility	[1/Pa]	5.4000E-10
Porosity	[-]	5.0000E-02

Model assumptions	
Flow model	Homogeneous
Boundary conditions	Constant rate
Well type	Source
Superposition type	Drawdown

Results of analysis		
Transmissibility	[m3]	3.9300E-11
Transmissivity	[m2/s]	3.8554E-04
Storage	[m/Pa]	3.5153E-06
Storativity	[-]	3.4485E-02
Wellbore storage	[m3/Pa]	1.2818E-06
Skin (assumed)	[-]	0.0000E+00
Inner shell flow dimension	[-]	2.0000E+00
Time match	[1/h]	6.9315E+02
Pressure match	[1/kPa]	4.6017E-02

Comments

FlowDim V2.14b Copyright (c) Golder Associates 1994

TEST ANALYSIS REPORT 15.11.1995

Identification

Site name	Florence, Arizona
Well name	P28.2-O
Interval name	Oxide
Event name	Obs. Well (P28.1-O)
Test date	8 - 11 Sep, 1995
Input file name	p282-obd.rec

Well parameters

Well depth	[m brp]	1.6150E+02
Reference point elevation	[m asl]	0.0000E+00
Wellbore radius	[m]	5.0800E-02
Interval length	[m]	3.0180E+01
Distance to active well	[m]	2.9910E+01

Testparameter

Flow rate	[l/min]	3.2170E+02
Test duration	[h]	7.3898E+01

Fluid and formation parameters

Viscosity	[Pa s]	1.0000E-03
Total compressibility	[1/Pa]	5.4000E-10
Porosity	[-]	5.0000E-02

Model assumptions

Flow model	Homogeneous
Boundary conditions	Constant rate
Well type	Observation
Superposition type	Drawdown

Results of analysis

Transmissibility	[m3]	2.8996E-11
Transmissivity	[m2/s]	2.8446E-04
Storage	[m/Pa]	2.9688E-08
Storativity	[-]	2.9124E-04
Inner shell flow dimension	[-]	2.0000E+00
Dimensionles obs. point distance	[-]	5.8878E+02
Time match	[1/h]	3.9303E+00
Pressure match	[1/kPa]	3.3963E-02

Comments

FlowDim V2.14b Copyright (c) Golder Associates 1994

TEST ANALYSIS REPORT 16.11.1995

Identification

Site name	Florence, Arizona
Well name	P28.2-O
Interval name	Oxide
Event name	Pumping Well
Test date	2 - 5 Oct. 1995
Input file name	p282-od.rec

Well parameters

Well depth	[m brp]	1.5820E+02
Reference point elevation	[m asl]	0.0000E+00
Wellbore radius	[m]	7.6200E-02
Interval length	[m]	3.0180E+01

Testparameter

Flow rate	[l/min]	2.8769E+02
Test duration	[h]	7.4052E+01

Fluid and formation parameters

Viscosity	[Pa s]	1.0000E-03
Total compressibility	[1/Pa]	5.4000E-10
Porosity	[-]	5.0000E-02

Model assumptions

Flow model	Homogeneous
Boundary conditions	Constant rate
Well type	Source
Superposition type	Drawdown

Results of analysis

Transmissibility	[m3]	3.3674E-11
Transmissivity	[m2/s]	3.3035E-04
Storage	[m/Pa]	3.8581E-04
Storativity	[-]	3.7848E+00
Wellbore storage	[m3/Pa]	1.4068E-04
Skin (assumed)	[-]	0.0000E+00
Inner shell flow dimension	[-]	2.0000E+00
Time match	[1/h]	5.4115E+00
Pressure match	[1/kPa]	4.4105E-02

Comments

FlowDim V2.14b Copyright (c) Golder Associates 1994

TEST ANALYSIS REPORT 25.11.1995

Identification		
Site name		Florence, Arizona
Well name		P49-O
Interval name		Oxide
Event name		Recovery
Test date		11 - 16 Oct. 1995
Input file name		p490r.rec

Well parameters		
Well depth	[m brp]	3.9258E+02
Reference point elevation	[m asl]	0.0000E+00
Wellbore radius	[m]	7.6200E-02
Interval length	[m]	1.2619E+02

Testparameter		
Production/Injection time	[h]	4.5700E+01
Flow rate	[l/min]	1.5142E+02
Test duration	[h]	4.7164E+01

Fluid and formation parameters		
Viscosity	[Pa s]	1.0000E-03
Total compressibility	[1/Pa]	5.4000E-10
Porosity	[-]	5.0000E-03

Model assumptions		
Flow model		Homogeneous
Boundary conditions		Constant rate
Well type		Source
Superposition type		Buildup

Results of analysis		
Transmissibility	[m3]	3.5205E-13
Transmissivity	[m2/s]	3.4536E-06
Storage	[m/Pa]	8.1397E-05
Storativity	[-]	7.9851E-01
Wellbore storage	[m3/Pa]	1.7804E-06
Skin (assumed)	[-]	0.0000E+00
Inner shell flow dimension	[-]	3.0000E+00
Time match	[1/h]	8.9386E+00
Pressure match	[1/kPa]	1.7517E-03

Comments

FlowDim V2.14b Copyright (c) Golder Associates 1994

MEMORANDUM

TO: Mr. Steven A. Mellon
Brown and Caldwell
3636 N. Central Ave., Suite 300
Phoenix, Arizona 85012

FROM: Amado Guzman
Tucson Office

Our Reference: 953-2908

DATE: December 1, 1995

RE: Florence Electronic Data

Dear Steve:

Please find enclosed the reduced data files for the hydraulic tests included in our interpretation report. I have prepared a list of these files and their relationship to the figures presented in Appendix B. Please let me know if you need any additional information.

Cheers!

Enc. (12) Diskettes

cc. Mr. John Kline
Magma Copper Co.
Resource Development Technology Group
7400 N. Oracle Rd. Suite 162
Tucson, Arizona 85704
WITH ENCLOSURES (1) Diskette

Reduced data files and corresponding figures within Appendix B. Files contain two columns; time (hours) versus head (KPa).

Figure	Well ID	Name of Data File			
1B,	M1-GL	M1-GLD DAT	7,342	11-16-95	3:41a
2B,	M3-GL	M3GLPD DAT	6,354	08-29-95	9:31p
3B,	M14-GL	M14-GLD DAT	5,302	11-16-95	3:43a
4B,	M14-GL (3-D)	Same as previous			
5B,	M15-GU	M15-GUD DAT	7,138	11-16-95	3:42a
6B,	M18-GL	M18-GUD DAT	6,186	11-16-95	3:40a
7B,	P39-O	MF39PWPD DAT	7,920	11-15-95	12:01p
8B,	O39-O	MF39OWPD DAT	4,758	11-15-95	12:02p
9B,	OB7-1	OB7-1OD DAT	8,328	12-01-95	2:25p
10B,	O12-O	O12-ODDC FD1	22,449	10-27-95	11:44a
11B,	O28-GL	O28-GLD DAT	6,458	11-16-95	2:29a
12B,	O28.1-O	O281-OD DAT	6,220	11-16-95	1:24a
13B,	PW2-1	PW2-1D DAT	8,498	11-16-95	4:54p
14B,	M3-GL	M3GLODDB FDT	746	10-29-95	3:18p
15B,	PW4-1	PW4-1 DAT	7,478	11-16-95	4:29p
16B,	M4-O	M4OPD DAT	5,469	08-29-95	9:57p
17B,	PW7-1	PW7-1OD DAT	8,158	12-01-95	2:27p
18B,	P8-GU	P8-GUD DAT	6,696	11-16-95	2:26a
19B,	P12-O	P12-ODDB FDT	2,684	10-22-95	7:22p
20B,	P13.1-O	P131OD DAT	7,988	11-23-95	12:41p
21B,	P13.2-O (3-D)	P132OD DAT	8,294	11-23-95	12:44p
22B,	P15-O	P15OD DAT	8,260	11-25-95	12:06p
23B,	P19-O	P19-OD DAT	8,396	11-16-95	11:30a
24B,	P19-O (3-D)	Same as previous			
25B,	P19.1-O	P191-OD DAT	6,390	11-16-95	11:29a
26B,	P19.1-O (3-D)	Same as Previous			
27B,	P19.2-O	P192-OD DAT	8,838	11-16-95	11:32a
28B,	P19.2-O (3-D)	Same as Previous			
29B,	P28-GL	P28-GLD DAT	8,770	11-16-95	2:27a
30B,	P28.1-O	P281-OAD DAT	7,444	11-15-95	1:33p
31B,	P28.1-O (Test #2)	P281-OBD DAT	7,852	11-15-95	2:06p
32B,	P28.2-O (Test #2)	P282-OBD DAT	6,662	11-15-95	2:06p
33B,	P28.2-O	P282-OD DAT	8,090	11-16-95	1:22a
34B,	P49-O (3-D)	P49OR DAT	8,498	11-24-95	7:21p

M5-S Pump Out Slug Test
Brown and Caldwell

Project: 1899 for Magma Copper Company, Florence, AZ
Test Date: July 25-28, 1995

Depth of well, Dw=	380 ft		
Depth to water Dd=	122.13 ft		
D=Dw-Dd	257.87 ft		
b=D	257.87 ft		
d=	60 ft		
y=	211 ft		
rc=	0.2 ft		
rw=	0.35 ft		
d/rw=	171.4286		
b/rw=	736.7714		
from Fig 16.6			
C=	11.6		
ln(Re/rw)	4.268473	t=tx-to=	2005
		ln(ho/ht)=	0.300301
K=	3.1E-04 ft/day	slope=	0.00015

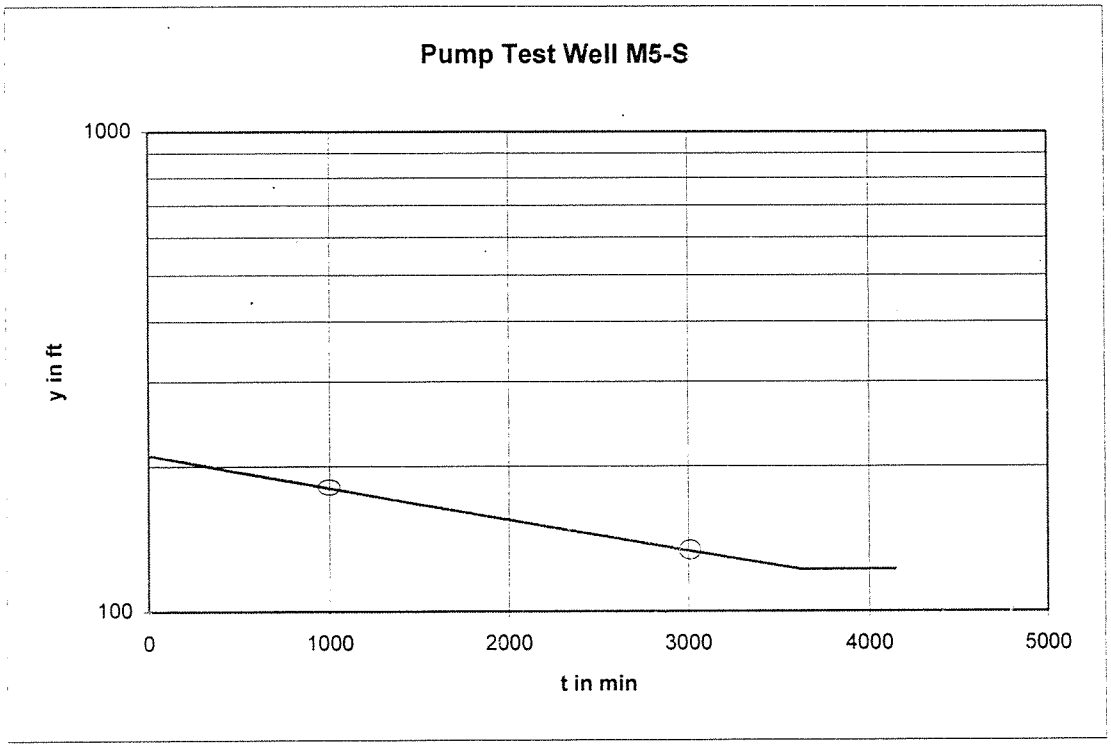

Reference: Bouwer, H., The Bouwer and Rice Slug Test - An Update. Ground Water Vol. 27, No. 3, 1989

M13-S Pump Out Slug Test
Brown and Caldwell

Project: 1899 for Magma Copper Company, Florence, AZ
Test Date: July 28 - Aug 1, 1995

Depth of well, Dw=	345 ft	t=tx-to=	4050
Depth to water Dd=	150.79 ft	ln(ho/ht)=	0.641854
D=Dw-Dd	194.21 ft	slope=	0.000158
b=D	194.21 ft		
d=	60 ft		
y=	349 ft		
rc=	0.2 ft		
rw=	0.35 ft		
d/rw=	171.4286		
b/rw=	554.8857		
from Fig 16.6			
C=	11.6		
ln(Re/rw)	4.136481		
K=	3.1E-04 ft/day		

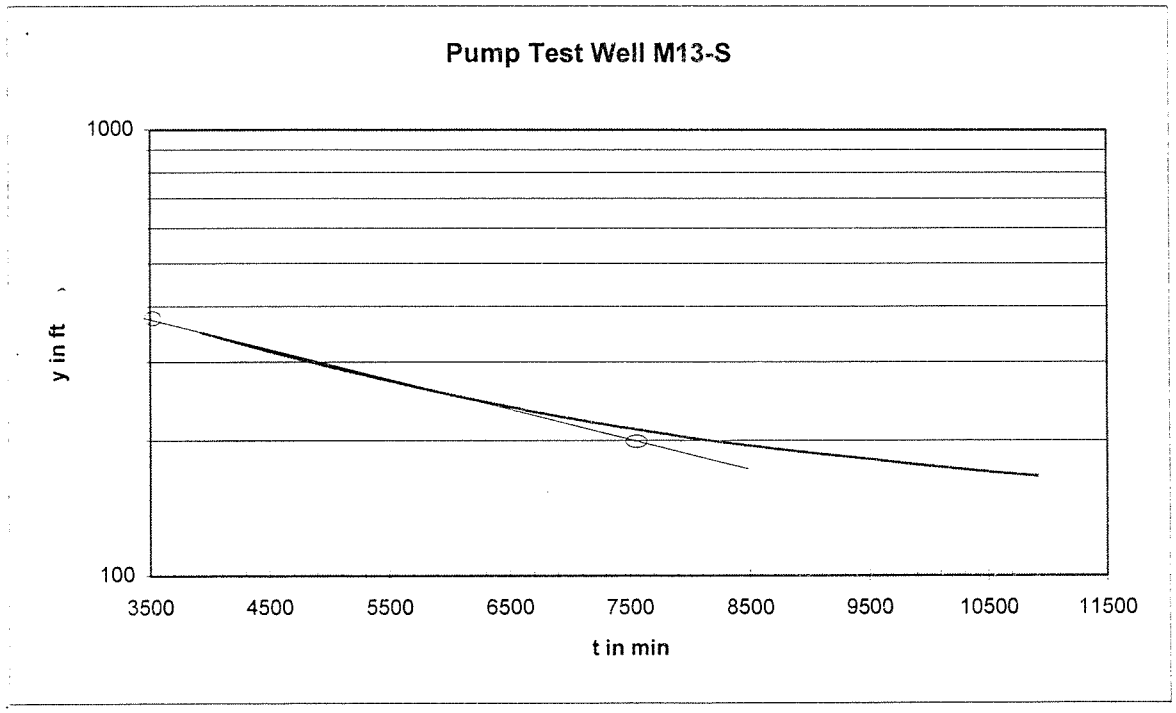

Reference: Bouwer, H., The Bouwer and Rice Slug Test - An Update. Ground Water Vol. 27, No. 3, 1989

Exhibit 14A-2

- **MFGU Hydraulic Conductivity Testing Laboratory Report (300), 1995**
- **MFGU Hydraulic Conductivity Testing Laboratory Report (283-288), 2011**
- **MFGU Hydraulic Conductivity Testing Laboratory Report (292-297), 2011**

CORE LABORATORIES

PARTICLE-SIZE ANALYSIS RESULTS

MAGMA FLORENCE

CL AURORA FILE # 57209-954427
CL BKRSFLD FILE # 57111-095334

PERFORMED BY:
CORE LABORATORIES
3430 UNICORN ROAD
BAKERSFIELD, CA 93308
(805) 392-8600

FINAL REPORT PRESENTED
OCTOBER 12, 1995

The analyses, opinions or interpretations contained in this report are based upon observations and material supplied by the client for whose exclusive and confidential use this report has been made. The interpretations or opinions expressed represent the best judgment of Core Laboratories. Core Laboratories, however, assumes no responsibility and makes no warranty or representations, express or implied, as to the productivity, proper operations, or profitableness of any oil, gas, coal or other mineral, property, well or sand in connection with which such report is used or relied upon for any reason whatsoever. This report shall not be reproduced except in its entirety, without the written approval of Core Laboratories.

CORE LAB

CORE LABORATORIES

Company	CORE LAB. - AURORA	Sample	P1-80-55	File Number	57111-95334
I.D.	954427-1	Proj.	Magma Florence	Date	11-OCT-95
County		State		Analysts	GC

Laser Particle Size Analysis

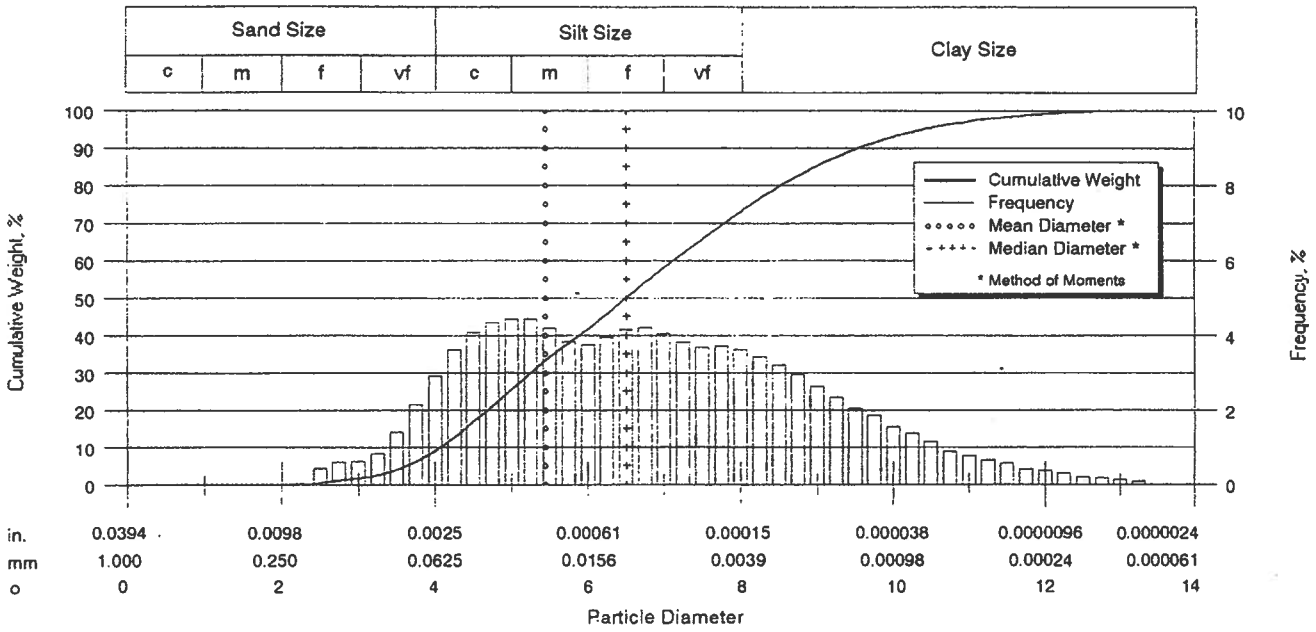

Particle Size Distribution

	[U.S. Sieve]	[in]	[mm]	[phi]	Weight, % [Inc.]	[Cum.]
Coarse	20	0.0331	0.84	0.25	0.00	0.00
Sand	25	0.0280	0.71	0.50	0.00	0.00
	30	0.0232	0.59	0.75	0.00	0.00
	35	0.0197	0.50	1.00	0.00	0.00
Medium	40	0.0165	0.42	1.25	0.00	0.00
Sand	45	0.0138	0.35	1.50	0.00	0.00
	50	0.0118	0.30	1.75	0.00	0.00
	60	0.0098	0.25	2.00	0.00	0.00
Fine	70	0.0083	0.210	2.25	0.03	0.03
Sand	80	0.0070	0.177	2.50	0.44	0.47
	100	0.0059	0.149	2.75	0.60	1.07
	120	0.0049	0.125	3.00	0.62	1.69
Very Fine	140	0.0041	0.105	3.25	0.84	2.53
Sand	170	0.0035	0.088	3.50	1.40	3.93
	200	0.0029	0.074	3.75	2.15	6.08
	230	0.0025	0.063	4.00	2.92	9.00
Silt	270	0.0021	0.053	4.25	3.62	12.62
	325	0.0017	0.044	4.50	4.11	16.73
	400	0.0015	0.037	4.75	4.32	21.05
	450	0.0012	0.031	5.00	4.44	25.49
	500	0.0010	0.025	5.32	5.65	31.14
	635	0.0008	0.020	5.64	5.16	36.30
		0.00061	0.0156	6.00	5.41	41.71
		0.00031	0.0078	7.00	16.36	58.07
		0.00015	0.0039	8.00	14.85	72.92
Clay		0.000079	0.0020	9.00	12.21	85.13
		0.000039	0.00098	10.0	7.80	92.93
		0.000019	0.00049	11.0	4.18	97.11
		0.0000094	0.00024	12.0	2.00	99.11
		0.0000047	0.00012	13.0	0.80	99.91
		0.0000039	0.00010	13.3	0.09	100.00

Sorting Statistics

Parameter	[Moment]	[Trask]	[Inman]	[Folk]
Mean, in	0.0009	0.0004	0.0004	0.0004
Mean, mm	0.0229	0.0106	0.0098	0.0102
Mean, phi	5.4472	6.5619	6.6725	6.6187
Median, in	0.0004	0.0004	0.0004	0.0004
Median, mm	0.0110	0.0110	0.0110	0.0110
Median, phi	6.5103	6.5110	6.5110	6.5110
Std Deviation, in	0.0012	0.0161	0.0084	0.0089
Std Deviation, mm	0.0298	0.4116	0.2152	0.2280
Std Deviation, phi	5.0700	1.2805	2.2160	2.1331
Skewness	2.5040	0.9561	0.2286	0.1113
Kurtosis	8.2100	0.2899	0.5264	0.8717
Mode, mm	0.0296			
95% Confidence	0.0171			
Limits, mm	0.0288			
Variance, mm2	0.0009			
Coef. of Variance, %	129.80			

Percentiles [Weight, %]	Particle Diameter [in]	[mm]	[phi]
5	0.0031	0.0805	3.6349
10	0.0023	0.0593	4.0749
16	0.0018	0.0455	4.4565
25	0.0012	0.0319	4.9716
50	0.0004	0.0110	6.5110
75	0.0001	0.0035	8.1523
84	0.0001	0.0021	8.8885
90	0.0001	0.0013	9.5609
95	0.0000	0.0007	10.4002

The analyses, opinions or interpretations contained in this report are based upon observations and material supplied by the client for whose exclusive and confidential use this report has been made. The interpretations or opinions expressed represent the best judgment of Core Laboratories. Core Laboratories however, assumes no responsibility and makes no warranty or representations, express or implied, as to the productivity, proper operations, or profitableness of any oil, gas, coal or other mineral property, well or sand in connection with which such report is used or relied upon for any reason whatsoever. This report shall not be reproduced except in its entirety, without the written approval of Core Laboratories.

CORELAB

CORE LABORATORIES

Company	CORE LAB. - AURORA	Sample	P1-80-80	File Number	57111-95334
I.D.	954427-2	Proj.	Magma Florence	Date	11-OCT-95
County		State		Analysts	GC

Laser Particle Size Analysis

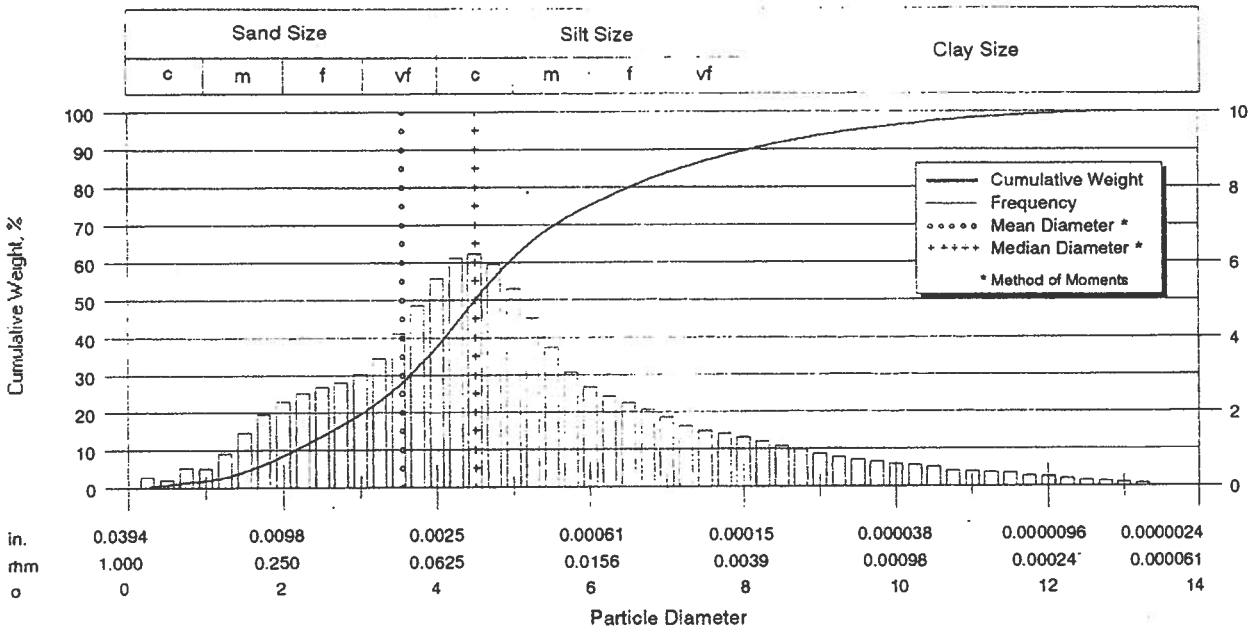

Particle Size Distribution

	[U.S. Sieve]	Diameter [in]	[mm]	[phi]	Weight, % [Inc.]	[Cum.]
Coarse Sand	20	0.0331	0.84	0.25	0.58	0.58
	25	0.0280	0.71	0.50	0.20	0.78
	30	0.0232	0.59	0.75	0.52	1.30
	35	0.0197	0.50	1.00	0.52	1.82
Medium Sand	40	0.0165	0.42	1.25	0.90	2.72
	45	0.0138	0.35	1.50	1.45	4.17
	50	0.0118	0.30	1.75	1.96	6.13
	60	0.0098	0.25	2.00	2.29	8.42
Fine Sand	70	0.0083	0.210	2.25	2.52	10.94
	80	0.0070	0.177	2.50	2.69	13.63
	100	0.0059	0.149	2.75	2.81	16.44
	120	0.0049	0.125	3.00	3.03	19.47
Very Fine Sand	140	0.0041	0.105	3.25	3.46	22.93
	170	0.0035	0.088	3.50	4.11	27.04
	200	0.0029	0.074	3.75	4.85	31.89
	230	0.0025	0.063	4.00	5.58	37.47
Silt	270	0.0021	0.053	4.25	6.12	43.59
	325	0.0017	0.044	4.50	6.24	49.83
	400	0.0015	0.037	4.75	5.93	55.76
	450	0.0012	0.031	5.00	5.29	61.05
	500	0.0010	0.025	5.32	5.64	66.69
	635	0.0008	0.020	5.64	4.39	71.08
		0.00061	0.0156	6.00	3.94	75.02
		0.00031	0.0078	7.00	8.57	83.59
		0.00015	0.0039	8.00	5.83	89.42
Clay		0.000079	0.0020	9.00	4.13	93.55
		0.000039	0.00098	10.0	2.73	96.28
		0.000019	0.00049	11.0	1.88	98.16
		0.0000094	0.00024	12.0	1.20	99.36
		0.0000047	0.00012	13.0	0.57	99.93
		0.0000039	0.00010	13.3	0.07	100.00

Sorting Statistics

Parameter	[Moment]	[Trask]	[Inman]	[Folk]
Mean, in	0.0033	0.0015	0.0013	0.0014
Mean, mm	0.0854	0.0388	0.0338	0.0369
Mean, phi	3.5495	4.6896	4.8856	4.7592
Median, in	0.0017	0.0017	0.0017	0.0017
Median, mm	0.0440	0.0440	0.0440	0.0440
Median, phi	4.5067	4.5065	4.5065	4.5065
Std Deviation, in	0.0047	0.0155	0.0086	0.0080
Std Deviation, mm	0.1217	0.3973	0.2215	0.2058
Std Deviation, phi	3.0386	1.3318	2.1745	2.2808
Skewness	3.0590	0.9986	0.4808	0.2199
Kurtosis	11.7700	0.2194	0.8113	1.2338
Mode, mm	0.0511			
95% Confidence	0.0616			
Limits, mm	0.1093			
Variance, mm2	0.0148			
Coef. of Variance, %	142.50			

Percentiles [Weight, %]	Particle Diameter [in]	[mm]	[phi]
5	0.0127	0.3268	1.6134
10	0.0087	0.2242	2.1572
16	0.0060	0.1527	2.7111
25	0.0037	0.0960	3.3813
50	0.0017	0.0440	4.5065
75	0.0006	0.0156	5.9979
84	0.0003	0.0075	7.0600
90	0.0001	0.0036	8.1190
95	0.0001	0.0014	9.4907

The analyses, opinions or interpretations contained in this report are based upon observations and material supplied by the client for whose exclusive and confidential use this report has been made. The interpretations or opinions expressed represent the best judgment of Core Laboratories. Core Laboratories, however, assumes no responsibility and makes no warranty or representations, express or implied, as to the productivity, proper operations, or profitableness of any oil, gas, coal or other mineral property, well or sand in connection with which such report is used or relied upon for any reason whatsoever. This report shall not be reproduced except in its entirety, without the written approval of Core Laboratories.

CORE LABORATORIES

Company	CORE LAB. - AURORA	Sample	P2-90-45	File Number	57111-95334
I.D.	954427-3	Proj.	Magma Florence	Date	11-OCT-95
County		State		Analysts	GC

Laser Particle Size Analysis

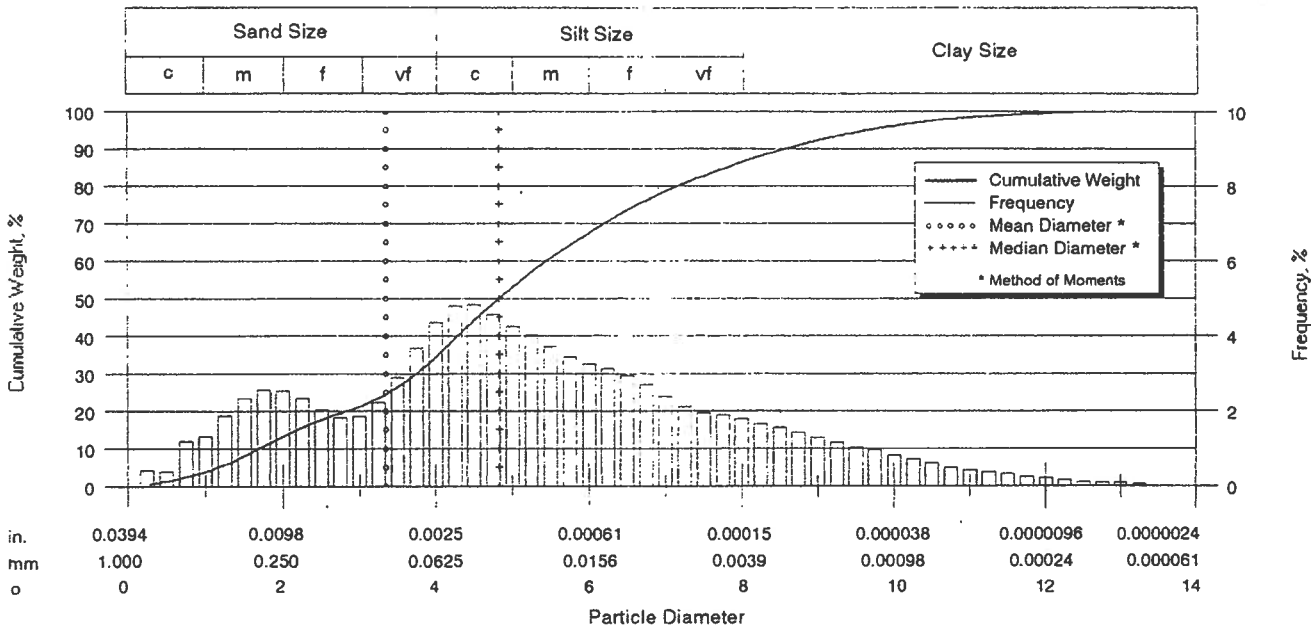

Particle Size Distribution

	[U.S. Sieve]	Diameter [in]	[mm]	[phi]	Weight, % [Inc.]	[Cum.]
Coarse Sand	20	0.0331	0.84	0.25	0.95	0.95
	25	0.0280	0.71	0.50	0.39	1.34
	30	0.0232	0.59	0.75	1.19	2.53
	35	0.0197	0.50	1.00	1.34	3.87
Medium Sand	40	0.0165	0.42	1.25	1.86	5.73
	45	0.0138	0.35	1.50	2.34	8.07
	50	0.0118	0.30	1.75	2.57	10.64
	60	0.0098	0.25	2.00	2.55	13.19
Fine Sand	70	0.0083	0.210	2.25	2.35	15.54
	80	0.0070	0.177	2.50	2.03	17.57
	100	0.0059	0.149	2.75	1.82	19.39
	120	0.0049	0.125	3.00	1.85	21.24
Very Fine Sand	140	0.0041	0.105	3.25	2.22	23.46
	170	0.0035	0.088	3.50	2.90	26.36
	200	0.0029	0.074	3.75	3.68	30.04
	230	0.0025	0.063	4.00	4.37	34.41
Silt	270	0.0021	0.053	4.25	4.80	39.21
	325	0.0017	0.044	4.50	4.85	44.06
	400	0.0015	0.037	4.75	4.56	48.62
	450	0.0012	0.031	5.00	4.26	52.88
	500	0.0010	0.025	5.32	5.08	57.96
	635	0.0008	0.020	5.64	4.60	62.56
		0.00061	0.0156	6.00	4.74	67.30
		0.00031	0.0078	7.00	11.16	78.46
		0.00015	0.0039	8.00	7.73	86.19
Clay		0.000079	0.0020	9.00	5.92	92.11
		0.000039	0.00098	10.0	3.95	96.06
		0.000019	0.00049	11.0	2.28	98.34
		0.0000094	0.00024	12.0	1.15	99.49
		0.0000047	0.00012	13.0	0.46	99.95
		0.0000039	0.00010	13.3	0.05	100.00

Sorting Statistics

Parameter	[Moment]	[Trask]	[Inman]	[Folk]
Mean, in	0.0038	0.0012	0.0012	0.0013
Mean, mm	0.0981	0.0308	0.0313	0.0325
Mean, phi	3.3498	5.0195	4.9989	4.9421
Median, in	0.0014	0.0014	0.0014	0.0014
Median, mm	0.0352	0.0352	0.0352	0.0352
Median, phi	4.8287	4.8286	4.8286	4.8286
Std Deviation, in	0.0060	0.0148	0.0060	0.0063
Std Deviation, mm	0.1551	0.3789	0.1544	0.1606
Std Deviation, phi	2.6887	1.4001	2.6952	2.6387
Skewness	2.4990	0.9669	0.2200	0.1012
Kurtosis	6.4300	0.2355	0.5809	1.0724
Mode, mm	0.0511			
95% Confidence Limits, mm	0.0677 – 0.1285			
Variance, mm2	0.0241			
Coef. of Variance, %	158.10			

Percentiles [Weight, %]	Particle Diameter [in]	[mm]	[phi]
5	0.0174	0.4472	1.1609
10	0.0121	0.3104	1.6877
16	0.0079	0.2025	2.3037
25	0.0037	0.0953	3.3911
50	0.0014	0.0352	4.8286
75	0.0004	0.0100	6.6479
84	0.0002	0.0048	7.6941
90	0.0001	0.0026	8.6029
95	0.0000	0.0012	9.6825

The analyses, opinions or interpretations contained in this report are based upon observations and material supplied by the client for whose exclusive and confidential use this report has been made. The interpretations or opinions expressed represent the best judgment of Core Laboratories. Core Laboratories, however assumes no responsibility and makes no warranty or representations, express or implied, as to the productivity, proper operations, or profitableness of any oil, gas, coal or other mineral, property, well or sand in connection with which such report is used or relied upon for any reason whatsoever. This report shall not be reproduced except in its entirety, without the written approval of Core Laboratories.

CORE LABORATORIES

Company	CORE LAB. - AURORA	Sample	P2-90-70	File Number	57111-95334
I.D.	954427-4	Proj.	Magma Florence	Date	11-OCT-95
County		State		Analysts	GC

Sieve and Laser Particle Size Analysis

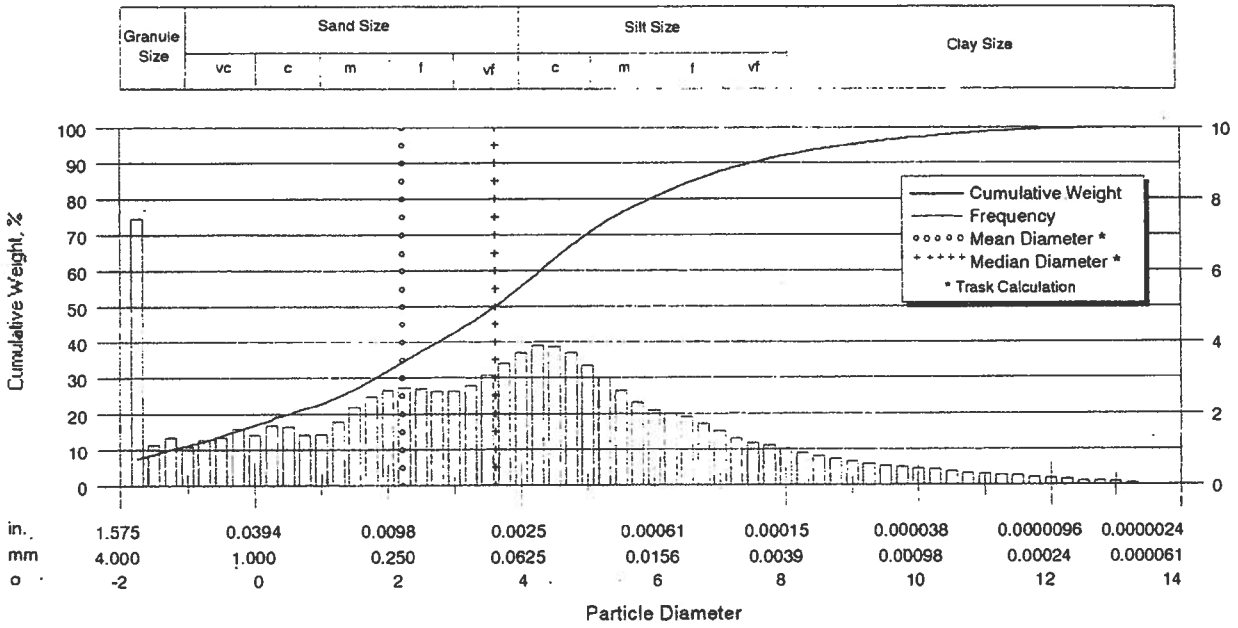

Particle Size Distribution

	[U.S. Sieve]	[in]	[mm]	[phi]	Weight, % [Inc.]	[Cum.]
Granule	6	0.1324	3.36	-1.75	7.46	7.46
	8	0.0936	2.38	-1.25	2.46	9.92
V Coarse Sand	12	0.0662	1.68	-0.75	2.35	12.27
	16	0.0468	1.19	-0.25	2.93	15.20
	20	0.0331	0.84	0.25	3.08	18.28
Coarse Sand	25	0.0280	0.71	0.50	1.63	19.91
	30	0.0232	0.59	0.75	1.42	21.33
	35	0.0197	0.50	1.00	1.43	22.76
	40	0.0165	0.42	1.25	1.78	24.54
Medium Sand	45	0.0138	0.35	1.50	2.18	26.72
	50	0.0118	0.30	1.75	2.47	29.19
	60	0.0098	0.25	2.00	2.66	31.85
	70	0.0083	0.210	2.25	2.74	34.59
Fine Sand	80	0.0070	0.177	2.50	2.70	37.29
	100	0.0059	0.149	2.75	2.63	39.92
	120	0.0049	0.125	3.00	2.63	42.55
	140	0.0041	0.105	3.25	2.77	45.32
Very Fine Sand	170	0.0035	0.088	3.50	3.08	48.40
	200	0.0029	0.074	3.75	3.39	51.79
	230	0.0025	0.063	4.00	3.70	55.49
	270	0.0021	0.053	4.25	3.90	59.39
Silt	325	0.0017	0.044	4.50	3.90	63.29
	400	0.0015	0.037	4.75	3.67	66.96
	450	0.0012	0.031	5.00	3.35	70.31
	500	0.0010	0.025	5.32	3.79	74.10
	635	0.0008	0.020	5.64	3.17	77.27
		0.00061	0.0156	6.00	3.07	80.34
		0.00031	0.0078	7.00	7.09	87.43
		0.00015	0.0039	8.00	4.58	92.01
		0.000079	0.0020	9.00	3.09	95.10
Clay		0.000039	0.00098	10.0	2.05	97.15
		0.000019	0.00049	11.0	1.43	98.58
		0.0000094	0.00024	12.0	0.93	99.51
		0.0000047	0.00012	13.0	0.44	99.95
		0.0000039	0.00010	13.3	0.05	100.00

Sorting Statistics

Parameter	Trask*	Inman**	Folk**
Mean, in	0.0083	0.0043	0.0039
Mean, mm	0.2139	0.1112	0.1002
Mean, phi	2.2249	3.1682	3.3191
Median, in	0.0032	0.0032	0.0032
Median, mm	0.0813	0.0813	0.0813
Median, phi	3.6209	3.6209	3.6209
Standard Deviation, in	0.1614	0.0039	
Standard Deviation, mm	4.1392	0.1013	
Standard Deviation, phi	-2.0493	3.3036	
Skewness	1.4436		
Kurtosis	0.0810		

* calculated using mm values
* *calculated using phi values

Percentiles [weight, %]	Particle Diameter [in]	[mm]	[phi]
5	ERR 5	ERR 5	ERR 5
10	0.0918	2.3543	-1.2353
16	0.0428	1.0983	-0.1353
25	0.0158	0.4042	1.3068
50	0.0032	0.0813	3.6209
75	0.0009	0.0236	5.4054
84	0.0004	0.0113	6.4718
90	0.0002	0.0054	7.5201
95	0.0001	0.0020	8.9587

The analyses, opinions or interpretations contained in this report are based upon observations and material supplied by the client for whose exclusive and confidential use this report has been made. The interpretations or opinions expressed represent the best judgment of Core Laboratories. Core Laboratories, however, assumes no responsibility and makes no warranty or representations, express or implied, as to the productivity, proper operations, or profitableness of any oil, gas, coal or other mineral, property, well or sand in connection with which such report is used or relied upon for any reason whatsoever. This report shall not be reproduced except in its entirety, without the written approval of Core Laboratories.

CORE LABORATORIES

Company	CORE LAB. - AURORA	Sample	B1-35	File Number	57111-95334
I.D.	954427-5	Proj.	Magma Florence	Date	11-OCT-95
County		State		Analysts	GC

Laser Particle Size Analysis

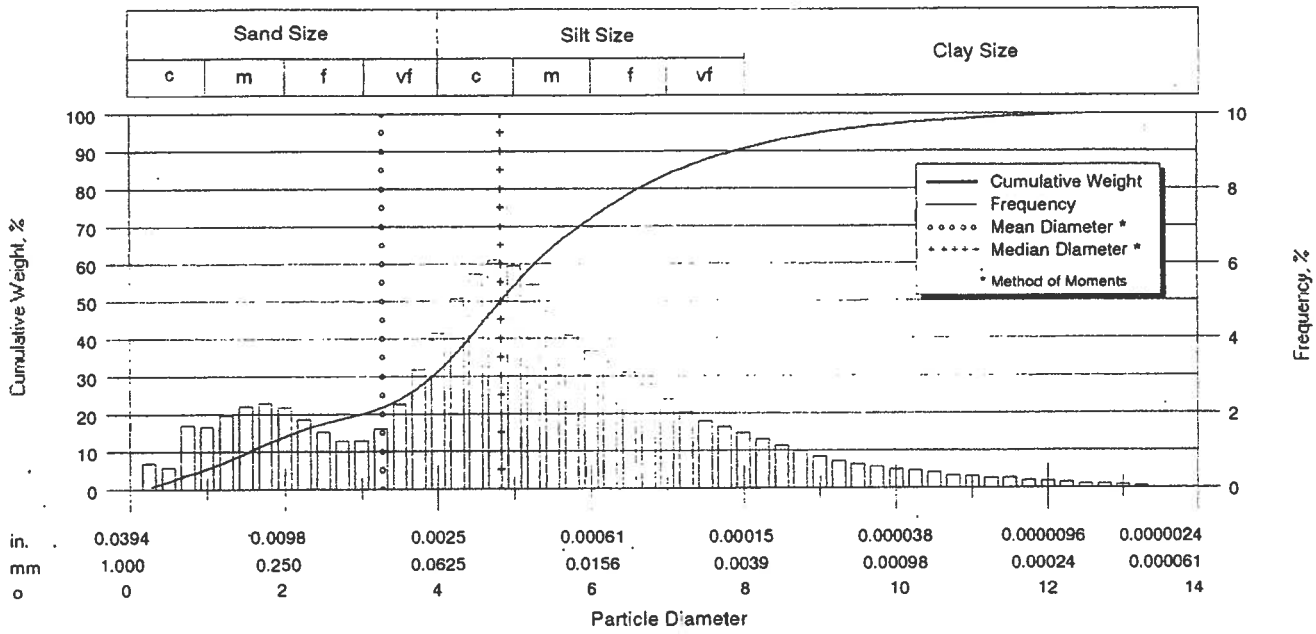

Particle Size Distribution

	[U.S. Sieve]	Diameter [in]	[mm]	[phi]	Weight, % [Inc.]	[Cum.]
Coarse Sand	20	0.0331	0.84	0.25	1.47	1.47
	25	0.0280	0.71	0.50	0.57	2.04
	30	0.0232	0.59	0.75	1.68	3.72
	35	0.0197	0.50	1.00	1.64	5.36
Medium Sand	40	0.0165	0.42	1.25	1.97	7.33
	45	0.0138	0.35	1.50	2.22	9.55
	50	0.0118	0.30	1.75	2.30	11.85
	60	0.0098	0.25	2.00	2.17	14.02
Fine Sand	70	0.0083	0.210	2.25	1.87	15.89
	80	0.0070	0.177	2.50	1.52	17.41
	100	0.0059	0.149	2.75	1.28	18.69
	120	0.0049	0.125	3.00	1.29	19.98
Very Fine Sand	140	0.0041	0.105	3.25	1.61	21.59
	170	0.0035	0.088	3.50	2.26	23.85
	200	0.0029	0.074	3.75	3.17	27.02
	230	0.0025	0.063	4.00	4.14	31.16
Silt	270	0.0021	0.053	4.25	5.06	36.22
	325	0.0017	0.044	4.50	5.75	41.97
	400	0.0015	0.037	4.75	6.06	48.03
	450	0.0012	0.031	5.00	5.95	53.98
	500	0.0010	0.025	5.32	6.84	60.82
	635	0.0008	0.020	5.64	5.68	66.50
		0.00061	0.0156	6.00	5.38	71.88
		0.00031	0.0078	7.00	11.64	83.52
		0.00015	0.0039	8.00	6.92	90.44
Clay		0.000079	0.0020	9.00	4.25	94.69
		0.000039	0.00098	10.0	2.41	97.10
		0.000019	0.00049	11.0	1.50	98.60
		0.0000094	0.00024	12.0	0.91	99.51
		0.0000047	0.00012	13.0	0.44	99.95
		0.0000039	0.00010	13.3	0.05	100.00

Sorting Statistics

Parameter	[Moment]	[Trask]	[Inman]	[Folk]
Mean, in	0.0040	0.0013	0.0015	0.0015
Mean, mm	0.1036	0.0331	0.0395	0.0380
Mean, phi	3.2709	4.9156	4.6609	4.7174
Median, in	0.0014	0.0014	0.0014	0.0014
Median, mm	0.0352	0.0351	0.0351	0.0351
Median, phi	4.8303	4.8305	4.8305	4.8305
Std Deviation, in	0.0067	0.0157	0.0074	0.0072
Std Deviation, mm	0.1707	0.4018	0.1901	0.1852
Std Deviation, phi	2.5505	1.3155	2.3950	2.4327
Skewness	2.4870	0.9614	0.0821	-0.0113
Kurtosis	5.8340	0.2063	0.7020	1.2704
Mode, mm	0.0389			
95% Confidence Limits, mm	0.0702 0.1371			
Variance, mm2	0.0291			
Coef. of Variance, %	164.70			

Percentiles [Weight, %]	Particle Diameter [in]	[mm]	[phi]
5	0.0202	0.5174	0.9508
10	0.0133	0.3419	1.5482
16	0.0081	0.2079	2.2659
25	0.0032	0.0824	3.6005
50	0.0014	0.0351	4.8305
75	0.0005	0.0133	6.2306
84	0.0003	0.0075	7.0558
90	0.0002	0.0041	7.9224
95	0.0001	0.0018	9.1034

The analyses, opinions or interpretations contained in this report are based upon observations and material supplied by the client for whose exclusive and confidential use this report has been made. The interpretations or opinions expressed represent the best judgment of Core Laboratories. Core Laboratories, however, assumes no responsibility and makes no warranty or representations, express or implied, as to the productivity, proper operations, or profitableness of any oil, gas, coal or other mineral, property, well or sand in connection with which such report is used or relied upon for any reason whatsoever. This report shall not be reproduced except in its entirety, without the written approval of Core Laboratories.

CORE LABORATORIES

Company	CORE LAB. - AURORA	Sample	B1-90	File Number	57111-95334
I.D.	954427-6	Proj.	Magma Florence	Date	11-OCT-95
County		State		Analysts	GC

Sieve and Laser Particle Size Analysis

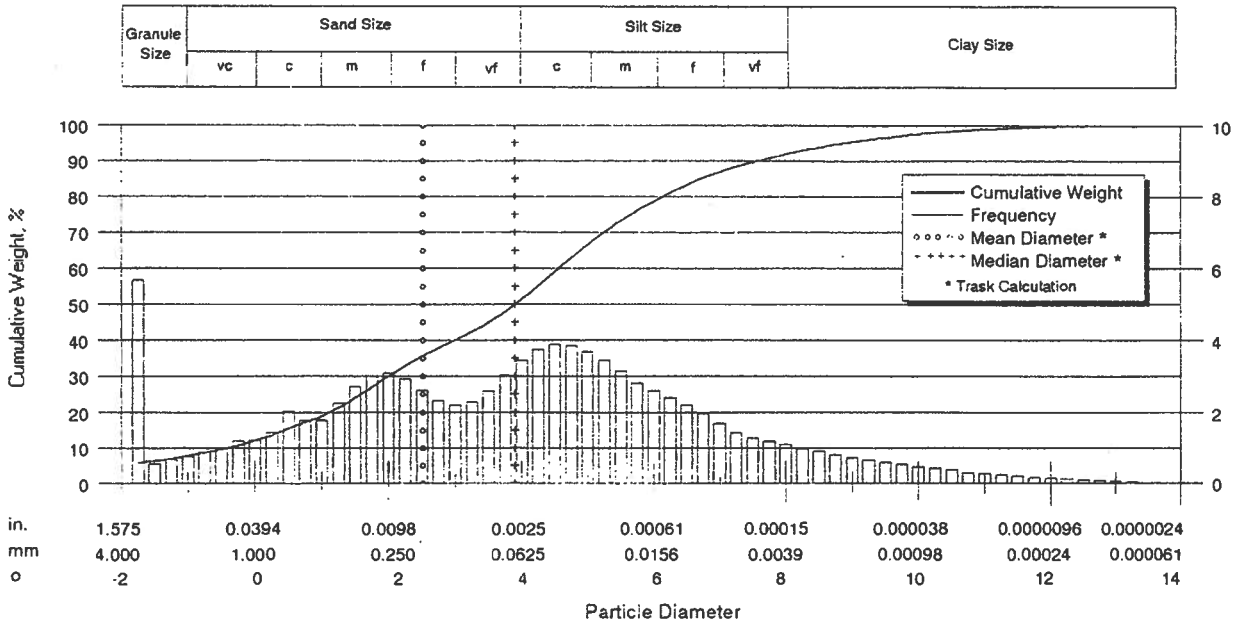

Particle Size Distribution

	[U.S. Sieve]	Diameter [in]	[mm]	[phi]	Weight, % [Inc.]	[Cum.]
Granule	6	0.1324	3.36	-1.75	5.67	5.67
	8	0.0936	2.38	-1.25	1.22	6.88
V Coarse Sand	12	0.0662	1.68	-0.75	1.64	8.52
	16	0.0468	1.19	-0.25	2.21	10.73
	20	0.0331	0.84	0.25	2.66	13.39
Coarse Sand	25	0.0280	0.71	0.50	2.03	15.42
	30	0.0232	0.59	0.75	1.76	17.18
	35	0.0197	0.50	1.00	1.78	18.96
	40	0.0165	0.42	1.25	2.24	21.20
Medium Sand	45	0.0138	0.35	1.50	2.71	23.91
	50	0.0118	0.30	1.75	3.01	26.92
	60	0.0098	0.25	2.00	3.10	30.02
	70	0.0083	0.210	2.25	2.92	32.94
Fine Sand	80	0.0070	0.177	2.50	2.61	35.55
	100	0.0059	0.149	2.75	2.32	37.87
	120	0.0049	0.125	3.00	2.19	40.06
	140	0.0041	0.105	3.25	2.29	42.35
Very Fine Sand	170	0.0035	0.088	3.50	2.59	44.94
	200	0.0029	0.074	3.75	3.03	47.97
	230	0.0025	0.063	4.00	3.45	51.42
	270	0.0021	0.053	4.25	3.75	55.17
Silt	325	0.0017	0.044	4.50	3.89	59.06
	400	0.0015	0.037	4.75	3.83	62.89
	450	0.0012	0.031	5.00	3.69	66.58
	500	0.0010	0.025	5.32	4.38	70.96
	635	0.0008	0.020	5.64	3.84	74.80
		0.00061	0.0156	6.00	3.78	78.58
		0.00031	0.0078	7.00	8.26	86.84
		0.00015	0.0039	8.00	4.98	91.82
		0.000079	0.0020	9.00	3.44	95.26
Clay		0.000039	0.00098	10.0	2.26	97.52
		0.000019	0.00049	11.0	1.37	98.89
		0.0000094	0.00024	12.0	0.75	99.64
		0.0000047	0.00012	13.0	0.33	99.97
		0.0000039	0.00010	13.3	0.03	100.00

Sorting Statistics

Parameter	Trask*	Inman**	Folk**
Mean, in	0.0068	0.0032	0.0030
Mean, mm	0.1756	0.0830	0.0773
Mean, phi	2.5097	3.5905	3.6937
Median, in	0.0026	0.0026	0.0026
Median, mm	0.0670	0.0670	0.0670
Median, phi	3.9000	3.9000	3.9000
Standard Deviation, in	0.1596	0.0048	
Standard Deviation, mm	4.0914	0.1243	
Standard Deviation, phi	-2.0326	3.0085	
Skewness	1.4621		
Kurtosis	0.1156		

* calculated using mm values
* *calculated using phi values

Percentiles [weight, %]	Particle Diameter [in]	[mm]	[phi]
5	ERR 5	ERR 5	ERR 5
10	0.0528	1.3527	-0.4359
16	0.0261	0.6680	0.5820
25	0.0129	0.3314	1.5934
50	0.0026	0.0670	3.9000
75	0.0008	0.0198	5.6586
84	0.0004	0.0103	6.5990
90	0.0002	0.0052	7.5926
95	0.0001	0.0021	8.9080

The analyses, opinions or interpretations contained in this report are based upon observations and material supplied by the client for whose exclusive and confidential use this report has been made. The interpretations or opinions expressed represent the best judgment of Core Laboratories. Core Laboratories, however, assumes no responsibility and makes no warranty or representations, express or implied, as to the productivity, proper operations, or profitableness of any oil, gas, coal or other mineral property, well or sand in connection with which such report is used or relied upon for any reason whatsoever. This report shall not be reproduced except in its entirety, without the written approval of Core Laboratories.

CORELAB

CORE LABORATORIES

Company	CORE LAB. - AURORA	Sample	B2-55	File Number	57111-95334
I.D.	954427-7	Proj.	Magma Florence	Date	11-OCT-95
County		State		Analysts	GC

Sieve and Laser Particle Size Analysis

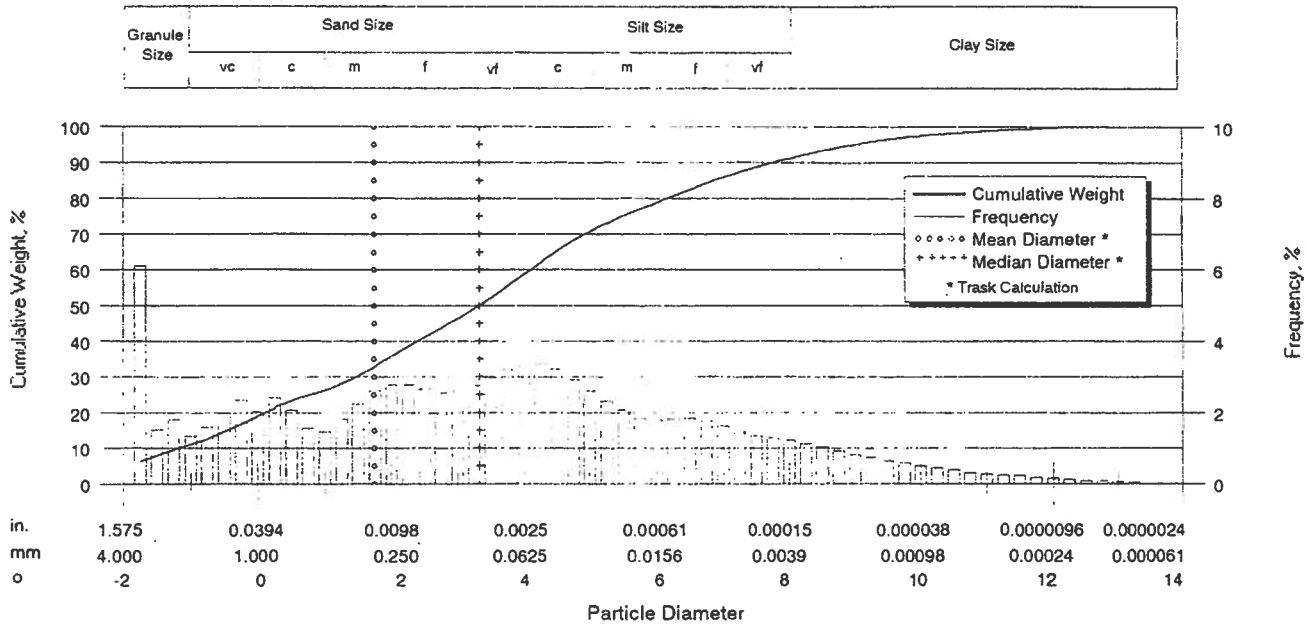

Particle Size Distribution

	[U.S. Sieve]	Diameter [in]	[mm]	[phi]	Weight, % [Inc.]	[Cum.]
Granule	6	0.1324	3.36	-1.75	6.11	6.11
	8	0.0936	2.38	-1.25	3.32	9.42
V Coarse	12	0.0662	1.68	-0.75	2.93	12.35
Sand	16	0.0468	1.19	-0.25	4.32	16.68
	20	0.0331	0.84	0.25	4.45	21.12
Coarse	25	0.0280	0.71	0.50	2.06	23.18
Sand	30	0.0232	0.59	0.75	1.57	24.75
	35	0.0197	0.50	1.00	1.45	26.20
	40	0.0165	0.42	1.25	1.83	28.03
Medium	45	0.0138	0.35	1.50	2.25	30.28
Sand	50	0.0118	0.30	1.75	2.61	32.89
	60	0.0098	0.25	2.00	2.79	35.68
	70	0.0083	0.210	2.25	2.77	38.45
Fine	80	0.0070	0.177	2.50	2.66	41.11
Sand	100	0.0059	0.149	2.75	2.56	43.67
	120	0.0049	0.125	3.00	2.60	46.27
	140	0.0041	0.105	3.25	2.76	49.03
Very Fine	170	0.0035	0.088	3.50	2.99	52.02
Sand	200	0.0029	0.074	3.75	3.21	55.23
	230	0.0025	0.063	4.00	3.33	58.56
	270	0.0021	0.053	4.25	3.36	61.92
Silt	325	0.0017	0.044	4.50	3.23	65.15
	400	0.0015	0.037	4.75	2.94	68.09
	450	0.0012	0.031	5.00	2.60	70.69
	500	0.0010	0.025	5.32	2.92	73.61
	635	0.0008	0.020	5.64	2.50	76.11
		0.00061	0.0156	6.00	2.58	78.69
		0.00031	0.0078	7.00	7.06	85.75
		0.00015	0.0039	8.00	5.31	91.06
		0.000079	0.0020	9.00	3.86	94.92
Clay		0.000039	0.00098	10.0	2.45	97.37
		0.000019	0.00049	11.0	1.45	98.82
		0.0000094	0.00024	12.0	0.79	99.61
		0.0000047	0.00012	13.0	0.35	99.96
		0.0000039	0.00010	13.3	0.04	100.00

Sorting Statistics

Parameter	Trask*	Inman**	Folk**
Mean, in	0.0117	0.0043	0.0041
Mean, mm	0.2988	0.1092	0.1057
Mean, phi	1.7428	3.1953	3.2415
Median, in	0.0039	0.0039	0.0039
Median, mm	0.0992	0.0992	0.0992
Median, phi	3.3339	3.3339	3.3339
Standard Deviation, in	0.1984	0.0034	
Standard Deviation, mm	5.0879	0.0862	
Standard Deviation, phi	-2.3471	3.5360	
Skewness	1.3002		
Kurtosis	0.1236		

* calculated using mm values
* *calculated using phi values

Percentiles [weight, %]	Particle Diameter [in]	[mm]	[phi]
5	ERR 5	ERR 5	ERR 5
10	0.0874	2.2415	-1.1645
16	0.0494	1.2663	-0.3407
25	0.0224	0.5754	0.7975
50	0.0039	0.0992	3.3339
75	0.0009	0.0222	5.4916
84	0.0004	0.0094	6.7313
90	0.0002	0.0045	7.7816
95	0.0001	0.0019	9.0256

The analyses, opinions or interpretations contained in this report are based upon observations and material supplied by the client for whose exclusive and confidential use this report has been made. The interpretations or opinions expressed represent the best judgment of Core Laboratories. Core Laboratories, however, assumes no responsibility and makes no warranty or representations, express or implied, as to the productivity, proper operations, or profitableness of any oil, gas, coal or other mineral property, well or sand in connection with which such report is used or relied upon for any reason whatsoever. This report shall not be reproduced except in its entirety, without the written approval of Core Laboratories.

CORE LAB

CORE LABORATORIES

Company	CORE LAB. - AURORA	Sample	B2-75	File Number	57111-95334
I.D.	954427-8	Proj.	Magma Florence	Date	11-OCT-95
County		State		Analysts	GC

Sieve and Laser Particle Size Analysis

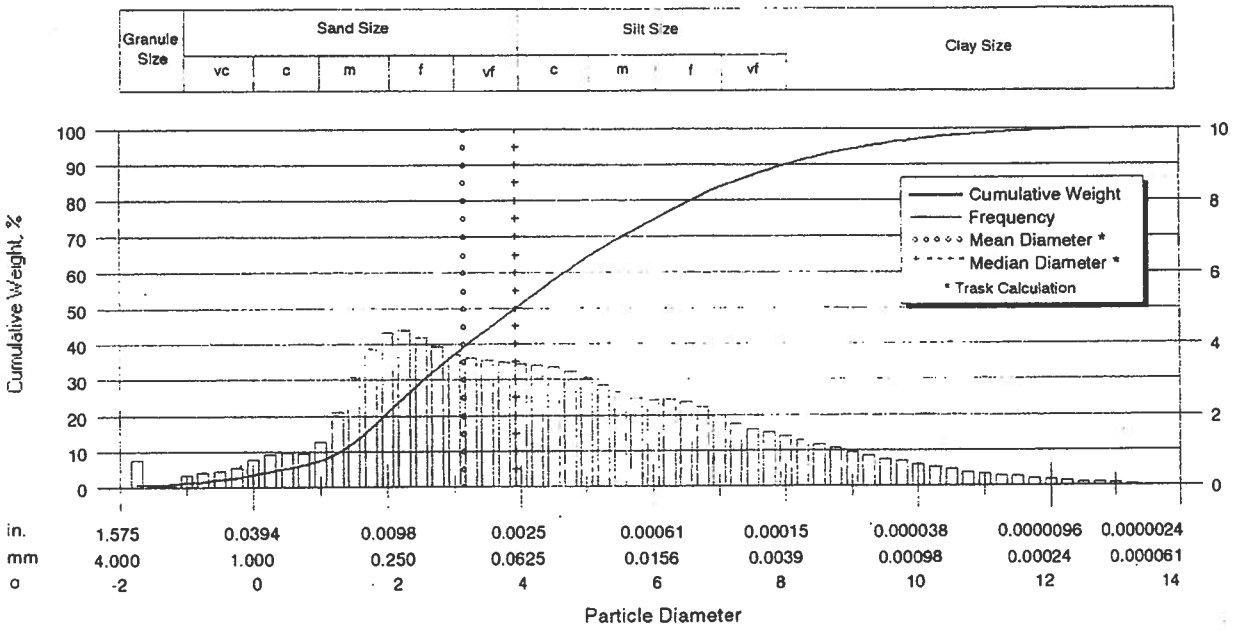

Particle Size Distribution

	[U.S. Sieve]	Diameter [in]	[mm]	[phi]	Weight, % [Inc.]	[Cum.]
Granule	6	0.1324	3.36	-1.75	0.75	0.75
	8	0.0936	2.38	-1.25	0.06	0.81
V Coarse	12	0.0662	1.68	-0.75	0.75	1.56
Sand	16	0.0468	1.19	-0.25	1.00	2.56
	20	0.0331	0.84	0.25	1.68	4.24
Coarse	25	0.0280	0.71	0.50	0.97	5.21
Sand	30	0.0232	0.59	0.75	0.94	6.15
	35	0.0197	0.50	1.00	1.26	7.41
	40	0.0165	0.42	1.25	2.09	9.50
Medium	45	0.0138	0.35	1.50	3.07	12.57
Sand	50	0.0118	0.30	1.75	3.87	16.44
	60	0.0098	0.25	2.00	4.32	20.76
	70	0.0083	0.210	2.25	4.39	25.15
Fine	80	0.0070	0.177	2.50	4.19	29.34
Sand	100	0.0059	0.149	2.75	3.92	33.26
	120	0.0049	0.125	3.00	3.72	36.98
	140	0.0041	0.105	3.25	3.60	40.58
Very Fine	170	0.0035	0.088	3.50	3.54	44.12
Sand	200	0.0029	0.074	3.75	3.48	47.60
	230	0.0025	0.063	4.00	3.44	51.04
	270	0.0021	0.053	4.25	3.39	54.43
Silt	325	0.0017	0.044	4.50	3.37	57.80
	400	0.0015	0.037	4.75	3.22	61.02
	450	0.0012	0.031	5.00	3.06	64.08
	500	0.0010	0.025	5.32	3.61	67.69
	635	0.0008	0.020	5.64	3.27	70.96
		0.00061	0.0156	6.00	3.51	74.47
		0.00031	0.0078	7.00	9.02	83.49
		0.00015	0.0039	8.00	6.26	89.75
		0.000079	0.0020	9.00	4.46	94.21
Clay		0.000039	0.00098	10.0	2.83	97.04
		0.000019	0.00049	11.0	1.65	98.69
		0.0000094	0.00024	12.0	0.89	99.58
		0.0000047	0.00012	13.0	0.38	99.96
		0.0000039	0.00010	13.3	0.04	100.00

Sorting Statistics

Parameter	Trask*	Inman**	Folk**
Mean, in	0.0044	0.0019	0.0021
Mean, mm	0.1133	0.0475	0.0529
Mean, phi	3.1421	4.3969	4.2394
Median, in	0.0026	0.0026	0.0026
Median, mm	0.0659	0.0659	0.0659
Median, phi	3.9244	3.9244	3.9244
Standard Deviation, in	0.1463	0.0061	0.0061
Standard Deviation, mm	3.7512	0.1569	0.1572
Standard Deviation, phi	-1.9074	2.6723	2.6694
Skewness	0.7329	0.3417	0.1922
Kurtosis	0.2437	0.6464	0.9453

* calculated using mm values
** calculated using phi values

Percentiles [weight, %]	Particle Diameter [in]	[mm]	[phi]
5	0.0288	0.7382	0.4379
10	0.0159	0.4069	1.2973
16	0.0118	0.3026	1.7246
25	0.0082	0.2115	2.2412
50	0.0026	0.0659	3.9244
75	0.0006	0.0150	6.0559
84	0.0003	0.0074	7.0692
90	0.0001	0.0038	8.0461
95	0.0001	0.0017	9.2371

The analyses, opinions or interpretations contained in this report are based upon observations and material supplied by the client for whose exclusive and confidential use this report has been made. The interpretations or opinions expressed represent the best judgment of Core Laboratories. Core Laboratories, however, assumes no responsibility and makes no warranty or representations, express or implied, as to the productivity, proper operations, or profitableness of any oil, gas, coal or other mineral property, well or sand in connection with which such report is used or relied upon for any reason whatsoever. This report shall not be reproduced except in its entirety, without the written approval of Core Laboratories.

CORELAB

CORE LABORATORIES

Company	CORE LAB. - AURORA	Sample	B3-10	File Number	57111-95334
I.D.	954427-9	Proj.	Magma Florence	Date	11-OCT-95
County		State		Analysts	GC

Sieve and Laser Particle Size Analysis

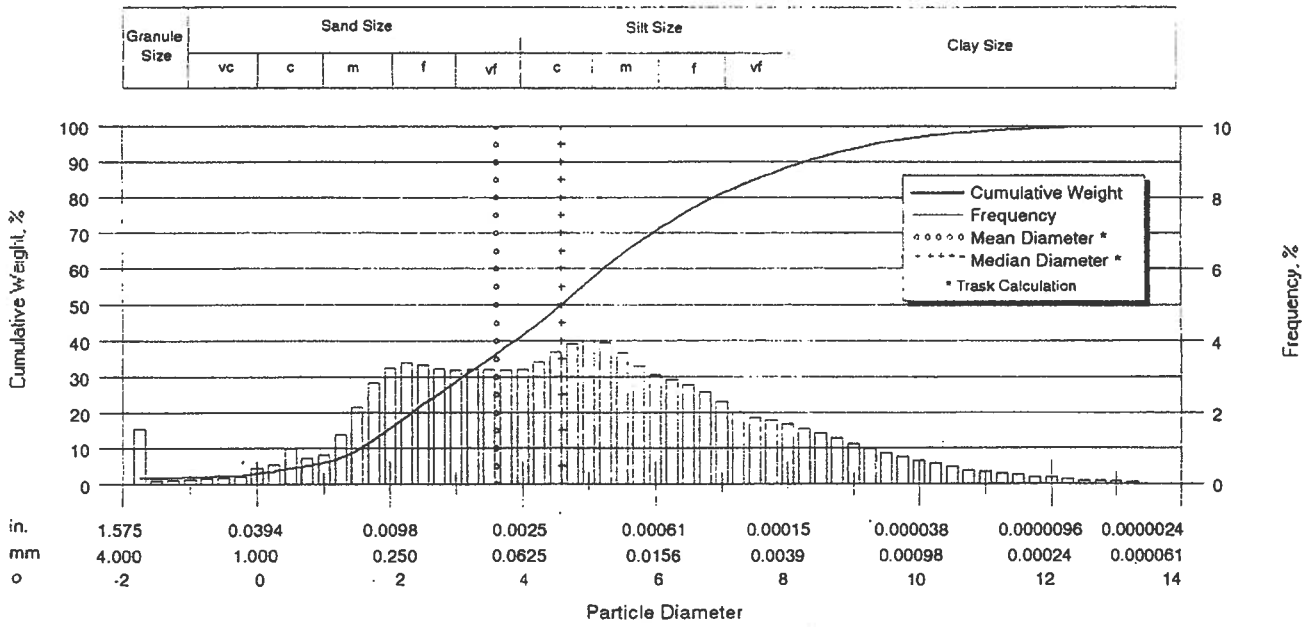

Particle Size Distribution

	[U.S. Sieve]	Diameter [in]	[mm]	[phi]	Weight, % [Inc.]	[Cum.]
Granule	6	0.1324	3.36	-1.75	1.53	1.53
	8	0.0936	2.38	-1.25	0.20	1.73
V Coarse Sand	12	0.0662	1.68	-0.75	0.27	2.00
	16	0.0468	1.19	-0.25	0.38	2.39
	20	0.0331	0.84	0.25	0.99	3.38
Coarse Sand	25	0.0280	0.71	0.50	0.97	4.35
	30	0.0232	0.59	0.75	0.71	5.06
	35	0.0197	0.50	1.00	0.81	5.87
	40	0.0165	0.42	1.25	1.38	7.25
Medium Sand	45	0.0138	0.35	1.50	2.15	9.40
	50	0.0118	0.30	1.75	2.84	12.24
	60	0.0098	0.25	2.00	3.24	15.48
	70	0.0083	0.210	2.25	3.40	18.88
Fine Sand	80	0.0070	0.177	2.50	3.33	22.21
	100	0.0059	0.149	2.75	3.23	25.44
	120	0.0049	0.125	3.00	3.20	28.64
	140	0.0041	0.105	3.25	3.20	31.84
Very Fine Sand	170	0.0035	0.088	3.50	3.22	35.06
	200	0.0029	0.074	3.75	3.18	38.24
	230	0.0025	0.063	4.00	3.22	41.46
	270	0.0021	0.053	4.25	3.41	44.87
Silt	325	0.0017	0.044	4.50	3.71	48.58
	400	0.0015	0.037	4.75	3.89	52.47
	450	0.0012	0.031	5.00	3.99	56.46
	500	0.0010	0.025	5.32	5.01	61.47
	635	0.0008	0.020	5.64	4.50	65.97
		0.00061	0.0156	6.00	4.46	70.43
		0.00031	0.0078	7.00	10.56	80.99
		0.00015	0.0039	8.00	7.32	88.31
		0.000079	0.0020	9.00	5.32	93.63
Clay		0.000039	0.00098	10.0	3.25	96.88
		0.000019	0.00049	11.0	1.77	98.65
		0.0000094	0.00024	12.0	0.92	99.57
		0.0000047	0.00012	13.0	0.38	99.95
		0.0000039	0.00010	13.3	0.05	100.00

Sorting Statistics

Parameter	Trask*	Inman**	Folk**
Mean, in	0.0032	0.0015	0.0015
Mean, mm	0.0821	0.0382	0.0393
Mean, phi	3.6067	4.7091	4.6700
Median, in	0.0016	0.0016	0.0016
Median, mm	0.0415	0.0415	0.0415
Median, phi	4.5917	4.5917	4.5917
Standard Deviation, in	0.1397	0.0061	0.0062
Standard Deviation, mm	3.5815	0.1569	0.1600
Standard Deviation, phi	-1.8406	2.6722	2.6437
Skewness	1.0514	0.1680	0.0740
Kurtosis	0.2085	0.6149	0.9609

* calculated using mm values
* *calculated using phi values

Percentiles [weight, %]	Particle Diameter [in]	[mm]	[phi]
5	0.0236	0.6048	0.7254
10	0.0133	0.3399	1.5567
16	0.0095	0.2437	2.0369
25	0.0059	0.1523	2.7150
50	0.0016	0.0415	4.5917
75	0.0005	0.0119	6.3961
84	0.0002	0.0060	7.3812
90	0.0001	0.0032	8.2768
95	0.0001	0.0015	9.3558

The analyses, opinions or interpretations contained in this report are based upon observations and material supplied by the client for whose exclusive and confidential use this report has been made. The interpretations or opinions expressed represent the best judgment of Core Laboratories. Core Laboratories, however, assumes no responsibility and makes no warranty or representations, express or implied, as to the productivity, proper operations, or profitableness of any oil, gas, coal or other mineral, property, well or sand in connection with which such report is used or relied upon for any reason whatsoever. This report shall not be reproduced except in its entirety, without the written approval of Core Laboratories.

CORELAB

CORE LABORATORIES

Company	CORE LAB. - AURORA	Sample	B3-45	File Number	57111-95334
I.D.	954427-10	Proj.	Magma Florence	Date	11-OCT-95
County		State		Analysts	GC

Laser Particle Size Analysis

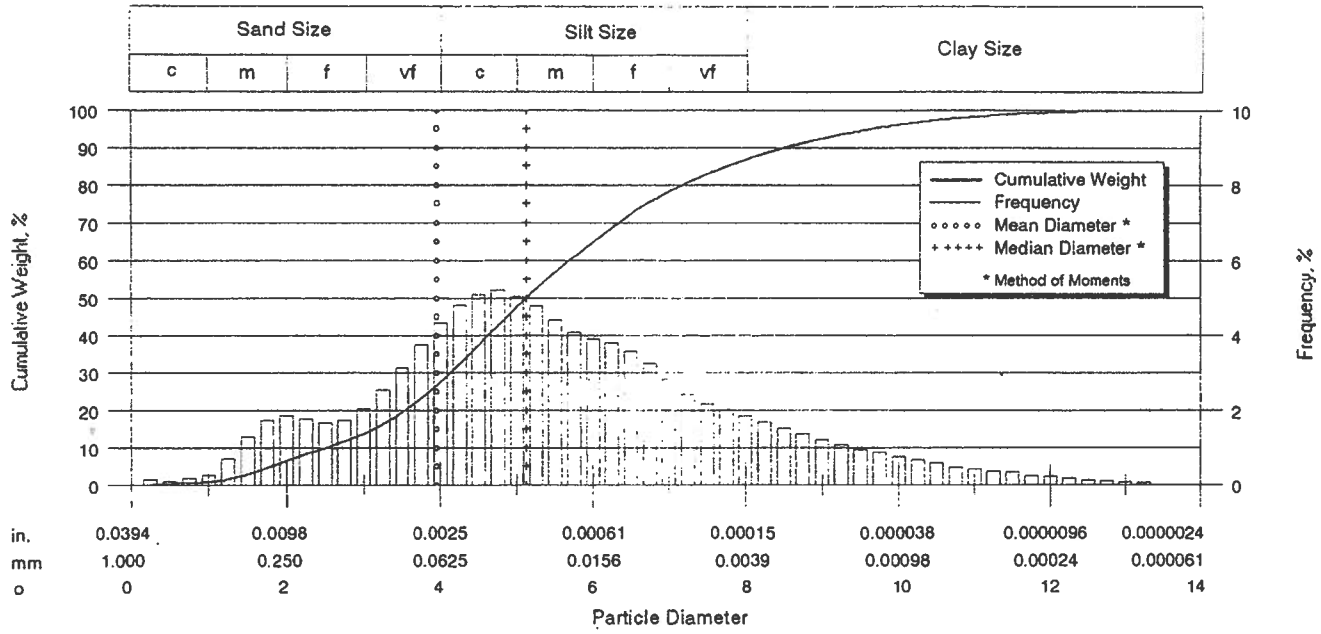

Particle Size Distribution

	[U.S. Sieve]	Diameter [in]	Diameter [mm]	Diameter [phi]	Weight, % [Inc.]	Weight, % [Cum.]
Coarse Sand	20	0.0331	0.84	0.25	0.33	0.33
	25	0.0280	0.71	0.50	0.09	0.42
	30	0.0232	0.59	0.75	0.19	0.61
	35	0.0197	0.50	1.00	0.26	0.87
Medium Sand	40	0.0165	0.42	1.25	0.71	1.58
	45	0.0138	0.35	1.50	1.30	2.88
	50	0.0118	0.30	1.75	1.74	4.62
	60	0.0098	0.25	2.00	1.87	6.49
Fine Sand	70	0.0083	0.210	2.25	1.78	8.27
	80	0.0070	0.177	2.50	1.67	9.94
	100	0.0059	0.149	2.75	1.73	11.67
	120	0.0049	0.125	3.00	2.04	13.71
Very Fine Sand	140	0.0041	0.105	3.25	2.54	16.25
	170	0.0035	0.088	3.50	3.12	19.37
	200	0.0029	0.074	3.75	3.75	23.12
	230	0.0025	0.063	4.00	4.32	27.44
Silt	270	0.0021	0.053	4.25	4.80	32.24
	325	0.0017	0.044	4.50	5.13	37.37
	400	0.0015	0.037	4.75	5.18	42.55
	450	0.0012	0.031	5.00	5.04	47.59
	500	0.0010	0.025	5.32	6.06	53.65
	635	0.0008	0.020	5.64	5.46	59.11
		0.00061	0.0156	6.00	5.66	64.77
		0.00031	0.0078	7.00	13.42	78.19
		0.00015	0.0039	8.00	8.46	86.65
Clay		0.000079	0.0020	9.00	5.78	92.43
		0.000039	0.00098	10.0	3.66	96.09
		0.000019	0.00049	11.0	2.17	98.26
		0.0000094	0.00024	12.0	1.18	99.44
		0.0000047	0.00012	13.0	0.50	99.94
		0.0000039	0.00010	13.3	0.06	100.00

Sorting Statistics

Parameter	[Moment]	[Trask]	[Inman]	[Folk]
Mean, in	0.0025	0.0010	0.0009	0.0010
Mean, mm	0.0649	0.0255	0.0231	0.0248
Mean, phi	3.9456	5.2916	5.4380	5.3334
Median, in	0.0011	0.0011	0.0011	0.0011
Median, mm	0.0287	0.0287	0.0287	0.0287
Median, phi	5.1243	5.1242	5.1242	5.1242
Std Deviation, in	0.0040	0.0156	0.0084	0.0079
Std Deviation, mm	0.1031	0.4008	0.2161	0.2038
Std Deviation, phi	3.2779	1.3189	2.2099	2.2947
Skewness	3.3970	0.9887	0.2723	0.1476
Kurtosis	15.2300	0.2375	0.7766	1.1264
Mode, mm	0.0426			
95% Confidence Limits, mm	0.0447 0.0851			
Variance, mm2	0.0106			
Coef. of Variance, %	158.80			

Percentiles [Weight, %]	Particle Diameter [in]	[mm]	[phi]
5	0.0112	0.2872	1.7998
10	0.0068	0.1755	2.5102
16	0.0042	0.1067	3.2280
25	0.0027	0.0687	3.8631
50	0.0011	0.0287	5.1242
75	0.0004	0.0095	6.7201
84	0.0002	0.0050	7.6479
90	0.0001	0.0027	8.5259
95	0.0000	0.0012	9.6520

The analyses, opinions or interpretations contained in this report are based upon observations and material supplied by the client for whose exclusive and confidential use this report has been made. The interpretations or opinions expressed represent the best judgment of Core Laboratories. Core Laboratories, however, assumes no responsibility and makes no warranty or representations, express or implied, as to the productivity, proper operations, or profitableness of any oil, gas, coal or other mineral, property, well or sand in connection with which such report is used or relied upon for any reason whatsoever. This report shall not be reproduced except in its entirety, without the written approval of Core Laboratories.

CORE LABORATORIES

Company	CORE LAB. - AURORA	Sample	B3-65	File Number	57111-95334
I.D.	954427-11	Proj.	Magma Florence	Date	11-OCT-95
County		State		Analysts	GC

Sieve and Laser Particle Size Analysis

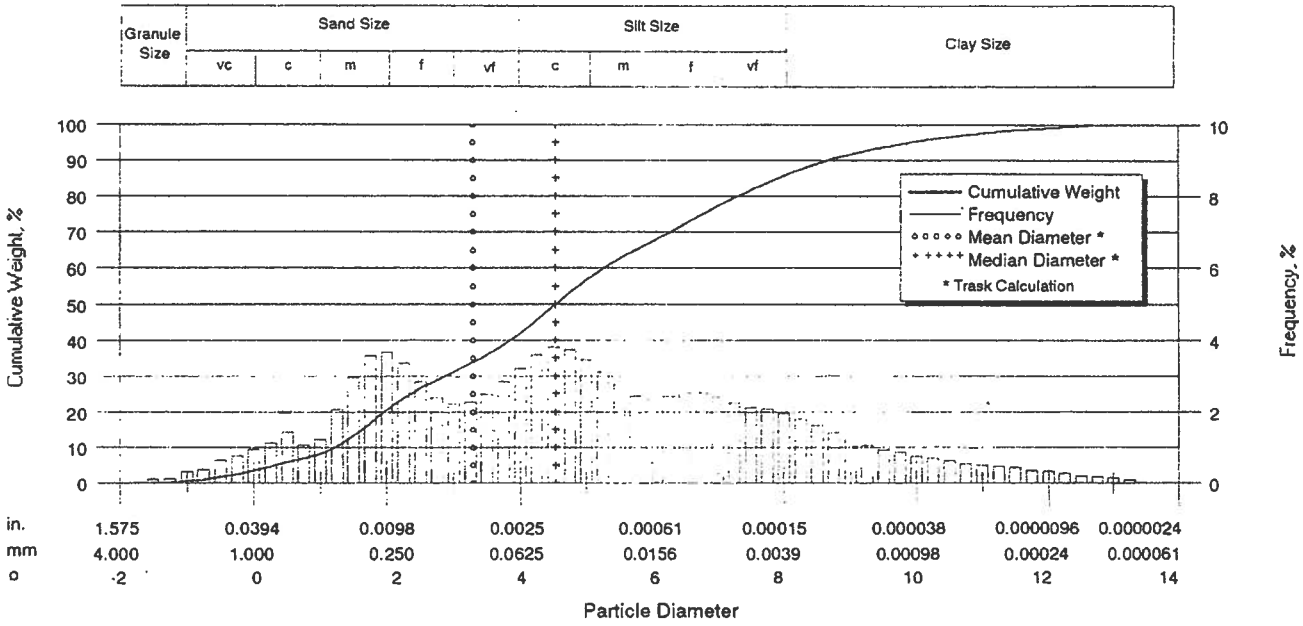

Particle Size Distribution

	[U.S. Sieve]	Diameter [in]	[mm]	[phi]	Weight, % [Inc.]	[Cum.]
Granule	6	0.1324	3.36	-1.75	0.00	0.00
	8	0.0936	2.38	-1.25	0.23	0.23
V Coarse Sand	12	0.0662	1.68	-0.75	0.70	0.93
	16	0.0468	1.19	-0.25	1.40	2.33
	20	0.0331	0.84	0.25	2.06	4.39
Coarse Sand	25	0.0280	0.71	0.50	1.42	5.81
	30	0.0232	0.59	0.75	1.08	6.89
	35	0.0197	0.50	1.00	1.22	8.11
	40	0.0165	0.42	1.25	2.05	10.16
Medium Sand	45	0.0138	0.35	1.50	2.98	13.14
	50	0.0118	0.30	1.75	3.56	16.70
	60	0.0098	0.25	2.00	3.67	20.37
	70	0.0083	0.210	2.25	3.36	23.73
Fine Sand	80	0.0070	0.177	2.50	2.85	26.58
	100	0.0059	0.149	2.75	2.40	28.98
	120	0.0049	0.125	3.00	2.21	31.19
	140	0.0041	0.105	3.25	2.26	33.45
Very Fine Sand	170	0.0035	0.088	3.50	2.50	35.95
	200	0.0029	0.074	3.75	2.84	38.79
	230	0.0025	0.063	4.00	3.21	42.00
	270	0.0021	0.053	4.25	3.59	45.59
Silt	325	0.0017	0.044	4.50	3.83	49.42
	400	0.0015	0.037	4.75	3.73	53.15
	450	0.0012	0.031	5.00	3.46	56.61
	500	0.0010	0.025	5.32	3.93	60.54
	635	0.0008	0.020	5.64	3.36	63.90
		0.00061	0.0156	6.00	3.39	67.29
		0.00031	0.0078	7.00	9.93	77.22
		0.00015	0.0039	8.00	8.38	85.60
		0.000079	0.0020	9.00	6.02	91.62
Clay		0.000039	0.00098	10.0	3.58	95.20
		0.000019	0.00049	11.0	2.35	97.55
		0.0000094	0.00024	12.0	1.58	99.13
		0.0000047	0.00012	13.0	0.77	99.90
		0.0000039	0.00010	13.3	0.10	100.00

Sorting Statistics

Parameter	Trask*	Inman**	Folk**
Mean, in	0.0040	0.0015	0.0015
Mean, mm	0.1023	0.0372	0.0391
Mean, phi	3.2897	4.7478	4.6777
Median, in	0.0017	0.0017	0.0017
Median, mm	0.0431	0.0431	0.0431
Median, phi	4.5373	4.5373	4.5373
Standard Deviation, in	0.1801	0.0047	0.0049
Standard Deviation, mm	4.6169	0.1211	0.1268
Standard Deviation, phi	-2.2069	3.0457	2.9794
Skewness	0.9653	0.1909	0.0951
Kurtosis	0.2204	0.5782	0.8926

* calculated using mm values
* *calculated using phi values

Percentiles [weight, %]	Particle Diameter [in]	[mm]	[phi]
5	0.0314	0.8054	0.3123
10	0.0166	0.4249	1.2347
16	0.0120	0.3073	1.7022
25	0.0076	0.1954	2.3558
50	0.0017	0.0431	4.5373
75	0.0004	0.0092	6.7697
84	0.0002	0.0045	7.7935
90	0.0001	0.0024	8.6768
95	0.0000	0.0010	9.9254

The analyses, opinions or interpretations contained in this report are based upon observations and material supplied by the client for whose exclusive and confidential use this report has been made. The interpretations or opinions expressed represent the best judgment of Core Laboratories. Core Laboratories, however, assumes no responsibility and makes no warranty or representations, express or implied, as to the productivity, proper operations, or profitableness of any oil, gas, coal or other mineral, property, well or sand in connection with which such report is used or relied upon for any reason whatsoever. This report shall not be reproduced except in its entirety, without the written approval of Core Laboratories.

CORE LAB

CORE LABORATORIES

Company	CORE LAB. - AURORA	Sample	B4-55	File Number	57111-95334
I.D.	954427-12	Proj.	Magma Florence	Date	11-OCT-95
County		State		Analysts	GC

Sieve and Laser Particle Size Analysis

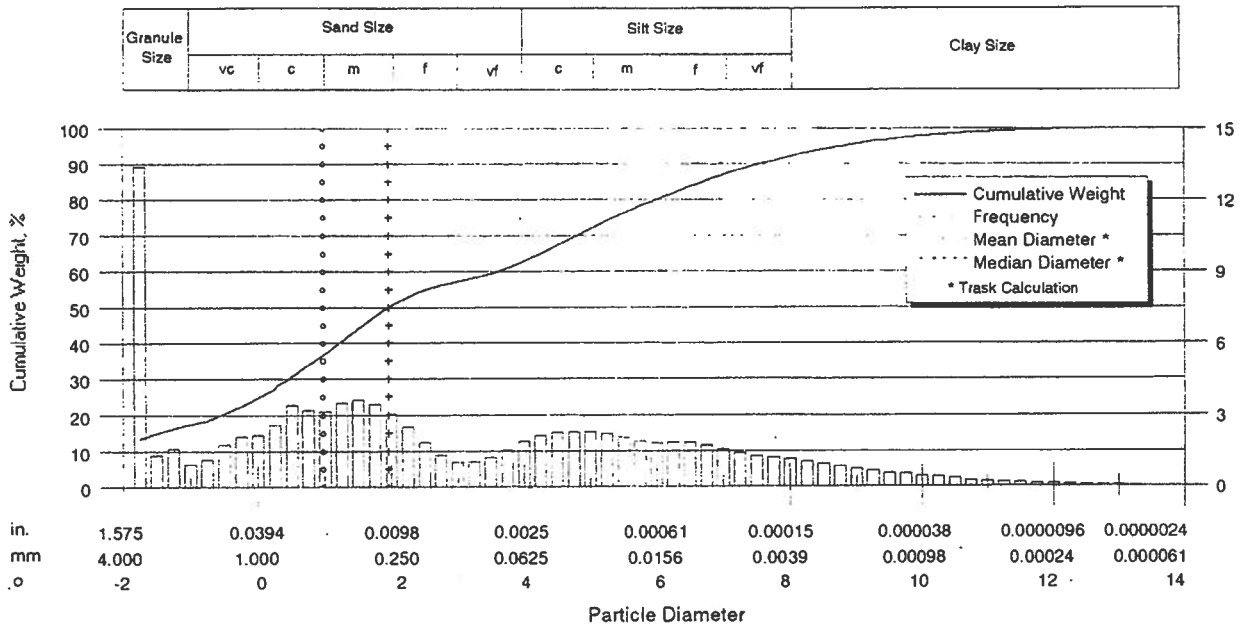

Particle Size Distribution

	[U.S. Sieve]	Diameter [in]	[mm]	[phi]	Weight, % [Inc.]	[Cum.]
Granule	6	0.1324	3.36	-1.75	13.39	13.39
	8	0.0936	2.38	-1.25	2.93	16.32
V Coarse Sand	12	0.0662	1.68	-0.75	2.12	18.44
	16	0.0468	1.19	-0.25	3.91	22.35
	20	0.0331	0.84	0.25	4.76	27.11
Coarse Sand	25	0.0280	0.71	0.50	3.39	30.50
	30	0.0232	0.59	0.75	3.19	33.69
	35	0.0197	0.50	1.00	3.16	36.85
	40	0.0165	0.42	1.25	3.49	40.34
Medium Sand	45	0.0138	0.35	1.50	3.62	43.96
	50	0.0118	0.30	1.75	3.43	47.39
	60	0.0098	0.25	2.00	3.05	50.44
	70	0.0083	0.210	2.25	2.49	52.93
Fine Sand	80	0.0070	0.177	2.50	1.86	54.79
	100	0.0059	0.149	2.75	1.35	56.14
	120	0.0049	0.125	3.00	1.04	57.18
	140	0.0041	0.105	3.25	1.02	58.20
Very Fine Sand	170	0.0035	0.088	3.50	1.23	59.43
	200	0.0029	0.074	3.75	1.56	60.99
	230	0.0025	0.063	4.00	1.88	62.87
	270	0.0021	0.053	4.25	2.15	65.02
Silt	325	0.0017	0.044	4.50	2.28	67.30
	400	0.0015	0.037	4.75	2.29	69.59
	450	0.0012	0.031	5.00	2.29	71.88
	500	0.0010	0.025	5.32	2.80	74.68
	635	0.0008	0.020	5.64	2.53	77.21
		0.00061	0.0156	6.00	2.66	79.87
		0.00031	0.0078	7.00	6.98	86.85
		0.00015	0.0039	8.00	5.08	91.93
		0.000079	0.0020	9.00	3.62	95.55
Clay		0.000039	0.00098	10.0	2.21	97.76
		0.000019	0.00049	11.0	1.26	99.02
		0.0000094	0.00024	12.0	0.67	99.69
		0.0000047	0.00012	13.0	0.28	99.97
		0.0000039	0.00010	13.3	0.03	100.00

Sorting Statistics

Parameter	Trask*	Inman**	Folk**
Mean, in	0.0199	0.0063	0.0074
Mean, mm	0.5098	0.1621	0.1889
Mean, phi	0.9721	2.6254	2.4040
Median, in	0.0100	0.0100	0.0100
Median, mm	0.2568	0.2568	0.2568
Median, phi	1.9612	1.9612	1.9612
Standard Deviation, in	0.2492	0.0025	
Standard Deviation, mm	6.3901	0.0652	
Standard Deviation, phi	-2.6758	3.9398	
Skewness	0.3677		
Kurtosis			

* calculated using mm values
**calculated using phi values

Percentiles [weight, %]	Particle Diameter [in]	[mm]	[phi]
5	ERR 5	ERR 5	ERR 5
10	ERR 5	ERR 5	ERR 5
16	0.0970	2.4870	-1.3144
25	0.0388	0.9951	0.0070
50	0.0100	0.2568	1.9612
75	0.0010	0.0244	5.3587
84	0.0004	0.0106	6.5652
90	0.0002	0.0052	7.5895
95	0.0001	0.0022	8.8171

The analyses, opinions or interpretations contained in this report are based upon observations and material supplied by the client for whose exclusive and confidential use this report has been made. The interpretations or opinions expressed represent the best judgment of Core Laboratories. Core Laboratories, however, assumes no responsibility and makes no warranty or representations, express or implied, as to the productivity, proper operations, or profitableness of any oil, gas, coal or other mineral property, well or sand in connection with which such report is used or relied upon for any reason whatsoever. This report shall not be reproduced except in its entirety, without the written approval of Core Laboratories

CORE LABORATORIES

Company	CORE LAB. - AURORA	Sample	B4-80	File Number	57111-95334
I.D.	954427-13	Proj.	Magma Florence	Date	11-OCT-95
County		State		Analysts	GC

Laser Particle Size Analysis

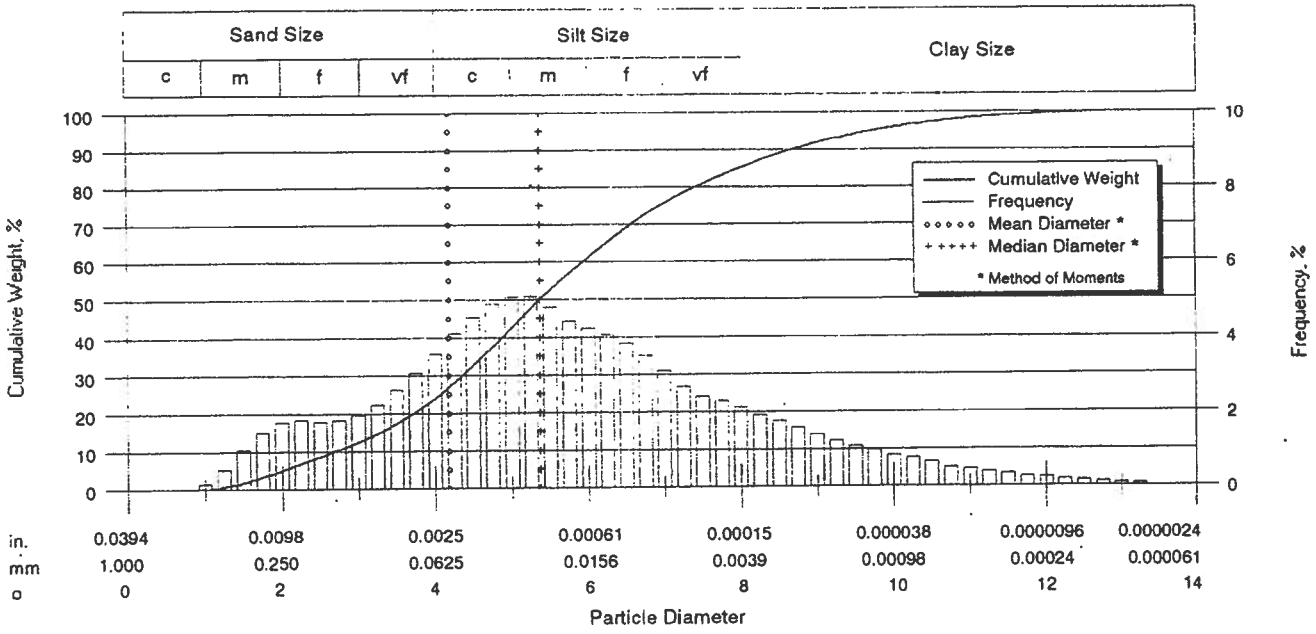

Particle Size Distribution

	[U.S. Sieve]	Diameter [in]	[mm]	[phi]	Weight, % [Inc.]	[Cum.]
Coarse Sand	20	0.0331	0.84	0.25	0.00	0.00
	25	0.0280	0.71	0.50	0.00	0.00
	30	0.0232	0.59	0.75	0.01	0.01
	35	0.0197	0.50	1.00	0.14	0.15
Medium Sand	40	0.0165	0.42	1.25	0.52	0.67
	45	0.0138	0.35	1.50	1.05	1.72
	50	0.0118	0.30	1.75	1.50	3.22
	60	0.0098	0.25	2.00	1.77	4.99
Fine Sand	70	0.0083	0.210	2.25	1.83	6.82
	80	0.0070	0.177	2.50	1.80	8.62
	100	0.0059	0.149	2.75	1.81	10.43
	120	0.0049	0.125	3.00	1.96	12.39
Very Fine Sand	140	0.0041	0.105	3.25	2.23	14.62
	170	0.0035	0.088	3.50	2.62	17.24
	200	0.0029	0.074	3.75	3.06	20.30
	230	0.0025	0.063	4.00	3.57	23.87
Silt	270	0.0021	0.053	4.25	4.11	27.98
	325	0.0017	0.044	4.50	4.56	32.54
	400	0.0015	0.037	4.75	4.85	37.39
	450	0.0012	0.031	5.00	5.06	42.45
	500	0.0010	0.025	5.32	6.46	48.91
	635	0.0008	0.020	5.64	5.94	54.85
		0.00061	0.0156	6.00	6.13	60.98
		0.00031	0.0078	7.00	14.50	75.48
		0.00015	0.0039	8.00	9.49	84.97
Clay		0.000079	0.0020	9.00	6.64	91.61
		0.000039	0.00098	10.0	4.14	95.75
		0.000019	0.00049	11.0	2.39	98.14
		0.0000094	0.00024	12.0	1.26	99.40
		0.0000047	0.00012	13.0	0.54	99.94
		0.0000039	0.00010	13.3	0.06	100.00

Sorting Statistics

Parameter	[Moment]	[Trask]	[Inman]	[Folk]
Mean, in	0.0021	0.0009	0.0008	0.0008
Mean, mm	0.0550	0.0219	0.0201	0.0214
Mean, phi	4.1836	5.5159	5.6354	5.5490
Median, in	0.0009	0.0009	0.0009	0.0009
Median, mm	0.0241	0.0241	0.0241	0.0241
Median, phi	5.3760	5.3764	5.3764	5.3764
Std Deviation, in	0.0032	0.0158	0.0082	0.0079
Std Deviation, mm	0.0822	0.4041	0.2104	0.2028
Std Deviation, phi	3.6042	1.3072	2.2487	2.3021
Skewness	2.6410	0.9805	0.2274	0.1234
Kurtosis	7.5020	0.2396	0.7283	1.1036
Mode, mm	0.0296			
95% Confidence Limits, mm	0.0389 to 0.0711			
Variance, mm2	0.0068			
Coef. of Variance, %	149.40			

Percentiles [Weight, %]	Particle Diameter [in]	[mm]	[phi]
5	0.0097	0.2498	2.0014
10	0.0060	0.1548	2.6912
16	0.0037	0.0956	3.3866
25	0.0023	0.0594	4.0727
50	0.0009	0.0241	5.3764
75	0.0003	0.0080	6.9591
84	0.0002	0.0042	7.8841
90	0.0001	0.0024	8.7136
95	0.0000	0.0011	9.7742

The analyses, opinions or interpretations contained in this report are based upon observations and material supplied by the client for whose exclusive and confidential use this report has been made. The interpretations or opinions expressed represent the best judgment of Core Laboratories. Core Laboratories, however, assumes no responsibility and makes no warranty or representations, express or implied, as to the productivity, proper operations, or profitableness of any oil, gas, coal or other mineral property, well or sand in connection with which such report is used or relied upon for any reason whatsoever. This report shall not be reproduced except in its entirety, without the written approval of Core Laboratories.

CORE LABORATORIES

Company	CORE LAB. - AURORA	Sample	M16-60-300	File Number	57111-95334
I.D.	954427-14	Proj.	Magma Florence	Date	11-OCT-95
County		State		Analysts	GC

Laser Particle Size Analysis

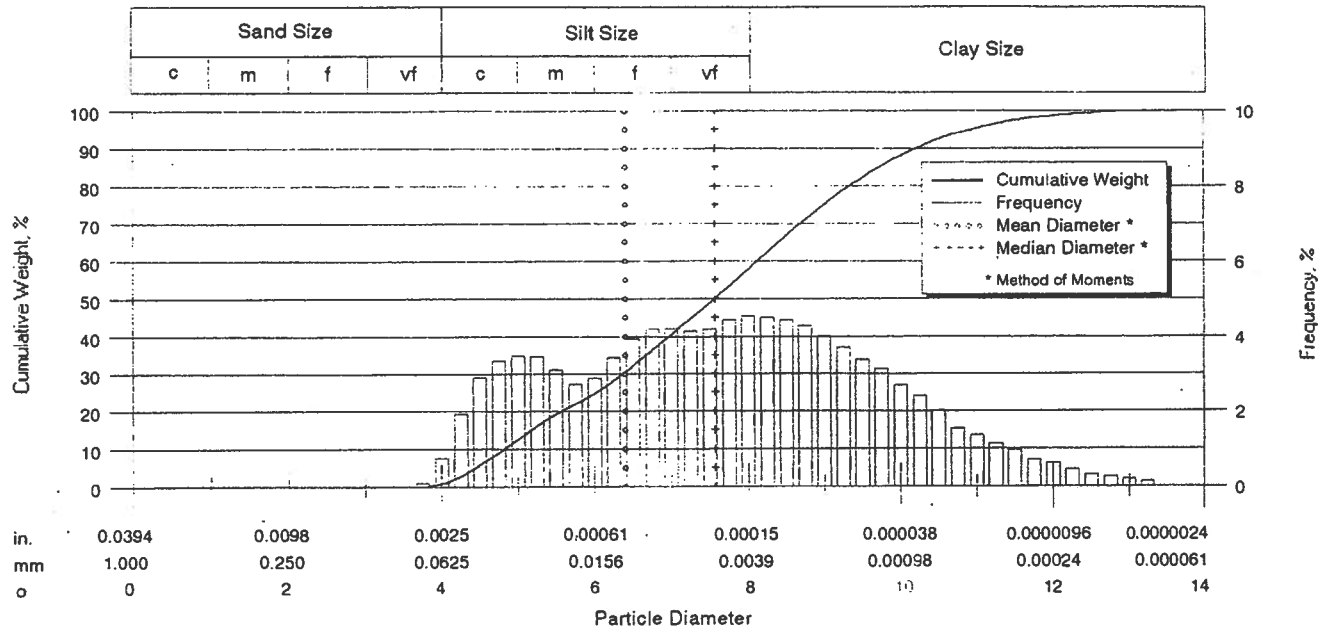

Particle Size Distribution

	[U.S. Sieve]	Diameter [in]	[mm]	[phi]	Weight, % [Inc.]	[Cum.]
Coarse Sand	20	0.0331	0.84	0.25	0.00	0.00
	25	0.0280	0.71	0.50	0.00	0.00
	30	0.0232	0.59	0.75	0.00	0.00
	35	0.0197	0.50	1.00	0.00	0.00
Medium Sand	40	0.0165	0.42	1.25	0.00	0.00
	45	0.0138	0.35	1.50	0.00	0.00
	50	0.0118	0.30	1.75	0.00	0.00
	60	0.0098	0.25	2.00	0.00	0.00
Fine Sand	70	0.0083	0.210	2.25	0.00	0.00
	80	0.0070	0.177	2.50	0.00	0.00
	100	0.0059	0.149	2.75	0.00	0.00
	120	0.0049	0.125	3.00	0.00	0.00
Very Fine Sand	140	0.0041	0.105	3.25	0.00	0.00
	170	0.0035	0.088	3.50	0.00	0.00
	200	0.0029	0.074	3.75	0.09	0.09
	230	0.0025	0.063	4.00	0.76	0.85
Silt	270	0.0021	0.053	4.25	1.91	2.76
	325	0.0017	0.044	4.50	2.92	5.68
	400	0.0015	0.037	4.75	3.33	9.01
	450	0.0012	0.031	5.00	3.50	12.51
	500	0.0010	0.025	5.32	4.38	16.89
	635	0.0008	0.020	5.64	3.74	20.63
		0.00061	0.0156	6.00	4.05	24.68
		0.00031	0.0078	7.00	15.78	40.46
		0.00015	0.0039	8.00	17.31	57.77
Clay		0.000079	0.0020	9.00	17.24	75.01
		0.000039	0.00098	10.0	12.88	87.89
		0.000019	0.00049	11.0	7.32	95.21
		0.0000094	0.00024	12.0	3.40	98.61
		0.0000047	0.00012	13.0	1.26	99.87
		0.0000039	0.00010	13.3	0.13	100.00

Sorting Statistics

Parameter	[Moment]	[Trask]	[Inman]	[Folk]
Mean, in	0.0005	0.0002	0.0002	0.0002
Mean, mm	0.0119	0.0055	0.0057	0.0056
Mean, phi	6.3990	7.5125	7.4508	7.4897
Median, in	0.0002	0.0002	0.0002	0.0002
Median, mm	0.0053	0.0053	0.0053	0.0053
Median, phi	7.5672	7.5674	7.5674	7.5674
Std Deviation, in	0.0006	0.0167	0.0085	0.0092
Std Deviation, mm	0.0147	0.4287	0.2178	0.2354
Std Deviation, phi	6.0841	1.2221	2.1988	2.0870
Skewness	1.7450	0.9469	0.0621	-0.0056
Kurtosis	2.4310	0.2755	0.4821	0.8983
Mode, mm	0.0036			
95% Confidence	0.0090			
Limits, mm	0.0147			
Variance, mm2	0.0002			
Coef. of Variance, %	124.40			

Percentiles [Weight, %]	Particle Diameter [in]	[mm]	[phi]
5	0.0018	0.0459	4.4450
10	0.0014	0.0354	4.8196
16	0.0010	0.0262	5.2520
25	0.0006	0.0154	6.0256
50	0.0002	0.0053	7.5674
75	0.0001	0.0020	8.9994
84	0.0000	0.0012	9.6496
90	0.0000	0.0008	10.2156
95	0.0000	0.0005	10.9629

The analyses, opinions or interpretations contained in this report are based upon observations and material supplied by the client for whose exclusive and confidential use this report has been made. The interpretations or opinions expressed represent the best judgment of Core Laboratories. Core Laboratories, however, assumes no responsibility and makes no warranty or representations, express or implied, as to the productivity, proper operations, or profitableness of any oil, gas, coal or other mineral, property, well or sand in connection with which such report is used or relied upon for any reason whatsoever. This report shall not be reproduced except in its entirety, without the written approval of Core Laboratories.

CORELAB

CORE LABORATORIES

SUMMARY OF HYDRAULIC CONDUCTIVITY
CORE LABORATORIES, AURORA
PROJECT NAME: MAGMA - FLORENCE

Sample I.D.	DEPTH, feet	Hydraulic Conductivity, md	Hydraulic Conductivity, cm/sec
P1 - 80 - 80	NA	32.2	2.76×10^{-5}
P2 - 90 - 45	NA	1.2	1.07×10^{-6}
B2 - 55	NA	0.618	5.30×10^{-7}
B3 - 45	NA	8.1	6.94×10^{-6}
B4 - 80	NA	0.613	5.26×10^{-7}
M16 - GU - 300	NA	0.0058	5.00×10^{-9}

The analyses, opinions or interpretations contained in this report are based upon observations and material supplied by the client for whose exclusive and confidential use this report has been made. The interpretations or opinions expressed represent the best judgment of Core Laboratories. Core Laboratories, however, assumes no responsibility and makes no warranty or representations, express or implied, as to the productivity, proper operations, or profitableness of any oil, gas, coal or other mineral, property, well or sand in connection with which such report is used or relied upon for any reason whatsoever. This report shall not be reproduced except in its entirety, without the written approval of Core Laboratories.

HYDRAULIC CONDUCTIVITY TEST REPORT

ASTM D5084

Project Name	Claridge - Hanlon #91100A	***Project No.***	106200-19
Client Name	Geosystems Analysis, Inc.	***Date Received***	8/11/2011
Client Address		***Date Tested***	8/11/2011
		Date Issued	8/18/2011
Boring No.	CMP-11-03		
Sample Type	Undisturbed		
Sample Depth	283-288 feet		
Sample Description	Clay, very stiff, brown to red brown		

	Before	***After***	***Units***
Moisture Content, w	28.6	29.2	*%*
Dry Unit Weight, Dd	94.8	95.0	*pcf*
Height, L	1.81	1.80	*inches*
Diameter, d	3.19	3.19	*inches*
Degree of Saturation, Sr	97.2	99.5	*%*

Chamber Pressure:	83.3	**psi**
Applied Pressure (influent):	78.3	**psi**
Applied Pressure (effluent):	75.0	**psi**
Consolidation Pressure:	5	**psi**

Test Number		***Temp. Deg. C***	***Time (sec)***	***Influent Reading***	***Effluent Reading***	***Hydraulic Conductivity (cm/sec) @ Test Temp.***	***Hydraulic Conductivity (cm/sec) @ 20° C***	***Hydraulic Gradient h/L***
1	Start	22.4	0	7.60	19.85			
	Finish	22.2	59220	8.20	19.30	4.52E-09	4.3E-09	53.09
2	Start	22.2	59220	8.20	19.30			
	Finish	22.5	90480	8.50	19.00	4.49E-09	4.3E-09	52.96
3	Start	22.5	90480	8.50	19.00			
	Finish	22.6	140400	9.05	18.55	4.70E-09	4.4E-09	52.73
4	Start	22.6	140400	9.05	18.55			
	Finish	22.7	229140	10.00	17.70	4.79E-09	4.5E-09	52.33

Average Hydraulic Conductivity "k" (cm/sec) @ Test Temp.	4.6E-09	
Average Hydraulic Conductivity "k" (cm/sec) @ 20° C		**4.4E-09**

Assumed Specific Gravity, SG 2.75

Area of Tube (cm^2), a (Pipette) 0.9721

Permeant : Deaired Tap Water

Formulas:

Permeability (Falling Head-Rising Tailwater Test)

k = [(a*L/(2*A*t)] ln(ho/h1)

k = Hydraulic Conductivity (cm/sec)

a = Area of Tube (cm^2)

L = Height or Length of Sample (cm)

A = Area of Sample (cm^2)

t = Time of Test Interval (sec)

h_o = Height of Head at Start of Test Interval (cm)

h_1 = Height of Head at End of Test Interval (cm)

Degree of Saturation

Sr = w*SG/e Dd = (SG/1+e)Dw

Therefore:

Sr = (w*SG)/((SG*Dw/Dd)-1)

Sr = Degree of Saturation (%)

w = Moisture Content (%)

SG = Specific Gravity

e = Void Ratio

Dd =Dry Unit Weight (pcf)

Dw = Unit Weight of Water (62.4 pcf)

L:\Quality\Labreports\Newperm.xls

KLEINFELDER
Bright People. Right Solutions.

HYDRAULIC CONDUCTIVITY TEST RESULTS (ASTM D5084)

Project Name	Claridge - Hanlon #91100A	***Job No.***	106200-19
Client Name	Geosystems Analysis, Inc.	***Date Received***	8/11/2011
Client Address		***Date Tested***	8/11/2011
		Date Issued	8/18/2011
Boring No.	CMP-11-03		
Sample Type	Undisturbed		
Sample Depth	283-288 feet		
Sample Description	Clay, very stiff, brown to red brown		
	0.0		

	Deviation from Average	Change in Influent(ml)	Change in Effluent (ml)	Ratio Effluent/Influent Change
Test1	0.98	0.58	-0.53	0.92
Test 2	0.97	0.29	-0.29	1.00
Test 3	1.02	0.53	-0.44	0.82
Test 4	1.04	0.92	-0.83	0.89
	ok if within 0.75-1.25			**ok if within 0.75-1.25**

1.0231881

0.022923341

HYDRAULIC CONDUCTIVITY TEST REPORT

ASTM D5084

Project Name	Claridge - Hanlon #91100A	***Project No.***	106200-19
Client Name	Geosystems Analysis, Inc.	***Date Received***	8/11/2011
Client Address		***Date Tested***	8/11/2011
		Date Issued	8/18/2011
Boring No.	CMP-11-03		
Sample Type	Undisturbed		
Sample Depth	292.5-297.5 feet		
Sample Description	Clay, very stiff, brown to red brown		

	Before	***After***	***Units***
Moisture Content, w	28.8	28.0	*%*
Dry Unit Weight, Dd	95.9	96.6	*pcf*
Height, L	1.95	1.95	*inches*
Diameter, d	3.16	3.16	*inches*
Degree of Saturation, Sr	100.4	99.0	*%*

Chamber Pressure:	83.5	**psi**
Applied Pressure (influent):	78.5	**psi**
Applied Pressure (effluent):	75.0	**psi**
Consolidation Pressure:	5	**psi**

Test Number		***Temp. Deg. C***	***Time (sec)***	***Influent Reading***	***Effluent Reading***	***Hydraulic Conductivity (cm/sec) @ Test Temp.***	***Hydraulic Conductivity (cm/sec) @ 20° C***	***Hydraulic Gradient h/L***
1	Start	22.4	0	7.60	19.70			
	Finish	22.2	59220	8.15	19.20	4.22E-09	4.0E-09	51.94
2	Start	22.2	59220	8.15	19.20			
	Finish	22.5	90480	8.50	18.85	5.35E-09	5.1E-09	51.80
3	Start	22.5	90480	8.50	18.85			
	Finish	22.6	140400	8.95	18.40	4.32E-09	4.1E-09	51.61
4	Start	22.6	140400	8.95	18.40			
	Finish	22.7	229140	9.80	17.60	4.48E-09	4.2E-09	51.27

Average Hydraulic Conductivity "k" (cm/sec) @ Test Temp.	4.6E-09	
Average Hydraulic Conductivity "k" (cm/sec) @ 20° C		**4.3E-09**

Assumed Specific Gravity, SG 2.75

Area of Tube (cm^2), a (Pipette) 0.9721

Permeant : Deaired Tap Water

Formulas:

Permeability (Falling Head-Rising Tailwater Test)

k = [(a*L/(2*A*t)] ln(ho/h1)

k = Hydraulic Conductivity (cm/sec)

a = Area of Tube (cm^2)

L = Height or Length of Sample (cm)

A = Area of Sample (cm^2)

t = Time of Test Interval (sec)

h_o = Height of Head at Start of Test Interval (cm)

h_1 = Height of Head at End of Test Interval (cm)

Degree of Saturation

Sr = w*SG/e Dd = (SG/1+e)Dw

Therefore:

Sr = (w*SG)/((SG*Dw/Dd)-1)

Sr = Degree of Saturation (%)

w = Moisture Content (%)

SG = Specific Gravity

e = Void Ratio

Dd =Dry Unit Weight (pcf)

Dw = Unit Weight of Water (62.4 pcf)

L:\Quality\Labreports\Newperm.xls

KLEINFELDER
Bright People. Right Solutions.

HYDRAULIC CONDUCTIVITY TEST RESULTS (ASTM D5084)

Project Name	Claridge - Hanlon #91100A	***Job No.***	106200-19
Client Name	Geosystems Analysis, Inc.	***Date Received***	8/11/2011
Client Address		***Date Tested***	8/11/2011
		Date Issued	8/18/2011
Boring No.	CMP-11-03		
Sample Type	Undisturbed		
Sample Depth	292.5-297.5 feet		
Sample Description	Clay, very stiff, brown to red brown		

0.0

	Deviation from Average	Change in Influent(ml)	Change in Effluent (ml)	Ratio Effluent/Influent Change
Test1	0.92	0.53	-0.49	0.91
Test 2	1.16	0.34	-0.34	1.00
Test 3	0.94	0.44	-0.44	1.00
Test 4	0.98	0.83	-0.78	0.94
	ok if within 0.75-1.25			**ok if within 0.75-1.25**

1.0231881

0.022923341

Exhibit 14A-3

Site Characterization Report Section 2.3.1
Florence 1996 APP Application

and data storage procedures. Users of the data management plan include Magma, Brown and Caldwell and others involved with the completion of the environmental permit support investigations.

Purposes of the data management plan include: (1) to ensure that the necessary information is collected; (2) to provide a means of communication between individuals involved in the project; (3) to optimize time spent on data management; and (4) to ensure that different types of data can be combined to meet information goals.

As shown on Figure 2.2-1[II], the data management and analysis system consists of a number of components, including statistics, graphical data analysis and data presentation modules. All modules are accessible from a central database (Microsoft ACCESS).

Two types of QA/QC, technical and accuracy, are performed on all data types. Technical QA consists of a review to ensure that data is consistent, both with expectations and with other data. Accuracy QA is a review to ensure that the data are transferred correctly from the raw data format into the data management and analysis system. Generalized procedures for lithologic, water quality, aquifer test, packer test and other data sets include the following elements:

- Manual measurements are obtained, when possible, to verify data collected on data loggers.
- Field data hard copies are generated and reviewed by qualified personnel.
- Field data are compiled, edited and summarized. Hard copies are then signed, dated and stored.
- Electronic copies of the data are used for input into the database system, and subsequently verified.
- Any unusual findings are identified and discussed with the appropriate parties.

Further discussions of QA protocols concerning groundwater quality sampling are presented in Volume III of this application. Further details concerning data management are presented in the project-specific Data Management Plan (BC, 1995h).

2.3 INVESTIGATION DESIGN AND PROCEDURES

This section describes the design of the field investigation, including scope of work, and field and laboratory procedures, where appropriate.

2.3.1 Vadose Zone Characterization

As discussed in Section 2.1.1, the following aspects of the vadose zone in the proposed in-situ mine area were investigated: (1) the general physical and chemical baseline conditions; (2) the geotechnical conditions; and (3) the soil quality. This section addresses the general baseline characterization. Potential soil quality impacts are discussed in Section 4.4.2 and Appendix G

of this volume, and the geotechnical results are presented and discussed in Volume V of this application. Geochemical discussions relative to vadose zone baseline conditions are presented in Volume IV of this application.

The vadose zone baseline characterization investigation was conducted in September and October 1995. The vadose zone baseline field work included advancing a total of eight soil borings. Piezometers (permeameters) P1-80, P2-90, P3-60, and P4-40 were installed in 4 of the borings in order to conduct field hydraulic conductivity tests. A summary of vadose characterization boring and piezometer construction details is presented in Table 2.3-1. Locations of vadose zone baseline and geotechnical borings are illustrated on Figure 2.1-1[II]. Vadose characterization boring logs and piezometer construction details are presented in Appendix A.

2.3.1.1 Drilling Methods

Percussion hammer drilling techniques were employed to advance borings for soil sampling and hydraulic conductivity testing. A Becker AP-1000 dual-tube percussion hammer drilling rig was used to advance borings to a maximum depth of 95 feet below ground surface (bgs). Piezometer construction details are presented in Table 2.3-1.

The borings were advanced using 10-inch outside diameter, dual-tube drill pipe driven into the subsurface with a hydraulic hammer. The pipe was marked every foot to measure rate of penetration. The rate of penetration was recorded on the boring log as hammer blows per foot (usually at 1-foot intervals). The boring cuttings were brought to the surface by a pressurized pipe and discharged to a cyclone next to the rig. The cuttings were used to backfill the borehole in cases where a piezometer was not installed. If water was encountered, the hole was backfilled with bentonite grout, followed by a Portland cement cap.

2.3.1.2 Soil Sampling Procedures

Soil samples were collected from the vadose zone borings at depths ranging from ground surface to 95 feet bgs. Soil samples were collected at depths of 2 feet bgs and at 5-foot intervals beginning at 5 feet bgs to the total depth of each soil boring. Four soil borings, B1, B2, B3, and B4 were advanced to a maximum depth of 95 feet bgs. The borings for piezometers P3-60 and P4-40 were not sampled as they were installed approximately 10 feet from B3 and B4, respectively.

Soil Sampling Equipment:

- The soil samples were collected using a California-modified, split-spoon 2.5-inch diameter sampler that was 18 inches in length.
- Sample rings were 2.5 inches in diameter and 6 inches in length, and were constructed of brass.

Soil Sampling Procedures:

- The clean sampler was opened and clean sample collection rings and sand retainer were inserted.
- The sampler was closed and the end cap and drive shoe were hand tightened. No grease was used on the end cap or drive shoe threads.
- The clean, loaded sampler was attached to the downhole 140-pound sample hammer, and lowered into the boring.
- The sampler was driven ahead of the bit into undisturbed soil using a standard 140-pound weight that was allowed to drop 30 inches per blow.
- The number of blows required to drive the sampler 18 inches past the end of the drill bit was recorded on the boring logs.
- The sampler was then retrieved from the borehole, removed from the hammer, and opened.
- Teflon sheets were placed over the 2 exposed ends of the middle sample ring. Plastic endcaps were placed over the Teflon sheets. The sample was labeled, placed in a zip-lock bag and stored in a cooler maintained at approximately 4 degrees Celsius.
- To detect any potential volatile organic presence in the soil samples in the field, a portion of the sample was placed in a zip-lock bag and the bag was sealed. The sample was allowed to be heated by the sun for a few minutes to allow any volatile substances in the soil sample to volatilize. The presence of volatile organics was measured by placing the probe of an Organic Vapor Analyzer (OVA) into the bag. The OVA reading was recorded on the boring log.
- A soil sample was collected from the drive shoe, and described on the lithologic log form using American Society for Testing and Materials (ASTM) Methods D-1452, D-2487, and D-2488.

2.3.1.3 Hydraulic Conductivity Testing

Each of the 4 vadose zone piezometers (permeameters) listed in Table 2.3-1 was constructed using 2 3/8-inch (outside diameter) Schedule 80 PVC pipe, with a 10-foot screened section at the indicated depth interval in each boring. A filter pack consisting of No. 69 Colorado silica sand was installed to a depth of 5 feet above the top of the screen. One 100-pound bag of No. 30 silica sand (approximately 3 feet of annular length) was installed on top of the No. 6 - No. 9 mesh sand. Bentonite grout was installed to within 1 to 2 feet of the surface, followed by a Portland cement cap.

In October 1995, soil hydraulic conductivity tests were conducted in the piezometers (permeometers) installed during this investigation. The field permeability tests were performed in accordance with U.S. Bureau of Reclamation E-18 test methods, (Bureau of Reclamation [BOR], 1974). Hydraulic conductivity values were calculated using Method E-18 (BOR, 1974) and procedures described in Lamb and Whitman (1969). This test method assumes saturated conditions while testing, therefore pre-wetting was performed prior to conducting each of the tests. The tests were performed using constant head conditions.

Each field piezometer installation was pre-soaked for 24 to 48 hours prior to testing by filling the casings with water from a truck-mounted 1,000-gallon water tank. The piezometers were filled by pumping the water with a centrifugal pump until all air inside the casing was expelled and water spilled over the top of the casing. A flow meter pressure gauge and an air escape valve were connected to the top of the field piezometers using a well head attachment. A hose was connected from the attachment to the centrifugal pump and a hose was connected from the pump to the water tank. The water was pumped into the piezometer with the air escape valve opened until all air was expelled from the system. The air escape valve was closed, pressurizing the well. The pump rate was regulated to prevent the pressure from exceeding a static pressure level of 10 pounds per square inch (psi). The amount of water pumped into the well to maintain a static pressure was monitored using the flow meter. This procedure was repeated several times, providing results at several static pressure levels. Results of the soil hydraulic conductivity tests are discussed in Section 4.0. A report summarizing the field hydraulic conductivity vadose zone investigation conducted by AGRA E&E is presented in Appendix F of this volume.

2.3.1.4 Laboratory Analyses

Selected soil samples retrieved during the baseline vadose zone investigation were chemically and physically tested to measure background geochemical and attenuation properties, and assist in the description of the various soil types. Laboratory analyses were performed by Core Laboratories in Denver, Colorado on 13 soil samples collected as part of the vadose zone baseline investigation. The samples chosen for analyses were fine-grained soils such as clay, silt, and sandy silts. A summary of the vadose zone laboratory testing program is presented in Table 2.3-2. Soil samples selected for laboratory analyses included the following:

P1-80:	2 samples from 55 and 80 feet bgs;
P2-90:	2 samples from 45 and 70 feet bgs;
B1:	2 samples from 35 and 90 feet bgs;
B2:	2 samples from 55 and 75 feet bgs;
B3:	3 samples from 10, 45, and 65 feet bgs; and
B4:	2 samples from 55 and 80 feet bgs.

Each sample submitted was analyzed for each of the chemical constituents or properties listed on Table 2.3-2, except for triaxial permeability. One sample from each boring was analyzed for triaxial permeability. Physical laboratory results from Core Laboratories are presented in Appendix F and are discussed in Section 4.0. Chemical laboratory results associated with the vadose zone investigation are presented and discussed in Volume IV of the application.

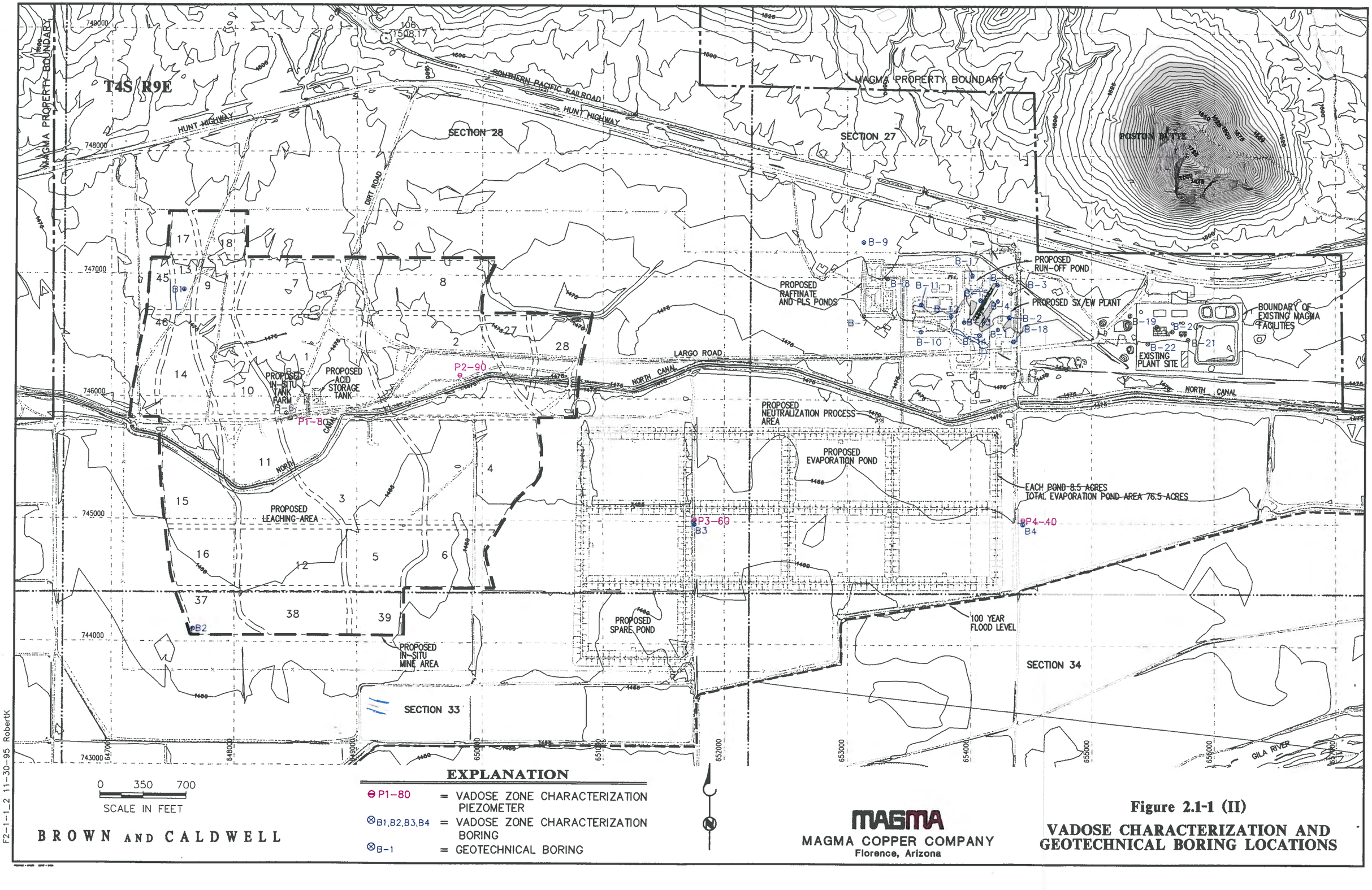

F2-1-1_2 11-30-95 RobertK

Figure 2.1-1 (II)

VADOSE CHARACTERIZATION AND GEOTECHNICAL BORING LOCATIONS

Table 2.3-1 Summary of Vadose Zone Characterization Borings and Piezometer Construction Details			
Boring Identification	**Drilling Method**	**Total Depth (feet bgs)**	**Piezometer Screen Interval (feet bgs)**
B1	Percussion Hammer	95	NA
B2	Percussion Hammer	80	NA
B3	Percussion Hammer	80	NA
B4	Percussion Hammer	95	NA
P1-80	Percussion Hammer	80	70'to 80'
P2-90	Percussion Hammer	90	80' to 90'
P3-60	Percussion Hammer	60	50' to 60'
P4-40	Percussion Hammer	40	30' to 40'

NA - Not Applicable
Percussion Hammer Drilling Method - AP-1000 Drilling Rig
See Figure 2.1-1[II] for Boring and Piezometer Locations
Lithologic Logs and Piezometer Construction Diagrams are presented in Appendix A [II].
bgs - below ground surface

Table 2.3-2 Summary of Vadose Zone Investigation Laboratory Analysis Program			
Analyses	**Analytical Method**	**Detection Limit**	**Reporting Units**
Geochemical Parameters			
Acid Neutralization Potential (ANP)	EPA 600 3.2.3	0.1	tons $CaCO_3$/Kt
Cation Exchange Capacity (CEC)	SW-846 9081	0.01	meq/100gm
Exchangeable Cations: Sodium	USDA 60 18	0.01	meq/100gm
Total Organic Carbon (TOC)	Agronomy 90-3	0.01	Percent
Total Sulfur as S Total Sulfur	ASTM D4239-85C	0.01 0.3	Percent (Leco Furnace) tons $CaCO_3$/Kt
Total Metals[a]			
Mercury	SW-846 7471	0.02	mg/Kg
Arsenic (As) Beryllium (Be) Cadmium (Cd) Chromium (Cr) Copper (Cu) Lead (Pb) Selenium (Se) Silver (Ag) Zinc (Zn)	SW-846 6010	0.05 0.005 0.005 0.01 0.01 0.05 0.1 0.01 0.01	mg/Kg mg/Kg mg/Kg mg/Kg mg/Kg mg/Kg mg/Kg mg/Kg mg/Kg
Miscellaneous Geochemical Parameters[b]			
Alkalinity	EPA 310.1	5	mg/L $CaCO_3$
Bicarbonate	SM 2320 B	5	mg/L
Chloride	EPA 325.2	0.5	mg/L
Nitrate and Nitrite	EPA 353.2	0.05	mg/L
Sulfate	EPA 375.2	NA	NA
Soluble Metals Analyses Calcium (Ca) Magnesium (Mg) Sodium (Na)	SW-846 6010	 0.1 0.1 1	 mg/L mg/L mg/L

Table 2.3-2 Summary of Vadose Zone Investigation Laboratory Analysis Program			
Analyses	**Analytical Method**	**Detection Limit**	**Reporting Units**
Physical Parameters			
Particle Size Distribution	ASTM D4464	NA	NA
Triaxial Permeability	ASTM 5048	NA	NA
Plasticity Index	ASTM D4318	NA	NA

[a]Performed with Solids Acid Digestion preparation (SW-846-3050)
[b]Performed with Soluble Soil Paste preparation (USDA Method 60 2)
NA - Not Applicable
mg/Kg - milligrams per Kilogram
meq/100gm - milliequivalent per 100 grams
mg/L - milligrams per Liter
Kt - Kiloton
$CaCO_3$ - Calcium Carbonate